



Thesis

By

**MOSTAFA ABD EL-
HAMEED MOHAMED**

**The Department of
Natural Resources
Institute of African
Research and
Studies, Cairo
University**

**Impact of climatic Variability on
Nile River Water resources and
its Flood Fluctuations in Ethiopia**

2013



04 SEP. 2015

16.02.02

MOH

16156

*Impact of Climatic variability on Nile
River water resources and its flood
fluctuations in Ethiopia*



By

MOSTAFA ABD EL-HAMEED MOHAMED

B.Sc. Astronomy and Meteorology, Al-Azhar University, 2001

*Diploma of African studies (Natural Resources) 2005 M.Sc. African studies
(Natural Resources, Meteorology), 2008, Institute of African Research and
Studies, Cairo University*

A Thesis Submitted to
The Department of Natural Resources
Institute of African Research and Studies, Cairo University

For the degree of
Ph.D.
In

AFRICAN STUDIES
(Natural Resources, Meteorology)

Natural Resources Department
Institute of African Research and Studies
Cairo University

2013

*Impact of Climatic variability on Nile
River water resources and its flood
fluctuations in Ethiopia*

By

MOSTAFA ABD EL-HAMEED MOHAMED

*B.Sc. Astronomy and Meteorology, Al-Azhar University, 2001
Diploma of African studies (Natural Resources) 2005 M.Sc. African studies
(Natural Resources, Meteorology), 2008, Institute of African Research and
Studies, Cairo University*

A thesis Submitted to
The Department of Natural Resources
Institute of African Research and Studies, Cairo University

For the degree of
Ph.D.
AFRICAN STUDIES
(Natural Resources, Meteorology)

Under supervision of

Prof. Dr. Fawzia Ibrahim Moursy
Prof. of Meteorology, Institute of African
Research and Studies, Cairo University

Dr. Abbas Mohamed Sharaky
Associate Prof. of Georesources (Economic
Geology) - Institute of African Research and
Studies, Cairo University

Dr. Abdellatif Esawy Awad
Associate Prof. of Meteorology- Egyptian
Meteorological Authority

2013



The approvals sheet

Impact of Climatic variability on Nile River water resources and its flood fluctuations in Ethiopia

By

MOSTAFA ABD EL-HAMEED MOHAMED

*B.Sc. Astronomy and Meteorology, Al-Azhar University, 2001
Diploma of African studies (Natural Resources) 2005 M.Sc. African studies (Natural Resources, Meteorology), 2008, Institute of African Research and Studies, Cairo University*

**A Thesis Submitted to
The Department of Natural Resources
Institute of African Research and Studies, Cairo University**

For the degree of

Ph.D.

In

AFRICAN STUDIES

(Natural Resources, Meteorology)

Approved by the examining committee

Prof. Fathy Mohamed El Hussainy Mohamed.....*Fathy*.....

Professor of Meteorology, Department of Meteorology, Faculty of Science, Al-Azhar University

Prof. El-Sayed Mohamed Abdel-Hamid Robaa.....*S. M. Robaa*.....

Professor of Environmental and Atmospheric Physics, Astronomy and Meteorology Department, Faculty of Science, Cairo University

Prof. Fawzia Ibrahim Moursy.....*Fawzia*.....

Professor of Meteorology, Institute of African Research and Studies, Cairo University

Prof. Abbas Mohamed Sharaky.....*A. Sharaky*.....

Associate Prof. of Georesources (Economic Geology), Institute of African Research and Studies, Cairo University

Acknowledgment

I would like to acknowledge all people who have made significant contribution to my Ph.D thesis studies. In particular, Prof. Fawzia Ibrahim Moursy, Prof. of Meteorology, Institute of African Research and Studies, Cairo University, for her permanent support, encouragements, supervision, guidance and useful comments throughout the course of this thesis.

Special thanks to Dr. Abbas Mohamed Sharaky Assi. Prof. of Georesources (Economic Geology), Institute of African Research and Studies, Cairo University, and Dr. Abdellatif Esawy Awad Assi. Prof. of Meteorology, for their permanent support, supervision and encouragements throughout this study.

I would like to thank all my professors, all my friends and colleagues at Department of Natural Resources, Institute of African Research and Studies, Cairo University, for their useful comments throughout this thesis.

I would like to extend my sincere gratitude to Council for the Development of Social Science Research in Africa for the opportunity of Small Grants Programme for Theses Writing given to me, and for the assistance and financial support for this study.

"My deep gratitude is to my parents, my brothers, my sisters and my wife for their patience and continuous support especially in time of difficulty".

ABSTRACT

The present study has been conducted to investigate climatic variability over Nile river water resources how stream flow in the Nile Basin has varied over the period of available records. Stream flow records from 5 flow gauging stations in three major river basins of the Nile and 26 meteorological stations all over Ethiopia were studied. Temperature and rainfall are the most indicative factors of climate change. The present study aimed at studying temporal variation in temperature and rainfall over Ethiopia during the period 1950–2005.

The climate data consisted of mean monthly and annual records of temperature (minimum and maximum), rainfall. Seasonal classification of the region, especially over Ethiopia, is from February to May, June to September and October to January called Belg, Kiremt and Bega, respectively.

The average of temperature and rainfall at the selected weather stations was used for this study. Statistics on measures (mean, minimum, maximum), dispersion (standard deviation) and distribution (skewness, kurtosis and variability coefficient) were calculated for the data. The data series was tested for normality using One-Sample Kolmogorov-Smirnov test, Homogeneity test was tested as indicator for the Homogeneity of data, trends in annual and seasonal temperature and rainfall series were analyzed using (The least squares method, Quadratic, Cubic and Exponential equations) and we Also used the Mann-Kendall test for cases where the trend may be assumed to be non-parametric tests and thus no seasonal or other cycle is present in the data. The Sen's method uses a linear model to estimate the slope of the trend and the variance of the residuals should be constant in time.

Time series were used in the present study with using (Box & Jenkins) method (Identification, Estimation, Diagnostic Checking of Model, and Forecasting) to find the best forecasting model to the Rainfall over Blue Nile basin in Ethiopia by using the monthly data for the period (1950-2005).

The study reveals overall increasing trends in temperature (significant at 95% confidence level) at different rates in the study period. The mean of maximum and minimum temperatures in Ethiopia has minimal increased by 0.02 and 0.027 °C over the whole period, respectively. We noted that the highest value for R^2 was at cubic equation at all stations so cubic equation is the best to express the trend equation than the other equations for maximum and minimum temperature.

Time series analysis and forecasting is an important tool which can be used to improve water resources management. After selecting the most appropriate model, it was found that ARIMA model $(0,0,0) \times (1,1,1)_{12}$, $(0,0,0) \times (1,1,1)_{12}$, $(0,0,0) \times (0,1,1)_{12}$ and $(0,0,1) \times (0,1,1)_{12}$ was among several models that passed all statistic tests required in the

Box-Jenkins methodology for Bahar Dar, Nekemte, DebreMarkos and Addis Ababa respectively, of the North, West and middle of Ethiopia.

After selection of the best trend equation for mean annual maximum and minimum temperature through the study period we depend on this equation to predict the temperature trend for 2006-2030, all stations will have a small increase in mean annual maximum temperature as regarding quadratic and cubic trend equation but every station represented by either quadratic or cubic trend equation.

The trends in stream flow computed by the Mann-Kendall test, the results indicate that there was no significant trend in the observed annual runoff at all stations El Diem, Khartoum, Malakal, Dongola and Aswan ($R^2 = 0.033, 0.00, 0.14, 0.09$ and 0.002 respectively). We note that, trend in the flow TS increased for the Blue Nile at (El Diem and Khartoum station), while the flow TS decreased for White Nile at Malakal station.

Keyword

Nile River Basin, Water Resources, Blue Nile, Flood, Climatic Variability, Trend, Time-series forecasting, ARIMA Models.

CODESRIA - LIBRARY

List of Content

	<i>Page</i>
List of tables.....	V
List of figures.....	VIII
List of abbreviations.....	XII
1. INTRODUCTION.....	1
1.1. Problem statement.....	4
1.2. Objective of the research.....	4
2. REVIEW OF LITERATURES.....	5
2.1. The Nile river basin.....	5
2.1.1. Hydrology.....	5
2.1.2. Ethiopian Nile basins.....	7
2.2. Description of Nile basin in Ethiopia.....	8
2.2.1. Blue Nile river sub basin.....	8
2.2.2. Atbara river sub basin.....	8
2.3. Climate and water resources of the Nile basin.....	10
3. DATA AND METHODS.....	26
3.1. Data.....	26
3.2. Methodology.....	30
3.2.1. Evaluation of station time series.....	30
3.2.1.1. Missing data.....	30
A. Simple arithmetic averaging (AA).....	30
B. Closest station method (CSM).....	30
C. Estimation methods for replacing missing values in SPSS.....	30
3.2.1.2. Quality control.....	32
3.2.1.3. Control charts.....	32
3.2.1.4. Homogeneity test for temperature.....	33
3.2.1.5. Homogeneity test for rainfall.....	35
3.2.2. Trend analysis of temperature and precipitation.....	36
3.2.2.1. The least squares method.....	37

3.2.2.2. Quadratic trends.....	37
3.2.2.3. Cubic trends.....	38
3.2.2.4. Exponential trends.....	38
3.2.3. Mann-Kendall test for trend detection.....	39
3.2.4. Low pass filter.....	41
3.2.5. The Correlation coefficient.....	42
3.2.6. Computer-used programs.....	43
3.2.7. Time series analysis.....	44
3.2.8. Sample size	44
3.2.9. Time Series components and decomposition.....	45
3.2.10. Moving averages and exponential smoothing methods.....	46
3.2.10.1. Simple moving averages.....	46
3.2.10.2. Double moving averages.....	46
3.2.11. Stationary of a TS process.....	47
3.2.12. Autocorrelation functions.....	47
3.2.12.1. Autocorrelation.....	47
3.2.12.2. Partial autocorrelation.....	48
3.2.12.3. Autocorrelation function (ACF) and partial autocorrelation function (PACF).....	48
3.2.13. ARIMA modeling.....	48
3.2.14. Seasonal ARIMA modeling.....	49
3.2.15. The Art of ARIMA model building.....	50
A. Identification.....	50
B. Estimation.....	51
C. Diagnostics.....	51
3.2.16. Assessment of forecast performance.....	53
A. Mean forecast error.....	53
B. Mean absolute deviation.....	53
C. Mean absolute percentage error.....	53
D. Mean squared error.....	53

4. RESULTS AND DISCUSSIONS.....	54
4.1. Missing data.....	54
4.2. Quality control.....	58
4.3. Control chart.....	63
4.4. Homogenization of long-term climatological series.....	77
4.5. Results of statistical analysis for maximum temperature.....	79
4.6. The skewness coefficient for maximum temperature.....	80
4.7. Maximal value and minimal value for maximum temperature.....	80
4.8. Test of normality for maximum temperature.....	81
4.9. Linear regression model for maximum temperature.....	81
4.10. R-Square for maximum temperature.....	83
4.11. Results of statistical analysis for minimum temperature.....	92
4.12. The skewness coefficient for minimum temperature.....	92
4.13. Maximal value and minimal value for minimum temperature.....	93
4.14. Test of normality for minimum temperature.....	93
4.15. Linear regression model for minimum temperature.....	93
4.16. R-Square for minimum temperature.....	94
4.17. Results of statistical analysis for annual rainfall.....	103
4.18. The skewness coefficient for annual rainfall.....	103
4.19. Maximal value and minimal value for annual rainfall.....	104
4.20. Test of normality for annual rainfall.....	104
4.21. Linear regression model for annual rainfall.....	104
4.22. R-Square for annual rainfall.....	105
4.23. Ethiopia climate.....	115
4.24. Seasonal classifications in Ethiopia.....	123
4.25. Rainfall regimes in Ethiopia.....	129
4.25.1. Local and regional factors affecting rainfall in Ethiopia.....	129
A. Topographic variation.....	129
B. Regional weather features affecting the climate system in Ethiopia...	130
4.26. Comparing linear, quadratic, cubic and exponential equations.....	134

4.27. Trends of Mann-Kendall test.....	156
4.28. Time series analyses.....	160
4.28.1. Study area and rainfall data.....	160
4.28.2. Box-Jenkins ARIMA model.....	161
4.28.3. Results and discussion of time series.....	163
4.29. Future climate change over Ethiopia.....	195
4.30. Trend analysis of the Nile Basin.....	206
5. CONCLUSIONS.....	215
6. RECOMMENDATIONS.....	218
7. REFERENCES.....	219
8. ARABIC SUMMERY.....	-

CODESRIA - LIBRARY

list of tables

Page

Table (1):	River regulation in Ethiopia.	9
Table (2):	A summary of climate change studies on the Nile River, type of study and main findings.	14
Table (3):	Selected weather stations of Ethiopia and their general geographic information.	28
Table (4):	Percentage of missing values for each station.	56
Table (5):	Comparisons between the different methods for finding missing data.	57
Table (6):	The results of quality control (QC) for maximum temperature.	60
Table (7):	The results of quality control (QC) for minimum temperature.	61
Table (8):	The results of quality control (QC) for rainfall.	62
Table (9):	Upper and lower control limit of mean annual maximum temperature.	64
Table (10):	Upper and lower control limit of mean annual minimum temperature.	65
Table (11):	Upper and lower control limit of annual rainfall (mm).	66
Table (12):	Statistical characteristics for mean annual maximum temperature.	85
Table (13):	Coefficient of skew and kurtosis for mean annual maximum temperature.	86
Table (14):	Statistical characteristics of mean annual maximum temperature as regarding (maximum, minimum value, 1st Q (25%), Median and 3rd Q (75%).	87
Table (15):	Statistical characteristics of mean annual maximum temperature as regarding (Normal distribution and linear regression model).	88
Table (16):	Accuracy measures of mean annual maximum temperature	89
Table (17):	Statistical characteristics for mean annual minimum temperature.	95
Table (18):	Coefficient of skew and kurtosis for mean annual minimum temperature.	96

Table (19):	Statistical characteristics of mean annual minimum temperature as regarding (maximum, minimum value, 1st Q (25%), Median and 3rd Q (75%).	97
Table (20):	Statistical characteristics of mean annual minimum temperature as regarding (normal distribution and linear regression model).	98
Table (21):	Accuracy measures of mean annual minimum temperature.	100
Table (22):	Statistical characteristics for total annual precipitation.	106
Table (23):	Coefficient of skew and kurtosis for total annual precipitation.	107
Table (24):	Statistical characteristics of total annual precipitation as regarding (maximum, minimum value, 1st Q (25%), Median and 3rd Q (75%).	108
Table (25):	Statistical characteristics of total annual precipitation as regarding (normal distribution and linear regression model).	109
Table (26):	Accuracy measures of total annual rainfall.	111
Table (27):	Mean monthly temperature for study period.	118
Table (28):	Mean monthly precipitation for study period.	119
Table (29):	Descriptive statistical of mean monthly temperature.	120
Table (30):	Seasonal classifications in Ethiopia.	125
Table (31):	Comparison between trend equations for mean annual maximum temperature.	139
Table (32):	Comparison between trend equations for mean annual minimum temperature.	144
Table (33):	Comparison between trend equations for total annual rainfall	149
Table (34):	Mean annual maximum temperature trends, Mann –Kendall test for long period 1950-2005.	157
Table (35):	Mean annual minimum temperature trends, Mann –Kendall test for long period 1950-2005.	158
Table (36):	Annual rainfall trends, Mann –Kendall test for long period 1950-2005.	159
Table (37):	Autocorrelation, partial autocorrelation, stander error and Box-Ljung statistic of rainfall (mm) for Addis Ababa station.	169
Table (38):	Autocorrelation, partial autocorrelation, stander error and	170

	Box-Ljung statistic of rainfall (mm) for Bahar Dar station.	
Table (39):	Autocorrelation, partial autocorrelation, stander error and Box-Ljung statistic of rainfall (mm) for Nekemte station.	171
Table (40):	Autocorrelation, partial autocorrelation, stander error and Box-Ljung statistic of rainfall (mm) for Debra Markos station.	172
Table (41):	Model type, model fit statistics and Ljung-Box of rainfall (mm) for Addis Ababa station.	173
Table (42):	Model type, model fit statistics and Ljung-Box of rainfall (mm) for Bahir Dar station.	173
Table (43):	Model type, model fit statistics and Ljung-Box of rainfall (mm) for Nekemte station.	174
Table (44):	Model type, model fit statistics and Ljung-Box of rainfall (mm) for Debra Markos station.	174
Table (45):	Step trend analyses.	211

CODESRIA - LIBRARY

List of figures

	<i>Page</i>
Figure (1): Distributions of elevation over Nile river basin.	6
Figure (2): Nile River Basin in Ethiopia.	9
Figure (3): Distributions of precipitation over Nile river basin.	13
Figure (4): Location of climatic stations under study in Ethiopia.	29
Figure (5): Comparisons between the different methods for finding missing data.	57
Figure (6): Control chart of mean annual maximum temperature.	67
Figure (7): Control chart of mean annual minimum temperature.	70
Figure (8): Control chart of annual total rainfall.	73
Figure (9): Trend of mean annual maximum temperature.	90
Figure (10): Trend of mean annual minimum temperature.	101
Figure (11): Trend of annual total precipitation.	112
Figure (12): Mean monthly temperature and precipitation for study period.	121
Figure (13): Temperature and rainfall in the Ethiopia seasons.	126
Figure (14): Map of Ethiopia showing rainfall regimes A, B, B1 and C.	131
Figure (15): Mean monthly rainfall distribution for Central and Eastern Ethiopia (Region A).	132
Figure (16): The same as figure (15), but for the western Ethiopia (Region B1).	132
Figure (17): The same as figure (15), but for north-western Ethiopia (Region B).	133
Figure (18): The same as figure (15), but for Southern and South-eastern Ethiopia (Region C).	133
Figure (19): Map of Ethiopia shows the meteorological stations; Bahar Dar, Nekemte, Debre Markos and Addis Ababa.	175
Figure (20): Outline of Box-Jenkins (1976) model.	175
Figure (21): Monthly rainfall data for Addis Ababa station for the	176

period (1900-2005).

Figure (22):	Autocorrelation function of rainfall (mm) for Addis Ababa station.	176
Figure (23):	Partial autocorrelation function of rainfall (mm) for Addis Ababa station.	177
Figure (24):	Autocorrelation and partial autocorrelation function of rainfall (mm) for Addis Ababa station.	177
Figure (25):	Residual plots of Addis Ababa ARIMA model $(0,0,1) \times (0,1,1)I_2$.	178
Figure (26):	Trend of monthly rainfall for Addis Ababa.	179
Figure (27):	Actual and forecasting Addis Ababa rainfall for the year 2005.	180
Figure (28):	Comparison between actual and forecast period according to mean monthly rainfall (mm) for Addis Ababa station.	180
Figure (29):	Observed and forecasted Ethiopian rainfall for Addis Ababa station.	181
Figure (30):	Time series plot of Bahar Dar station.	181
Figure (31):	Autocorrelation function of rainfall (mm) for Bahar Dar station.	182
Figure (32):	Partial autocorrelation function of rainfall (mm) for Bahar Dar station.	182
Figure (33):	Autocorrelation and partial autocorrelation function of rainfall (mm) for Bahar Dar station.	183
Figure (34):	Residual plots of Bahar Dar ARIMA model $(0,0,0) \times (1,1,1)I_2$.	183
Figure (35):	Trend of monthly rainfall for Bahir Dar.	184
Figure (36):	Actual and forecasting Bahar Dar rainfall for the year 2005.	185
Figure (37):	Comparison between actual and forecast period according to mean monthly rainfall (mm) for Bahar Dar station.	185
Figure (38):	Observed and forecasted Ethiopian rainfall for Bahar Dar station.	186
Figure (39):	Time series plot of Nekemte station.	186

Figure (40):	Autocorrelation function of rainfall (mm) for Nekemte station.	187
Figure (41):	Partial autocorrelation function of rainfall (mm) for Nekemte station.	187
Figure (42):	Autocorrelation and partial autocorrelation function of rainfall (mm) for Nekemte station.	188
Figure (43):	Residual plots of Nekemte ARIMA model $(0,0,0) \times (1,1,1)_{12}$.	188
Figure (44):	Trend of monthly rainfall for Addis Ababa Nekemte.	189
Figure (45):	Actual and forecasting Nekemte rainfall for the year 2005.	190
Figure (46):	Comparison between actual and forecast period according to mean monthly rainfall (mm) for Nekemte station.	190
Figure (47):	Observed and forecasted Ethiopian rainfall for Nekemte station.	191
Figure (48):	Autocorrelation and partial autocorrelation function of rainfall (mm) for Debra Markos station.	191
Figure (49):	Residual plots of Debra Markos ARIMA model $(0,0,0) \times (0,1,1)_{12}$.	192
Figure (50):	Trend of monthly rainfall for Debra Markos.	193
Figure (51):	Actual and forecasting Debra Markos rainfall for the year 2005.	194
Figure (52):	Comparison between actual and forecast period according to mean monthly rainfall (mm) for Debra Markos station.	194
Figure (53):	Actual and forecasted mean annual maximum temperature for Addis Ababa.	199
Figure (54):	Actual and forecasted mean annual maximum temperature for Arbaminch.	199
Figure (55):	Actual and forecasted mean annual maximum temperature for Assosa.	200
Figure (56):	Actual and forecasted mean annual maximum temperature for Gondar.	200
Figure (57):	Actual and forecasted mean annual maximum temperature for Jijiga.	201

Figure (58):	Actual and forecasted mean annual minimum temperature for Addis Ababa.	201
Figure (59):	Actual and forecasted mean annual minimum temperature for Arbaminch.	202
Figure (60):	Actual and forecasted mean annual minimum temperature for Assosa.	202
Figure (61):	Actual and forecasted mean annual minimum temperature for Gondar.	203
Figure (62):	Actual and forecasted mean annual minimum temperature for Jijiga.	203
Figure (63):	Actual and forecasted annual precipitation for Addis Ababa.	204
Figure (64):	Actual and forecasted annual precipitation for Bahir Dar.	204
Figure (65):	Actual and forecasted annual precipitation for Debremarkos.	205
Figure (66):	Actual and forecasted annual precipitation for Nekemte.	205
Figure (67):	Annual precipitation forecast for four stations (Addis Ababa, Bahir Dar, Debremarkos and Nekemte).	206
Figure (68):	Location of Nile river flow station.	212
Figure (69):	Observed discharge data for El Diem, Khartoum, Malakal, Dongola and Aswan.	213
Figure (70):	Step trends for: El Diem, Khartoum, Malakal, Dongola and Aswan stations.	214

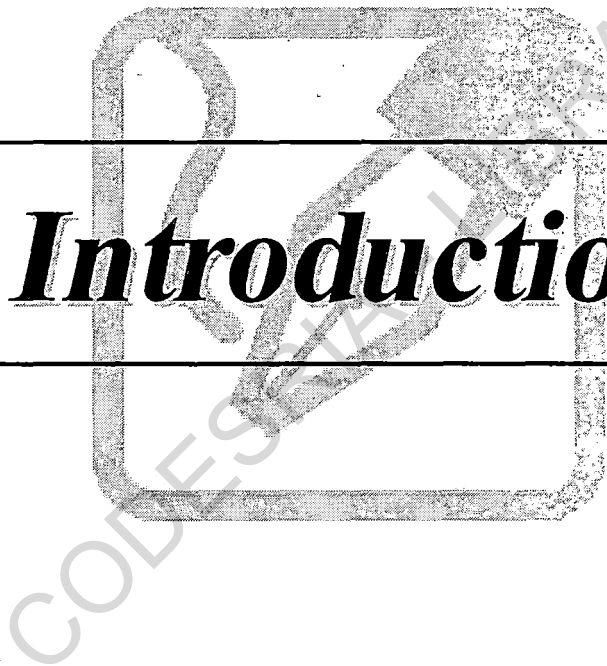
List of Abbreviations

(K-S)	Kolmogorov–Smirnov test
(p,d,q)	The order of the autoregressive, integrated, and moving average
AA	Arithmetic averaging
ACF	Autocorrelation function
AIC	Akaike Information Criteria
ANOVA	Analysis of variation
CSM	Closest station method
CV	Coefficient of variance
DF	Degree of freedom
ENMA	Ethiopia National Meteorological Agency
ENSO	El Niño southern oscillation
FAO	Food and agriculture organization
GCM	General circulation model
GCOS	Global Climate Observing System
GHCN	Global historical climate network
GIS	Geographic information system
GW	Global warming
IPCC	Intergovernmental panel on climate change
IQR	Interquartile range
ITCZ	Inter-tropical convergence zones
Km	Kilometer
ARIMA	Autoregressive integrated moving average
MAD	Mean absolute deviation
MAE	Mean absolute error
MAF	Mean Annual Flows
MFE	Mean forecast error
MSE	Mean squared error

MV	Mean value
°C	Celsius degree
PACF	Partial autocorrelation function
QC	Quality control
RMSE	Root-mean-square error
RSCZ	Red Sea convergence zone
SD	Standard deviation
SL	Significance level
SOI	Southern oscillation index
SPSS	Statistical Package for the Social Sciences
SST	Sea surface temperature
SWAT	Soil and Water Assessment Tool
TS	Time series
UCL and LCL	Upper and lower control limit
UNEP	United nations environment program
WMO	World meteorological organization



Introduction



INTRODUCTION

The climate of Africa is both varied and varying. Varied, because climate ranges from humid equatorial to seasonally arid and sub-tropical Mediterranean and varying because all these climates exhibit differing degrees of temporal and spatial variability. At the sub-regional scale, Africa is vulnerable to ENSO and related extreme events (Drought, floods, and changes in hydrologic patterns) (*Hulme, et al., 2001; Tsonis, et al., 2003*). That portion of sub-Saharan Africa that depends entirely on the Nile River for its water supply is particularly susceptible to hydrologic changes that might be associated with a warmer climate. Flooding and droughts will be increasingly difficult to cope with in the face of increasing pressures on water supplies due to rapid population growth and dwindling resources (*Beyene, et al., 2007*).

Current studies into the potential impacts of climate change remain largely uninformative to policy and decision makers in the water resources sector. Alarming trends in temperature and the potential for redistribution of fresh water has understandably led to concerns for the future availability of water resources (*Conway and Hulme, 1993*). Although some projections suggest that significant climate change may occur over the same scales as water resources development and management, policy makers continue to rely heavily on the assumption that historical conditions will persist into the future. This is largely due to a lack of integrative tools with realism to tie climate to hydrology to water resources and yield meaningful information for decision makers (*Conway and Hulme 1996; Conway, et al., 2008*).

Climate change impact assessments begin with developing scenarios of future climate. Typically, historical records of temperature and

precipitation are adjusted according to some specified change, often based on the output of general circulation models (GCMs). The adjusted climate, or climate scenario, is then used to drive hydrologic models in the area of interest. Finally, the resulting hydrologic sequences are analyzed with respect to a baseline. Many of these studies are inconclusive due to conflicting trends across a number of climate scenarios, often showing potentially large runoff increases in some scenarios and significant drying in others. Thus previous climate and hydrologic scenarios tended to be most informative as aides to sensitivity studies rather than true impact projections (*IPCC, 2007; Beyene, et al., 2007*).

During the 20th century, the amount of greenhouse gases in the atmosphere has increased, largely as a result of the burning of fossil fuels for energy and transportation, and land use changes. Global warming is now considered most probably to be due to the man-made increases in greenhouse gas emissions. Whilst other natural causes of climate change, including changes in the amount of energy coming from the sun and shifting patterns of ocean circulation, can cause global climate to change over similar periods of time, the balance of evidence now indicates that there is a discernible human influence on the global climate (*IPCC, 2008*).

Observational records and climate projections provide abundant evidence that freshwater resources are vulnerable and have the potential to be strongly impacted by climate change, with wide-ranging consequences for human societies and ecosystems (*Conway, et al., 2008; IPCC, 2008*).

Water is one of several current and future critical issues facing Africa. Water supplies from rivers, lakes and rainfall are characterised by their unequal natural geographical distribution and accessibility, and

unsustainable water use. Climate change has the potential to impose additional pressures on water availability and accessibility (*Amy, 2006; Conway, et al., 2008*). *Arnell, (2004)* described the implications of the IPCC's SRES scenarios for a river-runoff projection for 2050 using the HadCM320 climate model. These experiments indicate a significant decrease in runoff in the north and south of Africa, while the runoff in eastern Africa and parts of semi-arid sub-Saharan Africa is projected to increase. However, multi-model results show considerable variation among models, with the decrease in northern Africa and the increase in eastern Africa emerging as the most robust responses. There is a wide spread in projections of precipitation in sub-Saharan Africa, with some models projecting increases and others decreases (*IPCC, 2008*).

The stream flow of rivers is a good indicator of climate variations, because it provides an integral measure of the precipitation over the source regions, if other conditions remain unchanged. The flood levels of the Nile river are one example of a long time series analysed by hydrologists, climatologists and historians in order to gain information about the evolution of the systems involved and their interactions, and also to estimate future conditions which, in climatological context, means that the possibility of recurring past events provides a measure of the expected variability (*Fraedrich and Bantzer, 1991*).

1.1. Problem Statement

At the outset it is important to have a good sense of the definition of the problem to be studied. In the recent years, the implications of global warming on water resources have attracted increasing attention. The impact of climate variability on water resources is so integrated into different sectors. The consistent conclusions of climate variability modeling exercises are that many of the world's major river basins may experience more severe droughts and floods in the coming decades.

1.2. Objective of the research

The major aim of this thesis was the study of the impact of climatic variability on hydrology and water resources of Nile River.

The second aim was reaching to suitable model for prediction of the impact of climatic variability on hydrology and water resources of Nile River in the future (Evaluation of future available water).



Review of Literatures

COLLEGE LIBRARY

REVIEW OF LITERATURES

2.1. The Nile river basin

2.1.1. Hydrology

The River Nile extends 6,700 kilometers through a drainage area equaling approximately 3 million km². The Nile Basin is shown in figure 1. Although the foregoing discussion of East African climate reveals that some of this area is subject to very high rainfall, the average annual runoff from the basin is merely 30 mm. This low runoff is in large part due to the majority of Nile flow originating from a relatively small fraction of the basin. The two primary runoff producing regions in the Nile Basin are the lake plateau of equatorial East Africa and the Ethiopian, or Abyssinian, plateau (*Amy, 2006; Meseret, 2009; Zelalem, et al., 2009*)

Figure (1) shows the elevation difference from Lake Victoria to Mediterranean Sea. The Nile Basin constitutes a unique diversified geographically, starting from the highlands in the south and its decrease until the hike up to the spacious plains in the far north. Therefore, the Nile River is the only river which flows from south to north and that according to earth's slope (*Arsano, 2007; Zelalem, et al., 2009*)

The total flow reaching the main Nile approximately 85 % stem from Ethiopian plateau and the rest from the equatorial Lakes plateau (Lake Victoria, Lake Kyogo, Lake Kwania, and Lake Albert) (*Arsano, 2007*).

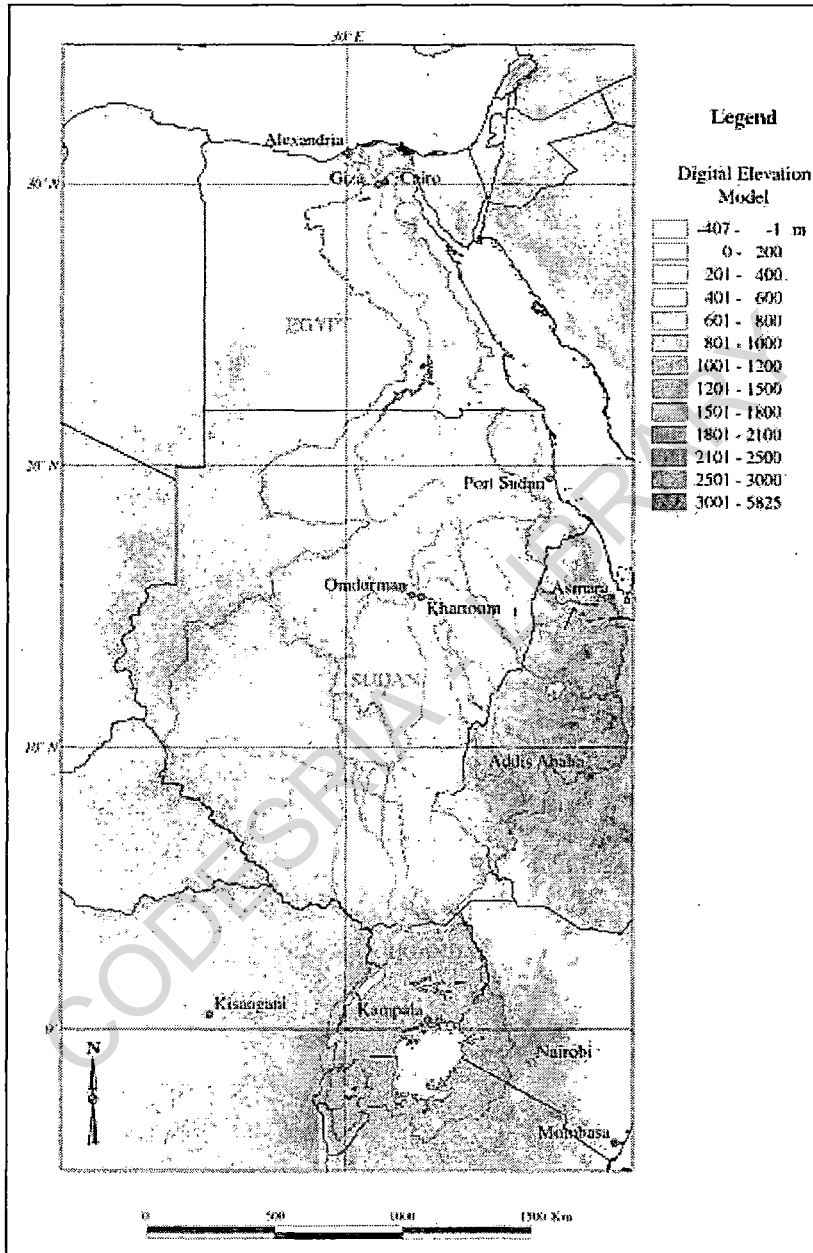


Figure (1): Distributions of elevation over Nile river basin.
 (<https://courseware.e-education.psu.edu/courses/earth105new/content/lesson>)

2.2. Description of Nile basin in Ethiopia

Nile basin of Ethiopia covers a total of about 358,889 km²-equivalent to 34% of the total geographic area of the country. Around 40% of the population of Ethiopia lives in this basin (*Meseret, 2009*) From south to north, the main river sub-basins flowing from the Ethiopian highlands into Sudan are the Baro-Akobo, the Abbay and the Tekeze. The sub-basins are illustrated in table (1) and figure (2) (*Amy, 2006*)

2.2.1. Blue Nile river sub basin

The Blue Nile River starts at the outlet of Lake Tana and flows to Khartoum where it meets the White Nile with basin area of 324,530 km². Blue Nile contributes about 60% of the flow of Main Nile (*Sutcliffe and Parks, 1999*) The topography of the Blue Nile composed of highlands, hills, valleys and occasional rock peaks. The average precipitation over the Blue Nile subbasin is 1394mm and is higher than the other subbasin of the Nile basin (Figure 2). The precipitation over the Blue Nile basin varies from 1000mm in the north-eastern part to 1450-2100mm over the south-western part of the sub basin (*Zelalem, et al., 2009*)

2.2.2. Atbara river sub basin

The Atbara River originates in the Northern Ethiopia and Eritrea and joins the Nile after the lowland in the eastern Sudan with total basin area of 112,400 km². The discharge of the river is extremely torrential. The rainfall is unimodal concentrated in August and September with mean annual rainfall 900 mm relatively high value over the Ethiopian highlands to less downstream at the confluence with the main Nile. Generally the average annual precipitation is lowest among the other Nile sub-basins (*Sutcliffe, and Parks, 1999*).

2.1.2. Ethiopian Nile basins

The White Nile is joined by three additional tributaries, the Sobat, Blue Nile, and Atbara Rivers, all of which have their origins in the Ethiopian plateau. The Sobat River joins the White Nile prior to Malakal, nearly doubling the flow from the Sudd. This basin is comprised of two distinct tributaries, the Baro (41,400 km²) and Pibor (109,000 km²) (*Amy, 2006*)

The Blue Nile basin adjoins the Sobat to the north and drains rugged terrain through deep canyons cut into the Ethiopian plateau. The river undergoes a steep 900 kilometer descent from its source in Lake Tana at 1,829 meters elevation to the Sudan plain at 490 m. The river continues to flow across the flat plain for another 800 km and intercepts two smaller rivers, Dinder and Rahad, bringing the total drainage area to 324,500 km² (*Shahin, 1985*). At Khartoum, the Blue and White Niles converge to form the Main Nile. 84% of the annual runoff in the Blue Nile basin occurs between June and October, resulting from heavy rains during the single rainy season. The Atbara River also flows from its headwaters in Ethiopia and has a drainage area of 112,400 km² (*Zelalem, et al., 2009*)

The Atbara shares many characteristics with the Blue Nile, though the upper portion of its basin has an even greater slope, the rainy season is shorter, and it does not have a large lake at its source. Consequently, the Atbara River is even more strongly seasonal than the Blue Nile, often receding to little or no flow in the dry season. From the mouth of the Atbara, the Nile continues its course through flat terrain within an arid climate towards Aswan, Egypt (*Shahin, 1985; Amy, 2006*)

Table (1): River regulation in Ethiopia

River	Capacity (m ³ *10 ⁶)	Catchment area (km ²)
Alwero (Baro-Akobo basin)	74	1043
Abbay	9000	15300
Finchaa (Abbay tributary)	900	2500
Koga (Tributary to L. Tana)	77	164
Tekeze	9293	30390

(Source: Moustafa, 2007)

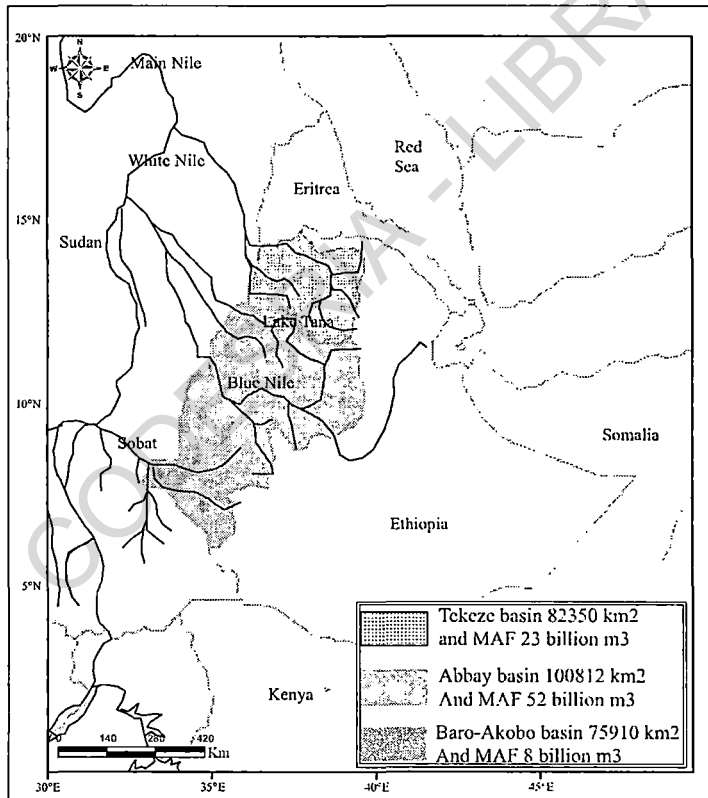


Figure (2): Nile River Basin in Ethiopia (Arsano, 2007)

2.3. Climate and water resources of the Nile basin

East African climate results from a complicated interplay of large scale atmospheric features such as monsoons and convergence zones, and highly heterogeneous local geographic features, such as steep topographic relief and large lakes. The region is influenced by two monsoons from the northeast and southeast of the continent, which in comparison to the Asian monsoons are relatively dry. In addition, westerly flow brings moist air from the Congo River Basin, which is associated with rainfall (*Amy, 2006*)

The monsoonal flows are separated by the Inter-Tropical Convergence Zone (ITCZ), while the Congo Air Boundary separates the westerly from the easterly flow. Largely due to topography, easterly flow predominates to the east of the East African highlands, while westerly flow is influential to the west, including the lake plateau region (*Zelalem, et al., 2009*).

Rainfall in East Africa is particularly variable and complex. Seasonal patterns range from a single rainy season to as many as three rainfall maxima, with average annual rainfall ranging from as much as 1800 mm in the mountains of Rwanda to less than 200 mm in the arid lowland regions of Sudan and Ethiopia (Figure 3). In the lake plateau, the extensive surface area of Lake Victoria itself strongly influences precipitation via the Lake Victoria Low (*Amy, 2006*)

The climate and vegetation cover in the Nile basin are highly related with the amount of precipitation. Precipitation increases southward and with altitude. The common area with high precipitation about 1200-1600mm/years on the highlands of Ethiopia and the Equatorial lakes plateaus. The potential evaporation over the basin increases as one move

downstream which show opposite trend to the precipitation (*Mohamed, et al., 2005*).

The climate of the Nile Basin is characterised by a strong latitudinal wetness gradient. Whereas the areas north of 18°N remain dry most of the year, to the south there is a gradual increase of monsoon precipitation amounts. Rainfall regimes can be divided into different types, among which summer peak regimes dominate. In the southern half of the basin, mesoscale circulation features and associated contrasts in local precipitation patterns develop as a result of a complex interplay involving topography, lakes and swamps. Precipitation changes and variability show up as 3 distinct modes of variability (*Camberlin 2009*). Drying trends since the 1950 are found in central Sudan and to some extent the Ethiopian Highlands. The equatorial lakes region is characterised by occasional very wet years (e.g. 1961, 1997). The interannual variations are strongly, but indirectly influenced by El-Nino / Southern Oscillation. Sea surface temperature variations over other ocean basins, especially the Indian and South Atlantic Oceans, also play a significant role (*Sutcliffe and Parks, 1999; Camberlin, 2009*)

Camberlin and Philippon, (2002) found that in the Ethiopian Highlands, the single rainy season is brought on with the passage of the ITCZ. Accordingly, the rainy season becomes progressively shorter in duration from south to north. In the southwestern portion of the highlands, the rains arrive around April-May and remain until as late as October. Near Lake Tana in the north, the rains do not materialize until June-July and remain through September. Temperature exhibits two annual minima and maxima. The onset of the summer rainy season acts to cool what would otherwise have been the warmest months of the year. Therefore,

temperatures begin to increase during the spring months, temporarily decrease during the rainy season, and again rise prior to the onset of fall (Amy, 2006)

CODESRIA - LIBRARY

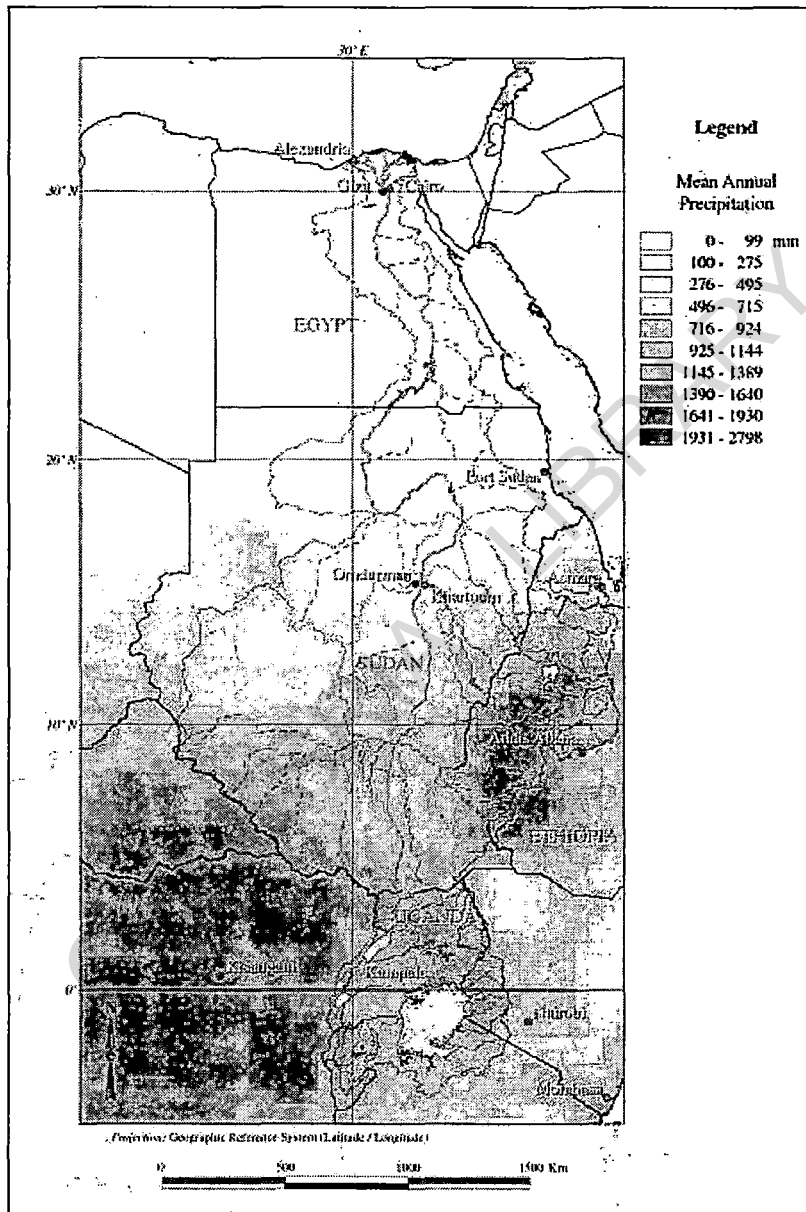


Figure (3): Distributions of precipitation over Nile river basin (https://www.google.com.eg/search?q=nile_precipitationb.gif).

Table (2): A summary of climate change studies on the Nile River, type of study and main findings

Authors	Type of study	Main results
<i>Gleick, (1991)</i>	Applied an annual water balance model to three subbasins of the Nile basin, the Upper White Nile, Sobat and Blue Nile/Atbara.	The model produced a 50% reduction in runoff in the Blue Nile catchment due to a 20% decrease in rainfall.
<i>Hulme, (1994)</i>	Review of future changes in temperature and rainfall based on GCM results for the Nile basin.	Qualitative discussion of their implications for Nile flows.
<i>Conwa, and Hulme, (1996)</i>	Used hydrologic models of the Blue Nile and Lake Victoria to assess impacts of future climate change on Nile flows. Sensitivity analysis of hypothetical changes in rainfall and evaporation, and a set of seven equilibrium GCM scenarios for 2025.	They obtained a range (due to differences between GCM scenarios) of -9% to +12% change in mean annual Nile flows for 2025. Results were used to estimate changes in the availability of Nile water in Egypt based on the Nile Waters Agreement.
<i>Nicholson, (1996)</i>	The correlation between sea surface temperatures in the tropical Atlantic and Indian Oceans and East African rainfall.	Suggest that spectral peaks around 5 years may be associated with similar peaks of sea surface temperatures in the

***Strzepek and
Yates (1996)***

Spatially aggregated monthly water balance model used to explore the sensitivity of Nile flows to climate change.

***Meigh, et al.,
(1998)***

Estimates of the possible changes in temperature, rainfall, evaporation and runoff for the decade of

tropical Atlantic and Indian Oceans, which may ultimately be the link between East African rainfall and the ENSO phenomena. Extremely high precipitation in an individual year can lead to dramatic changes in Lake Victoria or severe flooding below the Blue Nile. One such occurrence was observed in 1961/62 and was responsible for a profound 2.5 m increase in the level of Lake Victoria.

Divergence between climate model results for the Nile basin; from a sample of four models two produced increases and two produced decreases in flows.

The results showed fairly uniform increases in temperature of between 0.7

the 2020s as simulated by GCMs were compared to the reference period 1961-90.

and 1.0°C across the whole basin. Changes in rainfall were much more variable, generally increasing by between 0 and 19%, but with decreases in some areas. The expected changes in runoff are minor in most of the equatorial lakes basin, but quite substantial increases of 30% or even more were projected for some parts of the Ethiopian highlands and southern Sudan.

Five out of six climate models produced an increase in Nile flows at Aswan, with only one showing a small decrease.

Showed Blue Nile and Atbara flow are variable and declined in the 1970s and 1980s and Main Nile stations showed high flow up to 1990 and the variable

**Yates and
Strzepek
(1998)**

Follow-up study to *Strzepek and Yates, (1996)*

**Sutcliffe and
Parks, (1999)**

Blue Nile and Atbara flow

- Bayoumi, (2006)** Regional temperature trends
- Sene, (2000)** Investigated the influence of Lake Victoria on flows in the Upper White Nile using a model that represented the main river channel by a series of interconnected lakes and swamps.
- Conway, (2000)** Studied the spatial and temporal characteristics of climate in the region of central Ethiopia that
- flows until 1970 and low flow since 1970.
- Reveals an average increase in temperature over the basin by 2-4.3°C by the 2050 predicted by the different experiments. Temperature changes are not uniform over the basin, with higher temperature rises in the more arid regions of Northern Sudan and most of Egypt and lower rises around the equator.
- The results indicated extreme sensitivity of White Nile flows to changes in Lake Victoria levels and outflows, in particular to variations in direct rainfall on the lake surface.
- He indicated that rainfall is highly seasonal with roughly 70% of the annual

- comprises the upper Blue Nile basin by constructing a 99-year basin-wide area average time series of rainfall (1900-1998) from 11 gauges each with over 25 years length of record.
- IPCC, (2001)* Regional temperature trends
- rainfall occurring between June and September. He also showed that annual rainfall generally declines from over 2000 millimeters in the south-west to less than 1000 millimeters in the north-east.
- Trends for grid boxes located in Sudan and Ethiopia in the order of +0.2-0.3°C/decade (+0.2) from 1946 to 1975. Their overall conclusion from all methods is that climate change may lead to a slight increase in White Nile flows; and climate change scenarios for the Nile are dependent not only on the input climate and hydrological data and climate change scenarios, but also on the type of model used and its formulation.
- Sene, et al., (2001)* Used different modeling studies to model climate change impacts on the White Nile, and showed a very rough indication of the likely magnitude of those impacts.
- Strzpek et al., (2001)* Impacts – they used a sample population of
- A propensity for lower Nile flows (in 8

climate change scenarios for the basin that incorporate uncertainties due to differences between climate models, climate sensitivity estimates, and emission pathways. They selected nine representative scenarios from the full range to produce Nile flow scenarios using a suite of water balance models.

*Tate, et al.,
(2004)*

Analyzed the sensitivity of the water balance of Lake Victoria to climate change using HadCM3 A2a and B2 emission scenarios.

*Conway,
(2005)*

The effects of climate variability in the Ethiopian Highlands and Lake Victoria.

out of 8 scenarios). The wet scenario only produced moderate increases from the 2040 onwards, whilst 3 (4) of the flow scenarios produce large and rapid changes in flows of the order of 40–50% (20–40%) reductions in flow by 2025 (2020) and over 60% (Roughly 30–60%) by 2050.

Indicated that changes in annual rainfall and evaporation derived from HadCM3 implied that declines in water levels would occur during the 2021–2050 time horizon. This contrasted with projected increases in water levels later in the century (2070–2099).

The effects of climate variability in the Ethiopian Highlands and Lake Victoria

- Beyene, et al.,**
(2007) Runoff of all the tributaries of the Blue Nile are in the highlands of Ethiopia
- Kim, et al.,**
(2008) Evaluated the impacts of climate change on both hydrologic regimes and water resources of the

are shown to have caused significant interannual and interdecadal variability in the Nile River flows. He noted that, although there is low convergence among GCM simulations of rainfall, climate scenarios of rising temperatures are more consistent and could lead to large increases in evaporation because of the large expanses of open water and irrigated agriculture in the Nile River basin.

All the tributaries of the Blue Nile are in the highlands of Ethiopia, and the bulk of their runoff (70% on average) occurs between July and September.

They suggested that the climate in most of the upper Blue Nile River basin is

upper Blue Nile basin in Ethiopia using the outcomes of multiple general circulation models (GCMs) to perturb the baseline climate scenario representing the current temperature and precipitation patterns. They used a two-tank hydrologic model.

**Setegn, et al.,
(2008)**

Used Soil and Water Assessment Tool (SWAT) for hydrological modeling in the Tana basin, which is a subcatchment of the Blue Nile, Ethiopia.

**Elshamy, et al.,
(2009)**

Analyzed the output of 17 general circulation models (GCMs) included in the 4th IPCC assessment report (IPCC, 2007) for the period of 2081-2098 for the upper Blue Nile basin.

likely to become wetter and warmer in the 2050 (2040-2069), and mid-to-long term droughts are likely to become less frequent in the entire basin although uncertain with the accuracy of GCMs and limited data availability for the hydrologic model.

They found that the SWAT model can be used to investigate the impacts of various land use/cover, climate and management scenarios on the water resources of the catchment.

They concluded that there is no consensus among the GCMs on the direction of precipitation change. They found that changes in annual precipitation range between -15% to

+14% but more models reported reductions (10) than those reporting increases (7), though the ensemble mean of all models showed almost no change in the annual total rainfall. They noted that all models predict the temperature to increase between 2°C and 5°C and consequently the potential evapotranspiration to increase by 2-14% although uncertainties in the direction of precipitation.

**Mulugeta,
(2009)**

This study mainly deals with evaluation of the climate change impact on the Gilgel Abay reservoir which is found in Upper Blue Nile Basin, using the reliability, resilience and vulnerability indices (RRV-criteria). Projection of the future climate variables is done by using General

The performance of the model was assessed through calibration and validation process and resulted $R^2=0.82$ during calibration and $R^2=0.8$ during validation. The projected future climate variable shows an increasing trend for both maximum and minimum

Circulation Model (GCM) which is considered as the most advanced tool for estimating the future climatic condition.

temperature however, for the case precipitation it doesn't manifest a systematic increase or decreasing trend in the next century. The evaporation from the open water surface of reservoir reveals an average annual increase by 2.1 % when the projected average annual temperature and precipitation increases from the baseline period by an amount of 0.53°C and 0.82 % respectively in 2020 under the A2a emission scenario, when the average annual temperature is rise by 1.15 °C and the precipitation increase by 0.85 % in 2050 with A2a emission scenario, the reservoir open water evaporation will expected to increase by 6 %, while in the time horizon of 2080, the precipitation shows an increase

amount by 1.6 % and the temperature rise 1.97°C consequently the open water evaporation is expected to rise by 22 % for the same A2a emission scenario.

Lake Tana's flow system is governed by four main components: the inflow from surrounding river catchments into the lake, the outflow at Bahir Dar through the Blue Nile, the direct rainfall on the lake and the direct evaporation from the lake. While recent studies applied simple pragmatic approaches to estimate runoff from ungauged catchments, here emphasis is placed on more advanced approaches based on regionalization and spatial proximity principles. rainfall-runoff modelling of gauged catchments are transferred to ungauged catchments to allow runoff simulation. Lake areal rainfall is estimated by interpolation of

Wale, (2009)

Results show that runoff from ungauged catchments is around 880 mm per year for the simulation period 1995–2001 with a water balance closure error of 5%. In addition, use is made of river and lake water chemistry to arrive at an estimate of the unknown inflow and outflow components through the mixing cell approach. The results obtained with this method also provide independent information with regard to the errors in the individual water balance components.

the rain gauges around the lake, open water evaporation is estimated by the Penman-combination equation while observed inflows and outflow data are directly used in the lake water balance.

The water balance closure term was established by comparing the measured lake levels with the calculated levels.

CODESRIA - LIBRARY



Data and Methods

DATA AND METHODS

3.1. Data

In order to investigate climatic variability on Nile River water resources and its flood fluctuations, our attention fixed to variability of meteorological elements due to global or regional changes. Twenty-six stations covering different parts of Ethiopia have been chosen to study the variability of their data sets. The specifications of stations are listed in (Table 3 and Figure 4).

The climate data are consisted of mean monthly and annual records of temperature (minimum and maximum), precipitation. Annual means are the means of all 12 months from a respective year; seasonal classification of the region, especially over Ethiopia, is from February to May, June to September and October to January called Belg, Kiremt and Bega, respectively.

The main data used in the present study were assembled from several sources:

1. The Global Historical Climate Network Dataset (GHCN). GHCN reports data by year and month. Monthly means were calculated for the 1950–2000 period. GHCN has data for precipitation, mean temperature, and minimum and maximum temperatures.
2. World weather records (volume 1-2-3-5). Data for periods 1951-1960, 1961-1970, 1971-1980 and 1981-1990 (*National climatic data center*). These records are of monthly mean values of station pressure, sea level pressure, temperature, and monthly precipitation for stations listed in previous volumes. In addition to these parameters, mean monthly

maximum and minimum temperature have been collected for many stations and are archived in digital files by the national climatic data center, USA. New stations have been included.

3. Some climate information used in this study is represented by original data; the required data has been extracted from the reports of Ethiopia Meteorological Authority, Addis Ababa, Ethiopia.

4. Stream flow gauging stations were selected at points controlling the major area of the catchments. Monthly mean stream flow observations at five hydrological stations situated in the Nile were used: Aswan, Khartoum, Malakal, Eddim and Dongola. The stream flow data set for the Nile has been supplied by the Ministry of Water Resources and Irrigation of Egypt.

Table (3): Selected weather stations of Ethiopia and their general geographic information.

	Number of WMO	Station	Longitude (E)	Latitude (N)	Altitude (m)
1	63450	Addis Ababa	38.7	9.03	2408
2	63500	Arba Minch	37.55	6.05	1219
3	63043	Assosa	34.52	10.07	1560
4	63453	Awash	40.18	10.09	1052
5	63460	Awassa	39.48	7.08	1700
6	63332	Bahar Dar	37.42	11.06	1770
7		Bati	40.02	11.2	-
8	63333	Kombolcha	39.73	11.12	1916
9	63334	Debre Markos	37.67	10.33	2515
10		Debre Zeit	38.95	8.73	1900
11		Dessie	39.63	11.12	2460
12	63471	Diredawa	41.51	9.36	1260
13		Gambela	34.52	8.25	450
14	63402	Jima	36.43	7.47	1676
15		Gode	44.58	5.9	-
16	63331	Gondar	37.04	12.05	2004
17	63403	Gore	35.53	8.15	2002
18	63451	Harar	42.01	9.18	2100
19	63473	Jijiga	42.47	9.02	1775
20	63330	Mekele	39.05	13.05	2212
21	63453	Metehara	39.92	8.86	1062
22	63533	Negele	39.57	5.33	1544
23		Nekemte	36.45	9.08	2080
24		Robe	40.3	7.08	2450
25		Sibu Sire	36.09	9	1750
26		Wonji	39.25	8.48	1540

(Source: Ethiopia Meteorological Authority)

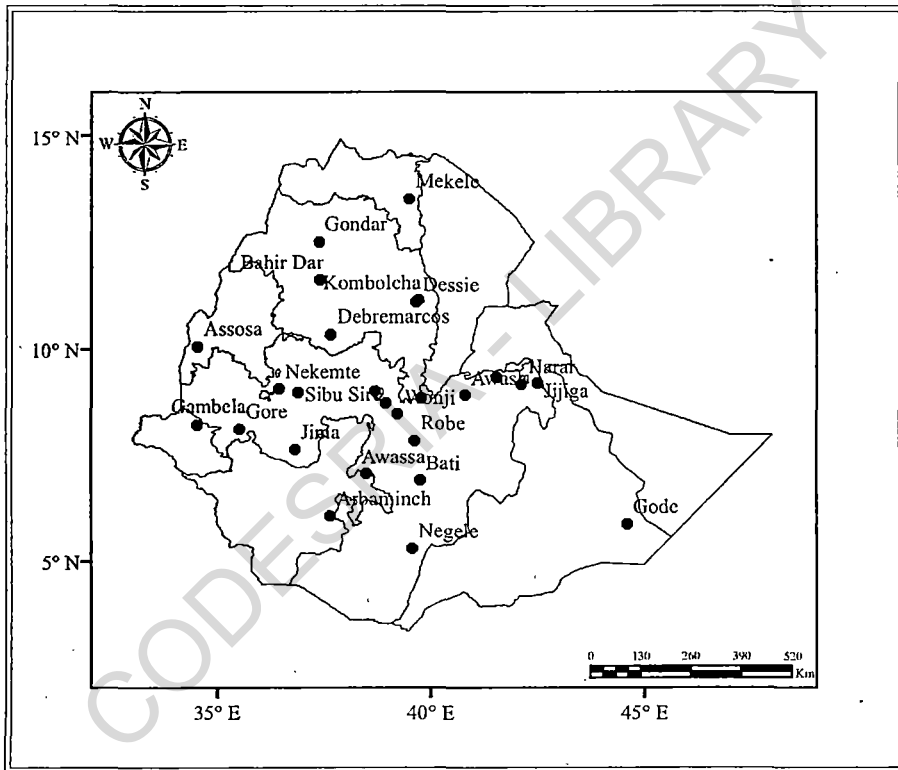


Figure (4): Location of climatic stations used in this study in Ethiopia.

(Source: Ethiopia Meteorological Authority)

3.2. Methodology

The following statistical approaches were used in the present study. Different statistical methods could be applied to study the basic properties of the time series, temperature variations and amount rainfall variations.

3.2.1. Evaluation of station time series

3.2.1.1. Missing data

The best methods of estimating missing data are in general depend upon the statistical properties of the data. In climatology, the most important factors are the inter-correlations in the station network and the seasonal variations in the relations between the stations. The following methods for estimating missing data are used in this study (*Xia, et al., 1999*).

A. Simple arithmetic averaging (AA)

This is the simplest method which is commonly used to fill the missing meteorological data in meteorology and climatology. The missing data are obtained by arithmetically averaging data of the five closest weather stations around a station (Which had missing data) (*Kemp, et al., 1983*).

B. Closest station method (CSM)

The closest station was identified, the missing data were estimated from the data of the closest station, and were adjusted by the ratio of the long-term means for that month. The method will be used for precipitation only (*Xia, et al., 1999*).

C. Estimation methods for replacing missing values in SPSS:

- **Series mean** replaces missing values with the mean for the entire series.
- **Mean of nearby points (moving average)** replaces missing values with the mean of valid surrounding values. The span of nearby points

is the number of valid values above and below the missing value used to compute the mean.

- **Median of nearby points** replaces missing values with the median of valid surrounding values. The span of nearby points is the number of valid values above and below the missing value used to compute the median.
- **Linear interpolation** replaces missing values using a linear interpolation. The last valid value before the missing value and the first valid value after the missing value are used for the interpolation. If the first or last case in the series has a missing value, the missing value is not replaced.
- **Interpolation** is a method used to determine a present or future value factor when the exact factor does not appear in either a present or future value table. Interpolation assumes that the change between two values is linear and that the margin of error is insignificant (*IBM, 2010*).

Linear interpolation involves estimating a new value by connecting two adjacent known values with a straight line.

If the two known values are (x_1, y_1) and (x_3, y_3) , then the y_2 value for some point x_2 is:

$$Y_2 = \frac{y_1 + (x_2 - x_1)(y_3 - y_1)}{(x_3 - x_1)}$$

Note: Linear interpolation works best when the function is not changing quickly between known values (*Paulhus and Kohler, 1952*).

- **Linear trend at point** replaces missing values with the linear trend for that point. The existing series is regressed on an index variable

scaled 1 to n . Missing values are replaced with their predicted values (*Tronci, et al., 1986*)

3.2.1.2. Quality control

The identification of outliers has been the primary emphasis of quality control work (*Mert, 2005*). Outliers are values greater than a threshold value specific for each time series, defined by

$$P_{\text{out}} = q_{0.75} + 3IQR$$

Where $q_{0.75}$ is the third quartile and IQR is the interquartile range. In order to reduce the size of distribution tails and make a safer use of the nonresistant homogeneity testing methods used later, also to keep the information from extreme events, outlier values of each annual precipitation series were replaced by the unique P_{out} value (*Mert, 2005*).

3.2.1.3. Control charts

A control chart provides a basis for deciding whether the variation in the output is due to common causes (in control) or assignable causes (out of control). Whenever an out-of-control situation is detected, adjustments and/or other corrective action will be taken to bring the process back into control (*Aguilar, et al., 2004*)

Control charts can be classified by the type of data they contain. An \bar{Y} chart is used if the quality of the output is measured in terms of a variable such as length, weight, temperature, and so on. In that case, the decision to continue or to adjust the production process will be based on the mean value found in a sample of the output. To introduce some of the concepts common to all control charts, let us consider some specific features of an \bar{Y} chart.

The two lines labeled UCL and LCL are important in determining whether the process is in control or out of control. The lines are called the

upper control limit and the lower control limit, respectively. They are chosen so that when the process is in control, there will be a high probability that the value of \bar{Y} will be between the two control limits. Values outside the control limits provide strong statistical evidence that the process is out of control and corrective action should be taken (Aguilar, et al., 2004)

Control Limits for an \bar{Y} Chart: Process mean and standard deviation known.

$$UCL = \mu + 3\alpha$$

$$LCL = \mu - 3\alpha$$

μ : mean and α : standard error

3.2.1.4. Homogeneity test for temperature

Climate data can provide a great deal of information about the atmospheric environment that affects almost all aspects of human life. To be accurate, the climate data used for long-term climate analyses, particularly climate change analyses, must be homogeneous.

A homogeneous climate time series defined as one where variations caused only by variations in weather and climate. Inhomogeneities in station data records are often caused by changes in observational routines, among which are station relocations, changes in measuring techniques and changes in observing practices (El-Tantawi, 2005).

A data series said to be homogeneous if it is a sample from a single population. Hence by definition a climatological series is homogeneous and elementary probability analysis must be applied only to climatological series.

Bartlett's test used to test if k samples have equal variances. Equal variances across samples called homogeneity of variances. Some statistical

tests, for example the analysis of variance, assume that variances are equal across groups or samples. The Bartlett test can be used to verify that assumption. Bartlett's test is sensitive to departures from normality. That is, if one's samples come from non-normal distributions, then Bartlett's test may simply be testing for non-normality (*Mitchell, et al., 1966*)

The Bartlett test defined as:

$$H_0: \sigma_1 = \sigma_2 = \dots = \sigma_k$$

$$H_a: \sigma_i \neq \sigma_j \text{ for at least one pair } (ij)$$

The Bartlett test statistic designed to test the equality of variances across groups against the alternative that variances are unequal for at least two groups.

$$T = \frac{N - K \ln S_p^2 - \sum_{i=1}^k (N_i - 1) \ln S_i^2}{1 + \frac{1}{3k-1} \sum_{i=1}^k \left(\frac{1}{N_i - 1} - \frac{1}{N - K} \right)}$$

In the above, S_i^2 is the variance of the i th group, N is the total sample size, N_i is the sample size of the i th group, k is the number of groups, and S_p^2 is the pooled variance. The pooled variance is a weighted average of the group variances and defined as:

$$S_p^2 = \frac{\sum_{i=1}^k (N_i - 1) S_i^2}{(N - K)}$$

Significance Level: α

The variances are judged to be unequal if,

$$T > X_{(\alpha, K-1)}^2$$

Where $X_{(\alpha, k-1)}^2$ are the upper critical value of the chi-square distribution with $k-1$ degrees of freedom and significance level of α .

In the above formulas for the critical regions, the Handbook follows the convention that X_{α}^2 is the upper critical value from the chi-square distribution and $X_{(1-\alpha)}^2$ is the lower critical value from the chi-square distribution (*Mitchell, et al., 1966*)

3.2.1.5. Homogeneity test for rainfall

Reliable rainfall records are usually very important in reaching useful decisions for the many applications of climatology and hydrology. A precipitation record can be considered homogeneous when a sequence of monthly or annual rainfall amounts is stationary (*Mohamed, 2006*).

The rainfall records over a long period may reflect non-uniform conditions (Nonhomogeneity). This could be due to a change in the observation site, or changes in the instrumentation or the location of the rain gauge with respect to obstructions such as trees, buildings, and the frequency of the observation. The observer also plays an important role in generation of the uncertain errors of the observation and error caused by low intensity precipitation below the resolution of the instrument is also common. Non-homogeneity can lead to serious bias in the analysis of the precipitation data i.e. slippage of mean, trend or some oscillation that may lead to difficulty in understanding of the climate. Various methods of evaluating the inhomogeneity of monthly or annual precipitation were described by *El-Tantawi, 2005*

The Von Neumann's ratio (N) is one of the methods used to test the homogeneity in a data series. Von Neumann's ratio has been used in homogeneity testing of rainfall (*Buishand, 1982*).

$$N = \frac{\sum_{i=1}^{N-1} Y_i - Y_{i+1}}{\sum_{i=1}^N (Y_i - \bar{Y})^2}$$

The Von Neumann's ratio tends to be smaller than one for a non-homogenous rainfall series with a jump in the mean. Also where there is more than one jump in the mean, the denominator tends to be larger resulting in values below one (*Buishand, 1982*).

Where:

Y = amount of rainfall (mm)

\bar{Y} = average of the Y_i s

i = i^{th} month

3.2.2. Trend analysis of temperature and precipitation

Trends of temperature and rainfall over Ethiopia were computed from the available data, from 1950-2005, as a "long-term trend".

Many time series have graphs, which at first glance appear fairly erratic in nature, but on closer inspection a general pattern can be observed over a long period of time. This long-term effect called the trend of the graph and is either a steady increase or decrease. If a particular time series is neither increasing nor decreasing over its range of time, it said to contain no trend. The trend can take a variety of shapes, and if the change from one period to the next is relatively constant, the trend is linear and can be represented by the usual equation of a straight line.

$$y = mx + c$$

However, trends may slow down or accelerate over the period and so would in these cases given by some other equation such as a quadratic. In time series analysis one of the most important first steps is to identify the trend. Many methods can be employed to do this, one of the most successful

being moving averages which will be discussed shortly. Seasonal variation refers to the periodic increases or decreases that occur within a calendar year in a time series (*Thom, 1966*).

3.2.2.1. The least squares method

The trend of temperature and rainfall variation could be studied by the method of least squares using line of the regression with time as independent variable. The slope of the regression line is computed and the corresponding relation could be easily found (*Thom, 1966*).

A simple linear regression analysis, namely the least square method or linear regression is used to detect climatic trends over time series at all stations under investigation, as the trend is the basic tool for describing and analysing the changes of climate parameters.

The least-square method (y) is a linear function of (x)

$$y = mx + b$$

Where the slope of the line is given by “ m ” (y over x) and the intercept of the y axis is given as “ b ”. For “ N ” data pairs, the equations used to find the slope “ m ” and intercept “ b ” are:

$$b = \frac{(\sum y \sum x^2 - \sum x \sum xy)}{(N \sum x^2 - (\sum x)^2)}$$

$$m = \frac{(N \sum xy - \sum y \sum x)}{(N \sum x^2 - (\sum x)^2)}$$

3.2.2.2. Quadratic trends

The goal is to forecast future observations given a linear function of observables. In the case of trend estimation, these observables are functions of the time index.

A quadratic equation in the form $y=kx^2$ (simplest form) has a dependent variable x which is to the second power, and a dependent y to the first. Here the x could take 2 different values for the same y .

$$\text{Quadratic model } (y = ax + bx^2 + c)$$

3.2.2.3. Cubic trends

We used the following cubic function to express the climatic element as a non-linear function of time t :

$$y = b_0 + b_1t + b_2t^2 + b_3t^3$$

Where b_0 , b_1 , b_2 and b_3 are empirical constants and calculated from observational data using least squares method. Short term climatic change (from several years to a dozen years scale) could be well reflected by Cubic function fitting curve (*Chen, et al., 2010*, and according to interim extreme values from the Cubic function, we could analyze the transformation character of element change qualitatively. A minimum value would correspond to the time when the element value turned from descending to ascending; a maximum value would correspond to the element value turning from ascending to descending (*Wang, et al., 2004*).

3.2.2.4. Exponential trends

To model this we will use an exponential trend

$$T_t = e^{c+ax}$$

Some time series which are growing (rainfall and temperature) are exponentially increasing. Percentage changes are stable in the long run; these series cannot be fit by a linear trend. So we can fit a linear trend to their (natural) logarithm.

3.2.3. Mann-Kendall test for trend detection

The Mann-Kendall test is based on the null hypothesis that a sample of data is independent and identically distributed, which means that there is no trend or serial correlation among the data points. The alternative hypothesis is that a trend exists in the data. First the statistic defined by variable S was computed which is the sum of the difference between the data points for a series $\{x_1, \dots, x_n\}$ come from a population where the random variables are independent and identically distributed shown in Esq.(1)

$$S = \sum_{i=1}^{n-1} \sum_{j=i+1}^n \text{sgn}(x_j - x_i), \text{ Where } \text{sgn} = \begin{cases} +1 & \theta > 0 \\ 0 & \theta = 0 \\ -1 & \theta < 0 \end{cases} \quad (1)$$

Salmi, et al., (2002) determined that the statistics S is normally distributed when $n \geq 8$ allowing for the computation of the standardized test statistics Z which represent an increasing or decreasing trends respectively. For the statistical trend test used in this study a 5-percent level of significance was selected. The 5- percent level of significance indicates that a 5-percent chance for error exists in concluding that a trend is statistically significant when in fact no trend exists.

$$Z = \begin{cases} \frac{S-1}{\sqrt{V(S)}} & S > 0 \\ 0 & S = 0 \\ \frac{S+1}{\sqrt{V(S)}} & S < 0 \end{cases} \quad \text{If} \quad (2)$$

Where $\text{Var}(S)$, the variance of the data point is given by,

$$\text{Var } s = \frac{1}{18} \left[n(n-1)(2n+5) - \sum_{i=1}^m t_i(t_i-1)(2t_i+5) \right] \quad (3)$$

Where m is the number of tied (i.e., equal values) groups in the data set and t_i is the number of data points in the i^{th} tied group. Under the null hypothesis, the quantity z defined in the following equation is approximately

standard normally distributed even for the sample size $n = 10$. The positive values of S indicate upward trends whereas negative S value indicate downward trend (*Salmi, et al., 2002; El-Tantawi, 2005*).

The slope of the data set can be estimated using the Thiel-Sen Approach (4). This equation is used instead of a linear regression because it limits the influence that the outliers have on the slope. To normalize the slopes calculated for streams of different size, the mean flow value of each parameter and station was used to find a percent change in flow rate.

$$\beta = \text{Median} \frac{X_j - X_i}{j - i} \quad \text{For all } i < j \quad (4)$$

Mann-Kendal approach requires the data to be serially independent. Serial correlation indicates the relation between a data point and its adjacent point. If the data are positively serially correlated then the Mann Kendal approach by itself tends to overestimate the significance of a trend. If, on the other hand, the data have a negative serial correlation then the significance of the trend is underestimated (*Yue, et al., 2002*).

$$Y_t = X_t - \beta t \quad (5)$$

To correct the serial correlation in the data a form of pre-whitening of the sample has been used (*Yue, et al., 2002*).

Where X_t is the series value at time t , β is the slope calculated using Equation (5), and Y_t is the detrended series. When the trend is removed from the data then an estimate of the lag-1 sample serial correlation using the detrended series is calculated using Equation (7). The use of an autoregressive AR (1) model is justified due to the weak serial correlation present in most hydrological time series. The lag-1 serial coefficient is calculated after the trend was removed in order to preserve the initial trend (*Yue, et al., 2002; El-Tantawi, 2005*).

$$r_k = \frac{\frac{1}{n-k} \sum_{t=1}^{n-k} (Y_t - \bar{Y}_t)(Y_{t+k} - \bar{Y}_t)}{\frac{1}{n} \sum_{t=1}^n (Y_t - \bar{Y}_t)^2} \quad (6)$$

If lag-1 serial correlation coefficient (r_k) is not significant at 5% significance level, then the Mann-Kendall test is applied to the original time series. Otherwise it is removed from Y_t as:

$$\hat{Y}_t = Y_t - r_1 Y_{t-1} \quad (7)$$

This procedure is known as the Trend-Free Pre-Whitening (TFPW) procedure. The third step is to add the trend back to \hat{Y}_t , by using Equation (8) and then the Mann-Kendall test is conducted on this new series.

$$Y = \hat{Y}_t + \beta t \quad (8)$$

3.2.4. Low pass filter

To understand the nature of this trend, the series was subjected to a "Low-pass filter" (*Mitchell, et al., 1966*), thus suppressing the high-frequency oscillations. The filter defined by equation (1) has a response function that depends on frequency. The weight used was the nine ordinates of the Gaussian probability curve (0.01, 0.05, 0.12, 0.20, 0.24, 0.20, 0.12, 0.05, and 0.01). The response curve of the Gaussian low-pass filter has a response function that is equal to unity at infinite wavelengths; It then tails off asymptotically to zero with decreasing wavelength. The response is approximately

$$X_{i=-n}^{i=+n} = \sum w_i X_{t+1} \quad (1)$$

$$R(f) = \exp[-2 \Pi^2 \sigma_g^2 f^2] \quad (2)$$

Where σ_g was the appropriate standard deviation (i.e., $6\sigma_g = 10$ Year). The trend was not linear but oscillatory, consisting of periods of more than 10 yr in duration (*Mitchell, et al., 1966*)

3.2.5. The Correlation coefficient

The correlation is one of the most common and most useful statistics. A correlation is a single number that describes the degree of relationship between two variables. There are several different correlation techniques. The most common type, called the Pearson or product-moment correlation. The module also includes a variation on this type called partial correlation. The latter is useful when you want to look at the relationship between two variables while removing the effect of one or two other variables (*Thom, 1966*).

If r is close to 0, it means there is no relationship between the variables. If r is positive, it means that as one variable gets larger the other gets larger. If r is negative it means that as one gets larger.

The Pearson Product-Moment Correlation Coefficient (r), or correlation coefficient for short is a measure of the degree of linear relationship between two variables, usually labeled X and Y (Daniel, S.W., 1995).

The formula for the correlation is:

$$r = \frac{N \sum xy - \sum y \sum x}{(N \sum x^2 - (\sum x)^2)(N \sum y^2 - (\sum y)^2)}$$

N = Number of pairs of scores

$\sum xy$ = Sum of the products of paired scores

$\sum x$ = Sum of x scores

$\sum y$ = Sum of y scores

$\sum x^2$ = Sum of squared x scores

$\sum y^2$ = Sum of squared y scores

The correlation coefficient may take any value between plus and minus one.

$$-1 \leq r \leq +1$$

The sign of the correlation coefficient (+, -) defines the direction of the relationship, either positive or negative. A positive correlation coefficient means that as the value of one variable increases, the value of the other variable increases; as one decreases the other decreases. A negative correlation coefficient indicates that as one variable increases, the other decreases, and vice-versa.

3.2.6. Computer-used programs

Illustrations and data analyses contained in this study were achieved using different programs: Minitab, SPSS 17, Excel 2007 and Surfer 8.

3.2.7. Time series analysis

Time series (TS) data refers to observations on a variable that occur in a time sequence. Mostly these observations are collected at equally spaced, discrete time intervals. When there is only one variable upon which observations are made then we call them a single time series or more specifically a univariate time series. A basic assumption in any time series analysis/ modeling is that some aspects of the past pattern will continue to remain in the future. Also under this set up, the time series process is based on past values of the main variable but not on explanatory variables which may affect the variable/ system. So the system acts as a black box and we may only be able to know about 'what' will happen rather than 'why' it happens. So if time series models are put to use, say, for instance, for forecasting purposes, then they are especially applicable in the 'short term'. Here it is assumed that information about the past is available in the form of numerical data (*Box, et al., 1994*).

Ideally, at least 50 observations are necessary for performing TS analysis/ modeling, as propounded by Box and Jenkins who were pioneers in TS modeling.

3.2.8. Sample size

Building an **ARIMA** model requires an adequate sample size. Box and Jenkins [suggest that about 50 observations is the minimum required number. Some analysts may occasionally use a smaller sample size, interpreting the results with caution. A large sample size is especially desirable when working with seasonal data (*Gerretsadikan and Sharma, 2011*).

3.2.9. Time Series components and decomposition

An important step in analysing TS data is to consider the types of data patterns, so that the models most appropriate to those patterns can be utilized. Four types of time series components can be distinguished. They are:

- I. Horizontal - when data values fluctuate around a constant value
- II. Trend - when there is long term increase or decrease in the data
- III. Seasonal - when a series is influenced by seasonal factor and recurs on a regular periodic basis
- IV. Cyclical - when the data exhibit rise and falls that are not of a fixed period

Many data series include combinations of the preceding patterns. After separating out the existing patterns in any time series data, the pattern that remains unidentifiable form the 'random' or 'error' component. Time plot (data plotted over time) and seasonal plot (data plotted against individual seasons in which the data were observed) help in visualizing these patterns while exploring the data. A crude yet practical way of decomposing the original data (ignoring cyclical pattern) is to go for a seasonal decomposition either by assuming an additive or multiplicative model viz.

$$Y_t = T_t + S_t + E_t \text{ or } Y_t = T_t \cdot S_t \cdot E_t$$

Where

Y_t - Original TS data

T_t - Trend component

S_t - Seasonal component

E_t - Error/ Irregular component

If the magnitude of a TS varies with the level of the series then one has to go for a multiplicative model else an additive model. This decomposition may enable one to study the TS components separately or will allow workers to do trend or to do seasonal adjustments if needed for further analysis (*Box, et al., 1994; Gerretsadikan and Sharma, 2011*).

3.2.10. Moving averages and exponential smoothing methods

3.2.10.1. Simple moving averages

A Moving Average (MA) is simply a numerical average of the last N data points. There is prior MA, centered MA etc. in the TS literature. In general, the moving average at time t, taken over N periods, is given by:

$$M_t^{[1]} = (T_t + T_{t-1} + \dots + T_{t-N+1})/N$$

Where Y_t is the observed response at time t. Another way of stating the above equation is:

$$M_t^{[1]} = M_{t-1}^{[1]} + (Y_t - Y_{t-N})/N$$

At each successive time period the most recent observation is included and the farthest observation is excluded for computing the average. Hence the name 'moving' averages.

3.2.10.2. Double moving averages

The simple moving average is intended for data of constant and no trend nature. If the data have a linear or quadratic trend, the simple moving average will be misleading. In order to correct for the bias and develop an improved forecasting equation, the double moving average can be calculated. To calculate this, simply treat the moving averages $Mt^{[1]}$ over time as individual data points and obtain a moving average of these averages (*Naill and Momani, 2009*).

3.2.11. Stationary of a TS process

A TS is said to be stationary if its underlying generating process is based on a constant mean and constant variance with its autocorrelation function (ACF) essentially constant through time. Thus, if different subsets of a realization are considered (time series 'sample') the different subsets will typically have means, variances and autocorrelation functions that do not differ significantly.

A statistical test for stationary is the most widely used Dickey Fuller test. To carry out the test, estimate by the regression model.

Where y_t denotes the differenced series ($y_t - y_{t-1}$). The number of terms in the regression, p , is usually set to be about 3. Then if $\hat{\alpha}$ is nearly zero the original series y_t needs differencing and if $\hat{\alpha} < 0$ then y_t is already stationary (*Naill and Momani, 2009*).

3.2.12. Autocorrelation functions

3.2.12.1. Autocorrelation

Autocorrelation refers to the way the observations in a time series are related to each other and is measured by the simple correlation between current observation (Y_t) and observation from p periods before the current one (Y_{t-p}). That is for a given series Y_t , autocorrelation at lag $p =$ correlation (Y_t, Y_{t-p}) and is given by:

$$r_p = \frac{\sum_{t=1}^{n-p} (Y_t - \bar{Y})(Y_{t-p} - \bar{Y})}{\sum_{t=1}^n (Y_t - \bar{Y})^2}$$

It ranges from -1 to +1. Box and Jenkins have suggested that maximum number of useful r_p are roughly $n/4$ where n is the number of periods upon which information on Y_t is available (*Box, et al., 1994*).

3.2.12.2. Partial autocorrelation

Partial autocorrelations are used to measure the degree of association between Y_t and Y_{t-p} when the Y -effects at other time lags 1, 2, 3, . . . , $p-1$ are removed.

3.2.12.3. Autocorrelation function (ACF) and partial autocorrelation function (PACF)

Theoretical ACFs and PACFs (Autocorrelations versus lags) are available for the various models chosen. Thus compare the correlograms (plot of sample ACFs versus lags) with these theoretical ACF/ PACFs, to find a reasonably good match and tentatively select one or more ARIMA models. The general characteristics of theoretical ACFs and PACFs are as follows:- (here 'spike' represents the line at various lags in the plot with length equal to magnitude of autocorrelations) (*Montgomery and Johnson, 1967*).

3.2.13. ARIMA modeling

In general, an ARIMA model is characterized by the notation ARIMA (p,d,q) where, p, d and q denote orders of auto-regression, integration (differencing) and moving average respectively. In ARIMA, TS is a linear function of past actual values and random shocks.

For instance, given a time series process $\{Y_t\}$, a first order autoregressive process is denoted by ARIMA (1, 0, 0) or simply AR(1) and is given by:

$$Y_t = \mu + \alpha_1 Y_{t-1} + \epsilon_t$$

And a first order moving average process is denoted by ARIMA (0,0,1) or simply MA(1) and is given by:

$$Y_t = \mu - \alpha_1 \epsilon_{t-1} + \epsilon_t$$

Alternatively, the model ultimately derived, may be a mixture of these processes and of higher orders as well. Thus a stationary ARIMA (p, q) process is defined by the equation:

$$Y_t = \phi_1 Y_{t-1} + \phi_2 Y_{t-2} + \dots + \phi_p Y_{t-p} - \theta_1 \epsilon_{t-1} - \theta_2 \epsilon_{t-2} - \dots - \theta_q \epsilon_{t-q} + \epsilon_t$$

Where ϵ_t 's are independently and normally distributed with zero mean and constant variance σ^2 for $t = 1, 2, \dots, n$. The values of p and q, in practice lie between 0 and 3 (*Gerretsadikan and Sharma, 2011*)

3.2.14. Seasonal ARIMA Modeling

Identification of relevant models and inclusion of suitable seasonal variables are necessary for seasonal modeling and their applications, say, forecasting production of crops. Seasonal forecasts of production of principal crops are of greater utility for planners, administrators and researchers alike. Agricultural seasons vary significantly among the states of India. For example, Tamil Nadu has unique three-season cropping pattern for paddy crop whereas two-season paddy rules elsewhere in the country. Thus seasonal forecasts of crop production can also be made using seasonal ARIMA models.

The Seasonal ARIMA i.e. ARIMA (p,d,q) (P,D,Q)S model is defined by:

$$\phi_p(B)\theta_P(B^S) \nabla^d \nabla_s^D Y_t = \Theta_Q(B^S)\phi_q(B)\epsilon_t$$

Where:

$$\phi_p(B) = 1 - \phi_1 B - \dots - \phi_p B^p$$

$$\phi_q(B) = 1 - \theta_1 B - \dots - \theta_q B^q$$

B is the backshift operator (i.e. $B Y_t = Y_{t-1}$, $B^2 Y_t = Y_{t-2}$ and so on), "S" the seasonal lag and ' ϵ_t ' a sequence of independent normal error variables with mean 0 and variance σ^2 . Θ 's and ϕ 's are respectively the seasonal and

non-seasonal autoregressive parameters. Θ 's and \square 's are respectively seasonal and non-seasonal moving average parameters, p and q are orders of non-seasonal autoregression and moving average parameters respectively whereas P and Q are that of the seasonal auto regression and moving average parameters respectively. Also d and D denote non-seasonal and seasonal differences respectively (*Salas and Boes, 1980*).

3.2.15. The Art of ARIMA model building

A. Identification

The foremost step in the process of modeling is to check for the stationarity of the series, as the estimation procedures are available only for stationary series. There are two kinds of stationarity, viz., stationarity in 'mean' and stationarity in 'variance'. A look at the graph of the data and structure of autocorrelation and partial correlation coefficients may provide clues for the presence of stationarity. Another way of checking for stationarity is to fit a first order autoregressive model for the raw data and test whether the coefficient ' \square ' is less than one. If the model is found to be non-stationary, stationarity could be achieved mostly by differencing the series. Or use a Dickey Fuller test. Stationarity in variance could be achieved by some modes of transformation, say, log transformation. This is applicable for both seasonal and non-seasonal stationarity (*Salas and Boes, 1980; Makridakis and Hison, 1995*).

Thus, if ' X_t ' denotes the original series, the non-seasonal difference of first order is:

$$Y_t = X_t - X_{t-1}$$

Followed by the seasonal differencing (if needed)

$$Z_t = Y_t - Y_{t-s} = (X_t - X_{t-1}) - (X_{t-s} - X_{t-s-1})$$

The next step in the identification process is to find the initial values for the orders of seasonal and non-seasonal parameters, p , q , and P , Q . They could be obtained by looking for significant autocorrelation and partial autocorrelation coefficients. Say, if second order auto correlation coefficient is significant, then an AR (2), or MA (2) or ARMA (2) model could be tried to start with. This is not a hard and fast rule, as sample autocorrelation coefficients are poor estimates of population autocorrelation coefficients. Still they can be used as initial values while the final models are achieved after going through the stages repeatedly (*Salas and Boes, 1980*).

B. Estimation

At the identification stage, one or more models are tentatively chosen that seem to provide statistically adequate representations of the available data. Then precise estimates of parameters of the model are obtained by least squares as advocated by Box and Jenkins. Standard computer packages like Minitab, SPSS etc. are available for finding the estimates of relevant parameters using iterative procedures (*Makridakis and Hison, 1995*).

C. Diagnostics

Different models can be obtained for various combinations of AR and MA individually and collectively. The best model is obtained with following diagnostics:

- Low Akaike Information Criteria (AIC)

AIC is given by $AIC = (-2 \log L + 2m)$ where $m=p+q+P+Q$ and L is the likelihood function. Since $-2 \log L$ is approximately equal to $\{n(1+\log 2\pi) + n \log \sigma^2\}$ where σ^2 is the model MSE, AIC can be written as $AIC=\{n(1+\log 2\pi) + n \log \sigma^2 + 2m\}$ and because first term in this equation is a constant, it is usually omitted while comparing between models. As an

alternative to AIC, sometimes SBC is also used which is given by $SBC = \log \sigma^2 + (m \log n) \ln$.

- Non-significance of autocorrelations of residuals via Portmonteau tests (Q-tests based on Chi-square statistics)-Box-Pierce or Ljung-Box texts (*Makridakis and Hison, 1995*).

After tentative model has been fitted to the data, it is important to perform diagnostic checks to test the adequacy of the model and, if need be, to suggest potential improvements. One way to accomplish this is through the analysis of residuals. It has been found that it is effective to measure the overall adequacy of the chosen model by examining a quantity Q known as Box-Pierce statistic (a function of autocorrelations of residuals) whose approximate distribution is chi-square and is computed as follows:

$$Q = N \sum r^2(j)$$

Where summation extends from 1 to k with k as the maximum lag considered, n is the number of observations in the series, r(j) is the estimated autocorrelation at lag j; k can be any positive integer and is usually around 20. Q follows Chi-square with (km_1) degrees of freedom where m_1 is the number of parameters estimated in the model (*Al-Ansari and Baban, 2005*).

A modified Q statistic is the Ljung-box statistic which is given by

$$Q = n(n-2) \sum r^2(j) / (n-j)$$

The Q Statistic is compared to critical values from chi-square distribution. If model is correctly specified, residuals should be uncorrected and Q should be small (the probability value should be large). A significant value indicates that the chosen model does not fit well (*Al-Ansari, et al., 2006*).

3.2.16. Assessment of forecast performance

A number of statistics are used to measure the forecast performance. They include; the correlation coefficient r between the forecast \hat{Y}_i and the observed value Y_i , the root-mean-square error (RMSE), the mean absolute error (MAE), and the bias. The referred four statistics may be determined as (Al-Ansari and Baban, 2005).

A. Mean forecast error:

$$\text{MFE} = \frac{1}{n} \sum_{t=1}^n (D_t - F_t)$$

B. Mean absolute deviation:

$$\text{MAD} = \frac{1}{n} \sum_{t=1}^n |D_t - F_t|$$

C. Mean absolute percentage error:

$$\text{MAPE} = \frac{100}{n} \sum_{t=1}^n \left| \frac{D_t - F_t}{D_t} \right|$$

D. Mean squared error:

$$\text{MSE} = \frac{1}{n} \sum_{t=1}^n (D_t - F_t)^2$$

Where D_t : actual data, F_t : forecast data and n : number of data.

In which \bar{Y} is the mean of the data Y_1, \dots, Y_N ; $\bar{\hat{Y}}$ is the mean of the predicted values $\hat{Y}_1, \dots, \hat{Y}_N$; and N is the sample size. For a given regression model, the coefficient of multiple determination R^2 is bounded between 0 and 1, with values closer to 1 denoting a better fitting model (Al-Ansari, et al., 2006).



Results and Discussions

CODES LIBRARY

RESULTS AND DISCUSSION

4.1. Missing data

Estimation of missing climatological data is an important task for meteorologists, hydrologists and environment protection workers all over the world. Missing data are problematic for a number of reasons. First, most statistical procedures rely on complete-data methods of analysis (*Kemp, et al., 1983*). That is, computational programs require that all cases contain values for all variables to be analyzed. Thus, as a default, most statistical software programs exclude from analysis cases that have missing data on any of the variables (*Degaetano, et al., 1995*).

Missing climate data existed at all weather stations (Table 4) due to relocation of a station or to interruptions in observations.

In a first reading of the data, we detect a small percentage of missing data. We try to recover it by some statistical methods, when they were available. The final rate of missing value is changes from station to station over the total of monthly data (Precipitation, maximum and minimum temperature). Although, this percentage is low, the major problem is that missing data are grouped in continuous months, which affect some homogeneity test. (Table 4), shows the final total percentage of missing data for each station, and for each variable (Precipitation, maximum and minimum temperature).

In Table (5), we compared between five methods for analyses of the missing data. To obtain the missing data by using some statistical methods (table 5) about 4 missing values through limited period for station. After analyses of the data by these statistical methods we found that any one of these methods can be used to obtain the missing data and give the same result by a percent more than 99% (Figure 5).

Table (4) showed the percent of the missing data for each station for each element of the climatic elements.

The percent of the missing data ranges from (0.7 to 2.8%) for all stations, it was low for each station data so the station that has data of about 30-year, contains 360 values ($12 \times 30 = 360$) and if the percent of the missing data was 2.8% (it means that the missing data equal 10 value from about 360 value). So it is low as regarding the sum of the total value.

CODESRIA - LIBRARY

Table (4): Percentage of missing values for each station.

No.	Station	Total missing data (%)		
		Maximum	Minimum	Rainfall
1	Addis Ababa	1.8	1.1	0.8
2	Arbaminch	1.8	1.7	1.1
3	Assosa	0.9	2	1.6
4	Awassa	1.6	2	1.2
5	Bahir Dar	1.9	0.4	0.4
6	Kombolcha	0.9	1.5	0.8
7	Diredawa	1.7	1.1	1.8
8	Negele	1.7	1.8	0.8
9	Debre Zeit	1.6	2.1	1.5
10	Gode	1.4	1.5	1.3
11	Gondar	2.8	2.1	1.1
12	Jima	0.7	1.3	1
13	Gore	1.7	1.5	1.8
14	Jijiga	0.7	1.6	0.7
15	Nekemte	1.2	1.4	1.5
16	Mekele	0.8	1.9	1
17	Debremarkos	1.3	1.9	1.8
18	Awash	1.5	1.8	1.6
19	Bati	-	-	1.3
20	Dessie	-	-	1.6
21	Gambela	-	-	0.7
22	Harara	-	-	1.1
23	Metehara	-	-	0.9
24	Robe	-	-	0.7
25	Sibu Sire	-	-	1.7
26	Wonji	-	-	1.5

Table (5): Comparison between the different methods for finding missing data.

Method	Missing	Percent (%)
Series mean	4	99.9
Mean of nearby points	4	99.8
Median of nearby points	4	99.6
Linear interpolation	4	99.5
Linear trend at point	4	99.6

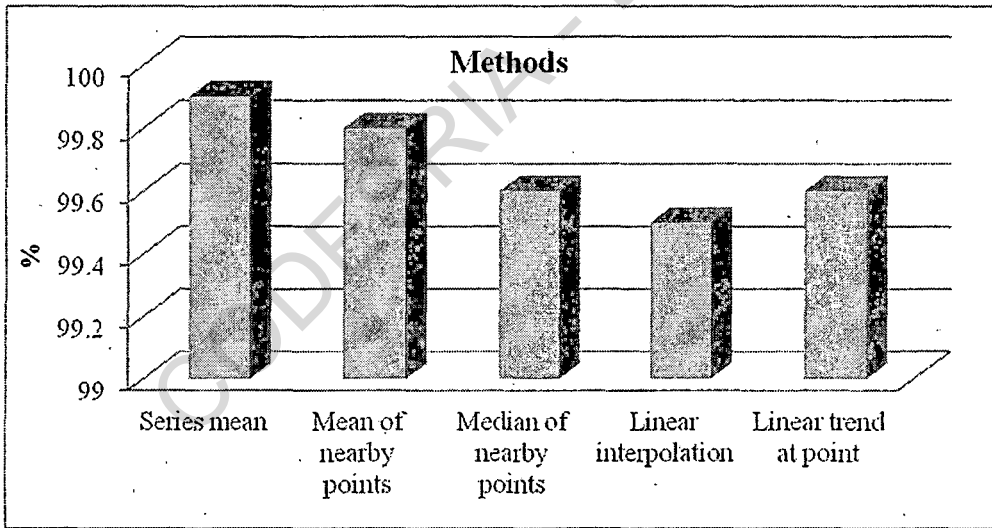


Figure (5): Comparison between the different methods for finding missing data.

4.2. Quality control

The World Meteorological Organization (*WMO, 1981a*) prescribes that certain quality control procedures must be applied to all meteorological data for international exchange.

WMO (1981b) prescribes that quality control must be applied by meteorological data-processing centres to most kinds of weather reports exchanged internationally, to check for coding errors, internal consistency, time and space consistency and physical - climatological limits. The same document specifies the minimum frequency and times for quality control.

WMO (1989) gives general guidance on procedures and emphasizes the importance of quality control at the station. A detailed description of the procedures that may be used by numerical analysis centres is given in *WMO (1993)*.

Quality control and homogenization has to be undertaken prior to any data analysis in order to eliminate any erroneous values and non climatic biases in time series (*Stepanek and Zahradnicek, 2009*).

The management and processing of climatological and meteorological data include quality control (QC). It is important to check the consistency of the data coming from the stations for a single observation term, to calculate derived variables, to verify the values using an enlarged set of tests including tests for temporal variability, to fill data gaps and estimate replacement values for obviously erroneous data points, and to be able to correct actual as well as historical data (*Alexandersson, 1995*).

Quality Control (QC) procedures are applied to detect and identify the errors made in the process of recording, manipulating, formatting, transmitting and archiving data. Therefore, knowledge of the applied procedures will allow

assessment of the validity of the observations and improve the data usage. Global Climate Observing System (GCOS) Climate Monitoring Principles recommend to regularly assess as part of routine operations the quality control and homogeneity operations (*Eischeid, et al., 1995*).

The results of quality control process are given in tables (6, 7 and 8) in which P_{out} values and extreme year (s) corrected for each station are tabulated. These tables show the variation of data that reaches maximum values along southern and northern border of the basin.

The total number of corrected values is detected in all stations. But some stations of Ethiopia have total annual precipitations which were higher than their corresponding P_{out} values in the same years.

After analyses of all climatic data (annual maximum and minimum temperature) of all stations in Ethiopia, the P_{out} values of all data for each station were found higher than all annual values for this station through the study period.

For the annual precipitation, it is found that the total number of corrected values is only ten stations shown in table (8), total annual precipitation values at these stations were found higher than P_{out} value, so it was replaced by the corresponding P_{out} value.

Table (6): The results of quality control (QC) for maximum temperature.

No.	Station	Period	Median	3 rd Q (75%)	IQR	P _{out}	Extreme year(s) replaced by P _{out}
1	Addis Ababa	(1960-2005)	22.9	23.3	0.4	24.5	-
2	Arbaminch	(1970-2005)	30.1	30.4	0.3	31.3	-
3	Assosa	(1970-2005)	28.2	28.4	0.2	29	-
4	Awash	(1970-2000)	33.2	33.5	0.3	34.4	-
5	Awassa	(1970-2005)	27	27.3	0.3	28.2	-
6	Bahir Dar	(1960-2005)	26.7	27.1	0.4	28.3	-
7	Kombolcha	(1950-2005)	26.2	26.6	0.4	27.8	-
8	Debremarkos	(1950-2005)	22.4	22.6	0.2	23.2	-
9	Debre Zeit	(1950-2005)	26.3	26.5	0.2	27.1	-
10	Diredawa	(1950-2005)	31.5	31.8	0.3	32.7	-
11	Gode	(1970-2000)	34.8	35	0.2	35.6	-
12	Gondar	(1950-2005)	26.5	26.8	0.3	27.7	-
13	Gore	(1950-2005)	23.4	23.8	0.4	25	-
14	Jijiga	(1950-2005)	27.3	27.6	0.3	28.5	-
15	Jima	(1950-2005)	26.9	27	0.1	27.3	-
16	Mekele	(1960-2005)	24.3	24.9	0.6	26.7	-
17	Negele	(1950-2005)	25.9	26.4	0.5	27.9	-
18	Nekemte	(1970-2005)	24	24.3	0.3	25.2	-

Table (7): The results of quality control (QC) for minimum temperature.

No.	Station	Period	Median	3 rd Q (75%)	IQR	P _{out}	Extreme year(s) replaced by P _{out}
1	Addis Ababa	(1950-2005)	9.6	10.3	0.7	12.4	-
2	Arbaminch	(1970-2005)	16.4	17.3	0.9	20	-
3	Assosa	(1970-2005)	15	15.7	0.7	17.8	-
4	Awassa	(1970-2005)	12.4	12.8	0.4	14	-
5	Bahir Dar	(1960-2005)	12.1	12.7	0.6	14.5	-
6	Kombolcha	(1950-2005)	12.2	12.7	0.5	14.2	-
7	Debremarkos	(1950-2005)	9.6	10.1	0.5	11.6	-
8	Debre Zeit	(1950-2005)	11.6	12	0.4	13.2	-
9	Diredawa	(1950-2005)	18.6	19.1	0.5	20.6	-
10	Gode	(1970-2005)	22.8	22.9	0.1	23.2	-
11	Gondar	(1950-2005)	13	13.5	0.5	15	-
12	Gore	(1950-2000)	13.3	13.6	0.3	14.5	-
13	Jijiga	(1950-2005)	11.3	12.1	0.8	14.5	-
14	Jima	(1950-2005)	11	11.4	0.4	12.6	-
15	Mekele	(1960-2005)	11.5	11.7	0.2	12.3	-
16	Metehara	(1970-2005)	18.3	18.9	0.6	20.7	-
17	Negele	(1950-2005)	13.5	15.4	1.9	21.1	-
18	Nekemte	(1970-2005)	12.7	13	0.3	13.9	-

Table (8): The results of quality control (QC) for rainfall.

No.	Station	Period	Median	3 rd Q (75%)	IQR	P _{out}	Extreme year(s) replaced by P _{out}
1	Addis Ababa	(1900-2005)	1177.8	1311	133.2	1710.6	1947
2	Arbaminch	(1960-2005)	855.1	933.3	78.2	1167.9	1997
3	Assosa	(1960-2005)	1057.7	1227.0	169.3	1734.9	1962-2001
4	Awash	(1950-2000)	631.0	719.8	88.8	986.2	-
5	Awassa	(1970-2005)	939.3	1020.4	81.1	1263.7	-
6	Bahar Dar	(1960-2005)	1482.8	1569.8	87	1830.8	1973-1974
7	Bati	(1950-1990)	1067.0	1177.5	110.5	1509	-
8	Kombolcha	(1940-2005)	1048.2	1166.0	117.8	1519.4	-
9	Debremarkos	(1953-2005)	1326.7	1415.5	88.8	1681.9	-
10	Debre Zeit	(1951-2005)	833.7	947.2	113.5	1287.7	-
11	Dessie	(1960-2005)	1228.1	1334.7	106.6	1654.5	-
12	Diredawa	(1950-2009)	623.7	721.7	98	1015.7	1956
13	Gambela	(1950-2009)	630.7	721.7	91	994.7	-
14	Jima	(1950-2009)	1486.7	1624.1	137.4	2036.3	-
15	Gode	(1966-2005)	216.1	283.9	67.8	487.3	1967-1968
16	Gondar	(1950-2009)	1121	1295.5	174.5	1819	2001
17	Gore	(1910-2005)	2093	2231.3	138.3	2646.2	1939-1960-1961
18	Harara	(1950-1985)	869.2	999.2	130	1389.2	-
19	Jijiga	(1950-2005)	598.1	694.8	96.7	984.9	1967-1972
20	Mekele	(1954-2005)	612.6	714	101.4	1018.2	-
21	Metehara	(1970-2005)	582	708.7	126.7	1088.8	-
22	Negele	(1960-2005)	730.4	843.8	113.4	1184	1972
23	Nekemte	(1970-2005)	2079.9	2219.3	139.4	2637.5	-
24	Robe	(1970-2000)	907.8	1157.3	249.5	1905.8	-
25	Sibu Sire	(1954-2005)	1336.1	1469.8	133.7	1870.9	-
26	Wonji	(1951-1985)	742	927.5	185.5	1484	-

4.3. Control chart

A control chart (also called process chart or quality control chart) is a graph that shows whether a sample of data falls within the common or normal range of variation.

A control chart has upper and lower control limits that separate common from assignable causes of variation. The common range of variation is defined by the use of control chart limits. The process is called out of control when a plot of data reveals that one or more samples fall outside the control limits (Tables 9, 10 and 11).

After analyses of about 26 climatic stations as regarding (maximum, minimum temperature and total annual precipitation) through the climatic periods in Ethiopia (Figures 6, 7 and 8), it was found that the control chart for most stations data was out of control, because the distance between upper and lower level was limited by that equation:

$$UCL = \mu + 3\alpha$$

$$LCL = \mu - 3\alpha$$

The equation for UCL and LCL was limited by the mean and standard error. The standard error was low so the difference between UCL and LCL was low, while the data frequency was high so it is mostly out of the distance between upper and lower limit.

Table (9): Upper and lower control limit of mean annual maximum temperature.

M.	Station	N	Min.	Max.	Mean	SE	SD	UCL	LCL
1	Addis Ababa	46	21.3	24.3	22.7	0.1	0.8	23	22.4
2	Arba Minch	36	28.8	31.6	30.0	0.1	0.6	30.3	29.7
3	Assosa	36	26.8	29.9	28.2	0.1	0.7	28.5	27.9
4	Awash	31	32.4	34.8	33.3	0.1	0.5	33.6	33
5	Awassa	36	25.6	27.9	26.9	0.1	0.6	27.2	26.6
6	Bahir Dar	46	25.6	28.2	26.8	0.1	0.7	27.1	26.5
7	Combolcha	56	23.4	29.2	26.2	0.1	0.8	26.5	25.9
8	Debre Markos	56	21.4	23.3	22.4	0.1	0.4	22.7	22.1
9	Debre Zeit	56	25.4	28.1	26.3	0.1	0.5	26.6	26
10	Dire Dawa	56	30	33	31.5	0.1	0.5	31.8	31.2
11	Gode	31	33.9	35.7	34.8	0.1	0.4	35.1	34.5
12	Gondar	56	25.6	28.1	26.5	0.1	0.5	26.8	26.2
13	Gore	56	22.4	24.5	23.5	0.1	0.5	23.8	23.2
14	Jijiga	56	26.1	28.2	27.3	0.1	0.5	27.6	27
15	Jimma	56	26	28.3	26.9	0.1	0.5	27.2	26.6
16	Mekele	46	22.6	25.8	24.3	0.1	0.8	24.6	24
17	Negele	56	25	27.1	25.9	0.1	0.5	26.2	25.6
18	Nekemte	36	23.1	24.9	24.0	0.1	0.5	24.3	23.7

Table (10): Upper and lower control limit of mean annual minimum temperature.

M.	Station	N	Min.	Max.	Mean	SE	SD	UCL	LCL
1	Addis Ababa	56	6.8	11.5	9.6	0.1	0.9	9.9	9.3
2	Arbaminch	36	13.1	18.2	16.3	0.2	1.2	16.9	15.7
3	Assosa	36	13.7	16.4	15.1	0.1	0.7	15.4	14.8
4	Awassa	36	10.6	13.7	12.4	0.1	0.7	12.7	12.1
5	Bahir Dar	46	7.8	13.8	11.7	0.2	1.4	12.3	11.1
6	Kombolcha	56	7.1	13.5	11.9	0.2	1.2	12.5	11.3
7	Debremarkos	56	6.2	10.9	9.4	0.1	1.0	9.7	9.1
8	Debre Zeit	56	10	13.1	11.6	0.1	0.7	11.9	11.3
9	Diredawa	56	13.6	19.6	18.5	0.1	1.1	18.8	18.2
10	Gode	36	19.6	23.8	22.7	0.1	0.8	23	22.4
11	Gondar	56	11.2	14.4	13.0	0.1	0.7	13.3	12.7
12	Gore	56	12.4	14.6	13.5	0.1	0.5	13.8	13.2
13	Jijiga	56	8.1	14	11.4	0.1	1.0	11.7	11.1
14	Jima	56	9.2	11.9	11.0	0.1	0.5	11.3	10.7
15	Mekele	46	8.8	12.2	11.2	0.1	0.8	11.5	10.9
16	Metehara	36	16.5	20.3	18.4	0.1	0.8	18.7	18.1
17	Negele	56	10.5	16.3	13.9	0.2	1.4	14.5	13.3
18	Nekemte	36	10.8	13.5	12.6	0.1	0.6	12.9	12.3

Table (11): Upper and lower control limit of annual rainfall (mm).

M.	Station	N	Min.	Max.	Mean	SE	SD	UCL	LCL
1	Addis Ababa	84	922	1936.7	1206.1	21.3	194.8	1270	1142.2
2	Gore	84	1448	3282	2137.1	37.8	346.4	2250.5	2023.7
3	Arbaminch	46	617.9	1312.6	872.8	20.8	140.9	935.2	810.4
4	Assosa	46	206.6	1875.5	1063.5	54.2	367.3	1226.1	900.9
5	Bahir Dar	46	894.6	2036	1444.5	34.4	233.2	1547.7	1341.3
6	Dessie	46	706.8	1576.3	1191.2	28.0	190.0	1275.2	1107.2
7	Negele	46	358.8	1381.2	752.3	27.9	189.1	836	668.6
8	Bati	40	625	1322	1039.5	27.4	173.4	1121.7	957.3
9	Goba	40	189.4	1279.2	878.2	34.3	217.1	981.1	775.3
10	Gode	40	38.8	686.3	242.0	21.9	138.6	307.7	176.3
11	Debremarkos	51	1057	1769	1342.0	21.4	152.9	1406.2	1277.8
12	Debre Zeit	51	412	1355.4	851.0	24.1	172.1	923.3	778.7
13	Mekele	51	293.2	1171.7	630.5	26.5	189.0	710	551
14	Sibu Sire	51	835.4	2081	1351.7	31.0	221.4	1444.7	1258.7
15	Jijiga	51	379.1	1477.8	666.2	32.0	228.5	762.2	570.2
16	Awassa	31	724.5	1226.1	937.0	24.9	138.6	1011.7	862.3
17	Gobe	31	38.8	687.3	247.8	28.7	159.6	333.9	161.7
18	Harer	31	412.1	1302.8	878.7	41.9	233.3	1004.4	753
19	Metehara	31	418.9	1008.5	633.8	26.1	145.4	712.1	555.5
20	Nekemte	31	1714.7	2551.4	2108.8	39.5	220.0	2227.3	1990.3
21	Wonji	31	503	1181	802.8	35.8	199.2	910.2	695.4
22	Robe	31	327.1	2184	1056.1	72.6	404.4	1273.9	838.3
24	Kombolcha	60	593	1433	1051.0	22.8	176.3	1119.4	982.6
25	Diredawa	60	283.9	1187.5	624.3	22.3	172.5	691.2	557.4
26	Gambela	60	283.9	1197.5	628.3	22.1	171.3	694.6	562
27	Jima	60	1204	2079.5	1508.2	24.0	185.9	1580.2	1436.2
28	Gondar	60	713	1875.6	1172.2	32.1	248.4	1268.5	1075.9

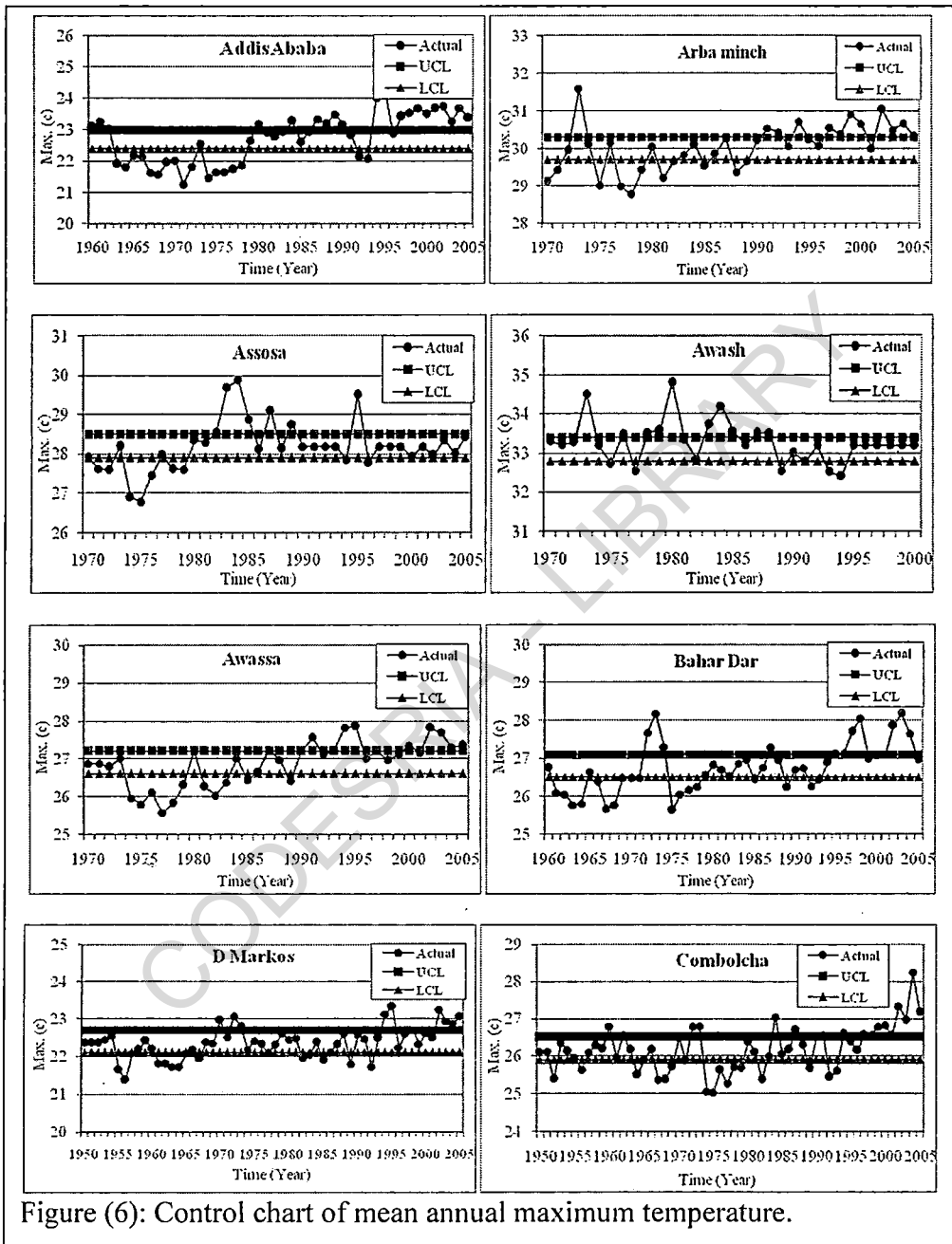
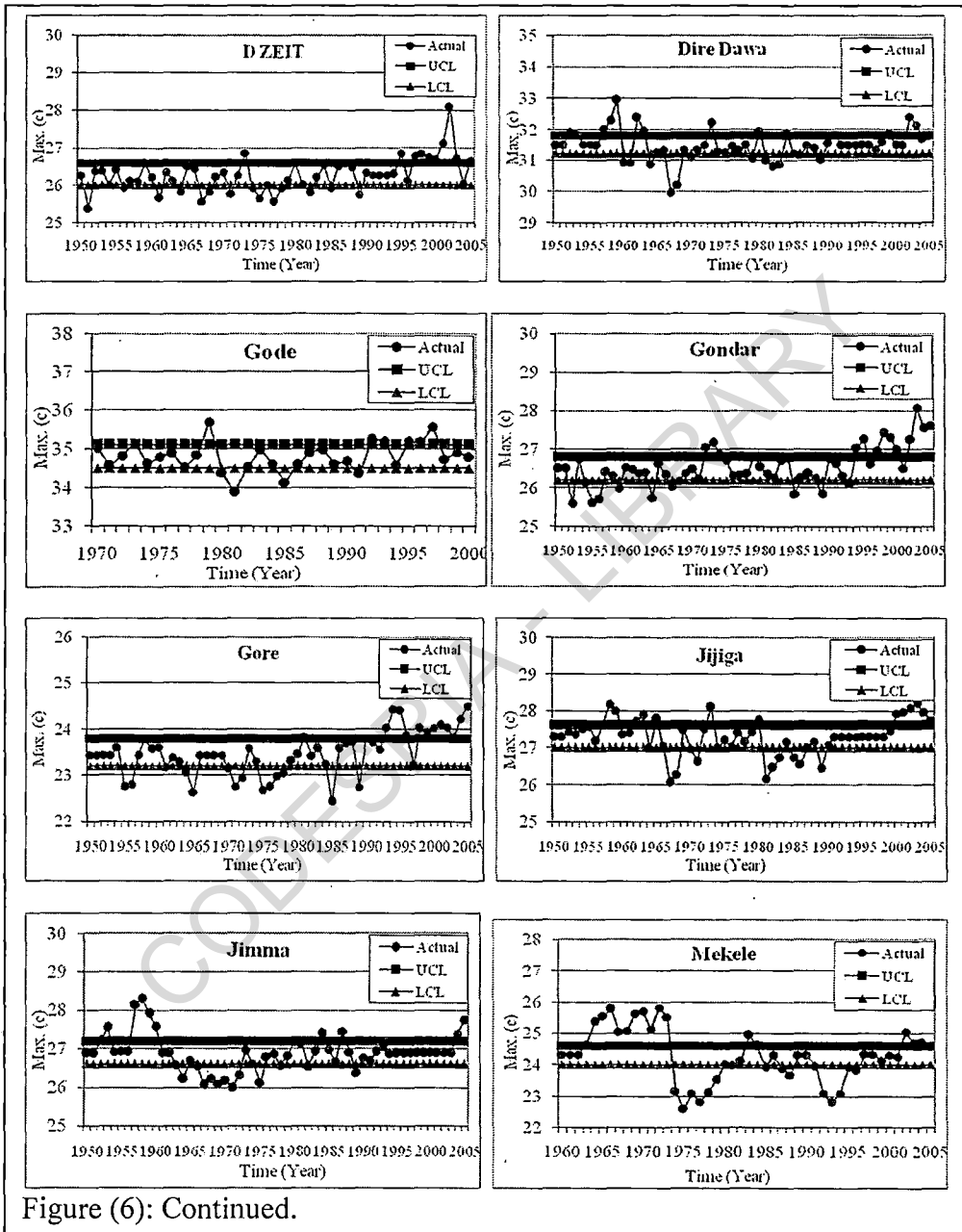


Figure (6): Control chart of mean annual maximum temperature.



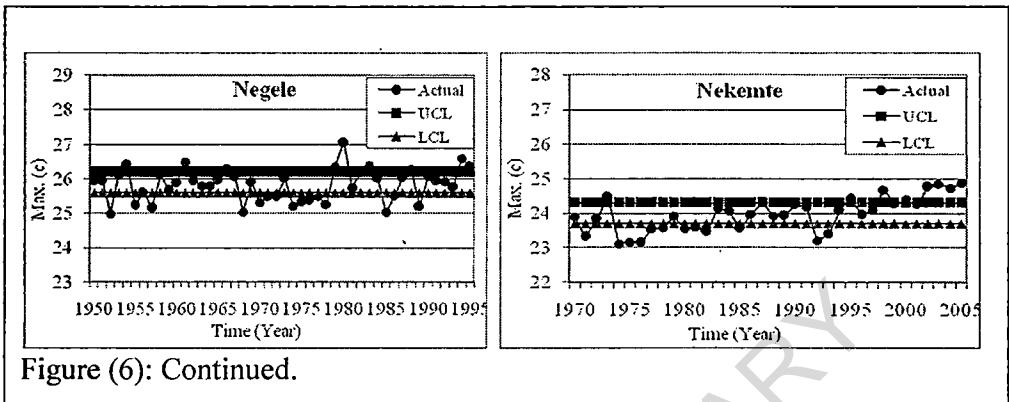
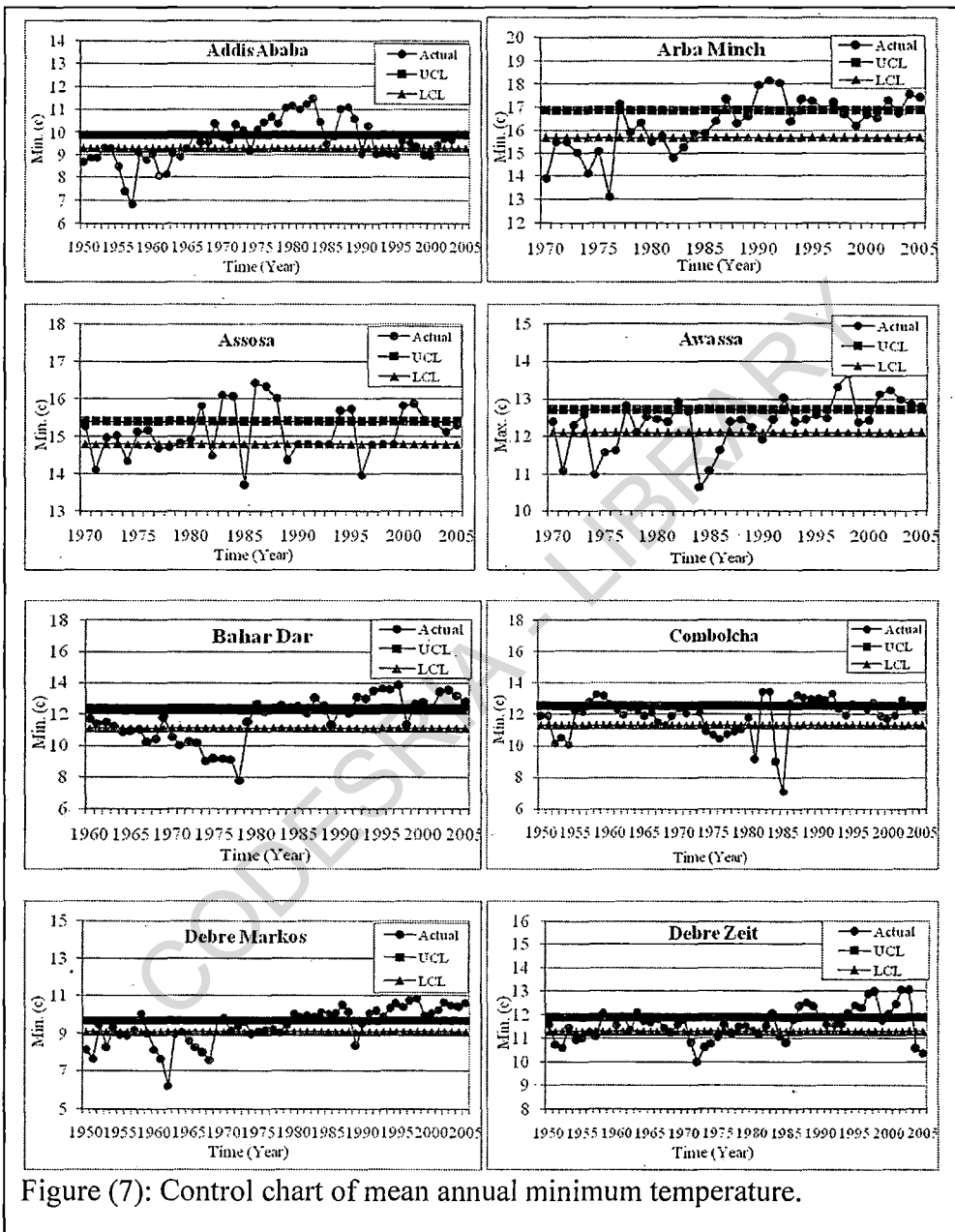


Figure (6): Continued.



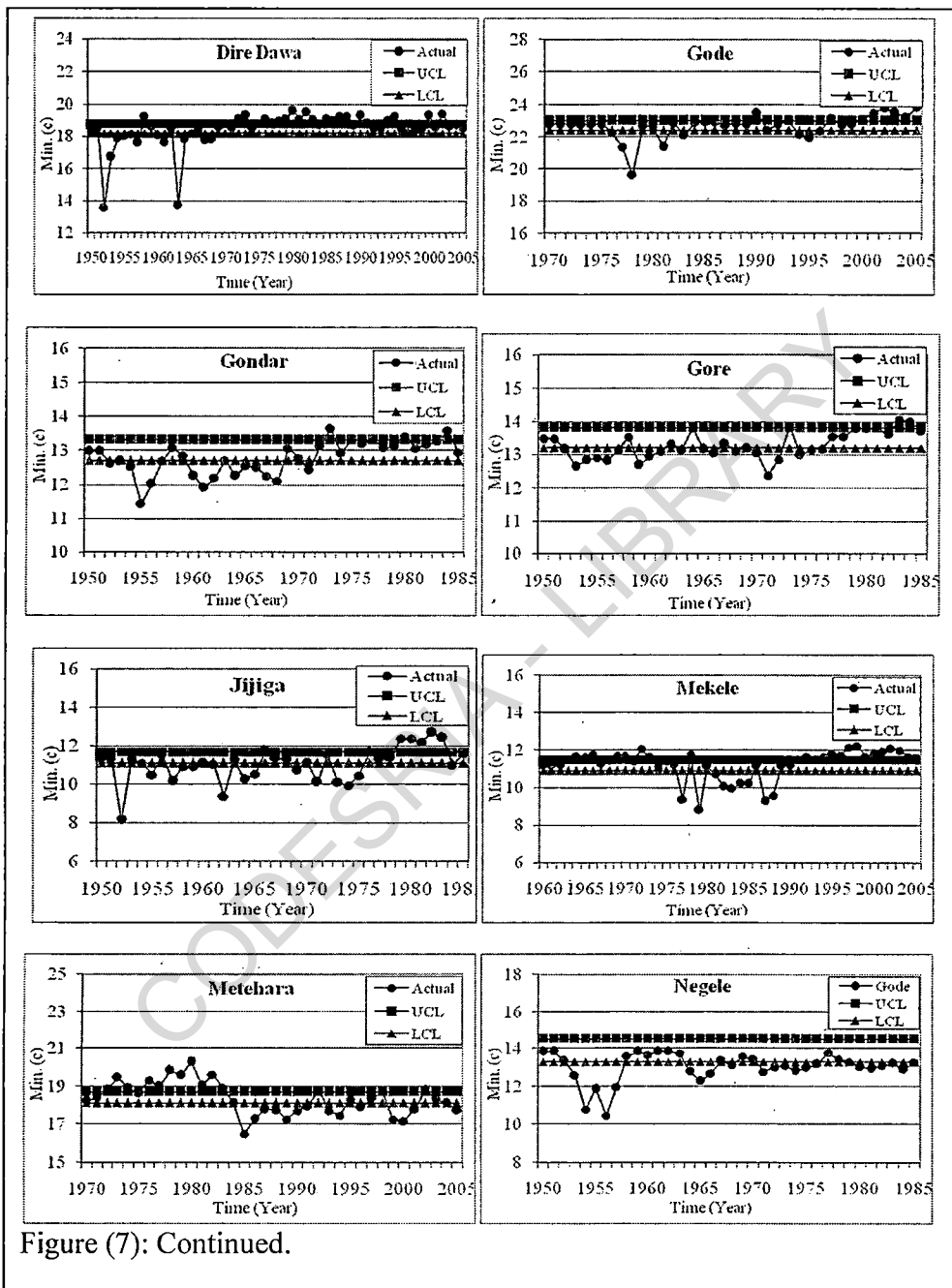


Figure (7): Continued.

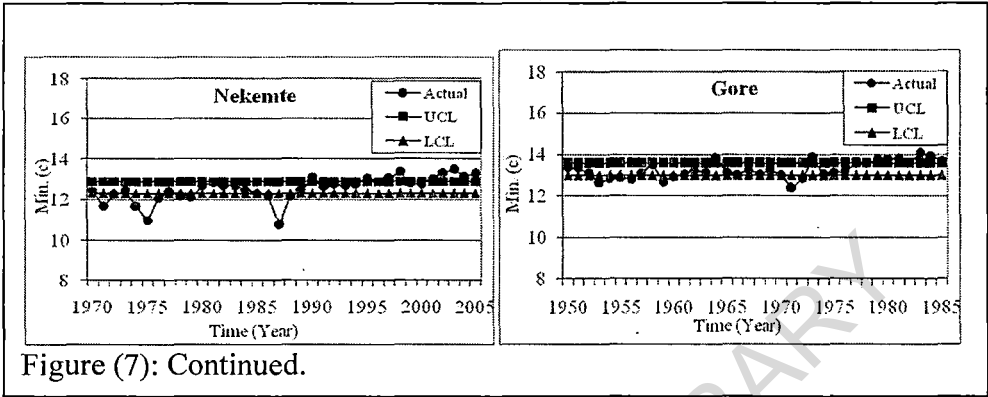


Figure (7): Continued.

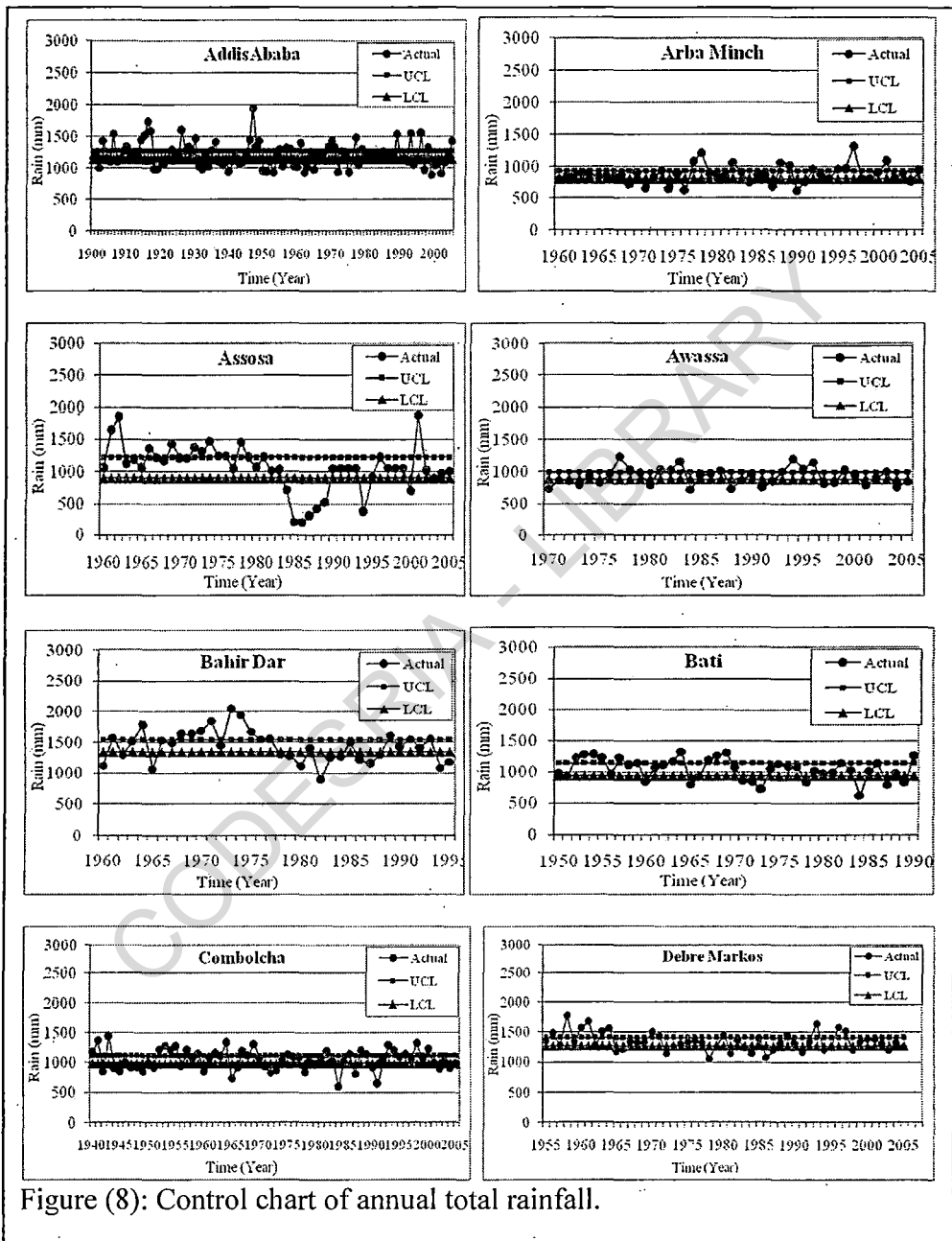
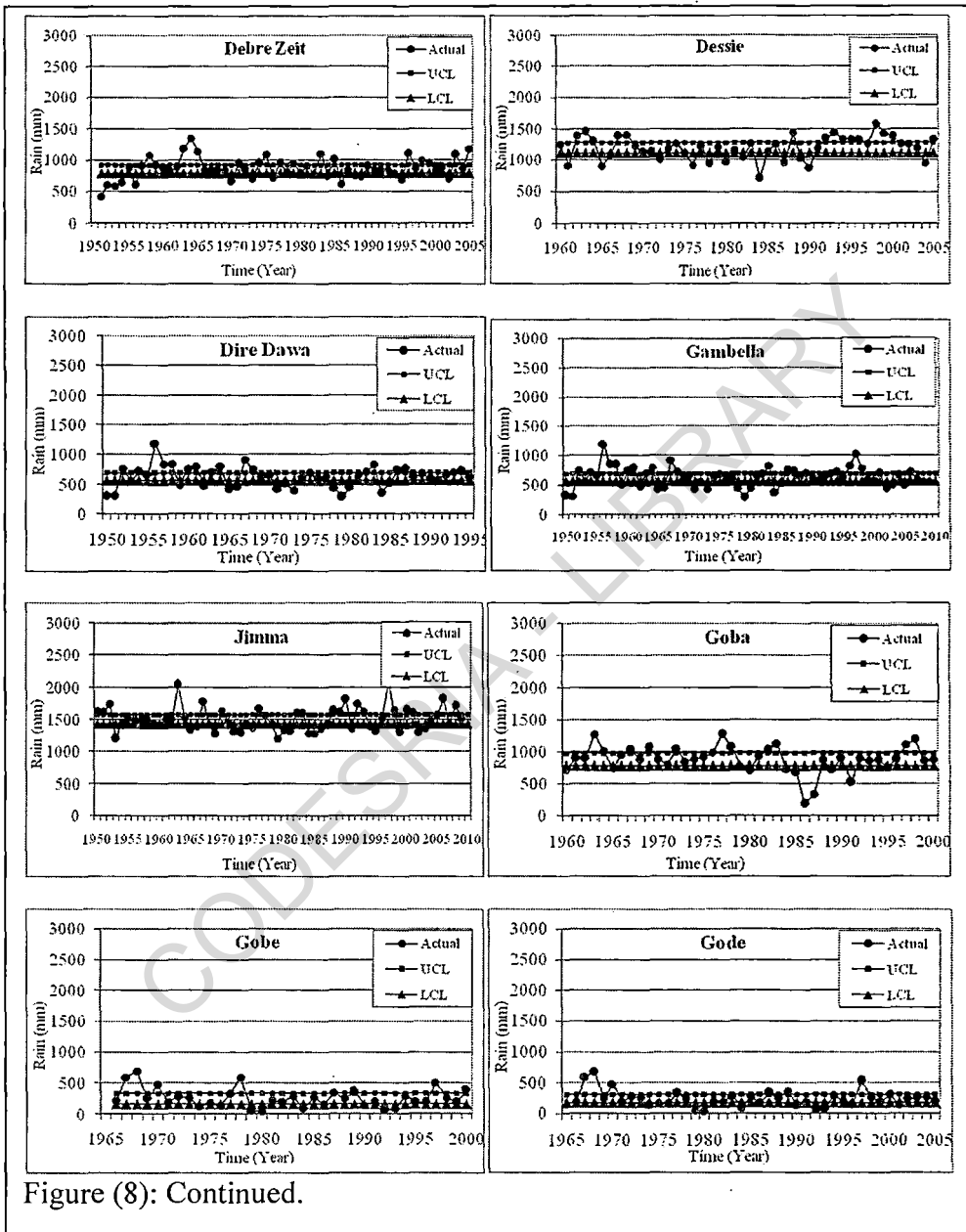


Figure (8): Control chart of annual total rainfall.



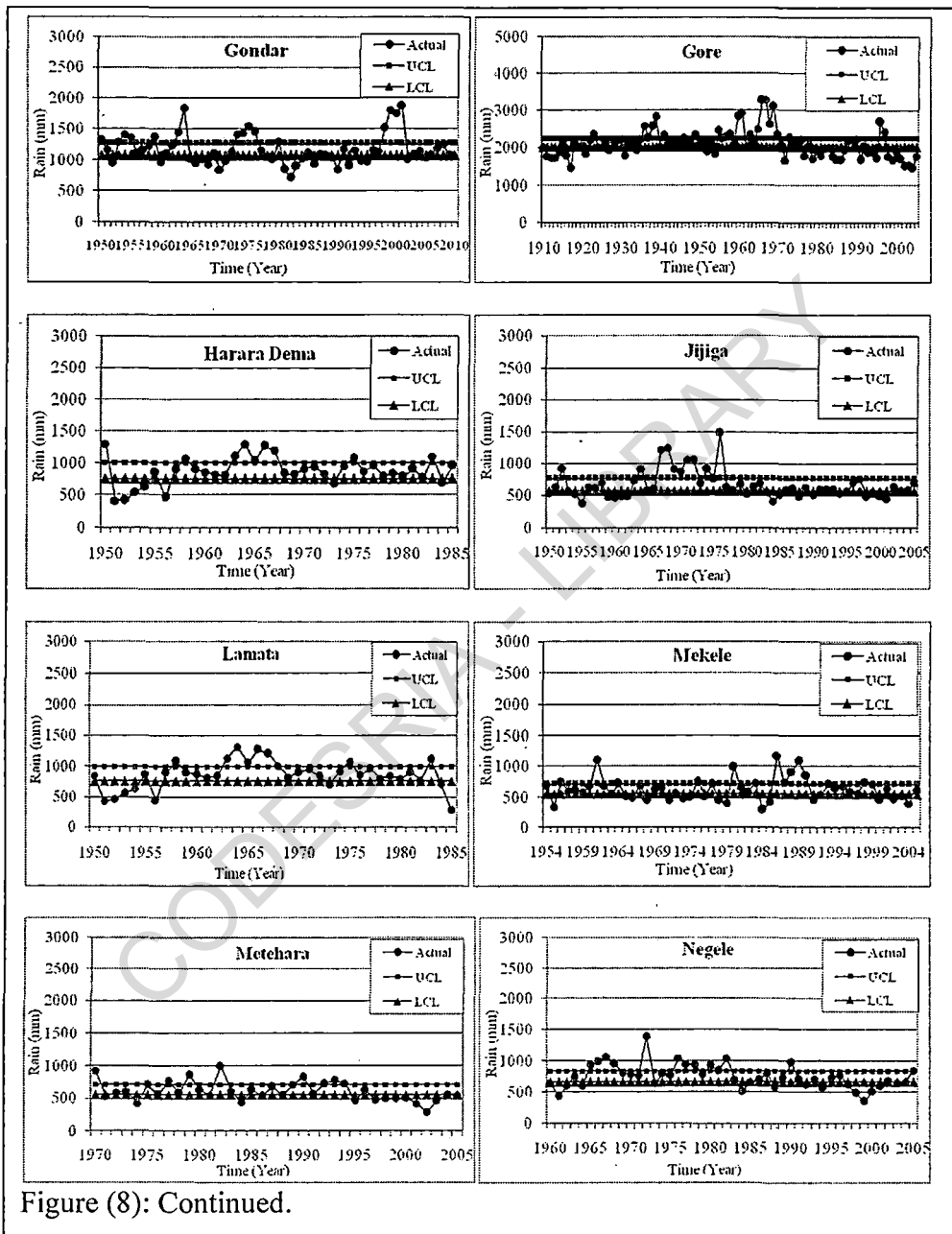


Figure (8): Continued.

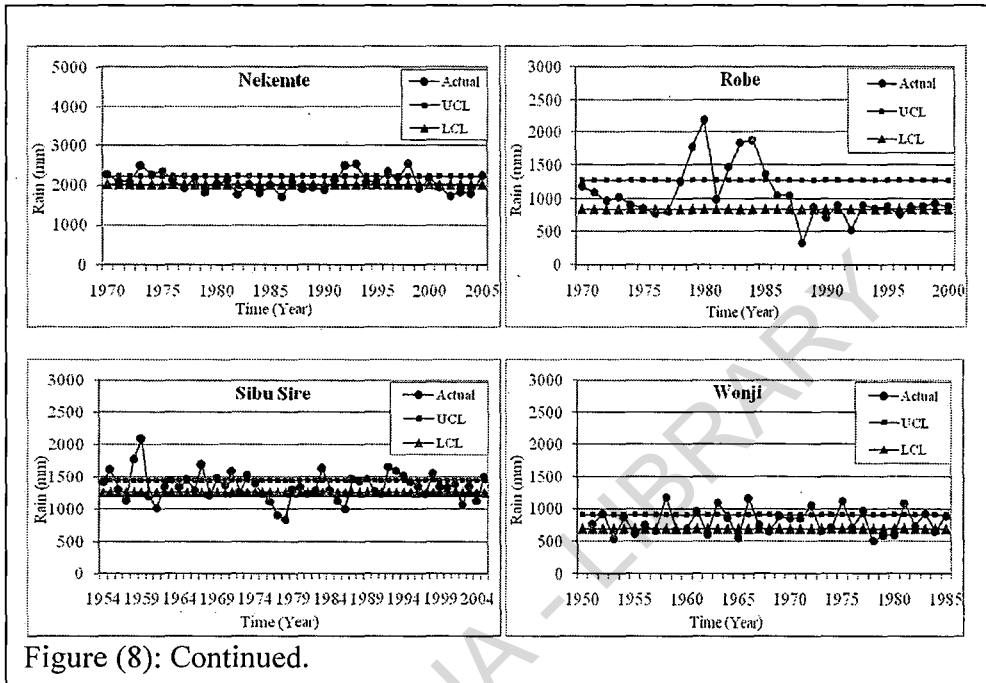


Figure (8): Continued.

4.4. Homogenization of long-term climatological series

Climate data can provide a great deal of information about the atmospheric environment that impacts almost all aspects of human life. To be accurate, the climate data used for long-term climate analyses, particularly climate change analyses, must be homogeneous. A homogeneous climate series is defined as one where variations are caused only by changes in weather and climate (*Alexandersson, 1995*). Most of the long-term climatic time series have been affected by a number of non-climatic factors that make these data unrepresentative of actual climate variations occurring over the time. These non-climatic factors which make data inhomogeneous are changes in location of the stations, instruments, formulae used to calculate means, observing practices and station environment. If a precipitation time series is homogeneous, all variability and changes of the series then can be considered due to the atmospheric processes (*Rusticucci and Renom, 2004*).

The first stage in climate change studies based on long climate records is almost inevitably a homogeneity testing of climate data. One type of non-homogeneity in long meteorological time series is sudden shifts of the mean level compared with surrounding sites. Such unrepresentative shifts are often related to relocations of the station but also may be caused by changes in observing schedules and practices, changes in instrument exposure or abrupt changes in the immediate environment (*Heino, 1994*). Changes in the surroundings also may be more gradual in the case of an urban influence, which affects mainly temperature data. Gradual changes also may be caused by trees growing in height, which reduces wind speeds and causes changes in the catchment efficiency of precipitation gauges.

Numerous methods have been used to evaluate the homogeneity of monthly and annual climate data series (*Folland and Salinger, 1995*).

Different homogenization procedures were used together with the aim of comparison. The selected test methods are: the ANOVA and Bartlett test. The temperature time series records may be influenced by various sources of homogeneity. Non-climatic variations may be caused by site change, change in means of measurement, change in observational time and the method of estimating daily and monthly averages.

An investigation of climatic change must be based on a homogeneous climatological time series. The non-homogeneity of the data usually creates some problems to researchers which study the time series analysis.

According to the statistical test for homogeneity, all data series under study were shown as homogeneous data, except precipitation for some stations.

Annual precipitation totals of each station were tested by the ANOVA and Bartlett test. The results of the ANOVA showed that 20 out of 26 stations have an inhomogeneity. According to the Bartlett test, 22 out of 26 stations were found to be inhomogeneous. 20 out of 26 stations have an inhomogeneity according to the results of both tests.

4.5. Results of statistical analysis for maximum temperature

The climatological characteristics of the climatic changes including the overall long-term mean (\bar{x}), the standard deviation (s), and the coefficient of variation (CV) are computed for each parameter in the study.

Different statistical characteristics like mean and coefficients of variation (CV) of annual maximum temperature over different stations under consideration in Ethiopia are calculated for different months and for the season as a whole.

The new results of this work concern (1) the presentation of characteristic coefficients of variation ($CV=SD/MV$; SD =Standard deviation; MV =mean value) for a comprehensive set of lake variables, (2) the use of these CV-values in describe the variation, and (3) the implication this has for the structuring of data management models.

In Table (12), it is found that the study period has mean value range between (22.4 and 34.8), standard deviation (0.4-0.8), variance (0.1-0.7) and coefficients of variation (1.1%-3.48%).

The standard deviation was low and the highest value was 0.8 at Addis Ababa, Kombolcha and Mekele stations and that indicated the maximum temperature value from different stations did not had extreme value, so this data is good and the coefficients of variation not more than 4 %.

The highest value of coefficients of variation was 3.48 % at Mekele station also this station has the highest standard deviation (0.8), so there is no extreme values at any station; as standard deviation was low. It is noted that coefficients of variation not more than 5% and that indicated the data did not had extreme values at any station. Standard deviation and coefficients of variation are the best statistical analyses tests to know the values of extreme data.

4.6. The skewness coefficient for maximum temperature

The skewness coefficient provides, to some degree, a statistical measure for extreme events; a larger absolute value of the skewness coefficient indicates that there are stronger monthly maximum temperature anomalies and/or more frequent occurrences of them. Since the standard deviation and mean used to estimate the skewness coefficient are based on each annual record, the results mainly measure the intra-annual variability of large or extreme monthly maximum temperature anomalies (*Dao-yi and Chang-hoi, 2004*).

The mean condition of the skewness coefficients displays well-defined features (Table 13). There are 9 positively skewed stations and 5 negatively skewed stations.

The main negatively skewed region covers about 6 to 12°N, including most of the center and eastern Ethiopia. On the other hand, there are two positively skewed regions, one located in southern Ethiopia and the other in northeastern Ethiopia.

The Kurtosis coefficient displays well-defined features (Table 13). There are 9 positively kurtosis stations and 9 negatively kurtosis stations.

4.7. Maximal value and minimal value for maximum temperature

Higher values of extreme maximum temperature were recorded mostly during the hot season (Belg). In particular, the extreme maximum temperature values had exceeded 35.7°C over Gode. On the other hand, nights and early mornings were cold over the highlands of northeast, central and southern Ethiopia during the dry season (Bega) (*ENMA, 2011*).

In Table (14), it is found that gradual increase in the mean for maximum temperature from the 1st Quarter (25%) to the last 3rd Quarter (75%) for all stations [1st Quarter (25%) < median < 3rd Quarter (75%)].

4.8. Test of normality for maximum temperature

The Kolmogorov-Smirnov test of normality, we note that if the normality test indicates a departure from normality then it may be that the statistical model is correct except that the error distribution is not normal, or that the statistical model and normality is correct but the data are not independent, or that the statistical model is wrong.

It is important to know whether the experimental data can be fitted to some type of theoretical distribution. The fit of the annual values of maximum temperature to a normal distribution was carried out by the Kolmogorov-Smirnov test (K-S) with a significance level. The value of the statistic K-S appears in the first column of (Table 15) and the significance level (SL) in the same column. The null hypothesis in the K-S test accept a normal distribution if the value of non significance level is higher than 0.05.

As the data are not normally distributed, the non-parametric test of Kruskal-Wallis was used with the aim of finding out whether the median of the different annual are statistically the same (Gondar, 1998). It was found that significant differences exist between the medians of each annual with a confidence level of 95%.

In Table (15), Kolmogorov-Smirnov test showed that all stations had normal distribution except one station (Jima). The results of this test were no significant and that indicate similarity and normal distribution for the all data.

4.9. Linear regression model for maximum temperature

Regression models have become standard actuarial tools for analyzing trends in frequency, severity, pure premium, reserves, development factors, and so on. One of the simplest methods of trend detection and estimation is simple linear regression. In this method the expected annual summary statistic is assumed to be linear in the year, so the estimated means plot as a straight line. This statistical model is usually fitted by least squares, which is defined as finding the straight line such that the squared errors about that line (Squared differences between the observed annual summary statistic and the estimate from the straight line trend) are minimized. That method is most appropriate when the annual summary statistics are normally distributed with a constant variance (*Abdullah and Al-Mazroui, 1998*).

The study reveals overall increasing trends in maximum temperature (significant at 95% confidence level) at different rates in the study period.

Maximum surface temperatures have risen in Ethiopia during the last 50 years period (1955-2004), as observed from instrumental recorded data obtained from Meteorological Agency of Ethiopia. The change of maximum surface air temperatures in Ethiopia is similar with global trend shown in (*IPCC, 2007*).

The observed yearly mean of maximum surface air temperatures of 16 meteorological stations in Ethiopia shows minimal increasing trend during the period 1950-2005. This increase of mean of maximum temperatures has been observed since the beginning of 1990 (*Fekadu, 2009*). The mean of maximum temperatures in Ethiopia has minimal increased by 0.02°C for 16 meteorological stations.

According to the least-square method test for trend (Table 16), positive trends of the mean annual maximum temperature (Long period) were observed at

all study stations. The trends ranged between 0 and 0.06 C°/years at Diredawa (East Ethiopia) (Figure 9).

For significance of trends, according to least-square method test for trend, the trends at all stations were significant at 0.05 level except Assosa, Awash, Diredawa, Gode, Jijiga, Jima and Mekele were not significant in this period.

4.10. R-Square for maximum temperature

The curve fitting toolbox supports the goodness of fit statistics for parametric models:

- The sum of squares due to error (SSE)
- R-square
- Adjusted R-square
- Mean squared error (MSE)

Sum of squares due to error: this statistics measures the total deviation of the response values from the fit to the response values. It is also called summed squared of residuals and is usually labeled as SSE (*Al-Ansari, et al., 2006*).

R-Square: this statistics measure how successful the fit is in explaining the variation of the data. Put in a different way, R-square is the square of the correlation between the response values and the predicated response values. It is also called the square of the multiple correlation coefficients and the coefficient of multiple determinations. R-square is defined as the ratio of the sum of squares of the regression (SSR) and the total sum of squares (SST) (*Draper and Smith, 1998*).

R-Squared is a statistical term saying how good one term is at predicting another. If R-Squared is 1.0 then given the value of one term, you can perfectly predict the value of another term. If R-squared is 0 then knowing one term doesn't

not help you to predict the other term at all. More generally, a higher value of R-Squared means that you can better predict one term from another.

In (Table 16), it is found that R-squared (0-0.48), so the highest value is 0.48 and this value is low as regarding linear regression model. If we divided all stations as regarding R-squared we found that all stations had R-squared less than 0.4 except four stations Addis Ababa, Awassa, Gonder and Nekemte. While sum of squares due to error was (18-29.5) the highest value was at Mekele station and the lowest value was at Gode station.

Mean squared error (MSE) was (0.1-0.7) the highest value was at Mekele station and the lowest value was at Gode and DebraMarkos station.

Table (12): Statistical characteristics for mean annual maximum temperature.

Station	Period	N	Arithmetic mean	SD	Variance	Coefficient of variation
Addis Ababa	(1960-2005)	46	22.7	0.8	0.6	3.47
Arbaminch	(1970-2005)	36	30	0.6	0.4	2.12
Assosa	(1970-2005)	36	28.2	0.7	0.4	2.31
Awash	(1970-2000)	31	33.3	0.5	0.3	1.6
Awassa	(1970-2005)	36	26.9	0.6	0.4	2.28
Bahar Dar	(1960-2005)	46	26.8	0.7	0.4	2.49
Kombolcha	(1950-2005)	56	26.2	0.8	0.6	2.94
Debramarkos	(1950-2005)	56	22.4	0.4	0.2	1.87
Debre Zeit	(1950-2005)	56	26.3	0.5	0.2	1.74
Diredawa	(1950-2005)	56	31.5	0.5	0.3	1.62
Gode	(1970-2000)	31	34.8	0.4	0.1	1.11
Gondar	(1950-2005)	56	26.5	0.5	0.3	1.95
Gore	(1950-2005)	56	23.5	0.5	0.2	2.03
Jijiga	(1950-2005)	56	27.3	0.5	0.2	1.81
Jima	(1950-2005)	56	26.9	0.5	0.2	1.8
Mekele	(1960-2005)	46	24.3	0.8	0.7	3.48
Negele	(1950-2005)	56	25.9	0.5	0.3	1.95
Nekemte	(1970-2005)	36	24	0.5	0.3	2.12

Table (13): Coefficient of skew and kurtosis for mean annual maximum temperature.

Station	Coefficient of Skew	Coefficient of Kurtosis
Addis Ababa	-0.1	-1.1
Arbaminch	0	-0.1
Assosa	0.6	1.5
Awash	0.9	1.7
Awassa	-0.4	-0.6
Bahar Dar	0.5	-0.2
Kombolcha	0.2	5.8
Debramarkos	0.1	-0.1
Debre Zeit	1	3.4
Diredawa	0	1.8
Gode	0.1	0.7
Gondar	0.6	0.6
Gore	0	-0.2
Jijiga	-0.4	0
Jima	0.7	1.2
Mekele	-0.1	-0.6
Negele	-0.1	-0.7
Nekemte	0	-0.8

Table (14): Statistical characteristics of mean annual maximum temperature as regarding (maximum, minimum value, 1st Q (25%), Median and 3rd Q (75%).

Station	Maximal value (year)	Minimal value (year)	1 st Q (25%)	Median	3 rd Q (75%)
Addis Ababa	24.3 (1995)	21.3 (1971)	22	22.9	23.3
Arbaminch	31.6 (1973)	28.8 (1978)	29.6	30.1	30.4
Assosa	29.9 (1984)	26.8 (1975)	27.9	28.2	28.4
Awash	34.8 (1980)	32.4 (1994)	33	33.2	33.5
Awassa	27.9 (1995)	25.6 (1977)	26.4	27	27.3
Bahar Dar	28.2 (1973,2003)	25.6 (1975)	26.3	26.7	27.1
Kombolcha	29.2 (2004)	23.4 (1952)	25.7	26.2	26.6
Debramarkos	23.3 (1995)	21.4 (1956)	22.1	22.4	22.6
Debre Zeit	28.1 (2002)	25.4 (1951)	25.9	26.3	26.5
Diredawa	33.0 (1959)	30.0 (1967)	31.3	31.5	31.8
Gode	35.7 (1979)	33.9 (1981)	34.6	34.8	35
Gondar	28.1 (2003)	25.6 (1952, 1955)	26.3	26.5	26.8
Gore	24.5 (2005)	22.4 (1985)	23.2	23.4	23.8
Jijiga	28.2 (1958, 2003)	26.1 (1967)	27.1	27.3	27.6
Jima	28.3 (1958)	26.0 (1971)	26.6	26.9	27
Mekele	25.8 (1966,1972)	22.6 (1975)	23.9	24.3	24.9
Negele	27.1 (1980)	25.0 (1952,1968,1985)	25.5	25.9	26.4
Nekemte	24.9 (2003,2005)	23.1 (1974)	23.6	24	24.3

Table (15): Statistical characteristics of mean annual maximum temperature as regarding (normal distribution and linear regression model).

Station	Kolmogorov-Smirnov test for Normal Distribution	Linear Regression Model ($y=b_0+b_1*x$)		T-test for Coefficient b_1	Trend /10 years
		b_0	b_1		
Addis Ababa	0.537	21.8026	0.039	5.959 *	0.4
Arbaminch	0.733	29.4175	0.03	3.907 *	0.3
Assosa	0.151	27.8843	0.016	1.628	0.2
Awash	0.271	33.5548	-0.016	-1.623	-0.2
Awassa	0.336	26.1654	0.039	5.274 *	0.4
Bahar Dar	0.677	26.06	0.029	4.858 *	0.3
Kombolcha	0.438	25.55	0.021	3.787 *	0.2
Debramarkos	0.570	22.02	0.01	3.792 *	0.1
Debre Zeit	0.687	25.90	0.012	3.705 *	0.1
Diredawa	0.087	31.45	0.001	0.259	0.0
Gode	0.897	34.7	0.008	1.079	0.1
Gondar	0.346	26	0.018	5.422 *	0.2
Gore	0.489	23.02	0.015	4.466 *	0.2
Jijiga	0.337	27.3	0.001	0.419	0.0
Jima	0.007*	26.9	-0.00	-0.133	0.0
Mekele	0.445	24.7	-0.017	-1.964	-0.2
Negele	0.757	25.5	0.01	3.710 *	0.1
Nekemte	0.780	23.4	0.03	5.626 *	0.3

* p- Value < 0.05 is significant, p-value > 0.05 non significant

Table (16): Accuracy measures of mean annual maximum temperature.

Station	Linear trend equation ($y=b_0+b_1*x$)	R-square	Sum square error (SSE)	Mean square error (MSE)
Addis Ababa	0.04*	0.45	15.4	0.4
Arbaminch	0.03*	0.31	9.8	0.3
Assosa	0.02	0.10	13.8	0.4
Awash	-0.01	0.10	7.8	0.3
Awassa	0.04*	0.45	7.2	0.2
Bahar Dar	0.03*	0.35	13.0	0.3
Kombolcha	0.02*	0.21	25.6	0.5
Debramarkos	0.01*	0.21	7.6	0.1
Debre Zeit	0.01*	0.20	9.2	0.2
Diredawa	0.00	0.0	14.2	0.3
Gode	0.00	0.0	4.3	0.1
Gondar	0.02*	0.40	9.6	0.2
Gore	0.02*	0.35	9.1	0.2
Jijiga	0.00	0.0	13.5	0.2
Jima	0.00	0.0	12.9	0.2
Mekele	-0.02	0.10	29.5	0.7
Negele	0.01*	0.20	11.2	0.2
Nekemte	0.03*	0.48	4.7	0.1

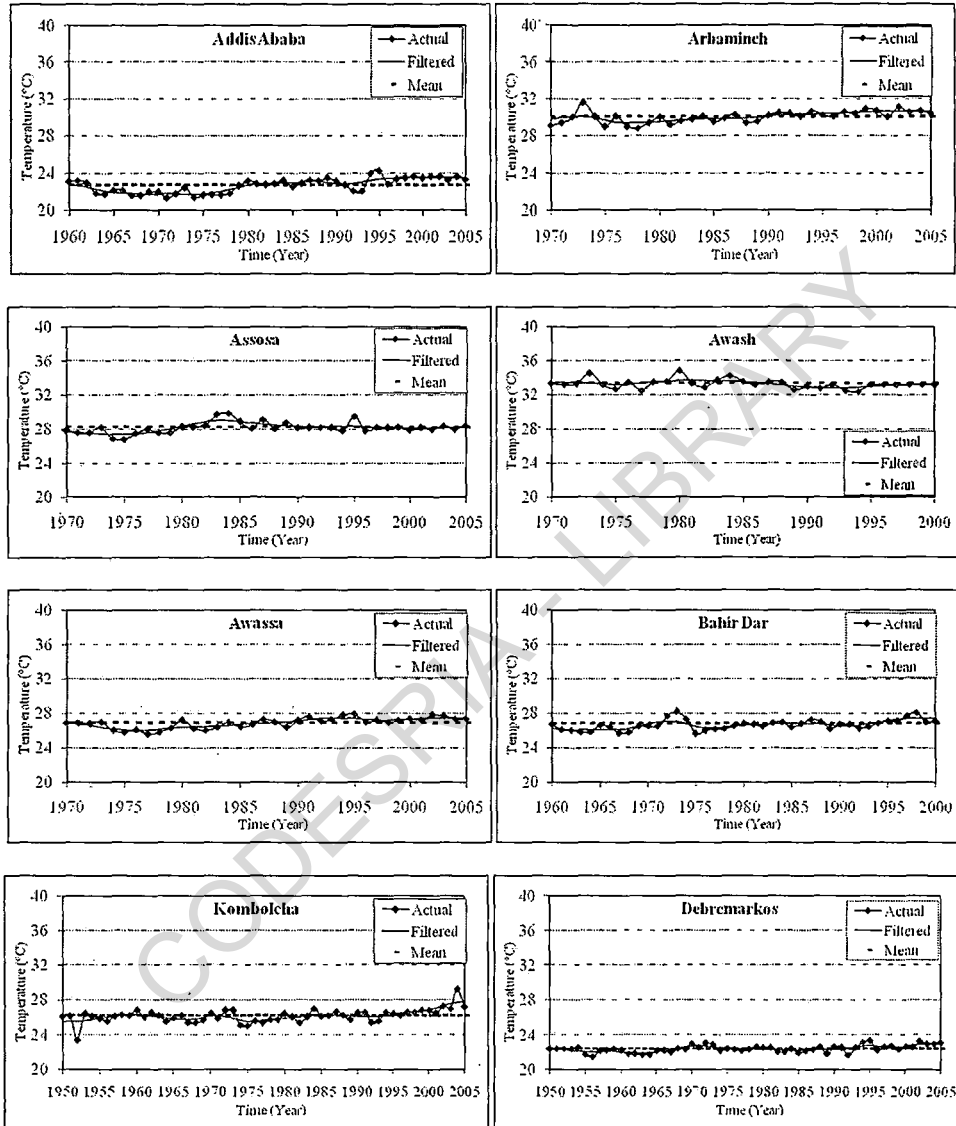


Figure (9): Trend of mean annual maximum temperature.

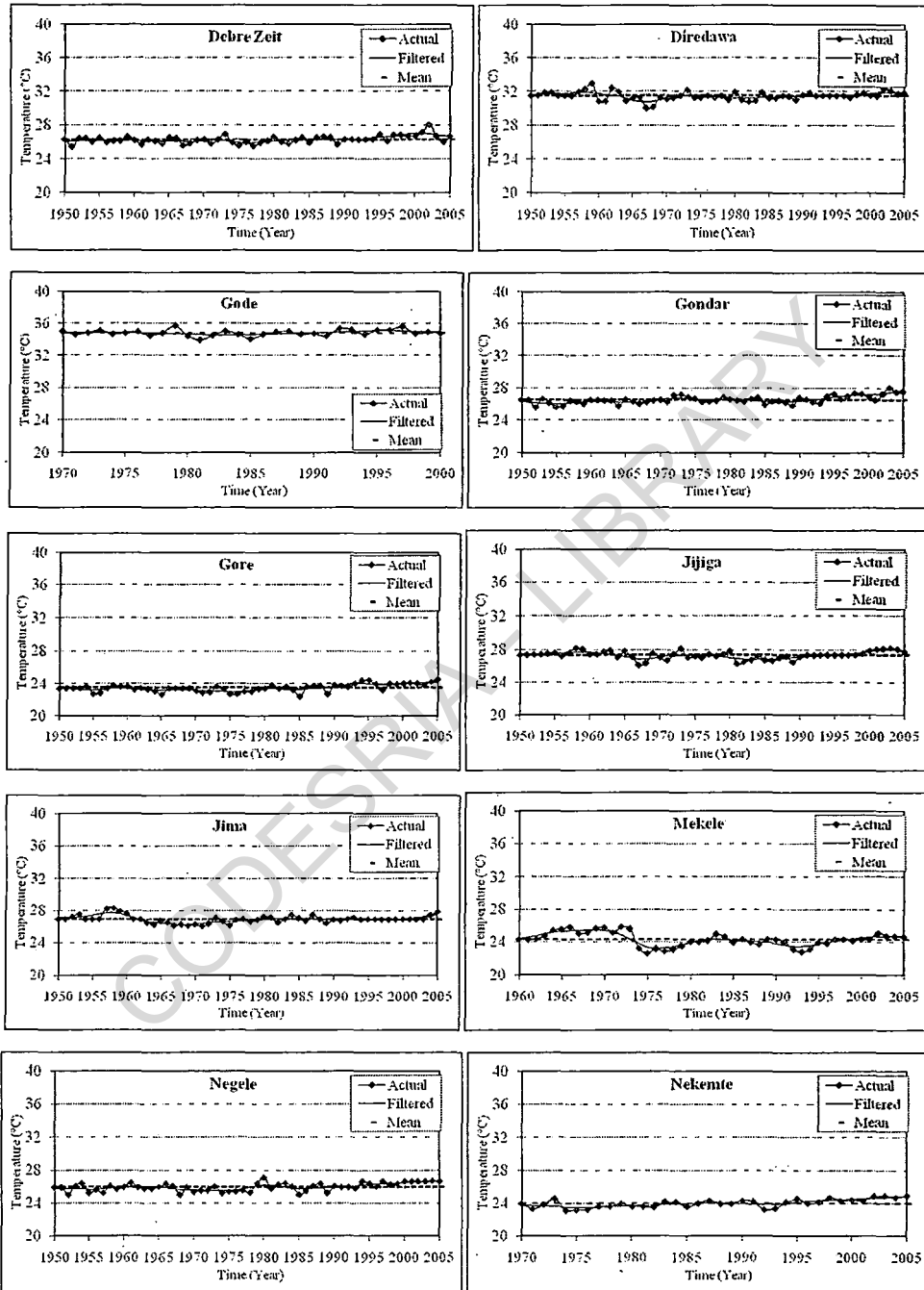


Figure (9): Continued.

4.11. Results of statistical analysis for minimum temperature

The past observed climate change impact has been analyzed employing meteorological station data obtained from Meteorology Agency of Ethiopia. Observed minimum surface air temperature for the period 1950-2005 has been analyzed using 18 stations data collected from different climatic zone over the country.

In (Table 17), it is found that the study period from (1950-2005) had mean (9.4-22.7), standard deviation (0.4-1.4), variance (0.2-2.1) and coefficients of variation (3.2%-12.3%). We noted that standard deviation was low and the highest value was 1.4 at Bahir Dar and Negele station and that indicated the minimum temperature value from different station did not had extreme value, so this data is good and the coefficients of variation not more than 13%.

The highest value of coefficients of variation was 12.3 % at Bahir Dar station also this station had the highest standard deviation (1.4). It is noted that coefficients of variation not more than 13% and that indicated the data did not had extreme values at any station.

Coefficients of variation was more than 10% at Bahir Dar, Kombolcha, Debremarkos and Negele station, while it was (More than 5% and less than 10%) at Addis Ababa, Arbaminch, Awassa, Debre Zeit, Diredawa, Gondar, Jijiga, Mekele and Negele.

4.12. The skewness coefficient for minimum temperature

The mean condition of the skewness coefficients displays well-defined features (Table 18). There are 5 positively skewed stations and 13 negatively skewed stations. And the Kurtosis coefficient displays well-defined features (Table 18). There are 12 positively skewed stations and 3 negatively skewed stations.

4.13. Maximal value and minimal value for minimum temperature

Mean of minimum surface air temperatures of 18 stations in Ethiopia, 1962 is the lowest year (6.2 °C) during the period 1950-2005 at Debremarkos station in the Ethiopia, In Table (19), we found that gradual increase in the mean for minimum temperature from the 1st Quarter (25%) to the last 3rd Quarter (75%) for all stations [1st Quarter (25%) < median < 3rd Quarter (75%)].

4.14. Test of normality for minimum temperature

In Table (20), Kolmogorov-Smirnov test showed that all stations had normal distribution except five stations (Kombolcha, Diredawa, Gode, Mekele and Negele). The results of this test were no significant and that indicate similarity and normal distribution for the all data.

4.15. Linear regression model for minimum temperature

Changes in temperature and rainfall patterns are widely observed in many semi-arid parts of the developing world that are likely to become even hotter and dryer with time (*Collier and Dercon, 2008*). Recent observational and modeling studies showed that the warmest temperature extremes, particularly those derived from minimum temperature, have significantly increased over the 20th century and will continue to increase throughout the 21st century (*Gebrehiwot and Anne, 2013*).

Evidences suggest that globally, there have been more flood/drought-inducing events, which are set to escalate in frequency and intensity in the future. The average temperature rise in Africa is faster than the global average and is likely to persist in the future. This warming occurred at the rate of about 0.5°C per decade with a slightly larger warming in crops are grown close to the thermal tolerance limits (*Collier and Dercon, 2008*).

The observed yearly mean of minimum surface air temperatures of 18 meteorological stations in Ethiopia shows minimal increasing trend during the period 1950-2005. The mean of minimum temperatures in Ethiopia has minimal increased by 0.027 °C for all meteorological stations except one station (Metehara).

According to the least-square method test for trend (Table 21), positive trends of the mean annual minimum temperature (Long period) were observed at all study stations except one station. The trends ranged between 0.01 and 0.07 C°/years at Arbaminch (South Ethiopia) (Figure 10).

For significance of trends, according to least-square method test for trend, the trends at all stations were significant at 0.05 level except three stations Assosa, Kombolcha and Mekele were not significant in this period.

4.16. R-Square for minimum temperature

In (Table 21), it is found that R-squared (0.01-0.58), so the highest value is 0.58 and this value is low as regarding linear regression model. If we divided all stations as regarding R-squared we found that all stations had R-squared less than 0.40 except four stations Arbaminch, Debremarkos, Gore, Metehara, Negele and Nekemte. While sum of squares error was (6.8-77.8) the highest value was at Kombolcha station and the lowest value was at Negele station.

Mean squared error (MSE) was (0.1-1.4) the highest value was at Kombolcha station and the lowest value was at Nekemte and debramarkos station.

Table (17): Statistical characteristics for mean annual minimum temperature.

Station	Period	N	Arithmetic mean	SD	Variance	Coefficient of variation
Addis Ababa	(1950-2005)	56	9.6	0.9	0.9	9.9
Arbaminch	(1970-2005)	36	16.3	1.2	1.4	7.3
Assosa	(1970-2005)	36	15.1	0.7	0.4	4.4
Awassa	(1970-2005)	36	12.4	0.7	0.5	5.5
Bahir Dar	(1960-2005)	46	11.7	1.4	2.1	12.3
Kombolcha	(1950-2005)	56	11.9	1.2	1.4	10.1
Debremarkos	(1950-2005)	56	9.4	1	0.9	10.1
Debre Zeit	(1950-2005)	56	11.6	0.7	0.5	5.9
Diredawa	(1950-2005)	56	18.5	1.1	1.2	5.9
Gode	(1970-2005)	36	22.7	0.8	0.6	3.3
Gondar	(1950-2005)	56	13	0.7	0.5	5.3
Gore	(1950-2000)	51	13.3	0.4	0.2	3.2
Jijiga	(1950-2005)	56	11.4	1	1	8.7
Jima	(1950-2005)	56	11	0.5	0.2	4.4
Mekele	(1960-2005)	46	11.2	0.8	0.7	7.2
Metehara	(1970-2005)	36	18.4	0.8	0.7	4.6
Negele	(1950-2005)	56	13.9	1.4	2.1	10.4
Nekemte	(1970-2005)	36	12.6	0.6	0.4	4.9

Table (18): Coefficient of skew and kurtosis for mean annual minimum temperature.

Station	Coefficient of Skew	Coefficient of Kurtosis
Addis Ababa	-0.2	0.6
Arbaminch	-0.7	0.4
Assosa	0.1	-0.5
Awassa	-0.8	0.6
Bahir Dar	-0.7	0
Kombolcha	-1.7	4
Debremarkos	-0.9	1.1
Debre Zeit	0.2	0
Diredawa	-3.2	12.6
Gode	-2.1	7.5
Gondar	-0.2	0
Gore	0.4	0.1
Jijiga	-0.3	2
Jima	-1.2	2.8
Mekele	-1.5	1.5
Metehara	0.2	-0.3
Negele	0.2	-0.5
Nekemte	-1	1.4

Table (19): Statistical characteristics of mean annual minimum temperature as regarding (maximum, minimum value, 1st Q (25%), Median and 3rd Q (75%).

Station	Maximal Value (year)	Minimal Value (year)	1st Q (25%)	Median	3 rd Q (75%)
Addis Ababa	11.5 (1983)	6.8 (1957)	9	9.6	10.3
Arbaminch	18.2 (1991)	13.1 (1976)	15.5	16.4	17.3
Assosa	16.4 (1986)	13.7 (1985)	14.8	15	15.7
Awassa	13.7 (1998)	10.6 (1984)	12.1	12.4	12.8
Bahir Dar	13.8 (1997)	7.8 (1978)	10.9	12.1	12.7
Kombolcha	13.5 (1983)	7.1 (1985)	11.7	12.2	12.7
Debremarkos	10.9 (1998)	6.2 (1962)	8.9	9.6	10.1
Debre Zeit	13.1 (2002,2003)	10.0 (1972)	11.1	11.6	12
Diredawa	19.6 (1980)	13.6 (1952)	18.3	18.6	19.1
Gode	23.8 (2002,2005)	19.6 (1978)	22.5	22.8	22.9
Gondar	14.4 (1995)	11.2 (1989)	12.5	13	13.5
Gore	14.6 (2002,2005)	12.4 (1971)	13.1	13.5	13.8
Jijiga	14.0 (1997)	8.1 (1952)	11	11.3	12.1
Jima	11.9 (1977)	9.2 (1956)	10.8	11	11.4
Mekele	12.2 (1997,1998)	8.8 (1979)	11.2	11.5	11.7
Metehara	20.3 (1980)	16.5 (1985)	17.8	18.3	18.9
Negele	16.3 (2002)	10.5 (1956)	13	13.5	15.4
Nekemte	13.5 (2003)	10.8 (1987)	12.3	12.7	13

Table (20): Statistical characteristics of mean annual minimum temperature as regarding (normal distribution and linear regression model).

Station	Kolmogorov-Smirnov test for Normal Distribution	Linear Regression Model ($y=b_0+b_1*x$)		T-test for Coefficient b1	Trend /10 years
		b0	b1		
Addis Ababa	0.576	8.99	0.02	2.898 *	0.2
Arbaminch	0.896	14.82	0.07	5.744 *	0.9
Assosa	0.543	14.9	0.01	1.117	0.2
Awassa	0.060	11.7	0.03	3.607 *	0.4
Bahir Dar	0.427	10.1	0.07	5.640 *	0.7
Kombolcha	0.015*	11.6	0.01	1.141	0.1
Debremarkos	0.426	8.2	0.04	7.788 *	0.4
Debre Zeit	0.831	11.1	0.017	3.300 *	0.2
Diredawa	0.006*	17.6	0.03	3.629 *	0.3
Gode	0.045*	22.1	0.03	2.736 *	0.3
Gondar	0.987	12.2	0.02	5.184 *	0.2
Gore	0.279	12.9	0.01	3.844 *	0.1
Jijiga	0.483	10.4	0.03	5.049 *	0.3
Jima	0.338	10.6	0.01	3.289 *	0.1
Mekele	0.003*	10.9	0.01	1.140	0.1

* p-value < 0.05 is significant, p-value > 0.05 non significant

Table (20): Continued.

Station	Kolmogorov-Smirnov test for Normal Distribution	Linear Regression Model ($y=b_0+b_1*x$)		T-test for Coefficient b_1	Trend /10 years
		b_0	b_1		
Metehara	0.965	19.1	-0.04	-3.261 *	-0.4
Negele	0.011*	11.9	0.06	8.615 *	0.7
Nekemte	0.644	11.8	0.03	5.577 *	0.4

* p- value < 0.05 is significant, p-value > 0.05 non significant

Table (21): Accuracy measures of mean annual minimum temperature.

Station	Linear trend equation	R-square	Sum square error (SSE)	Mean square error (MSE)
Addis Ababa	$Y_t = 8.9947 + 0.021302 * t$	0.13	42.7	0.8
Arbaminch	$Y_t = 14.822 + 0.078829 * t$	0.49	24.9	0.7
Assosa	$Y_t = 14.907 + 0.011776 * t$	0.04	14.7	0.4
Awassa	$Y_t = 11.729 + 0.033874 * t$	0.28	11.7	0.3
Bahir Dar	$Y_t = 10.067 + 0.070085 * t$	0.38	53.4	1.3
Kombolcha	$Y_t = 11.602 + 0.011319 * t$	0.02	77.8	1.4
Debremarkos	$Y_t = 8.2166 + 0.042587 * t$	0.53	23.6	0.4
Debre Zeit	$Y_t = 11.115 + 0.017085 * t$	0.20	21.2	0.4
Diredawa	$Y_t = 17.622 + 0.029563 * t$	0.20	52.4	1.0
Gode	$Y_t = 22.125 + 0.030309 * t$	0.18	16.2	0.5
Gondar	$Y_t = 12.29 + 0.02446 * t$	0.33	17.6	0.3
Gore	$Y_t = 12.888 + 0.02055 * t$	0.42	8.7	0.2
Jijiga	$Y_t = 10.693 + 0.012269 * t$	0.17	11.0	0.2
Jima	$Y_t = 12.076 + 0.0035081 * t$	0.01	7.5	0.3
Mekele	$Y_t = 19.085 - 0.039266 * t$	0.24	19.2	0.6
Metehara	$Y_t = 11.958 + 0.067006 * t$	0.58	47.8	0.9
Negele	$Y_t = 11.814 + 0.039936 * t$	0.46	6.8	0.2
Nekemte	$Y_t = 12.974 + 0.013837 * t$	0.48	7.0	0.1

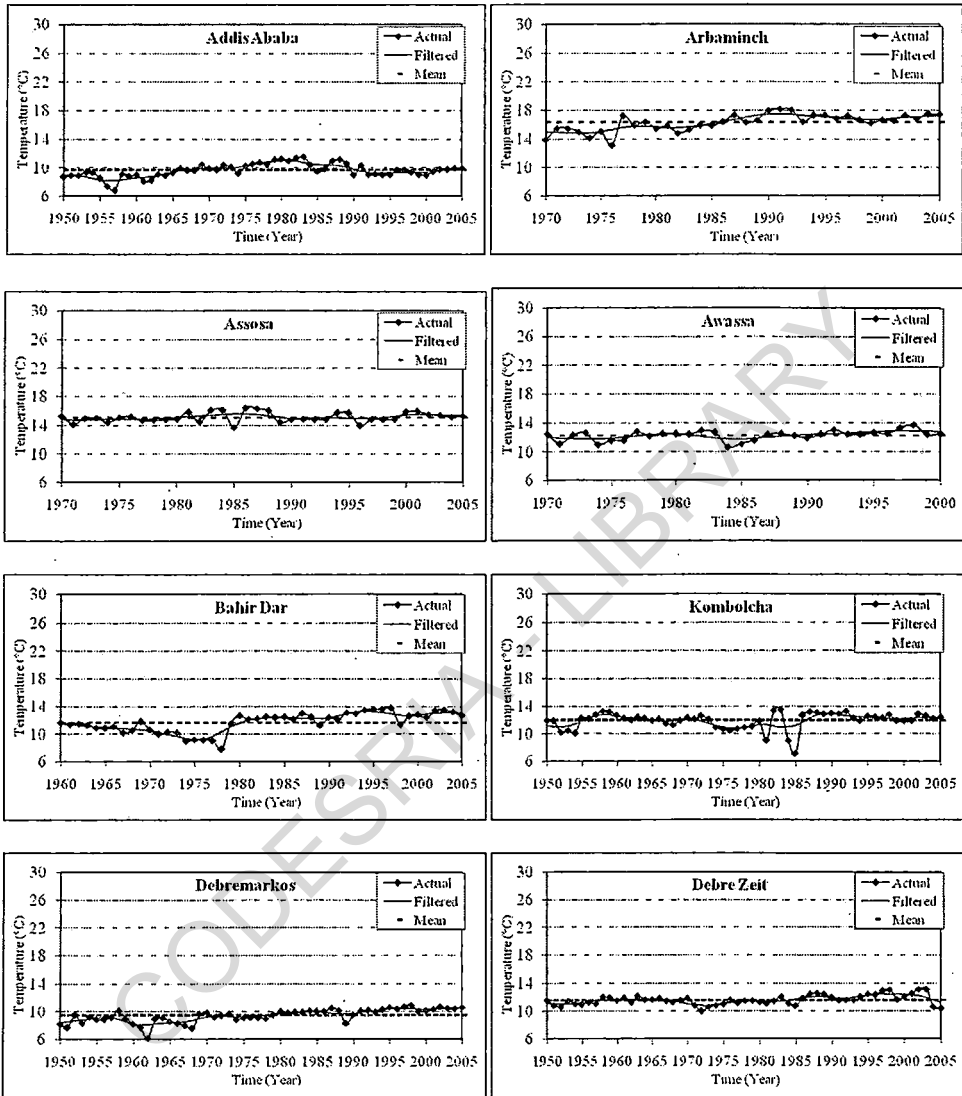


Figure (10): Trend of mean annual minimum temperature.

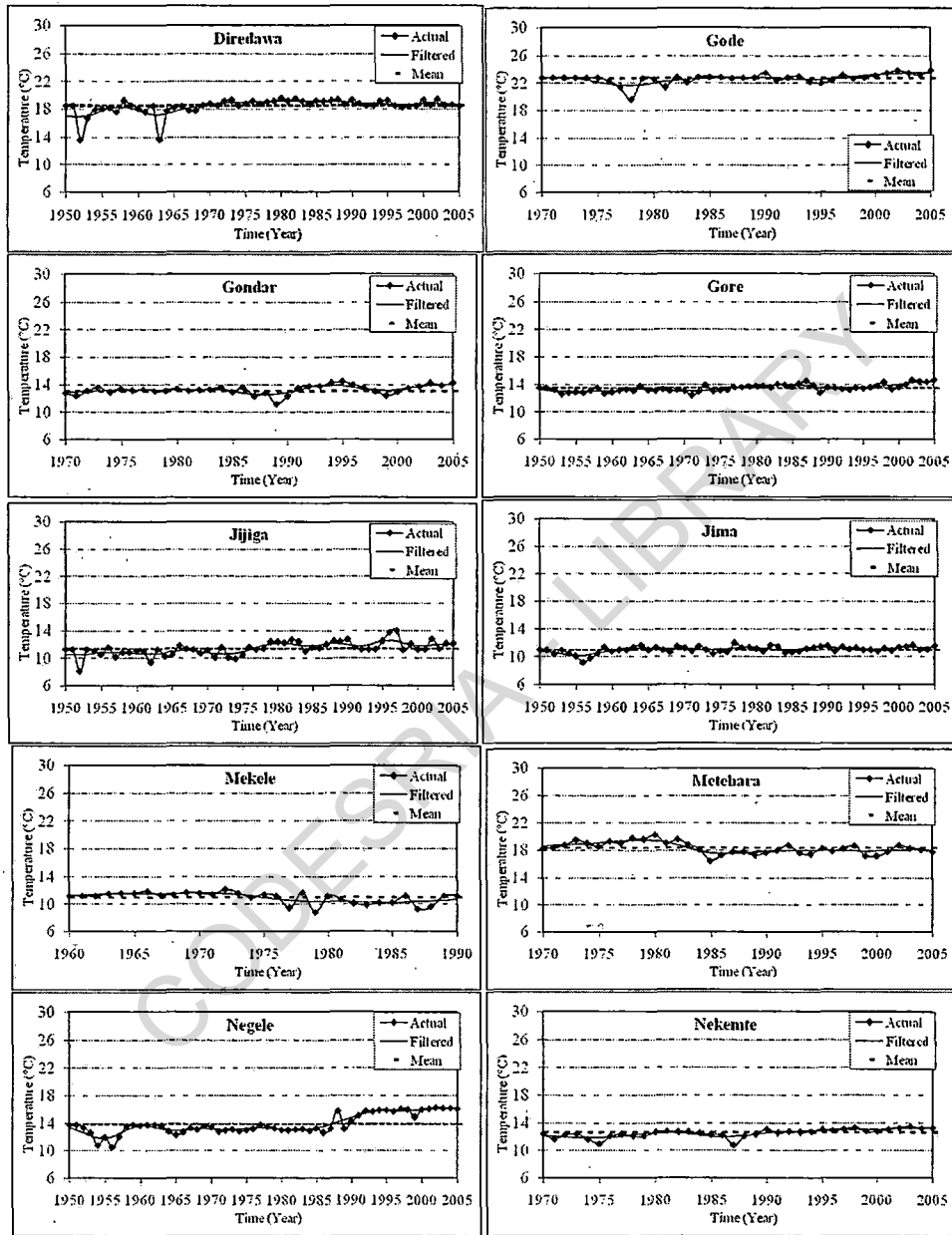


Figure (10): Continued.

4.17. Results of statistical analysis for annual rainfall

Ethiopia is a large complex country, with complex patterns of rainfall and livelihoods. In Ethiopia, higher elevations receive more rainfall than low arid areas and support agricultural livelihoods and higher population densities (Cheung, *et al.*, 2008).

Historical records of monthly rainfall from 26 stations for the period 1950-2005 were provided by Meteorology Agency of Ethiopia. However, the period of records for these stations varies and some have missing records. Thus, the period of study has been chosen as long as possible depending on the availability of the recorded data collected from different climatic zones in Ethiopia (ENMA, 2001).

In (Table 22), it is found that the study period from (1950-2005) had mean (242-2099.6), standard deviation (125.5-404.4), variance (15753.5-163500.8) and coefficients of variation (10.9%-57.3%). We noted that standard deviation was high and the highest value was 404.4 at Robe station and that indicated the total annual precipitation value from different station had extreme value.

The highest value of coefficient variation was 57.3 % at Gode station that had standard deviation (138.6). It is noted that coefficients of variation are more than 50% indicating that data had extreme values in some stations.

Coefficients of variation were higher than 50% at only one station (Gode station), while it was (higher than 30% and less than 50%) at three stations (Assosa, Jijiga and Robe).

4.18. The skewness coefficient for annual rainfall

The mean condition of the skewness coefficients displays well-defined features (Table 23). There are 21 positively skewed stations and 5 negatively skewed stations. The Kurtosis coefficient displays well-defined features (Table 23). There are 20 positively skewed stations and 6 negatively skewed stations.

4.19. Maximal and minimal values for annual rainfall

Total annual precipitation of 26 stations in Ethiopia, we noted that 1967 had the highest value (3282 mm) during the period 1950-2005 at gore station in the Ethiopia, In (Table 24), we found that gradual increase in the total annual precipitation from the 1st Quarter (25%) to the last 3rd Quarter (75%) for all stations [1st Quarter (25%) < median < 3rd Quarter (75%)].

4.20. Test of normality for annual rainfall

In Table (25), Kolmogorov-Smirnov test showed that all stations had normal distribution except only one station (Jijiga). The results of this test were insignificant and indicating similarity and normal distribution for the all data.

4.21. Linear regression model for annual rainfall

Rainfall, which is the main climatic factor, is distributed very unevenly in the study area. The climate is characterized by large spatial variations which range from about 1000-1260 mm year⁻¹ in some pockets areas in the southwest to about less than 300 mm yr⁻¹ in the Northeast lowlands (*Funk, et al., 2005*). Estimates from the historical records of precipitation for the period 1954-2008 indicate that the mean annual rainfall is 560.7mm while the mean annual kiremt rainfall is 473mm, 84% of the annual rainfall. Most areas receive less than 400 mm of rainfall yearly indicating the existence of spatial variations in precipitation consistent with topographic difference (*Gebrehiwot, and Anne, 2013*).

According to the least-square method test for trend (Table 26), positive trends of the total annual precipitation (Long period) were observed at eight stations (Arbaminch, Awash, Awassa, Debre Zeit, Dessie, Jima, Harer and Wonji) and 18 stations had negative trends of the total annual precipitation.

The trend of the observed total annual precipitation in Ethiopia for 26 meteorological stations showed decrease during the period 1950-2005 at most of stations but this decrease not high (Figure 11).

4.22. R-Square for annual rainfall

In Table (26), it is found that R-squared (0.0-0.15), so the highest value is 0.15 at (Assosa and Metehara stations) and this value is low as regarding linear regression model. All stations were divided as regarding R-squared so it is found that all stations had R-squared less than 0.05 except six stations Assosa, Bati, Gode, Metehara, Negele and Robe. While sum of squares error was (628596-12103291) the highest value was at gore station and the lowest value was at Awassa station.

Mean squared error (MSE) was (15652.5-153495.1) the highest value was at Robe station and the lowest one was at Awash station.

Table (22): Statistical characteristics for total annual precipitation.

Station	Period	N	Arithmetic mean	SD	Variance	Coefficient of variation
Addis Ababa	(1900-2005)	106	1203.6	193.2	37320.7	16.1
Arbaminch	(1960-2005)	46	872.8	140.9	19856.6	16.2
Assosa	(1960-2005)	46	1063.5	367.3	134937.2	34.5
Awash	(1950-2000)	51	643.5	125.5	15753.5	19.5
Awassa	(1970-2005)	36	926.2	135.2	18289.3	14.6
Bahir Dar	(1960-2005)	46	1444.5	233.2	54389.2	16.2
Bati	(1950-1990)	41	1044.7	174.5	30435.6	16.7
Kombolcha	(1940-2005)	66	1046.3	171.8	29501.4	16.4
Debremarkos	(1953-2005)	53	1339.8	150.5	22644.5	11.2
Debre Zeit	(1951-2005)	55	858.3	175.8	30904.7	20.5
Dessie	(1960-2005)	46	1191.2	190	36085.1	16
Diredawa	(1950-2009)	60	624.3	172.5	29739.5	27.6
Gambela	(1950-2009)	60	628.3	171.3	29343.9	27.3
Jima	(1950-2009)	60	1508.2	185.9	34569.8	12.3
Gode	(1966-2005)	40	242	138.6	19197.7	57.3
Gondar	(1950-2009)	60	1172.2	248.4	61706.9	21.2
Gore	(1910-2005)	96	2099.6	359.4	129176.7	17.1
Harer	(1950-1985)	36	879.9	223	49745.2	25.4
Jijiga	(1950-2005)	56	660.6	219.1	48007.3	33.2
Mekele	(1954-2005)	52	629.9	187.2	35041.2	29.7
Metehara	(1970-2005)	36	608.8	153.6	23595.7	25.2
Negele	(1960-2005)	46	752.3	189.1	35762.2	25.1
Nekemte	(1970-2005)	36	2081.4	225.8	51006.9	10.9
Robe	(1970-2000)	31	1056.1	404.4	163500.8	38.3
Sibu Sire	(1954-2005)	52	1354.6	220.2	48474.8	16.3
Wonji (63373)	(1951-1985)	35	802.7	191.1	36527	23.8

Table (23): Coefficient of skew and kurtosis for total annual precipitation.

Station	Coefficient of Skew	Coefficient of Kurtosis
Addis Ababa	0.9	1.2
Arbaminch	0.8	1.6
Assosa	-0.5	0.9
Awash	0.7	0.5
Awassa	0.4	-0.6
Bahir Dar	0.1	0.3
Bati	-0.4	-0.5
Kombolcha	-0.2	-0.1
Debremarkos	0.7	0.5
Debre Zeit	0.3	0.6
Dessie	-0.4	-0.4
Diredawa	0.5	1.1
Gambela	0.5	1.2
Jima	0.9	1
Gode	1.4	2.5
Gondar	1.1	1.2
Gore	1	1.8
Harer	-0.1	0.1
Jijiga	1.8	3.4
Mekele	1	1.3
Metehara	0.6	0.5
Negele	0.7	1.5
Nekemte	0.4	-0.5
Robe	1.2	1.5
Sibu Sire	0.4	1.6
Wonji (63373)	0.3	-0.4

Table (24): Statistical characteristics of total annual precipitation as regarding (maximum, minimum value, 1st Q (25%), Median and 3rd Q (75%).

Station	Maximal Value (year)	Minimal Value (year)	1st Q (25%)	Median	3 rd Q (75%)
Addis Ababa	1936.7 (1947)	895.6 (1999)	1067.2	1177.8	1311
Arbaminch	1312.6 (1997)	617.9 (1976)	808.7	855.1	933.3
Assosa	1875.5 (2001)	206.6 (1986)	1005.4	1057.7	1227.0
Awash	998.5 (1982)	418.9 (1974)	544.4	631.0	719.8
Awassa	1226.1 (1977)	724.5 (1984)	815.2	939.3	1020.4
Bahir Dar	2036.0 (1973)	894.6 (1982)	1280.0	1482.8	1569.8
Bati	1322.0 (1964)	625.0 (1984)	921.8	1067.0	1177.5
Kombolcha	1433.0 (1943)	593.0 (1984)	917.8	1048.2	1166.0
Debremarkos	1769.0 (1958)	1057.0 (1978)	1243.0	1326.7	1415.5
Debre Zeit	1355.4 (1964)	412.0 (1951)	747	833.7	947.2
Dessie	1576.3 (1998)	706.8 (1984)	1040.6	1228.1	1334.7
Diredawa	1187.5 (1956)	283.9 (1979)	504.4	623.7	721.7
Gambela	1197.5 (1956)	283.9 (1979)	509.9	630.7	721.7
Jima	2079.5 (1997)	1204.0 (1979)	1363.2	1486.7	1624.1
Gode	686.3 (1968)	38.8 (1980)	159.2	216.1	283.9
Gondar	1875.6 (2001)	713.0 (1982)	1015	1121	1295.5
Gore	3282.0 (1967)	1445.9 (2004)	1848.6	2093	2231.3
Harer	1302.8 (1950,1964)	412.1 (1951)	788.3	869.2	999.2
Jijiga	1477.8 (1976)	379.1 (1955)	522.6	598.1	694.8
Mekele	1171.7 (1986)	293.2 (1984)	490.8	612.6	714
Metehara	1008.5 (1982)	276.5 (2002)	499.1	582	708.7
Negele	1381.2 (1972)	358.8 (1999)	632.3	730.4	843.8
Nekemte	2551.4 (1998)	1714.7 (1986)	1923.2	2079.9	2219.3
Robe	2184.0 (1980)	327.1 (1988)	860.7	907.8	1157.3
Sibu Sire	2081.0 (1959)	835.4 (1978)	1231.8	1336.1	1469.8
Wonji	1181.0 (1958)	544.0 (1950,1953)	700	815.6	913.5

Table (25): Statistical characteristics of total annual precipitation as regarding (normal distribution and linear regression model).

Station	Kolmogorov-Smirnov test for Normal Distribution	Linear Regression Model ($y=b_0+b_1*x$)		T-test for Coefficient b_1	Trend /10 years
		b_0	b_1		
Addis Ababa	0.613	1244.6	-0.8	-1.253	-7.7
Arbaminch	0.451	825.5	2.0	1.294	20.1
Assosa	0.054	1312.3	-10.6	-2.784 *	-105.9
Awash	0.311	607.9	1.4	1.150	13.7
Awassa	0.738	923.1	0.2	0.078	1.8
Bahir Dar	0.892	1511.4	-2.8	-1.102	-28.5
Bati	0.969	1143.5	-4.7	-2.132 *	-47.1
Kombolcha	0.931	1068.0	-0.6	-0.580	-6.5
Debre markos	0.202	1391.5	-1.9	-1.431	-19.1
Debre Zeit	0.662	802.1	2.0	1.354	20.1
Dessie	0.790	1136.2	2.3	1.112	23.4
Diredawa	0.992	635.2	-0.4	-0.276	-3.6
Gambela	0.984	641.7	0.4	-0.342	-4.4
Jima	0.703	1484.3	0.8	0.564	7.6
Gode	0.303	295.8	-2.6	-1.401	-26.3
Gondar	0.076	1175.8	-0.1	-0.063	-1.2
Gore	0.104	2172.9	-1.5	-1.143	-15.2
Harer	0.698	808.3	3.9	1.083	38.7

* p- value < 0.05 is significant, p-value > 0.05 non significant

Table (25): Continued.

Station	Kolmogorov-Smirnov test for Normal Distribution	Linear Regression Model ($y=b_0+b_1*x$)		T-test for Coefficient b_1	Trend /10 years
		b_0	b_1		
Jijiga	0.009*	729.4	-2.4	-1.34	-24.2
Mekele	0.528	631.3	-0.1	-0.03	-0.5
Metehara	0.727	712.2	-5.5	-2.42 *	-55.9
Negele	0.732	860.9	-4.6	-2.30 *	-46.2
Nekemte	0.962	2131.9	-2.7	-0.74	-27.325
Robe	0.121	1272.4	-13.5	-1.71	-135.3
Sibu Sire	0.930	1401.6	-1.7	-0.87	-17.8
Wonji	0.868	763.1	2.3	1.26	23.1

* p- value < 0.05 is significant, p-value > 0.05 non significant

Table (26): Accuracy measures of total annual rainfall.

Station	Linear trend equation	R-square	Sum square error (SSE)	Mean square error (MSE)
Addis Ababa	$Y_t = 1244.6 - 0.7665 * t$	0.01	3860362.5	37118.9
Arbaminch	$Y_t = 825.52 + 2.01 * t$	0.04	860791.8	19563.5
Assosa	$Y_t = 1312.3 - 10.591 * t$	0.15	5162719.4	117334.5
Awash	$Y_t = 607.91 + 1.3687 * t$	0.03	766972.4	15652.5
Awassa	$Y_t = 908.57 + 1.2972 * t$	0.01	628596.0	18488.1
Bahir Dar	$Y_t = 1511.4 - 2.8475 * t$	0.03	2381777.0	54131.3
Bati	$Y_t = 1143.5 - 4.7055 * t$	0.10	1090330.2	27957.2
Kombolcha	$Y_t = 1068 - 0.64693 * t$	0.01	1907566.6	29805.7
Debre markos	$Y_t = 1391.5 - 1.914 * t$	0.04	1132079.6	22197.6
Debre Zeit	$Y_t = 802.1 + 2.0058 * t$	0.03	1613091.8	30435.7
Dessie	$Y_t = 1136.2 + 2.3391 * t$	0.03	1579471.1	35897.1
Diredawa	$Y_t = 630.2 - 0.11412 * t$	0.0	1727724.0	31994.9
Gambela	$Y_t = 637.25 - 0.22367 * t$	0.0	1705977.8	31592.2
Jima	$Y_t = 1498 + 0.083264 * t$	0.0	1881415.8	34841.0
Gode	$Y_t = 295.8 - 2.6258 * t$	0.05	711961.2	18735.8
Gondar	$Y_t = 1175.8 - 0.11859 * t$	0.0	3640451.9	62766.4
Gore	$Y_t = 2172.9 - 1.5109 * t$	0.01	12103491.9	128760.6
Harer	$Y_t = 808.34 + 3.8658 * t$	0.03	1683022.3	49500.7
Jijiga	$Y_t = 730.27 - 2.4928 * t$	0.03	2564661.7	47493.7
Mekele	$Y_t = 631.34 - 0.054021 * t$	0.0	1787066.7	35741.3
Metehara	$Y_t = 712.26 - 5.5905 * t$	0.15	704432.2	20718.6
Negele	$Y_t = 860.94 - 4.6223 * t$	0.11	1436075.7	32638.1
Nekemte	$Y_t = 2131.9 - 2.7325 * t$	0.02	1756233.4	51653.9
Robe	$Y_t = 1272.5 - 13.525 * t$	0.10	4451358.8	153495.1
Sibu Sire	$Y_t = 1401.7 - 1.7751 * t$	0.01	2435305.5	48706.1
Wonji (63373)	$Y_t = 763.07 + 2.3068 * t$	0.03	1194552.0	27148.9

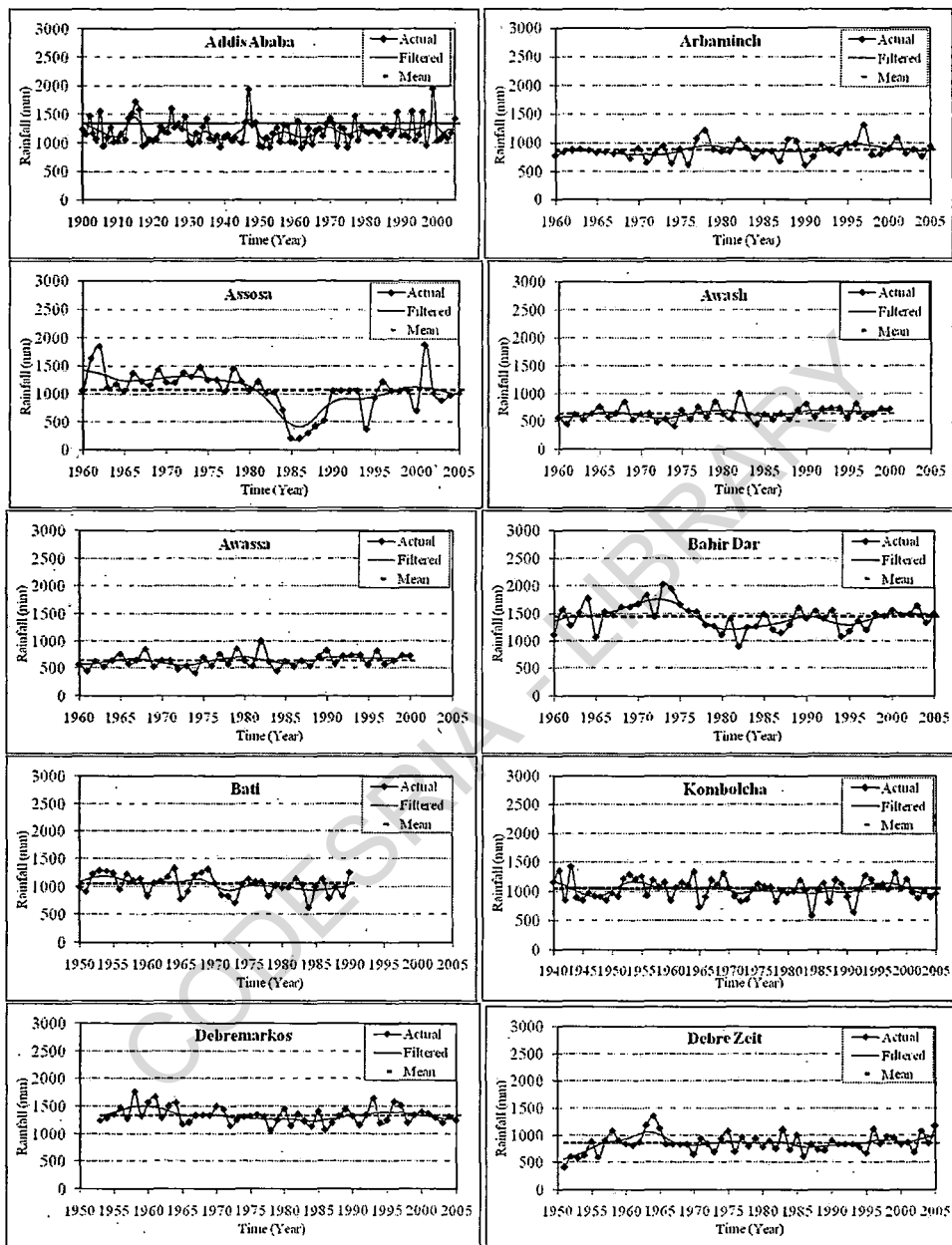


Figure (11): Trend of annual total precipitation.

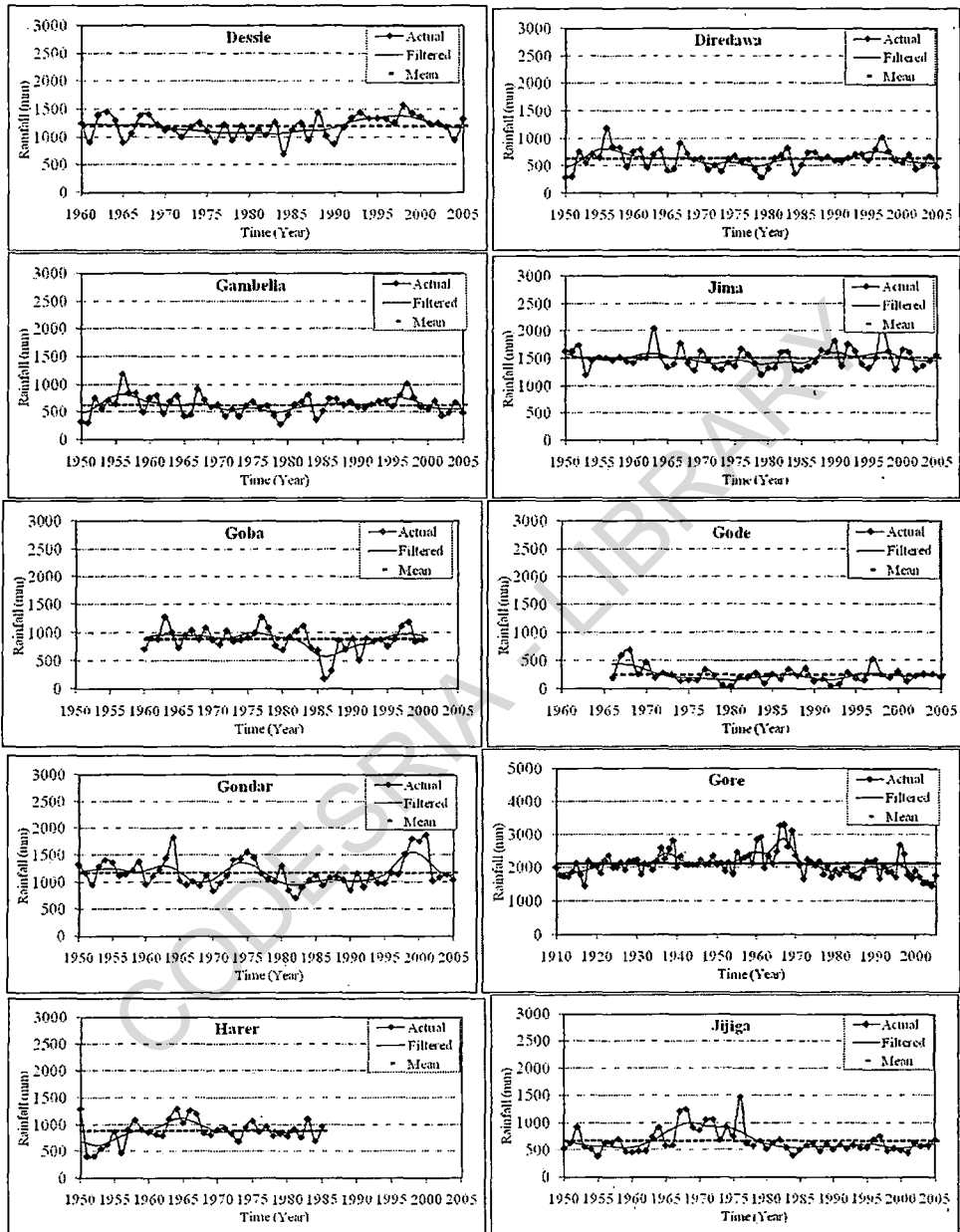


Figure (11): Continued.

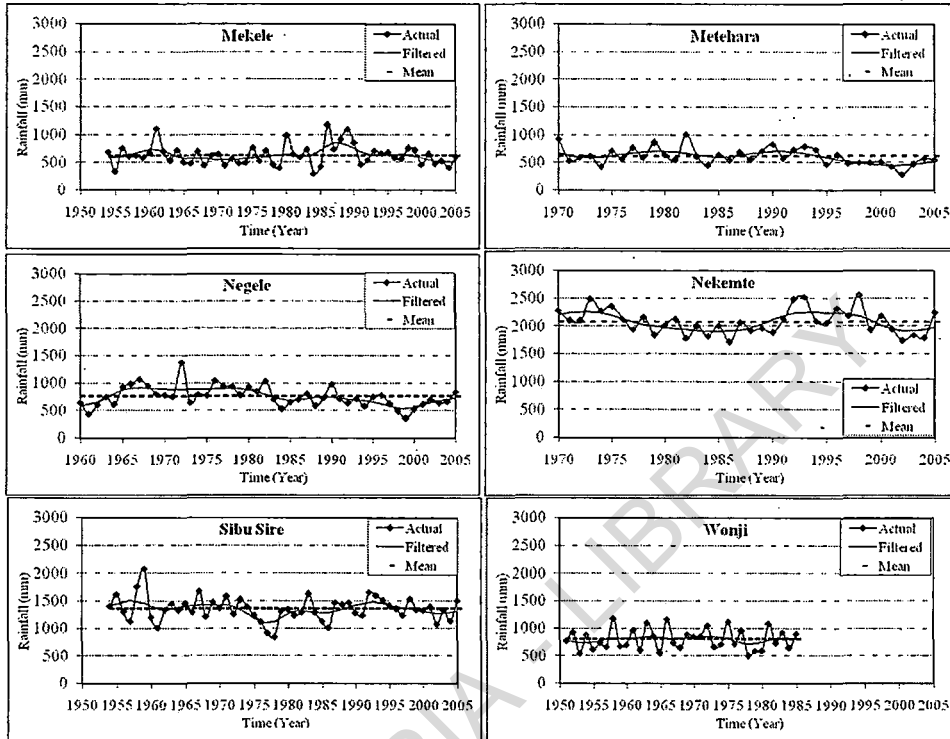


Figure (11): Continued.

4.23. Ethiopian climate

Climate is often described by the statistical interpretation of precipitation and temperature data recorded over a long period of time for a given region or location. Mean annual rainfall distribution over the country is characterized by large spatial variation which ranges from about 2000 mm over some pocket areas in the southwest to less than 250 mm over the Afar and Ogaden low lands (*ENMA, 2001*).

According to the *FAO (2005)*, Ethiopia's tropical monsoon climate is subjected to wide topographic induced variations. Therefore, three climatic zones can be distinguished: a cool zone comprising the central parts of the western and eastern section of the high plateaus, a temperate zone between 1500 and 2400 meters above sea level, and the hot lowlands (below 1500 m) with arid to semi-arid conditions. The mean annual temperature ranges from below 7 to 12°C in the cool zone to more than 25°C in the hot lowlands. Mean annual potential evapotranspiration varies between 1700 and 2600 mm in arid and semi-arid areas and 1600 - 2100 mm in dry sub-humid areas. Annual rainfall for the country averages out at 848 mm, varying from about 2000 mm within some small areas in southwest Ethiopia to less than 100 mm in the Afar Lowlands in the northeastern.

Temperatures are also very much modified by the varied altitude of the country. In general, the country experiences mild temperatures for its tropical latitude because of topography. Mean annual temperature distribution over the country varies from about 10°C over the highlands of northwest, central and southeast to about 35°C over north-eastern lowlands. Daily maximum temperature varies from more than 37°C over the lowlands of northeast and southeast to about 15°C over the highlands of central and northern Ethiopia. Generally speaking the months of March through May are the hottest during the year (*Tadege, 2007*).

Lowest annual minimum temperatures occur over the highlands particularly between November to January. Generally minimum temperatures that reach frost point during the Bega season are not uncommon over the highlands. Also temperatures lower than 5°C occur during high rainfall months (July & August) over northwest; central and southeast due to high cloud cover (*Seleshi and Zanke, 2004*).

Addis Ababa has a subtropical highland climate. The city has a complex mix of highland climate zones, with temperature differences of up to 10°C, depending on elevation and prevailing wind patterns. The high elevation moderates temperatures year-round, and the city's position near the equator means that temperatures are very constant from month to month (*Fekadu, 2009*).

Bahir Dar in the northwestern part of Ethiopia on Lake Tana and at an altitude of more than 1800 meters, has a tropical savannah climate with one distinct rainy period. That lasts from May up to and including October. During the rainy period the average temperatures are somewhat low and the average air humidity is somewhat high (*Seleshi and Camberlin, 2006*).

Debre Markos is a city in the Blue Nile River basin on the northwestern highlands of Ethiopia. It has latitude 10° 20' N, longitude 37°43' E, and elevation 2446 meters. Although the topography of Ethiopia is highly diverse, more than 45% of the country is dominated by highlands with elevations greater than 1500 meters (*Shang, et al., 2011*). Strong seasonality naturally exists in the data. As most areas in Ethiopia, there are three seasons in Debre Markos: main rainy season (June to September), dry season (October to January), and small rainy season (February to May), which are locally known as Kiremt, Bega, and Belg, respectively. High precipitations are observed in summer months and low precipitations are observed in winter months (*Seleshi and Zanke, 2004*).

Results of data analysis of precipitation and temperature in Ethiopia are shown in (Tables 27 and 28), we can know number of humid and arid months by Walter-Lieth method.

The diagrams compiled show the variation of the mean temperature and precipitation from 1951 to 2005 (Figures 12).

The highest aridity index values were obtained in January and February, during these months.

The mean monthly temperature shown in (Table 29): Where the least mean monthly temperature was at Addis Ababa (Mean $14.8 \pm SD$) at December, while the highest mean monthly temperature was at Dire Dana at July (Kiremt season).

The standard error not more than the 0.5 at all monthly stations, it is found that SD was not more than 1.7.

It is noted that the value of SD and SE was low so there are no extreme values through all monthly stations.

Table (27): Mean monthly temperature for study period.

Station	Month											
	J	F	M	A	M	J	J	A	S	O	N	D
Addis Ababa	15.6	16.65	17.5	17.75	17.9	16.65	15.6	15.65	15.8	15.6	14.9	14.75
Arbaminch	23.5	24.6	24.95	24.05	22.9	22.4	22.15	22.85	23.1	22.85	22.7	22.85
Assosa	22.25	23.65	24.35	24.3	22.3	20.55	19.95	19.75	20.1	20.45	21.3	21.5
Awash	19.6	20.45	21.05	20.85	20.35	19.65	18.95	19.1	19.15	19.25	18.65	18.95
Awassa	17.95	19.25	20.7	20.7	20.55	19.65	18.75	18.9	18.95	19.5	19	17.95
Bahar Dar	18.3	19.5	21	21.55	21.3	20.55	19	18.8	19.05	18.4	17.4	17.45
Kombolcha	15.95	17.2	18.4	18.9	19.75	20	18.85	18.2	17.55	16.9	16.15	15.6
Debramarkos	16.7	18	19	19.25	18.45	16.6	15.9	15.85	16.2	15.95	15.9	15.9
Debre Zeit	20.65	21.9	23.3	23.75	24.8	24.65	22.25	21.75	22.55	22.2	20.85	20.1
Diredawa	24.95	25.95	27.7	27.85	28.8	29.1	28	27.45	27.95	27.55	25.8	24.65
Gode	23.2	24.55	25.8	25.6	24.7	23.7	23.15	23.3	23.85	23.2	22.8	23.05
Gondar	20.7	21.6	22	21.95	20.95	19.05	17.75	17.75	18.7	19.6	20.1	20.25
Gore	16.15	17.55	18.6	19.15	18.75	18.3	17.7	17.85	17.95	16.3	15.8	15.7
Jijiga	17.45	19	20.1	20.15	20.5	20	19.55	19.6	19.9	19.4	17.85	16.8
Jima	19.95	20.75	21.1	21	20.05	18.75	17.85	18.1	18.65	19.35	19.5	19.4
Mekele	19.4	20.6	22.3	22.8	23.55	24.55	21.85	21.25	22.2	20.6	18.85	18.4
Negele	20.85	21.6	21.75	20.6	19.75	18.65	18.2	18.85	20.1	19.5	19.5	19.9
Nekemte	18.75	19.95	20.35	20.3	18.9	17	16.25	16.45	17.05	17.9	18.15	18.3

Table (28): Mean monthly precipitation for study period.

Station	Month											
	J	F	M	A	M	J	J	A	S	O	N	D
Addis Ababa	20.3	42.8	68.7	91.4	86.3	129.6	268.8	283	179	31.8	11.6	9.1
Arbaminch	40.9	35.2	69.8	148.3	143.1	60.9	49.2	56.5	88.9	117.1	65.8	35.5
Assosa	17	4.9	22.3	54.5	117.8	159.4	199.1	209.1	166.1	111.6	22.2	28.7
Awash	25.1	52.4	56.6	67.8	57.1	32.7	117.7	140.5	63.1	23.7	16.4	13.3
Awassa	31.8	47.1	74.3	102.9	120.2	99.9	119.3	125.1	120.1	84.2	31.6	20.3
Bahar Dar	3.2	2.6	11	26.3	88	195.7	440.7	391.8	204.7	97.7	19.6	3.4
Kombolcha	28.5	43.8	76.1	93.4	58.4	39.7	261.7	258.6	127	40.8	19.2	18
Debramarkos	20.7	19.3	51.5	72.4	94.5	163.1	297.4	306.2	211.7	92.4	26.3	19
Debre Zeit	12.8	27.6	52.7	58.9	57.6	100.8	217.8	224.6	108	29.8	4	4.9
Diredawa	24.4	37.8	74.4	105.2	52	28.3	94.7	126.6	68.6	28.8	19.2	7.3
Gode	20	6.3	20.1	82.8	53.1	49.3	297.4	303	7.2	56.7	45.2	5.5
Gondar	4.3	5.3	18.6	40.7	87.5	173.3	331.9	307.5	124.7	71.7	22.6	9.6
Gore	37	47	89.2	134.3	246.3	311.8	303.7	329.7	320.9	178	92.7	38.8
Jijiga	13.2	28.2	51.8	104.6	89.5	55.9	72.8	117.9	89.8	42.2	19.5	9.1
Jima	37.7	55.5	93.8	135.7	172	214	222.2	211.2	185.8	102.6	63.2	42.2
Mekele	3	8	26.6	32.4	29.6	46.3	218.9	236.8	47.7	6.1	6.3	2.2
Negele	9.3	31.1	65	211.6	167.6	11.5	6.9	4.8	42.1	167.3	61	16.7
Nekemte	11.9	19.7	63.5	90.3	237.2	390.6	411.1	391	280.4	149.9	54.9	22.6

Table (29): Descriptive statistical of mean monthly temperature.

Station	Minimum		Maximum		Mean	SE	SD	CV
	Value	Month	Value	Month				
Addis Ababa	14.8	Dec	17.9	MA	16.2	0.3	1.1	6.6
Arbaminch	22.2	Jul	25	Mar	23.3	0.3	0.9	3.7
Assosa	19.8	Aug	24.4	Mar	21.7	0.5	1.7	7.7
Awash	18.7	Nov	21.1	Mar	19.7	0.2	0.8	4.1
Awassa	17.9	Dec	20.7	Mar	19.3	0.3	0.9	4.9
Bahar Dar	17.4	Nov	21.6	Apr	19.4	0.4	1.4	7.5
Kombolcha	15.6	Dec	20	jun	17.8	0.4	1.5	8.3
Debramarkos	15.8	Aug	19.3	Apr	17.0	0.4	1.3	7.8
Debre Zeit	20.1	Dec	24.8	May	22.4	0.4	1.5	6.7
Diredawa	24.7	Dec	29.1	Jul	27.2	0.4	1.4	5.3
Gode	22.8	Nov	25.8	Mar	23.9	0.3	1.0	4.3
Gondar	17.7	Aug	22	Mar	20.0	0.4	1.5	7.4
Gore	15.7	Dec	19.2	Apr	17.5	0.3	1.2	6.9
Jijiga	16.8	Dec	20.5	May	19.2	0.3	1.2	6.2
Jima	17.9	Jul	21.1	Mar	19.5	0.3	1.1	5.5
Mekele	18.4	Des	24.6	Jun	21.4	0.5	1.9	8.8
Negele	18.2	Jul	21.8	Mar	19.9	0.3	1.1	5.6
Nekemte	16.3	Jul	20.4	Mar	18.3	0.4	1.4	7.8

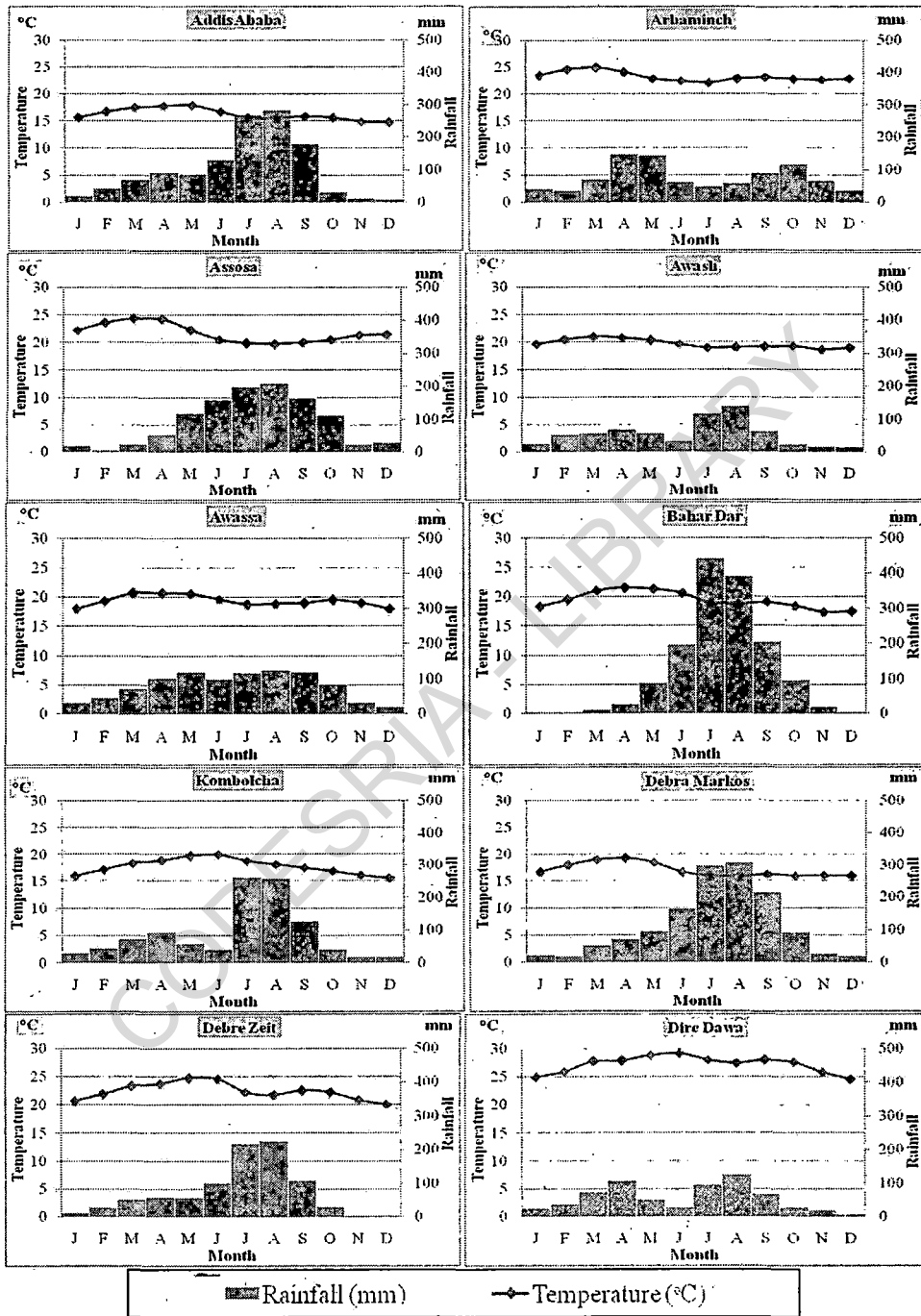


Figure (12): Mean monthly temperature and precipitation of study period.

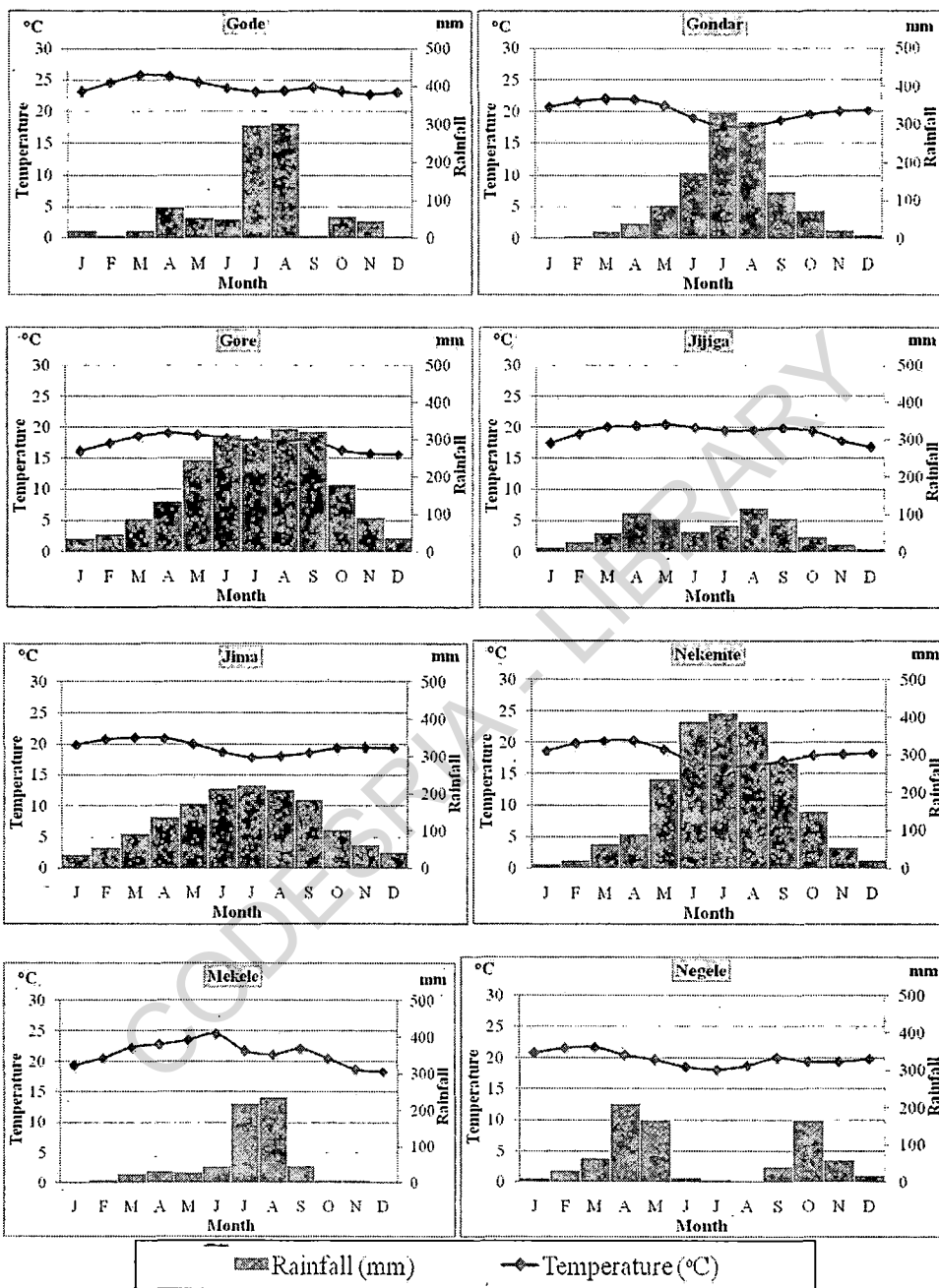


Figure (12): Continued.

4.24. Seasonal classifications in Ethiopia

Within each climatic zone, seasonal variations and atmospheric pressure systems contribute to the creation of three seasons, which are known as the Kiremt, Belg, and Bega. The Kiremt season is the main rainy season and usually lasts from June to September, covering all of Ethiopia except the southern and southeastern parts. The Belg season is the light rainy season and usually lasts from March to May; it is the main source of rainfall for the water-deficient southern and southeastern parts of Ethiopia. The Bega season is the dry season and usually lasts from October to February (Table 30 and figure 13), during which the entire country is dry, with the exception of occasional rainfall that is received in the central sections (*Seleshi and Zanke, 2004*). A brief description of the mechanisms for rainfall formation for each season.

- During Kiremt the air flow is dominated by a zone of convergence in low-pressure systems accompanied by the oscillatory intertropical convergence zone (ITCZ) extending from West Africa through the north of Ethiopia towards India. Major rain-producing systems during Kiremt are: the northward migration of the ITCZ; development and persistence of the Arabian and the Sudan thermal lows along 20 °N latitude; development of quasi-permanent high-pressure systems over the South Atlantic and south Indian Oceans; development of the tropical easterly jet and its persistence; and the generation of the low-level 'Somali jet', which enhances low level southwesterly flow. It is to be noted that Kiremt rainfall covers most of the country with the exception of the south and southeast of Ethiopia (e.g. Gode, Negele) (*Seleshi and Demaree, 1995*).
- During Bega, the country predominantly falls under the influence of warm and cool northeasterly winds. These dry air masses originate either from the

Saharan anticyclone and/or from the ridge of high pressure extending into Arabia from a large high over central Asia (Siberia). However, very occasionally, northeasterly winds get interrupted when migratory low-pressure systems originating in the Mediterranean area move eastward and interact with the equatorial/tropical systems, resulting in rainfall over parts of central Ethiopia. In addition to this, occasional development of the Red Sea convergence zone (RSCZ) affects coastal areas (*Conway, 2000*).

- In Bega, most of the country is generally dry; the exception is the south and southeast of Ethiopia, which receives its second important seasonal rainfall in this period (*Seleshi and Zanke, 2004*).

The Belg season coincides with the domination of the Arabian high as it moves towards the north Arabian Sea. Major systems during the Belg are the development of a thermal low (Cyclone) over the south of Sudan, and winds from the Gulf of Aden and the Indian Ocean highs that are drawn towards this centre and blow across central and southern Ethiopia. These moist, easterly and southeasterly winds produce the main rains in southern and southeastern Ethiopia and the Belg rains to the east-central part of the northwestern highlands (*Conway, 2000*).

The forward and retreat pace of the African sector of the ITCZ and their ending and beginning times vary annually, causing most of the interannual variability in rainfall over Ethiopia. The dynamics of the ITCZ over most of Ethiopia are known to be teleconnected to El Nino occurrence. Studies have shown that, in general, El Nino years are accompanied by below-average Kiremt rainfall years in large parts of Ethiopia (*Haile, 1988; Seleshi and Demaree, 1995; Nicholson and Kim, 1997*).

Table (30): Seasonal classifications in Ethiopia.

Station	Temperature (°C)			Precipitation (mm)		
	Bega (ONDJ)	Belg (FMAM)	Kiremt (JJAS)	Bega (ONDJ)	Belg (FMAM)	Kiremt (JJAS)
Addis Ababa	15.2	17.5	15.9	72.8	289.2	860.4
Arbaminch	23.0	24.1	22.6	259.3	396.4	255.5
Assosa	21.4	23.7	20.1	179.5	199.5	733.7
Awash	19.1	20.7	19.2	78.5	233.9	354
Awassa	18.6	20.3	19.1	167.9	344.5	464.4
Bahir Dar	17.9	20.8	19.4	123.9	127.9	1232.9
Kombolcha	16.2	18.6	18.7	106.5	271.7	687
Debra Markos	16.1	18.7	16.1	158.4	237.7	978.4
Debre Zeit	21.0	23.4	22.8	51.5	196.8	651.2
Diredawa	25.7	27.6	28.1	79.7	269.4	318.2
Gode	23.1	25.2	23.5	127.4	162.3	656.9
Gondar	20.2	21.6	18.3	108.2	152.1	937.4
Gore	16.0	18.5	18.0	346.5	516.8	1266.1
Jijiga	17.9	19.9	19.8	84	274.1	336.4
Jima	19.6	20.7	18.3	245.7	457	833.2
Mekele	19.3	22.3	22.5	17.6	96.6	549.7
Negele	19.9	20.9	19.0	254.3	475.3	65.3
Nekemte	18.3	19.9	16.7	239.3	410.7	1473.1

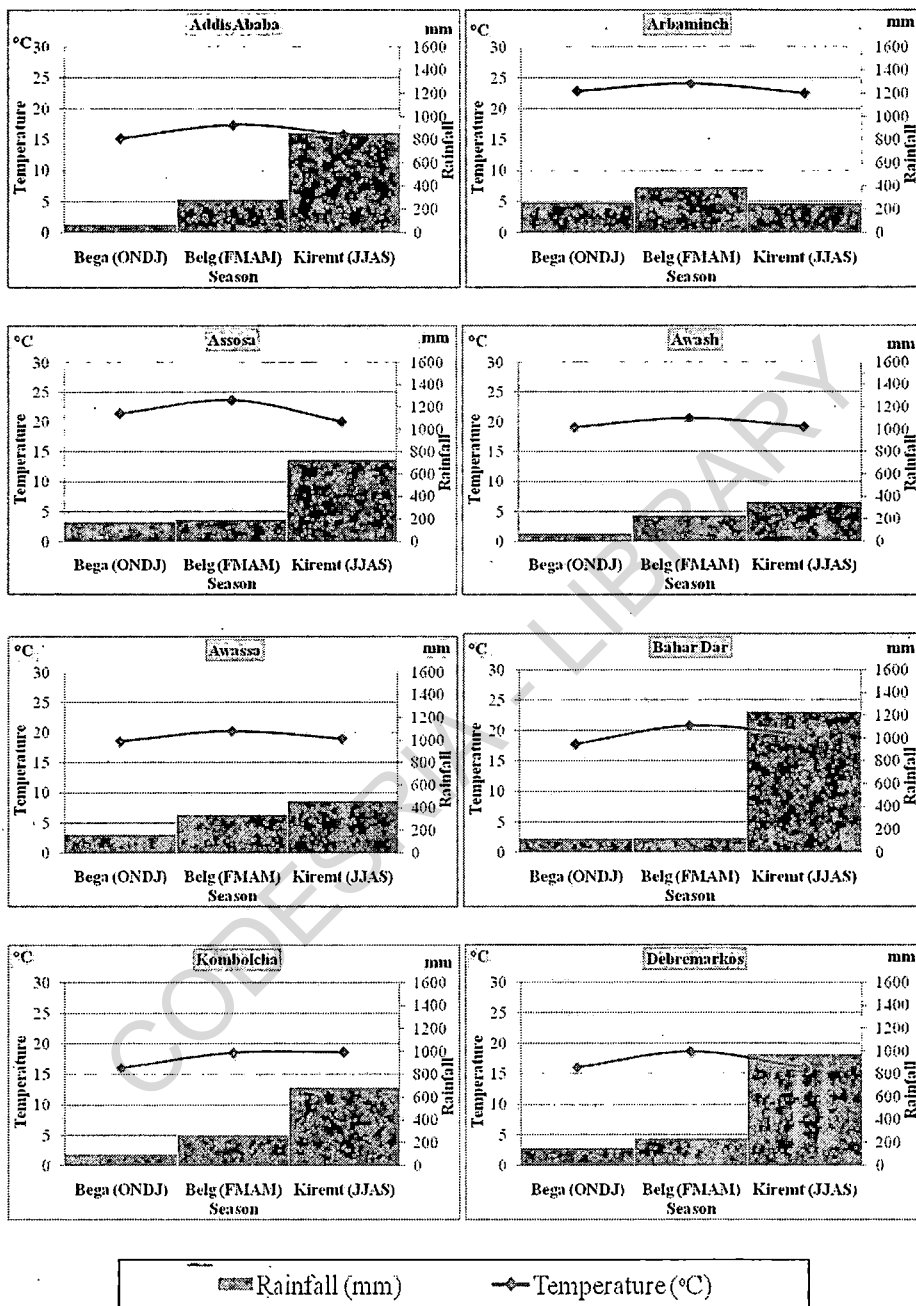


Figure (13): Temperature and rainfall in the Ethiopian seasons.

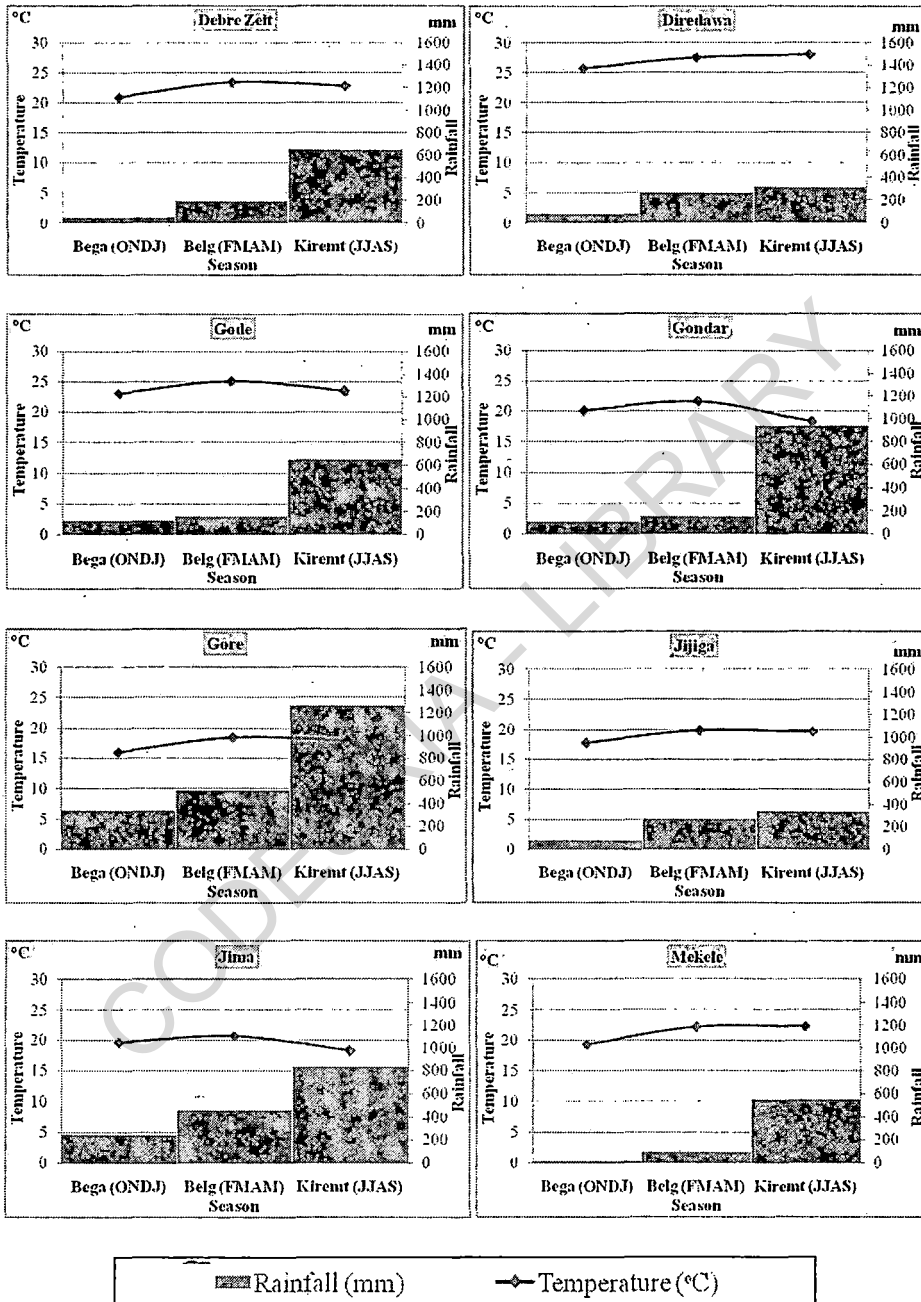


Figure (13): Continued.

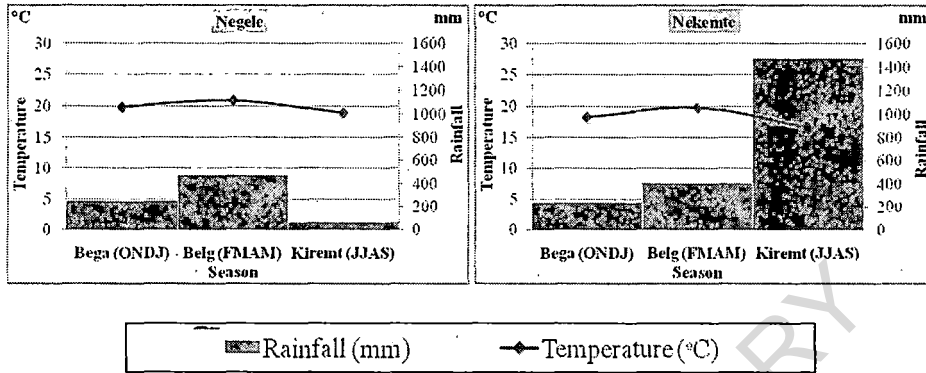


Figure (13): Continued.

4.25. Rainfall regimes in Ethiopia

The rainfall regime in Ethiopia is described as uni-modal and bi-modal systems influenced by topographical variation in the country, seasonal cycles and opposing responses to regional and global weather systems, consequently, three rainfall regimes are commonly identified (Figure 14) (*Abebe, 2010*).

Regime A that comprises the central and the eastern parts of the country has a bi-modal rain classified as the long rainy season (June –September) and short rains (March-May) locally referred as Kiremt and Belg rains respectively (Figure 15). The rest of the months (October to February) are dry period.

Regime B in the western part of the country (from southwest through to northwest) has a mono-modal rainfall pattern (June – September), and the rainy period ranges from February through November mainly in the western and south-western part of the country (Figure 16), and decreases northwards (Figure 17).

Regime C that comprises the south and south-eastern part of Ethiopia has two distinct wet and dry seasons. The main rain season is from February through May, and short rains from October to November, and the dry periods are June to September and December to February (Figure 18).

4.25.1. Local and regional factors affecting rainfall in Ethiopia

Ethiopia has different rainy seasons influenced by topographic variation and rain-bearing system.

A. Topographic variation

Three major physiographic regions are identified in Ethiopia: the North, Central, and South-western Highlands and surrounding Lowlands; the South-eastern Highlands and the surrounding Lowlands; and the Rift Valley that is an extension of the Great East African Rift Valley dividing the highlands into two. As a result of the topographic variation and geographical location, rainfall in Ethiopia

characterised by high spatial and temporal variability, generally speaking, the amount of rain over the mountain areas is higher than the lowlands, with the maximum rain received over the southwest and the minimum over southeast of the country (*Abebe, 2010*).

B. Regional weather features affecting the climate system in Ethiopia

The rainfall seasons in Ethiopia influenced by different factors. Kiremt rain (JJAS) is the main rainy season for most part of the country except in the south and south-eastern, where the Belg rain (MAM) is the main rainy season. Southern and south-eastern part of the country characterised by bi-modal seasonal cycle and receives short rain during SON, which is Belg (Dry) season for the rest of the country. The rainy seasons in Ethiopia are influenced by different global and regional rain-bearing factors (*Abebe, 2010*).

The main features that affect the Kiremt rain include the ITCZ, Tropical Easterly Jet (TEJ), South Atlantic Ocean and South West Indian Ocean anticyclone, East African Low Level Jet (EALLJ) or Somali Jet and ENSO. The global and regional weather features that affect the Belg rain includes the ITCZ, Subtropical Westerly Jet (SWJ) stream, Arabian High, the frequency of tropical cyclones over the Southwest Indian Ocean and ENSO (*ENMA, 2011*).

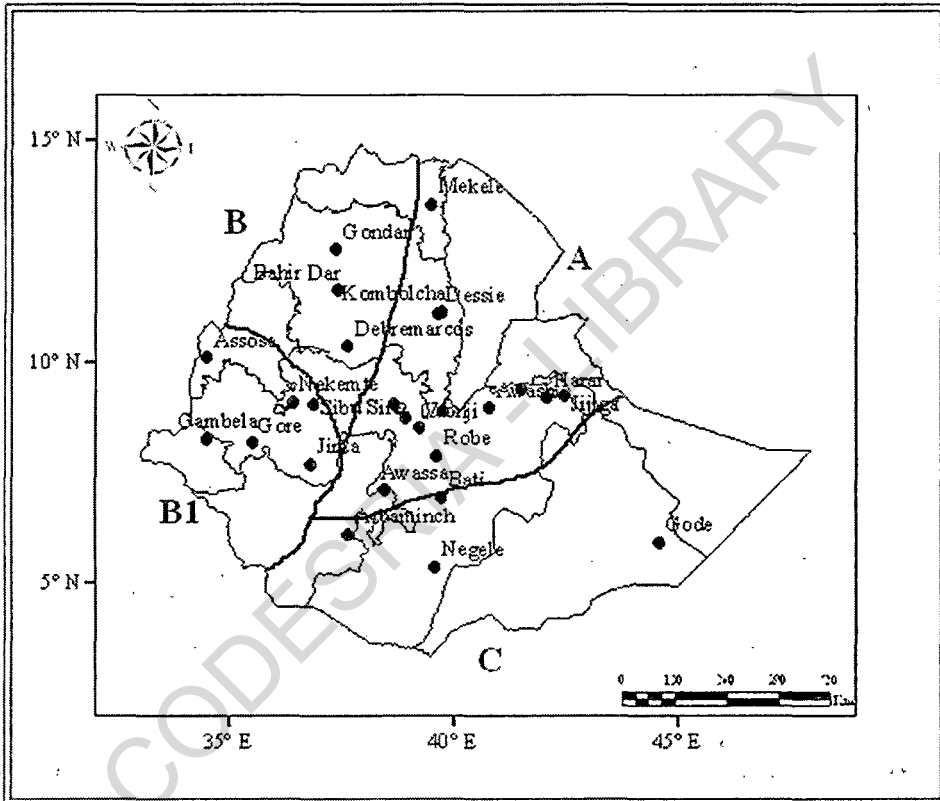


Figure (14): Map of Ethiopia showing rainfall regimes A, B, B1 and C (Abebe, 2010).

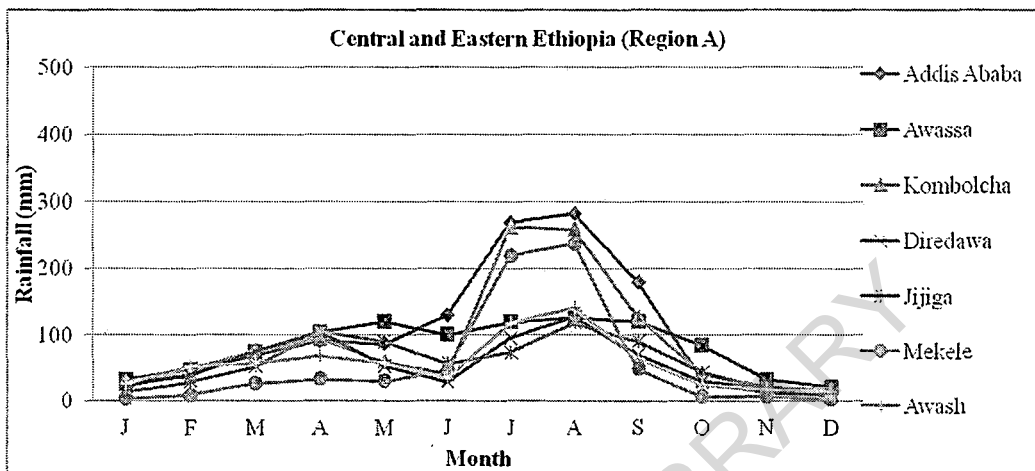


Figure (15): Mean monthly rainfall distribution for Central and Eastern Ethiopia (Region A).

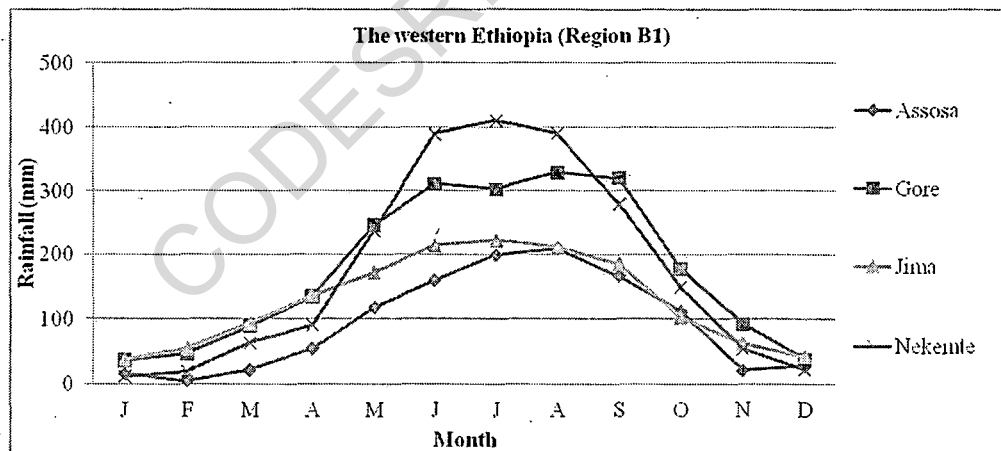


Figure (16): The same as figure (15), but for the western Ethiopia (Region B1).

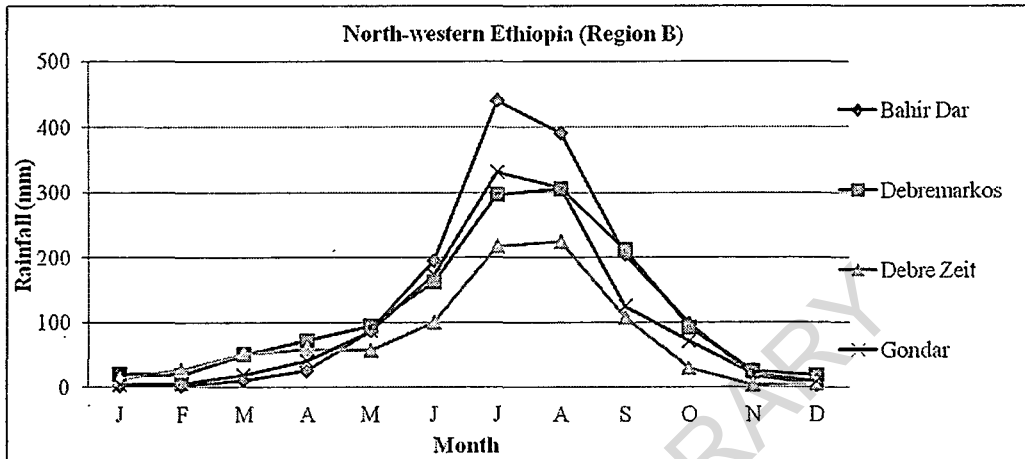


Figure (17): The same as figure (15), but for north-western Ethiopia (Region B).

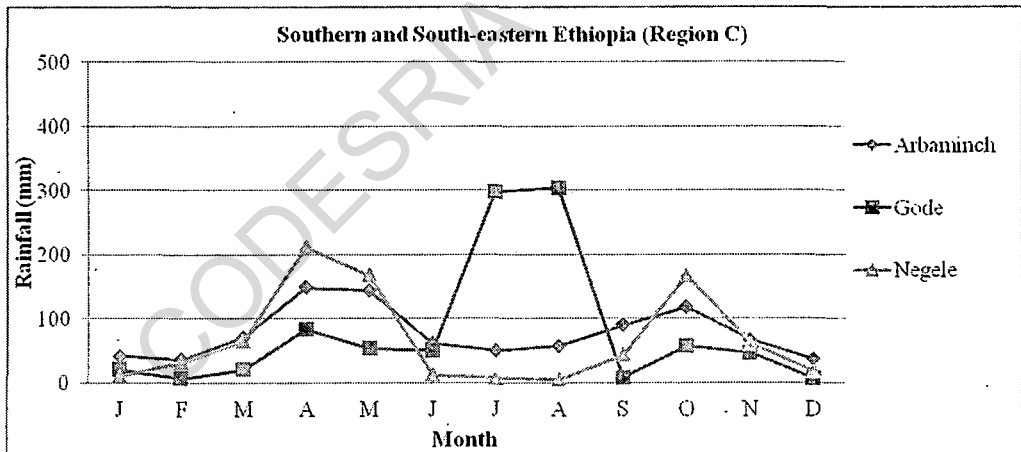


Figure (18): The same as figure (15), but for Southern and South-eastern Ethiopia (Region C).

4.26. Comparing linear, quadratic, cubic and exponential equations

The goal is to forecast future observations by a linear function of observables. In the case of trend estimation, these observables are functions of the time index.

A linear equation in the form $(y=mx+b)$ has two variables and both are to the first power. It is used to describe situation where the independent variables x and y , the dependent variable, so they are related simply by a one on one increase or a steady increase.

A quadratic equation in the form $y=kx^2$ (Simplest form) has independent variable x which is to the second power, and a dependent y to the first. Here the x could take 2 different values for the same y .

Finally an exponential equation in the form $y=ka^x$ which helps you understand how some particular situation or sets behave.

Some time series which are growing (Rainfall and temperature) are exponentially increasing. Percentage changes are stable in the long run; these series cannot be fit by a linear trend. So we can fit a linear trend to their (Natural) logarithm.

The average maximum temperature warming across the whole region was 0.02°C , with 95% of the stations showing significantly increased temperatures.

Table (31) shows the comparison between trend equations for mean annual maximum temperature, which include (Linear, quadratic, cubic and exponential), we noted that the highest value for R^2 was at cubic equation at all stations so cubic equation is the best to express the trend equation than the other equations.

It is found that R^2 was 64% (the highest value) at Addis Ababa station (Medial of Ethiopia) and it was 13% (the lowest value) at Gode station.

R^2 can be divide to more than 50% at three stations (Addis ababa, Awassa and Nekemte) and more than 30% and less than 50% at nine stations (Arbaminch, Bahir dar, Kombolcha, Debre zeit, Gondar, Gore, Jijiga, Mekele and Negele) and less than 30% at the rest of the stations.

In Table (31), it is found that the highest value for R^2 was at the middle of Ethiopia at Addis Ababa and Awassa stations which were 64% and 61%, respectively, while the lower value ($R^2=13\%$) at Gode station (East of Ethiopia).

It is noted that the best equation to represented minimum and maximum temperature trend at all stations was cubic equation as it contains, the highest value for R^2 than the other trend equations.

In (Table 32), it is noted that the highest value for R^2 was at the north of Ethiopia at Bahir Dar as regarding the mean of minimum temperature, R^2 was not more than 40% as regarding rainfall, the highest value was at the south of Ethiopia at Negele station while the lowest values was at middle and west of Ethiopia at Diredawa and Gambela, respectively.

It is noted that R^2 for rainfall was lower than maximum and minimum temperature for all stations, as R^2 was more than 60% for maximum and minimum temperature while it was not more than 40% for rainfall, as rainfall data had extreme oscillation from year to year, while maximum and minimum temperature had minimal oscillation so it can be represented by the trend equation.

Rainfall trends of Ethiopia from 1950-2005 have been decreasing in most of the stations (16 out of 26 stations). The decrease was minimal through the study period while 8 out of 26 (Arbaminch, Awash, Awassa, Debre Zeit, Dessie, Jima, Harer and Wonji) stations showed increase in rainfall and this increase was minimal (Table 33).

Climate change is the sever problem that the whole world facing today. It is now widely accepted that climate change is already happening and further change is inevitable; over the last century (between 1906 and 2005), the average global temperature rose by about 0.74°C. This has occurred in two phases, from 1910 to 1940 and more strongly from the 1970 to the present (*IPCC, 2007*).

Many studies into the detection and attribution of climate change have found that most of the increase in average global surface temperature over the last 50 years is attributable to human activities (*IPCC, 2001*).

The study of *ENMA (2001)* for 40 meteorological stations showed that there have been very warm and very cold years. However, the general trend showed that there was an increase in temperature over the last 50 years. The study also noted that the minimum temperature is increasing at a higher rate than the maximum temperature.

The observed yearly mean of maximum surface air temperatures of 18 meteorological stations in Ethiopia shows increasing trend during the period 1950-2005. Increase of mean maximum temperatures has been observed since the beginning of 1990. The mean of maximum temperatures in Ethiopia has increased by 0.87°C comparing two periods (Mean of 1955-1964 minus 1995-2004) for 8 meteorological stations (*Fekadu, 2009*).

Observed maximum surface air temperature and rainfall change for the period 1950-2005 has been analyzed using 18 and 26 stations data respectively collected from different climatic zone over the country. Because of limitation of recorded long period data only one station has been used for precipitation to analysis long-term trend. There are locations with large year-to-year variability and, the warming has been neither steady nor the same in different seasons or in different locations. (*Cheung, et al., 2008*) compared the mean annual rainfall of the

period 1985-2004 with mean annual of 1955-1974 and 1955-2004. For temperature the two periods compared the mean of 1955-1964 and of 1995-2004. Availability of data for both temperature and rainfall is more than 90% in the stations of Addis Ababa, Debre-Markos, Gonder, Gore, Combolcha, Dire-Dawa, Jimma, Meiso and Negele. In case of rainfall changes to annual, JJA and MAM have been analyzed. JJA and MAM are rainy seasons in Ethiopia. Maximum surface temperatures have risen in Ethiopia during the last 50 years (1955-2004), as observed from instrumental recorded data obtained from Meteorological Agency of Ethiopia. The change of maximum surface air temperatures in Ethiopia is similar with global trend shown in *IPCC (2007)*.

Seleshi and Camberlin, (2006) found that the mean of maximum surface air temperatures of 8 stations in Ethiopia, indicates $0.82^{\circ}\text{C} \pm 0.078^{\circ}\text{C}$ and $0.66^{\circ}\text{C} \pm 0.043^{\circ}\text{C}$ rise as observed from mean of 1995-2004 relative to 1955-1964 and 1955-2004, respectively. The standard deviation of stations varies from 0.44°C to 0.699°C . Monthly mean of maximum temperatures varies from 0.5°C in June to 1.27°C in February for two compared periods 1995-2004 relative to 1955-1964. The 2004 is the hottest year during the period 1955-2004 in the country, for annual temperatures of the 8 stations considered. The rate of warming over the last 50 years (1955-2004) varies widely from 0.14°C to 0.693°C per decade in Ethiopia for the observed station.

Both instrumental and proxy records have shown significant variations in the spatial and temporal patterns of climate in Ethiopia. According to *Tadege, (2007)* the country experienced 10 wet years and 11 dry years over 55 years analyzed, demonstrating the strong inter-annual variability. Between 1951 and 2006, annual minimum temperature in Ethiopia increased by about 0.37°C every decade. The UNDP Climate Change Profile for Ethiopia (*McSweeney, et al., 2008*) also shows

that the mean annual temperature increased by 1.3°C between 1960 and 2006, at an average rate of 0.28°C per decade. The temperature increase has been most rapid from July to September (0.32°C per decade). It is reported that the average number of hot days per year has increased by 73 (an additional 20% of days) and the number of hot nights has increased by 137 (an additional 37.5% of nights) between 1960 and 2006. The rate of increase was highest in June, July and August. Over the same period, the average number of cold days and nights decreased by 21 (5.8% of days) and 41 (11.2% of nights), respectively. These reductions have mainly occurred in the months of September to November (McSweeney, et al., 2008).

The year to year variation of annual minimum temperatures expressed in terms of temperature differences from the mean and averaged over 40 stations, the country has experienced both warm and cool years over the last 55 years. However, the recent years are the warmest compared to the early years. There has been a warming trend in the annual minimum temperature over the past 55 years. It has been increasing by about 0.37°C every ten years (Conway, 2000).

Table (31): Comparison between trend equations for mean annual maximum temperature.

Station	Trend	Trend equation	R	R ²	SSE	MSE
Addis Ababa	Linear	$Y_t = 21.803 + 0.039204 * t$	0.67	0.45	15.44	0.35
	Quadratic	$Y_t = 22.225 - 0.013538 * t + 0.0011222 * t^2$	0.71	0.5	14.01	0.33
	Cubic	$Y_t = 23.117 - 0.22991 * t + 0.012508 * t^2 - 0.00016151 * t^3$	0.80	0.64	9.97	0.24
	Exponential	$Y_t = 21.808 * (1.0017^t)$	0.67	0.44	0.01	0
Arbaminch	Linear	$Y_t = 29.417 + 0.033591 * t$	0.56	0.31	9.76	0.29
	Quadratic	$Y_t = 29.673 - 0.0066864 * t + 0.0010886 * t^2$	0.58	0.34	9.37	0.28
	Cubic	$Y_t = 30.032 - 0.11596 * t + 0.0083715 * t^2 - 0.00013122 * t^3$	0.61	0.37	8.89	0.28
	Exponential	$Y_t = 29.413 * (1.0011^t)$	0.56	0.31	0	0
Assosa	Linear	$Y_t = 27.884 + 0.016615 * t$	0.27	0.10	13.75	0.4
	Quadratic	$Y_t = 27.211 + 0.12293 * t - 0.0028733 * t^2$	0.51	0.26	10.99	0.33
	Cubic	$Y_t = 27.04 + 0.17492 * t - 0.0063384 * t^2 + 6.2433E-05 * t^3$	0.52	0.27	10.88	0.34
	Exponential	$Y_t = 27.872 * (1.0006^t)$	0.28	0.08	0	0
Awash	Linear	$Y_t = 33.555 - 0.016935 * t$	0.29	0.10	7.83	0.27

	Quadratic	$Y_t = 33.428 + 0.0061204 * t - 0.0007205 * t^2$	0.3	0.09	7.75	0.28
	Cubic	$Y_t = 32.984 + 0.16056 * t - 0.012596 * t^2 + 0.00024742 * t^3$	0.4	0.16	7.16	0.27
	Exponential	$Y_t = 33.55 * (0.9995^t)$	0.29	0.08	0	0
Awassa	Linear	$Y_t = 26.165 + 0.038958 * t$	0.67	0.45	7.21	0.21
	Quadratic	$Y_t = 26.336 + 0.012085 * t + 0.00072628 * t^2$	0.68	0.46	7.03	0.21
	Cubic	$Y_t = 27.051 - 0.20534 * t + 0.015218 * t^2 - 0.0002611 * t^3$	0.78	0.61	5.14	0.16
	Exponential	$Y_t = 26.166 * (1.0015^t)$	0.67	0.45	0	0
Bahir Dar	Linear	$Y_t = 26.066 + 0.029312 * t$	0.59	0.35	12.99	0.3
	Quadratic	$Y_t = 26.248 + 0.0065275 * t + 0.00048479 * t^2$	0.6	0.36	12.72	0.3
	Cubic	$Y_t = 25.985 + 0.070176 * t - 0.0028646 * t^2 + 4.751E-05 * t^3$	0.62	0.38	12.37	0.29
	Exponential	$Y_t = 26.067 * (1.0011^t)$	0.59	0.35	0	0
Kombolcha	Linear	$Y_t = 25.553 + 0.021579 * t$	0.46	0.21	25.65	0.47
	Quadratic	$Y_t = 26.106 - 0.035635 * t + 0.0010038 * t^2$	0.55	0.3	22.57	0.43
	Cubic	$Y_t = 25.492 + 0.088192 * t - 0.0043795 * t^2 + 6.2962E-05 * t^3$	0.62	0.38	20.14	0.39
	Exponential	$Y_t = 25.553 * (1.0008^t)$	0.46	0.21	0.01	0

Debremarkos	Linear	$Y_t = 22.026 + 0.011743 * t$	0.46	0.21	7.58	0.14
	Quadratic	$Y_t = 22.224 - 0.0087041 * t + 0.00035872 * t^2$	0.5	0.25	7.18	0.14
	Cubic	$Y_t = 22.134 + 0.0094258 * t - 0.00042946 * t^2 + 9.2184E-06 * t^3$	0.51	0.26	7.13	0.14
	Exponential	$Y_t = 22.026 * (1.0005^t)$	0.46	0.21	0	0
Debre Zeit	Linear	$Y_t = 25.906 + 0.012635 * t$	0.45	0.20	9.19	0.17
	Quadratic	$Y_t = 26.255 - 0.023424 * t + 0.00063262 * t^2$	0.56	0.31	7.97	0.15
	Cubic	$Y_t = 26.176 - 0.0076037 * t - 5.5167E-05 * t^2 + 8.0443E-06 * t^3$	0.56	0.31	7.93	0.15
	Exponential	$Y_t = 25.908 * (1.0005^t)$	0.45	0.20	0	0
Diredawa	Linear	$Y_t = 31.454 + 0.0011005 * t$	0.04	0.00	14.23	0.26
	Quadratic	$Y_t = 31.914 - 0.046448 * t + 0.00083418 * t^2$	0.39	0.15	12.11	0.23
	Cubic	$Y_t = 31.884 - 0.040331 * t + 0.00056825 * t^2 + 3.1103E-06 * t^3$	0.39	0.15	12.1	0.23
	Exponential	$Y_t = 31.447 * (1^t)$	0.04	0.00	0	0
Gode	Linear	$Y_t = 34.673 + 0.0083468 * t$	0.2	0.04	4.31	0.15
	Quadratic	$Y_t = 34.924 - 0.0373 * t + 0.0014265 * t^2$	0.33	0.11	3.98	0.14
	Cubic	$Y_t = 35.083 - 0.092747 * t + 0.0056903 * t^2 - 8.8829E-05 * t^3$	0.36	0.13	3.91	0.14

	Exponential	$Y_t = 34.671 * (1.0002^t)$	0.2	0.04	0	0
Gondar	Linear	$Y_t = 26.009 + 0.018859 * t$	0.59	0.40	9.56	0.18
	Quadratic	$Y_t = 26.311 - 0.012385 * t + 0.00054813 * t^2$	0.64	0.41	8.64	0.16
	Cubic	$Y_t = 25.934 + 0.063712 * t - 0.0027601 * t^2 + 3.8693E-05 * t^3$	0.69	0.48	7.72	0.15
	Exponential	$Y_t = 26.013 * (1.0007^t)$	0.59	0.35	0	0
Gore	Linear	$Y_t = 23.026 + 0.015178 * t$	0.52	0.27	9.13	0.17
	Quadratic	$Y_t = 23.509 - 0.034738 * t + 0.00087572 * t^2$	0.68	0.46	6.78	0.13
	Cubic	$Y_t = 23.51 - 0.034894 * t + 0.0008825 * t^2 - 7.9291E-08 * t^3$	0.68	0.46	6.78	0.13
	Exponential	$Y_t = 23.029 * (1.0006^t)$	0.51	0.26	0	0
Jijiga	Linear	$Y_t = 27.261 + 0.0017293 * t$	0.06	0.00	13.47	0.25
	Quadratic	$Y_t = 27.851 - 0.059216 * t + 0.0010692 * t^2$	0.51	0.26	9.98	0.19
	Cubic	$Y_t = 27.415 + 0.028607 * t - 0.0027488 * t^2 + 4.4655E-05 * t^3$	0.59	0.35	8.75	0.17
	Exponential	$Y_t = 27.258 * (1.0001^t)$	0.06	0.00	0	0
Jima	Linear	$Y_t = 26.905 - 0.00053999 * t$	0.02	0.00	12.95	0.24
	Quadratic	$Y_t = 27.402 - 0.051943 * t + 0.00090181 * t^2$	0.44	0.19	10.46	0.2

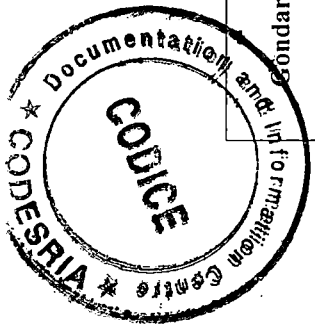
	Cubic	$Y_t = 27.518 - 0.075485*t + 0.0019253*t^2 - 1.197E-05*t^3$	0.45	0.2	10.38	0.2
	Exponential	$Y_t = 26.896 * (0.99999^t)$	0.01	0.00	0	0
Mekele	Linear	$Y_t = 24.713 - 0.017866*t$	0.28	0.10	29.52	0.67
	Quadratic	$Y_t = 25.484 - 0.11421*t + 0.0020499*t^2$	0.48	0.23	24.72	0.57
	Cubic	$Y_t = 24.807 + 0.049806*t - 0.0065813*t^2 + 0.00012243*t^3$	0.55	0.30	22.41	0.53
	Exponential	$Y_t = 24.692 * (0.99928^t)$	0.28	0.08	0.01	0
Negele	Linear	$Y_t = 25.546 + 0.013982*t$	0.45	0.20	11.22	0.21
	Quadratic	$Y_t = 25.912 - 0.023907*t + 0.0006647*t^2$	0.55	0.30	9.87	0.19
	Cubic	$Y_t = 25.755 + 0.0077829*t - 0.00071296*t^2 + 1.6113E-05*t^3$	0.56	0.31	9.71	0.19
	Exponential	$Y_t = 25.546 * (1.0005^t)$	0.45	0.20	0	0
Nekemte	Linear	$Y_t = 23.366 + 0.033501*t$	0.69	0.48	4.68	0.14
	Quadratic	$Y_t = 23.681 - 0.016216*t + 0.0013437*t^2$	0.74	0.55	4.08	0.12
	Cubic	$Y_t = 23.681 - 0.016216*t + 0.0013437*t^2$	0.74	0.55	4.08	0.12
	Exponential	$Y_t = 23.371 * (1.0014^t)$	0.69	0.48	0	0

Table (32): Comparison between trend equations for mean annual minimum temperature.

Station	Trend	Trend equation	R	R ²	SSE	MSE
Addis Ababa	Linear	$Y_t = 8.9947 + 0.021302 * t$	0.37	0.13	42.69	0.79
	Quadratic	$Y_t = 7.8204 + 0.14278 * t - 0.0021312 * t^2$	0.64	0.42	28.82	0.54
	Cubic	$Y_t = 8.0872 + 0.088976 * t + 0.0002079 * t^2 - 2.7358E-05 * t^3$	0.65	0.43	28.36	0.55
	Exponential	$Y_t = 8.9335 * (1.0024)^t$	0.38	0.14	0.09	0
Arbaminch	Linear	$Y_t = 14.822 + 0.078829 * t$	0.7	0.49	24.88	0.73
	Quadratic	$Y_t = 14.133 + 0.18759 * t - 0.0029395 * t^2$	0.74	0.55	21.98	0.67
	Cubic	$Y_t = 14.448 + 0.092103 * t + 0.0034248 * t^2 - 0.00011467 * t^3$	0.75	0.56	21.62	0.68
	Exponential	$Y_t = 14.808 * (1.005)^t$	0.7	0.49	0.02	0
Assosa	Linear	$Y_t = 14.907 + 0.011776 * t$	0.19	0.04	14.67	0.43
	Quadratic	$Y_t = 14.759 + 0.035206 * t - 0.00063324 * t^2$	0.21	0.04	14.53	0.44
	Cubic	$Y_t = 14.463 + 0.12495 * t - 0.006615 * t^2 + 0.00010778 * t^3$	0.26	0.07	14.21	0.44
	Exponential	$Y_t = 14.893 * (1.0008)^t$	0.19	0.04	0.01	0
Awassa	Linear	$Y_t = 11.729 + 0.033874 * t$	0.53	0.28	11.65	0.34

	Quadratic	$Y_t = 11.934 + 0.0014914 * t + 0.0008752 * t^2$	0.54	0.29	11.39	0.35
	Cubic	$Y_t = 12.055 - 0.035382 * t + 0.0033329 * t^2 - 4.4282E-05 * t^3$	0.54	0.30	11.34	0.35
	Exponential	$Y_t = 11.721 * (1.0028^t)$	0.52	0.27	0.02	0
Bahir Dar	Linear	$Y_t = 10.067 + 0.070085 * t$	0.62	0.38	53.35	1.3
	Quadratic	$Y_t = 10.947 - 0.047221 * t + 0.002666 * t^2$	0.67	0.45	47.56	1.19
	Cubic	$Y_t = 12.71 - 0.50203 * t + 0.028213 * t^2 - 0.00038707 * t^3$	0.78	0.61	33.13	0.85
	Exponential	$Y_t = 10.09 * (1.006^t)$	0.58	0.34	0.09	0
Kombolcha	Linear	$Y_t = 11.602 + 0.011319 * t$	0.15	0.02	77.77	1.44
	Quadratic	$Y_t = 12.012 - 0.03109 * t + 0.00074402 * t^2$	0.21	0.04	76.08	1.44
	Cubic	$Y_t = 11.635 + 0.045066 * t - 0.0025668 * t^2 + 3.8723E-05 * t^3$	0.24	0.06	75.16	1.45
	Exponential	$Y_t = 11.555 * (1.0009^t)$	0.13	0.02	0.13	0
Debremerkos	Linear	$Y_t = 8.2166 + 0.042587 * t$	0.73	0.53	23.62	0.44
	Quadratic	$Y_t = 8.3935 + 0.024288 * t + 0.00032104 * t^2$	0.73	0.54	23.31	0.44
	Cubic	$Y_t = 8.7657 - 0.050774 * t + 0.0035843 * t^2 - 3.8166E-05 * t^3$	0.74	0.55	22.42	0.43
	Exponential	$Y_t = 8.2233 * (1.0046^t)$	0.7	0.49	0.06	0

Debre Zeit	Linear	$Y_t = 11.115 + 0.017085 * t$	0.41	0.20	21.18	0.39
	Quadratic	$Y_t = 11.289 - 0.00095711 * t + 0.00031652 * t^2$	0.42	0.18	20.87	0.39
	Cubic	$Y_t = 11.497 - 0.042828 * t + 0.0021368 * t^2 - 2.129E-05 * t^3$	0.44	0.19	20.6	0.4
	Exponential	$Y_t = 11.123 * (1.0014)^t$	0.4	0.16	0.03	0
Direddawa	Linear	$Y_t = 17.622 + 0.029563 * t$	0.44	0.20	52.42	0.97
	Quadratic	$Y_t = 16.855 + 0.10893 * t - 0.0013925 * t^2$	0.54	0.29	46.5	0.88
	Cubic	$Y_t = 17.099 + 0.059563 * t + 0.00075384 * t^2 - 2.5103E-05 * t^3$	0.54	0.29	46.11	0.89
	Exponential	$Y_t = 17.546 * (1.0017)^t$	0.43	0.18	0.04	0
Gode	Linear	$Y_t = 22.125 + 0.030309 * t$	0.42	0.18	16.21	0.48
	Quadratic	$Y_t = 22.648 - 0.052158 * t + 0.0022288 * t^2$	0.51	0.26	14.55	0.44
	Cubic	$Y_t = 22.898 - 0.12817 * t + 0.0072953 * t^2 - 9.1287E-05 * t^3$	0.53	0.28	14.32	0.45
	Exponential	$Y_t = 22.114 * (1.0014)^t$	0.41	0.17	0.01	0
Gondar	Linear	$Y_t = 12.29 + 0.02446 * t$	0.57	0.33	17.59	0.33
	Quadratic	$Y_t = 12.454 + 0.0075601 * t + 0.00029649 * t^2$	0.59	0.34	17.32	0.33
	Cubic	$Y_t = 12.537 - 0.0092255 * t + 0.0010262 * t^2 - 8.5349E-06 * t^3$	0.59	0.34	17.27	0.33



	Exponential	$Y_t = 12.299 * (1.0019)^t$	0.57	0.32	0.02	0
Gore	Linear	$Y_t = 12.888 + 0.02055 * t$	0.65	0.42	8.67	0.16
	Quadratic	$Y_t = 13.055 + 0.0031988 * t + 0.00030441 * t^2$	0.66	0.44	8.39	0.16
	Cubic	$Y_t = 13.052 + 0.0039464 * t + 0.00027191 * t^2 + 3.8014E-07 * t^3$	0.66	0.44	8.39	0.16
	Exponential	$Y_t = 12.895 * (1.0015)^t$	0.64	0.41	0.01	0
Jijiga	Linear	$Y_t = 10.693 + 0.012269 * t$	0.41	0.17	10.99	0.2
	Quadratic	$Y_t = 10.486 + 0.033724 * t - 0.0003764 * t^2$	0.45	0.20	10.56	0.2
	Cubic	$Y_t = 10.341 + 0.062843 * t - 0.0016423 * t^2 + 1.4806E-05 * t^3$	0.46	0.21	10.43	0.2
	Exponential	$Y_t = 10.676 * (1.0011)^t$	0.41	0.17	0.02	0
Jima	Linear	$Y_t = 12.076 + 0.0035081 * t$	0.10	0.01	7.54	0.26
	Quadratic	$Y_t = 11.789 + 0.055707 * t - 0.0016312 * t^2$	0.24	0.06	7.12	0.25
	Cubic	$Y_t = 11.993 - 0.015249 * t + 0.0038252 * t^2 - 0.00011368 * t^3$	0.28	0.08	6.99	0.26
	Exponential	$Y_t = 12.07 * (1.0003)^t$	0.06	0.00	0.01	0
Mekele	Linear	$Y_t = 19.085 - 0.039266 * t$	0.49	0.24	19.16	0.56
	Quadratic	$Y_t = 19.355 - 0.081913 * t + 0.0011526 * t^2$	0.51	0.26	18.71	0.57

	Cubic	$Y_t = 18.465 + 0.18849*t - 0.01687*t^2 + 0.00032473*t^3$	0.61	0.37	15.79	0.49
	Exponential	$Y_t = 19.071 * (0.99789^t)$	0.48	0.23	0.01	0
Metehara	Linear	$Y_t = 11.958 + 0.067006*t$	0.67	0.58	47.8	0.89
	Quadratic	$Y_t = 13.095 - 0.050545*t + 0.0020623*t^2$	0.83	0.69	34.8	0.66
	Cubic	$Y_t = 13.03 - 0.037633*t + 0.001501*t^2 + 6.5652E-06*t^3$	0.83	0.69	34.78	0.67
	Exponential	$Y_t = 12.045 * (1.0048^t)$	0.75	0.56	0.05	0
Negele	Linear	$Y_t = 11.814 + 0.039936*t$	0.68	0.46	6.77	0.2
	Quadratic	$Y_t = 12.014 + 0.0083751*t + 0.00085299*t^2$	0.70	0.50	6.53	0.2
	Cubic	$Y_t = 12.074 - 0.0098596*t + 0.0020683*t^2 - 2.1898E-05*t^3$	0.71	0.50	6.52	0.2
	Exponential	$Y_t = 11.82 * (1.0032^t)$	0.67	0.46	0.01	0
Nekemte	Linear	$Y_t = 12.974 + 0.013837*t$	0.69	0.48	6.77	0.20
	Quadratic	$Y_t = 12.774 + 0.036382*t - 0.00043355*t^2$	0.70	0.50	6.53	0.20
	Cubic	$Y_t = 13.254 - 0.069258*t + 0.0045963*t^2 - 6.4485E-05*t^3$	0.71	0.50	6.52	0.20
	Exponential	$Y_t = 12.971 * (1.001^t)$	0.67	0.46	0.01	0.00

Table (33): Comparison between trend equations for total annual rainfall.

Station	Trend	Trend equation	R	R ²	SSE	MSE
Addis Ababa	Linear	$Y_t = 1244.6 - 0.7665 * t$	0.12	0.01	3860362	37118.87
	Quadratic	$Y_t = 1262.7 - 1.769 * t + 0.0093689 * t^2$	0.13	0.02	3853840	37415.92
	Cubic	$Y_t = 1264.6 - 1.9862 * t + 0.01442 * t^2 - 3.1473E-05 * t^3$	0.13	0.02	3853786	37782.22
	Exponential	$Y_t = 1229.7 * (0.99937)^t$	0.12	0.02	0.47	0
Arbaminch	Linear	$Y_t = 825.52 + 2.01 * t$	0.19	0.04	860791.8	19563.45
	Quadratic	$Y_t = 813.9 + 3.4625 * t - 0.030904 * t^2$	0.19	0.04	859701.6	19993.06
	Cubic	$Y_t = 848.28 - 4.8702 * t + 0.4076 * t^2 - 0.0062199 * t^3$	0.21	0.04	853719.8	20326.66
	Exponential	$Y_t = 819.73 * (1.0021)^t$	0.18	0.03	0.21	0
Assosa	Linear	$Y_t = 1312.3 - 10.591 * t$	0.39	0.15	5162719	117334.5
	Quadratic	$Y_t = 1589.4 - 45.221 * t + 0.73681 * t^2$	0.5	0.25	4542999	105651.1
	Cubic	$Y_t = 1319.8 + 20.117 * t - 2.7015 * t^2 + 0.048771 * t^3$	0.56	0.31	4175217	99409.93
	Exponential	$Y_t = 1269.8 * (0.98871)^t$	0.31	0.1	1.84	0.04
Awash	Linear	$Y_t = 607.91 + 1.3687 * t$	0.16	0.03	766972.4	15652.5
	Quadratic	$Y_t = 641.25 - 2.4066 * t + 0.072603 * t^2$	0.2	0.04	756887.8	15768.5
	Cubic	$Y_t = 646.6 - 3.5845 * t + 0.12868 * t^2 - 0.00071897 * t^3$	0.2	0.04	756723	16100.49

	Exponential	$Y_t = 596.24 * (1.0022)^t$	0.18	0.03	0.33	0.01
Awassa	Linear	$Y_t = 908.57 + 1.2972*t$	0.1	0.01	628596	18488.12
	Quadratic	$Y_t = 848.96 + 10.71*t - 0.25439*t^2$	0.21	0.04	606940.5	18392.14
	Cubic	$Y_t = 766.42 + 35.777*t - 1.9252*t^2 + 0.030104*t^3$	0.29	0.08	581850	18182.81
	Exponential	$Y_t = 898.04 * (1.0015)^t$	0.11	0.01	0.13	0
Bahir Dar	Linear	$Y_t = 1511.4 - 2.8475*t$	0.16	0.03	2381777	54131.3
	Quadratic	$Y_t = 1566.9 - 9.7896*t + 0.14771*t^2$	0.19	0.04	2356872	54810.99
	Cubic	$Y_t = 1292.4 + 56.752*t - 3.354*t^2 + 0.049669*t^3$	0.44	0.19	1975423	47033.88
	Exponential	$Y_t = 1482.1 * (0.99835)^t$	0.13	0.02	0.23	0.01
Bati	Linear	$Y_t = 1143.5 - 4.7055*t$	0.32	0.1	1090330	27957.18
	Quadratic	$Y_t = 1157.4 - 6.6399*t + 0.046057*t^2$	0.32	0.11	1088969	28657.08
	Cubic	$Y_t = 1067.3 + 17.654*t - 1.3827*t^2 + 0.022679*t^3$	0.37	0.13	1053492	28472.77
	Exponential	$Y_t = 1136.2 * (0.99531)^t$	0.32	0.1	0.21	0.01
Kombolcha	Linear	$Y_t = 1068 - 0.64693*t$	0.07	0.01	1907567	29805.73
	Quadratic	$Y_t = 1087.3 - 2.3539*t + 0.025477*t^2$	0.09	0.01	1903056	30207.24
	Cubic	$Y_t = 1085.1 - 1.9716*t + 0.011321*t^2 + 0.00014086*t^3$	0.09	0.01	1903017	30693.83
	Exponential	$Y_t = 1051.5 * (0.99943)^t$	0.06	0	0.36	0.01

Debremarkos	Linear	$Y_t = 1391.5 - 1.914 * t$	0.2	0.04	1132080	22197.64
	Quadratic	$Y_t = 1454.5 - 8.7891 * t + 0.12732 * t^2$	0.27	0.07	1094487	21889.73
	Cubic	$Y_t = 1438.8 - 5.4464 * t - 0.026004 * t^2 + 0.0018929 * t^3$	0.27	0.07	1092991	22305.94
	Exponential	$Y_t = 1381.3 * (0.99865)^t$	0.19	0.04	0.11	0
Debre Zeit	Linear	$Y_t = 802.1 + 2.0058 * t$	0.18	0.03	1613092	30435.69
	Quadratic	$Y_t = 748.05 + 7.6952 * t - 0.1016 * t^2$	0.23	0.05	1584279	30466.91
	Cubic	$Y_t = 500.82 + 58.403 * t - 2.3451 * t^2 + 0.026708 * t^3$	0.53	0.28	1198226	23494.64
	Exponential	$Y_t = 770.69 * (1.0031)^t$	0.23	0.05	0.43	0.01
Dessie	Linear	$Y_t = 1136.2 + 2.3391 * t$	0.17	0.03	1579471	35897.07
	Quadratic	$Y_t = 1253.7 - 12.353 * t + 0.31259 * t^2$	0.31	0.1	1467929	34137.87
	Cubic	$Y_t = 1357.4 - 37.473 * t + 1.6345 * t^2 - 0.018751 * t^3$	0.36	0.13	1413566	33656.33
	Exponential	$Y_t = 1122.1 * (1.002)^t$	0.16	0.02	0.24	0.01
Diredawa	Linear	$Y_t = 630.2 - 0.11412 * t$	0.01	0	1727724	31994.89
	Quadratic	$Y_t = 647.32 - 1.8846 * t + 0.031062 * t^2$	0.04	0	1724777	32542.96
	Cubic	$Y_t = 633.5 + 0.90247 * t - 0.090105 * t^2 + 0.0014172 * t^3$	0.05	0	1723543	33145.07
	Exponential	$Y_t = 585.67 * (1.0009)^t$	0.05	0	0.92	0.02
ambe	Linear	$Y_t = 637.25 - 0.22367 * t$	0.02	0	1705978	31592.18

	Quadratic	$Y_t = 653.98 - 1.9544*t + 0.030363*t^2$	0.05	0	1703162	32135.12
	Cubic	$Y_t = 641.74 + 0.51324*t - 0.076913*t^2 + 0.0012547*t^3$	0.05	0	1702195	32734.52
	Exponential	$Y_t = 594.6 * (1.0007^t)$	0.04	0	0.89	0.02
Jima	Linear	$Y_t = 1498 + 0.083264*t$	0.01	0	1881416	34841.03
	Quadratic	$Y_t = 1564.4 - 6.7942*t + 0.12066*t^2$	0.15	0.02	1836944	34659.33
	Cubic	$Y_t = 1621.8 - 18.358*t + 0.62339*t^2 - 0.0058799*t^3$	0.19	0.03	1815714	34917.58
	Exponential	$Y_t = 1489.4 * (1^t)$	0	0	0.15	0
Gode	Linear	$Y_t = 295.8 - 2.6258*t$	0.22	0.05	711961.2	18735.82
	Quadratic	$Y_t = 419.18 - 20.252*t + 0.42991*t^2$	0.43	0.19	607146.8	16409.37
	Cubic	$Y_t = 522.31 - 48.693*t + 2.1429*t^2 - 0.027853*t^3$	0.5	0.25	562147.1	15615.2
	Exponential	$Y_t = 232.4 * (0.99404^t)$	0.11	0.01	2.72	0.07
Gondar	Linear	$Y_t = 1175.8 - 0.11859*t$	0.01	0	3640452	62766.41
	Quadratic	$Y_t = 1293.9 - 11.549*t + 0.18738*t^2$	0.2	0.04	3488980	61210.17
	Cubic	$Y_t = 1282.3 - 9.3577*t + 0.098318*t^2 + 0.00097337*t^3$	0.2	0.04	3488036	62286.36
	Exponential	$Y_t = 1159.6 * (0.99969^t)$	0.03	0	0.44	0.01
Gore	Linear	$Y_t = 2172.9 - 1.5109*t$	0.12	0.01	1210349 2	128760.6
	Quadratic	$Y_t = 1747.3 + 24.546*t - 0.26863*t^2$	0.53	0.28	8836456	95015.65

	Cubic	$Y_t = 1759.4 + 23.092*t - 0.23136*t^2 - 0.00025616*t^3$	0.53	0.28	8834697	96029.32
	Exponential	$Y_t = 2162.5 * (0.99911)^t$	0.15	0.02	0.47	0
Harer	Linear	$Y_t = 808.34 + 3.8658*t$	0.18	0.03	1683022	49500.66
	Quadratic	$Y_t = 628.31 + 32.291*t - 0.76824*t^2$	0.38	0.15	1485527	45015.98
	Cubic	$Y_t = 566.04 + 51.204*t - 2.0288*t^2 + 0.022713*t^3$	0.39	0.15	1471244	45976.39
	Exponential	$Y_t = 740.07 * (1.0075)^t$	0.28	0.08	0.48	0.01
Jijiga	Linear	$Y_t = 730.27 - 2.4928*t$	0.19	0.03	2564662	47493.74
	Quadratic	$Y_t = 572.72 + 13.806*t - 0.28595*t^2$	0.36	0.13	2314880	43676.99
	Cubic	$Y_t = 382.61 + 52.143*t - 1.9526*t^2 + 0.019493*t^3$	0.46	0.22	2081550	40029.82
	Exponential	$Y_t = 687.86 * (0.99696)^t$	0.17	0.03	0.83	0.02
Mekele	Linear	$Y_t = 631.34 - 0.054021*t$	0	0	1787067	35741.33
	Quadratic	$Y_t = 580.77 + 5.5651*t - 0.10602*t^2$	0.12	0.01	1763368	35987.11
	Cubic	$Y_t = 716.3 - 23.735*t + 1.263*t^2 - 0.01722*t^3$	0.27	0.07	1655055	34480.32
	Exponential	$Y_t = 607.02 * (0.99985)^t$	0.01	0	0.8	0.02
Metehara	Linear	$Y_t = 712.26 - 5.5905*t$	0.38	0.15	704432.2	20718.59
	Quadratic	$Y_t = 621.61 + 8.722*t - 0.38682*t^2$	0.46	0.21	654361.1	19829.13
	Cubic	$Y_t = 648.01 + 0.70636*t + 0.14742*t^2 - 0.0096261*t^3$	0.46	0.21	651795.8	20368.62

	Exponential	$Y_t = 705.81 * (0.99038^t)$	0.4	0.16	0.36	0.01
Negele	Linear	$Y_t = 860.94 - 4.6223*t$	0.33	0.11	1436076	32638.08
	Quadratic	$Y_t = 727.68 + 12.035*t - 0.35442*t^2$	0.44	0.2	1292686	30062.47
	Cubic	$Y_t = 480.53 + 71.942*t - 3.5069*t^2 + 0.044716*t^3$	0.62	0.39	983511.6	23416.94
	Exponential	$Y_t = 839.34 * (0.99406^t)$	0.32	0.1	0.49	0.01
Nekemte	Linear	$Y_t = 2131.9 - 2.7325*t$	0.13	0.02	1756233	51653.92
	Quadratic	$Y_t = 2201.7 - 13.74*t + 0.2975*t^2$	0.18	0.03	1726617	52321.74
	Cubic	$Y_t = 2484.2 - 99.553*t + 6.017*t^2 - 0.10305*t^3$	0.44	0.2	1432592	44768.5
	Exponential	$Y_t = 2125.1 * (0.99857^t)$	0.14	0.02	0.07	0
Robe	Linear	$Y_t = 1272.5 - 13.525*t$	0.3	0.09	4451359	153495.1
	Quadratic	$Y_t = 1002.2 + 35.612*t - 1.5355*t^2$	0.41	0.17	4078282	145652.9
	Cubic	$Y_t = 598.2 + 176.09*t - 12.338*t^2 + 0.22506*t^3$	0.52	0.27	3587820	132882.2
	Exponential	$Y_t = 1215.8 * (0.98712^t)$	0.32	0.1	0.71	0.02
Sibu Sire	Linear	$Y_t = 1401.7 - 1.7751*t$	0.12	0.01	2435306	48706.11
	Quadratic	$Y_t = 1489.4 - 11.526*t + 0.18397*t^2$	0.21	0.04	2363946	48243.79
	Cubic	$Y_t = 1564.8 - 27.832*t + 0.94585*t^2 - 0.0095834*t^3$	0.24	0.06	2330399	48549.98
	Exponential	$Y_t = 1374 * (0.99897^t)$	0.09	0.01	0.26	0.01

Wonji (63373)	Linear	$Y_t = 763.07 + 2.3068 * t$	0.19	0.03	1194552	27148.91
	Quadratic	$Y_t = 722.71 + 7.3516 * t - 0.10734 * t^2$	0.21	0.05	1181400	27474.42
	Cubic	$Y_t = 646.01 + 25.943 * t - 1.0857 * t^2 + 0.013877 * t^3$	0.26	0.07	1151623	27419.59
	Exponential	$Y_t = 737.05 * (1.0035)^t$	0.23	0.05	0.34	0.01

4.27. Trends of Mann-Kendall test

According to the Mann-Kendall test for trend (Table 34), positive trends of the mean annual maximum temperature (Long period) were observed at all the studied stations. The trends ranged between 0 and 0.04 °C.

For significance of trends, according to Mann-Kendall test for trend, the trends at all stations were significant level except 6 stations (Awash, Diredawa, Gode, Jijiga, Jima and Mekele), while the trends of mean annual maximum temperature were significant at 0.1 level for Assosa station in this period.

From table (35), positive trends of the mean annual minimum temperature were observed at all study stations except Assosa, Kombolcha and Diredawa. The positive trends ranged between 0.01 and 0.07 °C at Assosa and Arba Minch, respectively.

Negative trends were not significant at Diredawa station, while Mekele and Metehara stations were significant at 0.01 level.

Table (36), it is noted that according to Mann-Kendall test for annual rainfall trend, the trends at all stations were not significant except Assosa, Negele, Bati, Wonji and Metehara.

Table (34): Mean annual maximum temperature trends, Mann –Kendall test for 1950-2005.

Station	First	Last	n	Test Z	Sig.	Q	B
Addis Ababa	1960	2005	46	4.8	***	0.04	21.2
Arba Minch	1970	2005	36	4.0	***	0.04	28.4
Assosa	1970	2005	36	1.7	+	0.01	27.6
Awash	1970	2000	31	-1.6		-0.01	33.6
Awassa	1970	2005	36	4.4	***	0.04	25.0
Bahar Dar	1960	2005	46	4.6	***	0.03	25.5
Kombolcha	1950	2005	56	3.3	**	0.02	25.7
Debre Markos	1950	2005	56	3.5	***	0.01	22.0
Debre Zeit	1950	2005	56	3.0	**	0.01	26.0
Diredawa	1950	2005	56	0.8		0.00	31.4
Gode	1970	2005	31	1.1		0.01	34.5
Gondar	1950	2005	56	3.9	***	0.02	26.0
Gore	1950	2005	56	4.0	***	0.01	23.1
Jijiga	1950	2005	56	0.5		0.00	27.2
Jima	1950	2005	56	0.3		0.00	26.9
Mekele	1960	2005	46	-1.1		-0.01	24.8
Negele	1950	2005	56	3.4	***	0.01	25.6
Nekemte	1970	2005	36	4.6	***	0.04	22.4

Sig. = the tested significance levels are 0.001, 0.01, 0.05 and 0.1 as:

*** = 0.001 level of significance - ** = 0.01 level of significance

* = 0.05 level of significance - + = 0.1 level of significance

If the cell is **blank**, the significance level is > 0.1

Table (35): Mean annual minimum temperature trends, Mann –Kendall test for 1950-2005.

Station	First	Last	n	Test Z	Sig.	Q	B
Addis Ababa	1950	2005	56	2.9	**	0.02	8.7
Arba Minch	1970	2005	36	4.5	***	0.07	13.2
Assosa	1970	2005	36	1.0		0.01	14.7
Awassa	1960	2000	31	2.0	*	0.03	11.3
Bahar Dar	1950	2005	46	4.6	***	0.06	9.7
Kombolcha	1950	2005	56	1.2		0.01	11.8
Debre Markos	1950	2005	56	6.8	***	0.04	8.3
Debre Zeit	1950	2005	56	3.2	**	0.02	11.0
Diredawa	1970	2005	36	-1.1		-0.01	19.2
Gode	1950	2005	36	2.8	**	0.02	22.1
Gondar	1950	2005	56	4.7	***	0.03	12.2
Gore	1950	2005	56	5.1	***	0.02	12.8
Jijiga	1950	2005	56	4.2	***	0.03	10.5
Jima	1950	2005	56	2.6	**	0.01	10.8
Mekele	1960	1990	31	-2.9	**	-0.04	12.3
Metehara	1970	2005	36	-2.6	**	-0.04	19.9
Negele	1950	2005	56	5.0	***	0.06	11.9
Nekemte	1970	2005	36	5.1	***	0.04	10.9

Sig. = the tested significance levels are 0.001, 0.01, 0.05 and 0.1 as:

*** = 0.001 level of significance - ** = 0.01 level of significance

* = 0.05 level of significance - + = 0.1 level of significance

If the cell is **blank**, the significance level is > 0.1

Table (36): Annual rainfall trends, Mann –Kendall test for 1950-2005.

Station	First	Last	n	Test Z	Sig.	Q	B
Addis Ababa	1900	2005	105	-1.2		-0.9	1215.4
Arba Minch	1960	2005	46	1.1		1.4	833.2
Assosa	1960	2005	46	-3.4	***	-8.9	1328.4
Bahar Dar	1960	2005	46	-0.9		-2.4	1535.6
Negele	1960	2005	46	-2.3	*	-4.4	846.1
Gode	1960	2000	41	-1.0		-1.7	917.4
Nekemte	1960	2000	41	-0.2		-0.6	2082.8
Awash	1950	2000	51	1.5		1.6	588.1
Bati	1950	1990	41	-2.1	*	-4.9	1165.0
Debre Zeit	1950	2005	56	1.6		2.4	789.0
Debre Markos	1950	2005	56	-0.8		-0.9	1351.4
Diredawa	1950	2005	56	-0.3		-0.4	647.8
Gambela	1950	2005	56	-0.3		-0.4	652.9
Jima	1950	2005	56	-0.3		-0.5	1484.5
Gondar	1950	2005	56	-0.5		-1.1	1146.8
Harar	1950	1985	36	0.7		2.9	827.5
Jijiga	1950	2005	56	-1.2		-1.3	638.9
Wonji	1950	1995	46	1.6	+	2.8	758.9
Mekele	1950	2005	56	-0.3		-0.4	622.9
Metehara	1970	2005	36	-2.0	*	-4.7	658.9
Nekemte	1970	2005	36	-0.9		-4.0	2116.4
Awassa	1970	2005	36	0.7		1.4	924.4
Kombolcha	1940	2005	66	-0.4		-0.4	1071.3
Gode	1966	2005	40	-0.6		-0.9	245.4
Gore	1910	2005	96	-1.6		-1.7	2156.2
Sibu Sire	1954	2005	52	-0.5		-0.9	1370.8

Sig. = the tested significance levels are 0.001, 0.01, 0.05 and 0.1 as:

*** = 0.001 level of significance - ** = 0.01 level of significance

* = 0.05 level of significance - + = 0.1 level of significance

If the cell is **blank**, the significance level is > 0.1

4.28. Time series analyses

4.28.1. Study area and rainfall data

The rainfall stations of Bahar Dar, Nekemte, Debre Markos and Addis Ababa are located within the vicinity of the Blue Nile basin district in the North, West and middle of Ethiopia (Figure 19). The data were provided by Ethiopia Meteorological Agency for the periods 1900-2005 (For Addis Ababa only (Figure 21)) and 1953-2005 (For the other stations) (Figure 30 and 39), assuming no missing data for all stations.

Rainfall on monthly basis of these 4 rainfall stations have been used to develop the ARIMA models. The mean monthly rainfall for the above stations was as follow: 120.4, 173.4, 111.7, and 100.3 (mm), respectively for the period 1953-2005.

All data of these stations, fluctuate greatly with wide variation where its value may ranged between zero to maximum value (more than 500 mm) in addition the maximum value rarely repeated, so it is not easy to find suitable ARIMA models to represent them unless enough trials have been applied. The complexity may be increased due to using monthly period to represent a seasonal period (S).

In general, there are about 12 monthly every year for the Ethiopia, which represent the S term in the general form of ARIMA model of $(p,d,q) \times (P,D,Q)_S$.

Seasonal differencing was applied on all the time series from the 4 stations after taking a log transformation function, and then applying ARIMA models using Minitab software Release 16 and SPSS 17. The ARIMA model describes the seasonal differencing time series.

The time series was divided into three periods: The first period, from 1953 to 2004 for all stations except Addis Ababa from 1900 to 2004, where the data were used to analyze the characteristics of the rainfall and selecting the most appropriate rainfall forecast models. The second period is the final year (2005) that was used for evaluating the performance of the selected models. The third period, the selected model was used to forecast rainfall time series for the up-coming 25 years (2005-2030).

4.28.2. Box-Jenkins ARIMA model

Box and Jenkins, (1976) described a methodology (Figure 20) in time series analysis to find the best fit of time series to past values in order to make future forecasts.

The methodology consists of four steps: 1) Model identification. 2) Estimation of model parameters. 3) Diagnostic checking for the identified model appropriateness for modeling and 4) Application of the model (forecasting).

The most important analytical tools used with time series analysis and forecasting are the Autocorrelation Function (ACF) and the Partial Autocorrelation Function (PACF). They measure the statistical relationships between observations in a single data series. Using ACF gives big advantage of measuring the amount of linear dependence between observations in a time series that are separated by a lag k . The PACF plot is used to decide how many auto regressive terms are necessary to expose one or more of the time lags where high correlations appear seasonality of the series, trend either in the mean level or in the variance of the series (*Zakaria, et al., 2013*).

The autocorrelation coefficient provides a measure of temporal correlation between rainfall data points with different time lags; namely 1, 2, 3, ..., n years. Thus, autocorrelation provides initial information relevant to the internal organisation of each time series data. The prevalence of autocorrelation in a data series is also an indication of persistence in the series of observations (*Zakaria, et al., 2013*). The auto-correlation coefficients provide an essential hint whether forecasting models can be developed based on the given data. For a purely incidental event, all autocorrelation coefficients are zero, apart from $r(0)$ which is equal to 1, shows the results of autocorrelation analysis of monthly rainfall time series data of the North, West and middle of Ethiopia. The autocorrelation coefficients of monthly rainfall lie between -0.14 and 0.86, each with standard error of 0.04 (Table 33, 34, 35 and 36).

In order to identify the model (step 1), ACF and PACF have to be estimated. They are used not only to help guess the form of the model, but also to obtain approximate estimates of the parameters (*Box, et al., 1994*).

The next step is to estimate the parameters in the model (step 2) using maximum likelihood estimation. Finding the parameters that maximize the probability of observations is the main goal of maximum likelihood.

The next, is checking the adequacy of the model for the series (step 3). The assumption is the residual is a white noise process and that the process is stationary and independent.

Model diagnostic checking is accomplished, in this work, through careful analysis of the residual series, the histogram of the residual, sample correlation and a diagnosis test.

The statistic Q has a chi-square (χ^2) distribution with degrees of freedom $(h-m)$ where m is the number of parameters in the model which has been fitted to the data, the chi-square value has been compared with the tabulated values; in order to evaluate the valid model otherwise the model will be rejected.

For successful models, it should be noted that a model with the less number of variables gives the best forecasting results, i.e. for a time series having more than one successful ARIMA model, in this case it should be consider the model with less variables (number of AR and/or MA), this is achieved by using Akaike's Information Criterion (AIC) (*Akaike, 1974*), in order to select the best ARIMA model among successful models. The smallest value of AIC should be chosen.

4.28.3. Results and discussion of time series

The data of Ethiopia stations were chosen as a sample of calculations. The first step in the application of the methodology is to check whether the time series (monthly rainfall) is stationary and has seasonality.

The monthly rainfall data (Figure 21) shows that there is a seasonal cycle of the series and it is not stationary. The plots of ACF and PACF of the original data (Figures 22 and 23) show also that the rainfall data is not stationary, where both ACF and PACF have significant values at different lags.

A stationary time series has a constant mean and has no trend over time. However it could satisfy stationary in variance by having log transformation and satisfy stationary in the mean by having differencing of the original data in order to fit an ARIMA model.

Seasonal trend could be removed by having seasonal differencing (D) through subtracting the current observation from the previous twelve observations, as described before that rainfall in Ethiopia district; it nearly extends for 12 monthly annually. In general the seasonality in a time series is a regular pattern of changes that repeats over time periods (S).

However, if differenced transformation is applied only once to a series, that means data has been "first differenced" (D=1). This process essentially eliminates the trend for a time series growing at a fairly constant rate. If it is growing at an increasing rate, the same procedure (Difference the data) can be applied again, then the data would be "second differenced" (D=2). If a trend is present in the data, then non-seasonal (regular) differencing (d) is required.

The monthly rainfall data, of Ethiopia stations, required to have a first seasonal difference of the original data in order to have stationary series. Then, the ACF and PACF for the differenced series should be tested to check stationary.

From all of the above, an ARIMA model of $(p, 0, q) \times (P, 1, Q)$ 12 could be identified.

In the Box-Jenkins methodology, the estimated model will be depending on the ACF and PACF. After ARIMA model was identified, the p, q, P and Q parameters need to be identified for Ethiopia monthly rainfall time series.

The data were tested to check the construction of the ARIMA model by selecting the required order of the D that making the series stationary, as well as specifying the necessary order of the p, P, q and Q to adequately represent the time series model.

It should be noted that, even if the ARIMA model has been correctly identified and giving good results, this will not mean that it is the only model that can be considered where most documentations of time series dealing with ARIMA models indicated that other ARIMA models with values of AR and/or MA less than same parameters of the considered ARIMA (for the seasonal or nonseasonal variables) might be available (Salas, et al., 1980). In this case, these models should be identified and tested. Box-Jenkins methodology has been used in this research to build Autoregressive Integrated Moving Average (ARIMA) models for monthly rainfall data from four rainfall stations (Bahar Dar, Nekemte, Debre Markos and Addis Ababa). After selecting the most appropriate model, it was found that ARIMA model $(0,0,0) \times (1,1,1)_{12}$, $(0,0,0) \times (1,1,1)_{12}$, $(0,0,0) \times (0,1,1)_{12}$ and $(0,0,1) \times (0,1,1)_{12}$ is among several models that passed all statistic tests required in the Box-Jenkins methodology for Bahar Dar, Nekemte, Debre Markos and Addis Ababa respectively, of the North, West and middle of Ethiopia.

Tables (41, 42, 43 and 44) show the estimated parameters for the successful Ethiopia ARIMA model $(0,0,0) \times (1,1,1)_{12}$, $(0,0,0) \times (1,1,1)_{12}$, $(0,0,0) \times (0,1,1)_{12}$ and $(0,0,1) \times (0,1,1)_{12}$.

The residuals from the fitted model are examined for the adequacy. This is done by testing the residual ACF and PACF plots that shows all the autocorrelation and partial autocorrelations of the residuals at different lags are within the 95 % confidence limits.

Tables (41, 42, 43 and 44) show the Ljung-Box Q-test of the residuals for the successful Ethiopia ARIMA model $(0,0,0) \times (1,1,1)_{12}$,

$(0,0,0) \times (1,1,1)_{12}$, $(0,0,0) \times (0,1,1)_{12}$ and $(0,0,1) \times (0,1,1)_{12}$. This model appears to fit the Ethiopia data.

Only the model with no significant residuals should be considered to indicate that the model is adequate to represent the considered time series. (Figures 24, 33, 42 and 48) show the residual ACF and PACF plots.

Figures (25, 34, 43 and 49) represent four graphical measures for the adequacy of the model.

The first measure is the normal probability of the residuals which is good as required for an adequate model. Almost all of the residuals are within acceptable limits which indicate the adequacy of the recommended model.

Although some other ARIMA models have been applied on the Ethiopia data such as $(0,0,1) \times (3,1,1)_{12}$, $(1,0,0) \times (3,1,1)_{12}$ and $(0,0,3) \times (1,1,1)_{12}$ that pass the probability and Ljung-Box Q-tests but they still contain little residuals which might not be significant and occur at late or delayed lag (60). These were not considered as the successful models. On the basis of the above, the selected ARIMA $(0,0,0) \times (1,1,1)_{12}$, $(0,0,0) \times (1,1,1)_{12}$, $(0,0,0) \times (0,1,1)_{12}$ and $(0,0,1) \times (0,1,1)_{12}$ model is adequate to represent the Ethiopia data and could be used to forecast the future rainfall data. After finding a valid model, monthly rainfall depth for the Ethiopia station is forecast (step 4) (Figure 26).

The performance of the Ethiopia ARIMA model $(0,0,0) \times (1,1,1)_{12}$, $(0,0,0) \times (1,1,1)_{12}$, $(0,0,0) \times (0,1,1)_{12}$ and $(0,0,1) \times (0,1,1)_{12}$ is evaluated by forecasting the data for the year 2005. Both the forecasted and Actual monthly rainfall of the Ethiopia station for the year 2005 were fitted on the

same plot to indicate the model adequacy, performance and comparison purposes (Figure 27).

The similarity and matching between the forecasted and Actual rainfall were good. The above comparison increases confidence with the ARIMA (0,0,1)x(0,1,1)₁₂ to represent the rainfall data at Addis Ababa station and can be use for forecasting the future rainfall data. Figure (28 and 29) shows the forecasting rainfall for the years 2006-2030 using ARIMA (0,0,1)x(0,1,1)₁₂.

The same procedures of the Box-Jenkins methodology were followed for the other three stations (Bahar Dar, Nekemte and Debre Markos) to forecast future rainfall.

In the following three stations (Bahar Dar, Nekemte and Debre Markos), it is found that some ARIMA models passed all the statistical tests required in the Box-Jenkins methodology without significant residuals for ACF and PACF plots. These models are the following.

For Bahar Dar data the ARIMA model was (0,0,0)x(1,1,1)₁₂, for Nekemte data the ARIMA model was (0,0,0)x(1,1,1)₁₂ for Debre Markos data the ARIMA model was (1,1,1)x(0,1,1)₁₂. (Table 42, 43 and 44) shows the ARIMA coefficients for the above models.

Tables (42, 43 and 44) show the results of the Ljung-Box Q-test of the residuals for the ARIMA models according to the stations.

The selected ARIMA models for the three stations (Bahar Dar, Nekemte and Debre Markos) have the biggest values of stationary R-squared (Tables 42, 43 and 44) among other successful ARIMA models.

Thus, these models can represent rainfall data and can be used with confidence to forecast future rainfall data.

Figures (34, 43 and 49) show the four graphical measures for the adequacy of the selected ARIMA models for the three stations (Bahar Dar, Nekemte and Debre Markos) respectively. The normal probability plots of the residuals show that most of the residuals are on the straight line having a good histograms shape. Follow-up the plots of residuals vs. fitted values and order of the data respectively, show that the errors have constant variance, the points on the plot appear to be randomly scattered around zero.

Almost all of the residuals are within acceptable limits which indicate the adequacy of the recommended models.

The performance of ARIMA models for the above three stations are evaluated by forecasting the data for the year 2005 to indicate the models adequacy, performance and comparison purposes (Figures 36, 45 and 51).

Figures (37 and 38) show forecast rainfall for the years 2006-2030 for Bahar Dar station.

Figures (46 and 47) show forecast rainfall for the years 2006-2030 for Nekemte station.

Figures (52) show forecast rainfall for the years 2006-2030 for Debre Markos station.

Table (37): Autocorrelation, partial autocorrelation, stander error and Box-Ljung statistic of rainfall (mm) for Addis Ababa station.

Lag	Autocorrelation	Std. Error ^a	Box-Ljung Statistic			Lag	Partial Autocorrelation	Std. Error ^a
			Value	df	Sig. ^b			
1	0.60	0.03	455.8	1	0.00	1	0.60	0.03
2	0.15	0.03	482.9	2	0.00	2	-0.33	0.03
3	-0.18	0.03	523.2	3	0.00	3	-0.17	0.03
4	-0.31	0.03	648.2	4	0.00	4	-0.09	0.03
5	-0.39	0.03	840.2	5	0.00	5	-0.23	0.03
6	-0.42	0.03	1065.1	6	0.00	6	-0.23	0.03
7	-0.39	0.03	1260.2	7	0.00	7	-0.22	0.03
8	-0.31	0.03	1386.3	8	0.00	8	-0.28	0.03
9	-0.17	0.03	1423.8	9	0.00	9	-0.25	0.03
10	0.16	0.03	1455.7	10	0.00	10	0.10	0.03
11	0.57	0.03	1875.3	11	0.00	11	0.36	0.03
12	0.78	0.03	2657.9	12	0.00	12	0.38	0.03
13	0.56	0.03	3067.8	13	0.00	13	0.09	0.03
14	0.14	0.03	3091.7	14	0.00	14	-0.10	0.03
15	-0.18	0.03	3132.7	15	0.00	15	-0.05	0.03
16	-0.32	0.03	3263.3	16	0.00	16	-0.02	0.03

a. The underlying process assumed is independence (white noise).

b. Based on the asymptotic chi-square approximation.

Table (38): Autocorrelation, partial autocorrelation, stander error and Box-Ljung statistic of rainfall (mm) for Bahar Dar station.

Lag	Autocorrelation	Std. Error ^a	Box-Ljung Statistic			Partial Autocorrelation	Std. Error
			Value	df	Sig. ^b		
1	0.66	0.04	239.3	1	0.001	0.66	0.04
2	0.22	0.04	266.6	2	0.001	-0.37	0.04
3	-0.14	0.04	277.6	3	0.001	-0.20	0.04
4	-0.39	0.04	360.9	4	0.001	-0.21	0.04
5	-0.50	0.04	501.8	5	0.001	-0.20	0.04
6	-0.52	0.04	654.9	6	0.001	-0.25	0.04
7	-0.49	0.04	791.0	7	0.001	-0.34	0.04
8	-0.38	0.04	870.8	8	0.001	-0.32	0.04
9	-0.14	0.04	882.0	9	0.001	-0.25	0.04
10	0.23	0.04	912.3	10	0.001	0.03	0.04
11	0.64	0.04	1144.2	11	0.001	0.34	0.04
12	0.86	0.04	1566.5	12	0.001	0.50	0.04
13	0.64	0.04	1800.2	13	0.001	0.05	0.04
14	0.23	0.04	1829.2	14	0.001	-0.04	0.04
15	-0.14	0.04	1840.4	15	0.001	-0.02	0.04
16	-0.39	0.04	1925.4	16	0.001	-0.02	0.04

a: The underlying process assumed is independence (white noise).

b: Based on the asymptotic chi-square approximation.

Table (39): Autocorrelation, partial autocorrelation, stander error and Box-Ljung statistic of rainfall (mm) for Nekemte station.

Lag	Autocorrelation	Std. Error ^a	Box-Ljung Statistic			Lag	Partial Autocorrelation	Std. Error ^a
			Value	df	Sig. ^b			
1	0.74	0.05	237.80	1	0.001	1	0.7	0.05
2	0.38	0.05	301.37	2	0.001	2	-0.4	0.05
3	-0.04	0.05	301.97	3	0.001	3	-0.4	0.05
4	-0.43	0.05	383.29	4	0.001	4	-0.4	0.05
5	-0.69	0.05	594.39	5	0.001	5	-0.3	0.05
6	-0.76	0.05	850.70	6	0.001	6	-0.2	0.05
7	-0.67	0.05	1045.86	7	0.001	7	-0.3	0.05
8	-0.41	0.05	1119.30	8	0.001	8	-0.2	0.05
9	-0.03	0.05	1119.77	9	0.001	9	-0.1	0.05
10	0.38	0.05	1182.49	10	0.001	10	0.1	0.05
11	0.72	0.05	1415.83	11	0.001	11	0.3	0.05
12	0.85	0.05	1738.51	12	0.001	12	0.2	0.05
13	0.71	0.05	1965.18	13	0.001	13	0.1	0.05
14	0.37	0.05	2025.47	14	0.001	14	-0.1	0.05
15	-0.04	0.05	2026.35	15	0.001	15	0.0	0.05
16	-0.42	0.05	2107.24	16	0.001	16	0.0	0.05

a. The underlying process assumed is independence (white noise).

b. Based on the asymptotic chi-square approximation.

Table (40): Autocorrelation, partial autocorrelation, stander error and Box-Ljung statistic of rainfall (mm) for Debra Markos station.

Lag	Autocorrelation	Std. Error ^a	Box-Ljung Statistic			Lag	Partial Autocorrelation	Std. Error ^a
			Value	df	Sig. ^b			
1	0.6	0.0	270.0	1	0.001	1	0.65	0.04
2	0.3	0.0	310.7	2	0.001	2	-0.29	0.04
3	-0.1	0.0	321.3	3	0.001	3	-0.28	0.04
4	-0.4	0.0	418.4	4	0.001	4	-0.19	0.04
5	-0.5	0.0	596.8	5	0.001	5	-0.22	0.04
6	-0.6	0.0	807.9	6	0.001	6	-0.29	0.04
7	-0.5	0.0	982.9	7	0.001	7	-0.31	0.04
8	-0.4	0.0	1071.4	8	0.001	8	-0.32	0.04
9	-0.1	0.0	1081.9	9	0.001	9	-0.31	0.04
10	0.2	0.0	1121.9	10	0.001	10	-0.01	0.04
11	0.6	0.0	1386.6	11	0.001	11	0.29	0.04
12	0.8	0.0	1817.1	12	0.001	12	0.33	0.04
13	0.6	0.0	2084.2	13	0.001	13	0.10	0.04
14	0.2	0.0	2123.2	14	0.001	14	-0.11	0.04
15	-0.1	0.0	2133.4	15	0.001	15	-0.05	0.04
16	-0.4	0.0	2226.1	16	0.001	16	0.00	0.04

a. The underlying process assumed is independence (white noise).

b. Based on the asymptotic chi-square approximation.

Table (41): Model type, model fit statistics and Ljung-Box of rainfall (mm) for Addis Ababa station.

Addis Ababa		Model
Model Type		ARIMA(0,0,1)(0,1,1)₁₂
Model Fit statistics	Stationary R-squared	0.50
	R-squared	0.79
	RMSE	48.5
	MAPE	165.6
Ljung-Box Q(12)	Statistics	11.3
	DF	16
	Sig.	0.690

Table (42): Model type, model fit statistics and Ljung-Box of rainfall (mm) for Bahir Dar station.

Bahar Dar		Model
Model Type		ARIMA (0,0,0)(1,1,1)₁₂
Model Fit statistics	Stationary R-squared	0.37
	R-squared	0.85
	RMSE	61.4
	MAPE	386.4
Ljung-Box Q(12)	Statistics	11.9
	DF	16
	Sig.	0.749

Table (43): Model type, model fit statistics and Ljung-Box of rainfall (mm) for Nekemte station.

Nekemte		Model
Model Type		ARIMA (0,0,0)(1,1,1)12
Model Fit statistics	Stationary R-squared	0.42
	R-squared	0.85
	RMSE	61.8
	MAPE	138.3
Ljung-Box Q(12)	Statistics	18.8
	DF	16
	Sig.	0.277

Table (44): Model type, model fit statistics and Ljung-Box of rainfall (mm) for Debra Markos station.

Debra Markos		Model
Model Type		ARIMA(0,0,0)(0,1,1)12
Model Fit statistics	Stationary R-squared	0.45
	R-squared	0.81
	RMSE	49.1
	MAPE	168.8
Ljung-Box Q(12)	Statistics	8.4
	DF	17
	Sig.	0.956

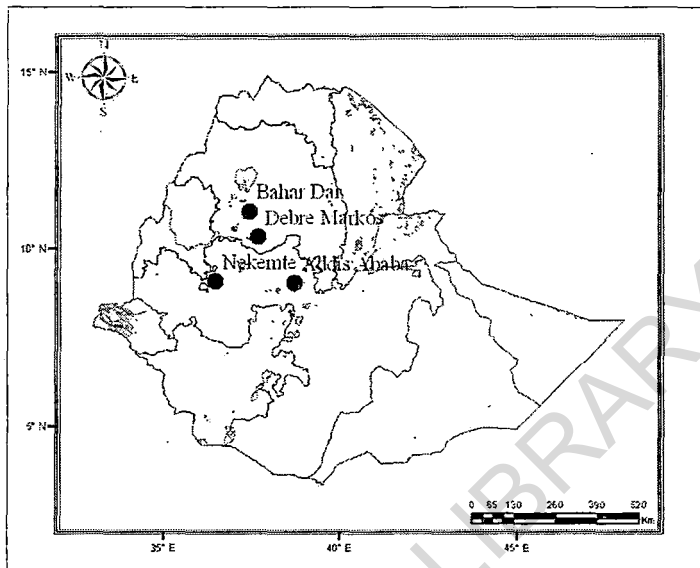


Figure (19): Map of Ethiopia shows the meteorological stations; Bahar Dar, Nekemte, Debre Markos and Addis Ababa (Source: ENMA, 2001).

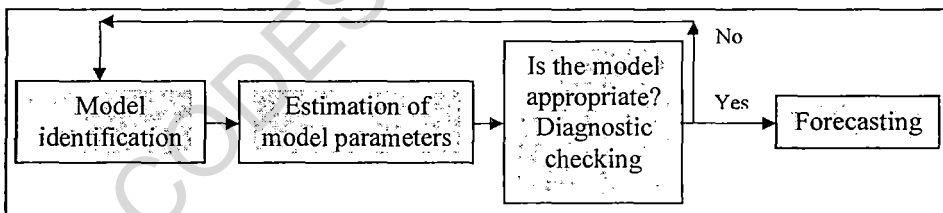


Figure (20): Outline of Box-Jenkins (1976) model.

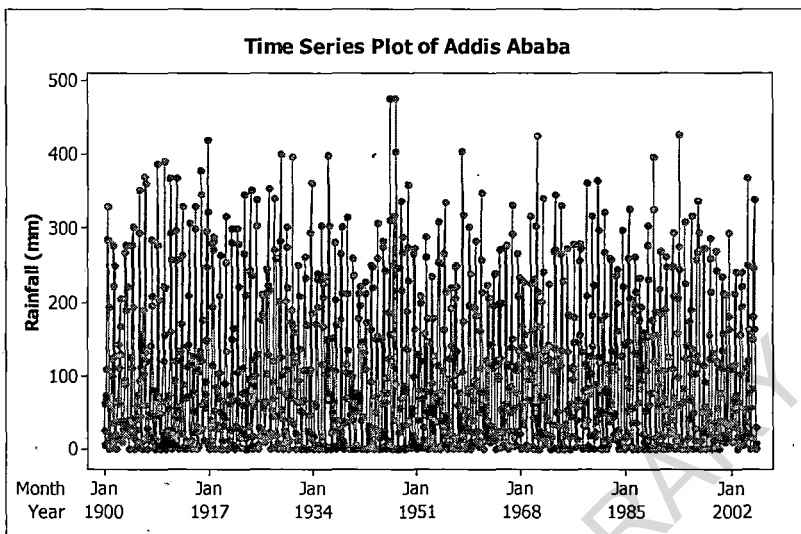


Figure (21): Monthly rainfall data for Addis Ababa station for the period (1900-2005).

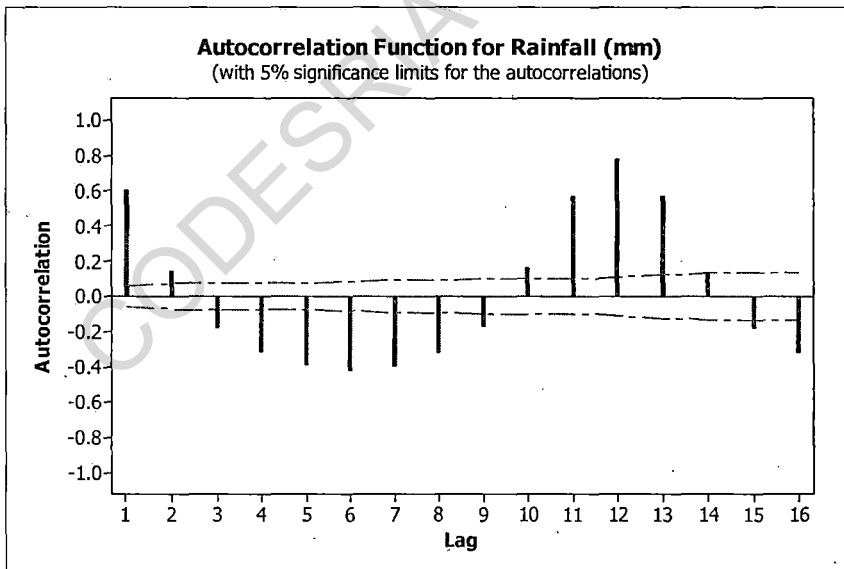


Figure (22): Autocorrelation function of rainfall (mm) for Addis Ababa station.

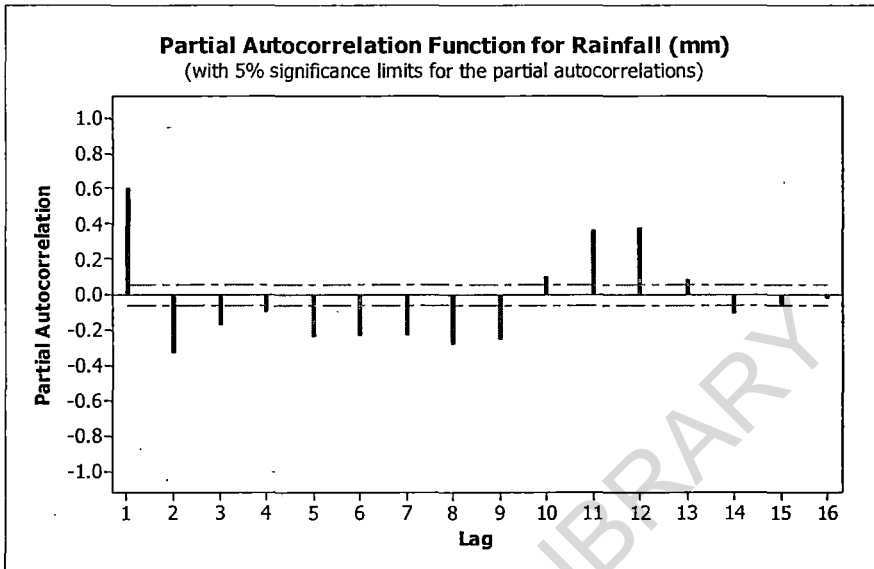


Figure (23): Partial autocorrelation function of rainfall (mm) for Addis Ababa station.

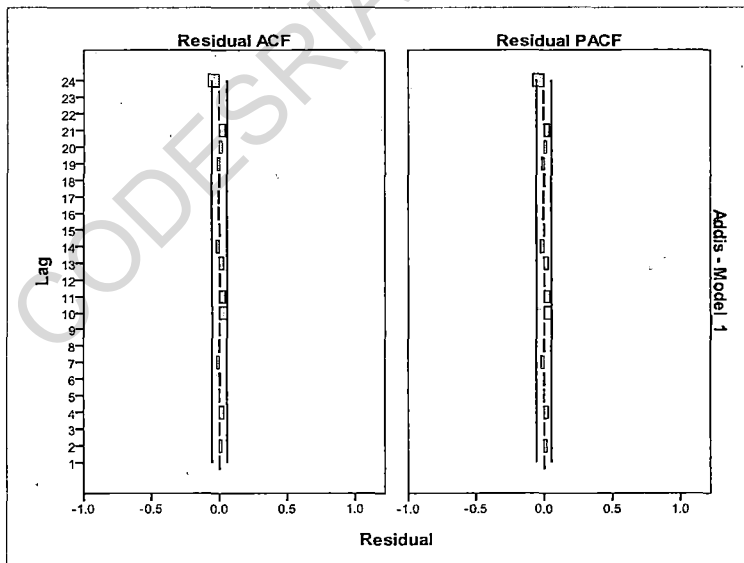


Figure (24): Autocorrelation and partial autocorrelation function of rainfall (mm) for Addis Ababa station.

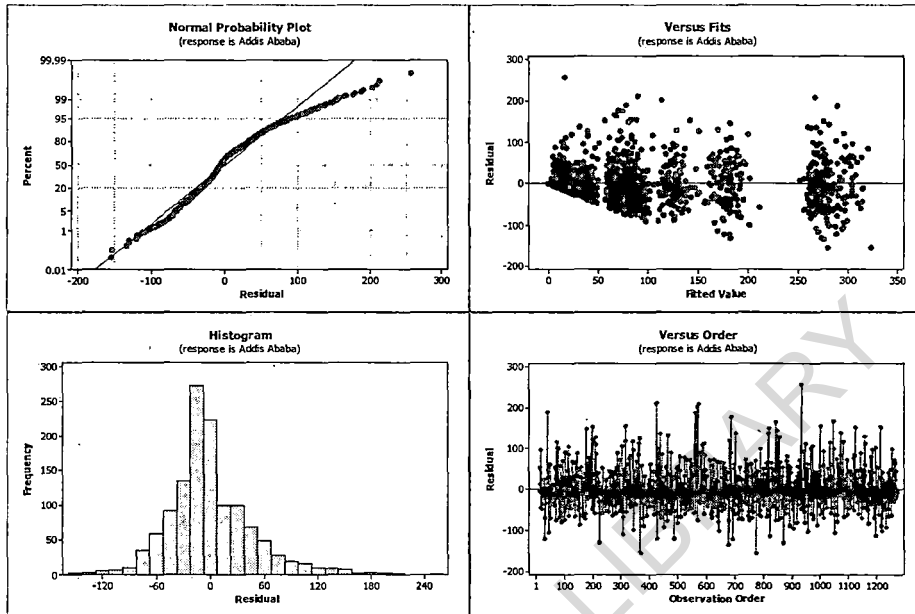


Figure (25): Residual plots of Addis Ababa ARIMA model $(0,0,1) \times (0,1,1)_{12}$.

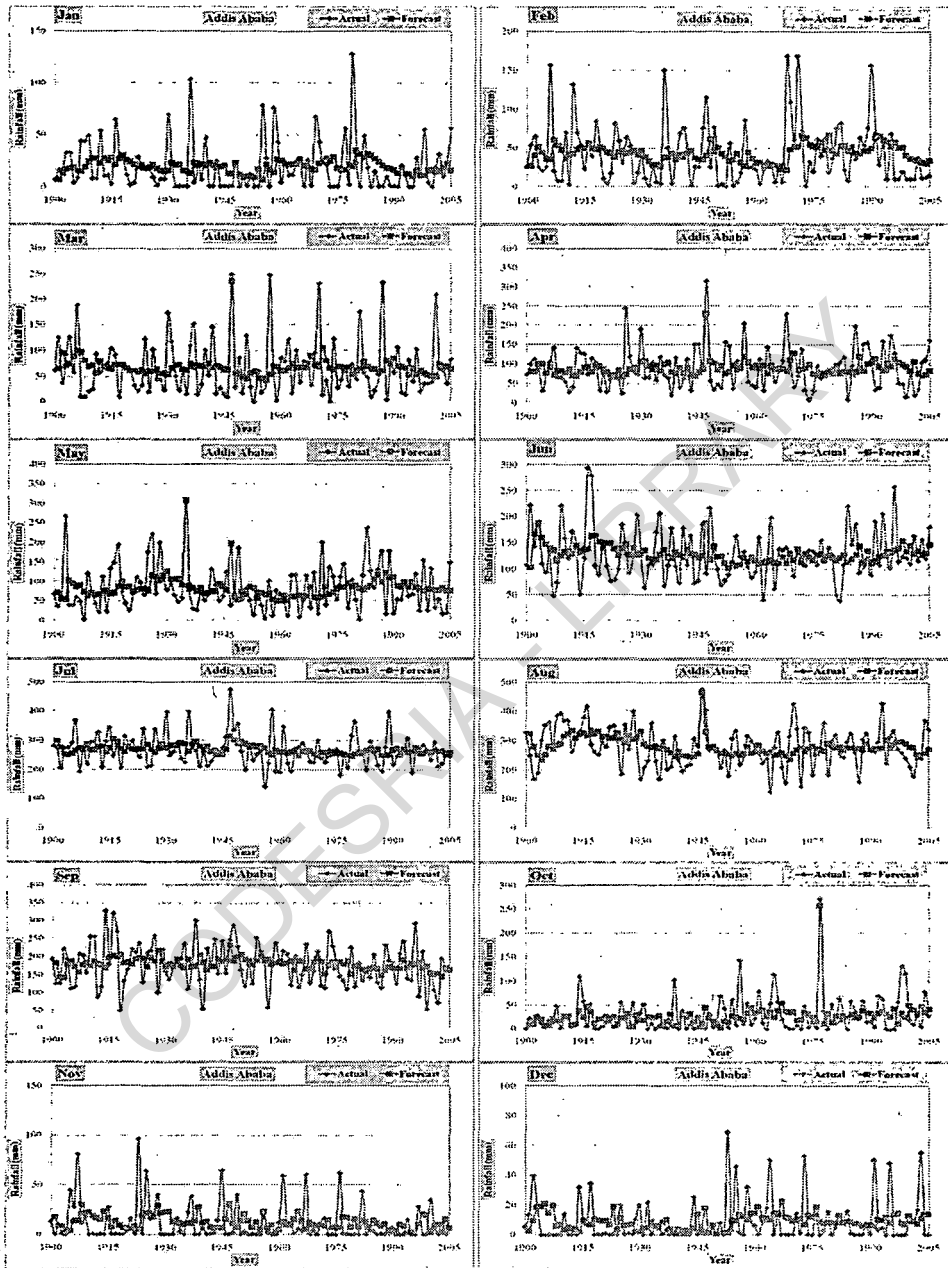


Figure (26): Trend of monthly rainfall for Addis Ababa.

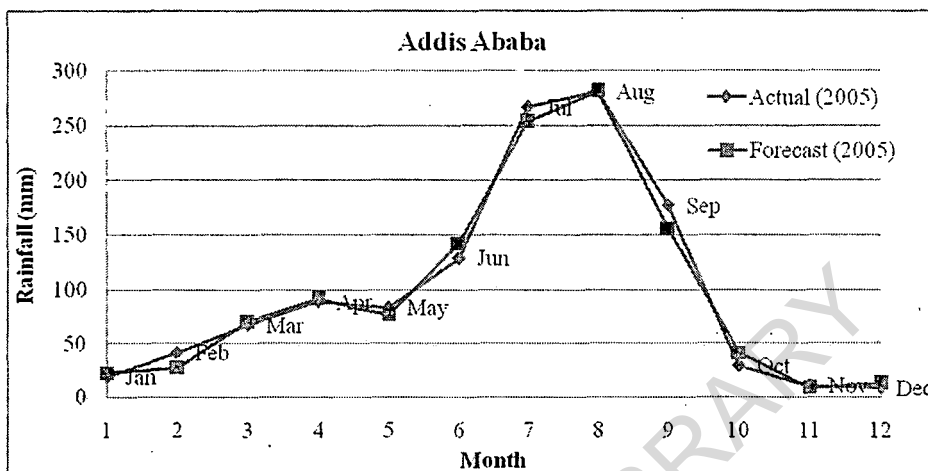


Figure (27): Actual and forecasting Addis Ababa rainfall for the year 2005.

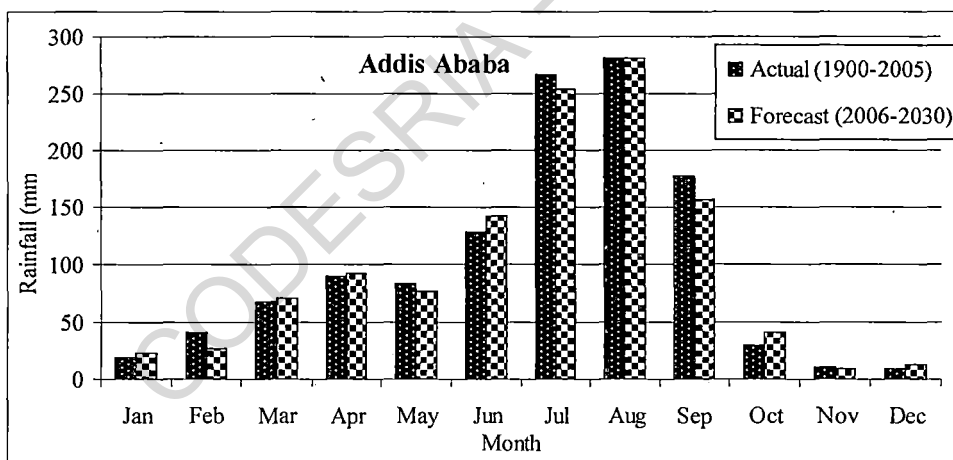


Figure (28): Comparison between actual and forecast period according to mean monthly rainfall (mm) for Addis Ababa station.

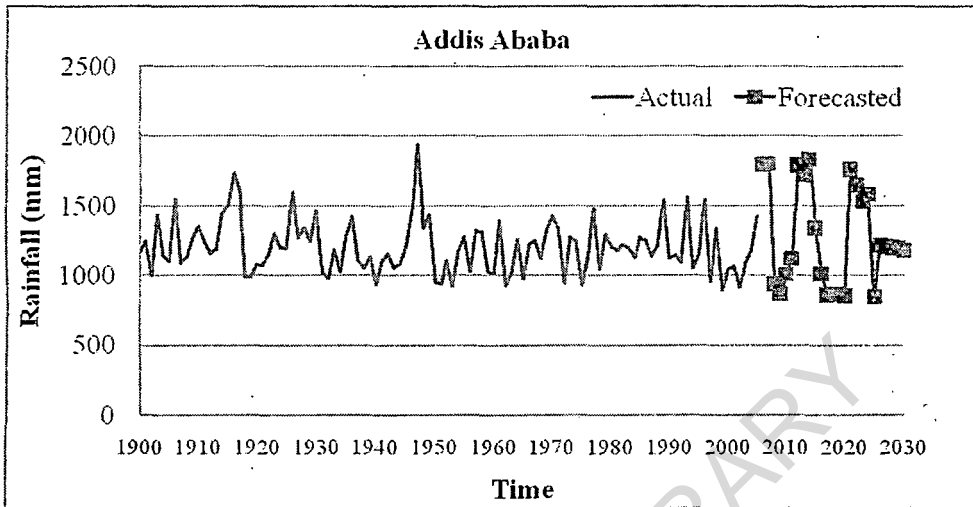


Figure (29): Observed and forecasted Ethiopian rainfall for Addis Ababa station.

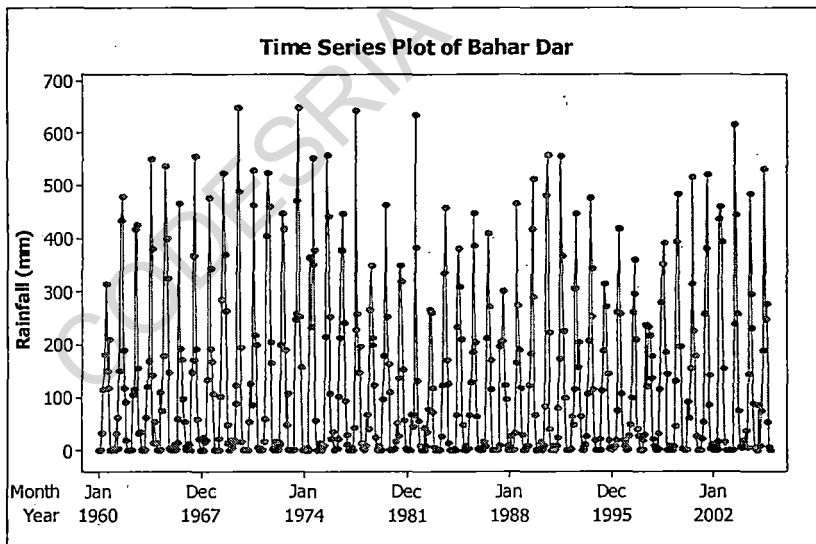


Figure (30): Time series plot of Bahar Dar station.

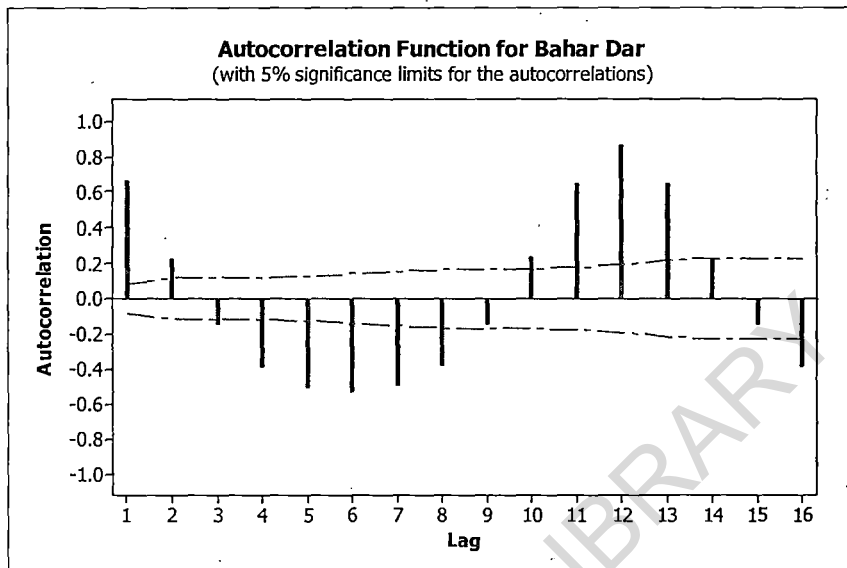


Figure (31): Autocorrelation function of rainfall (mm) for Bahar Dar station.

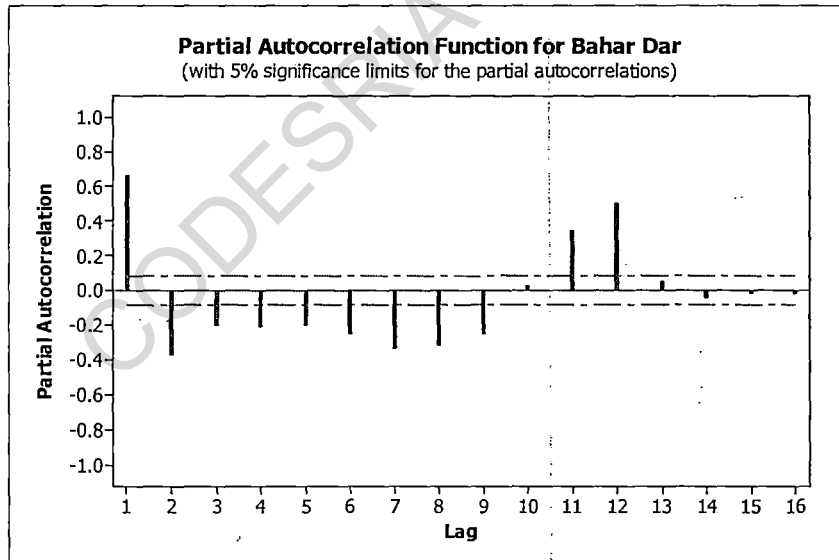


Figure (32): Partial autocorrelation function of rainfall (mm) for Bahar Dar station.

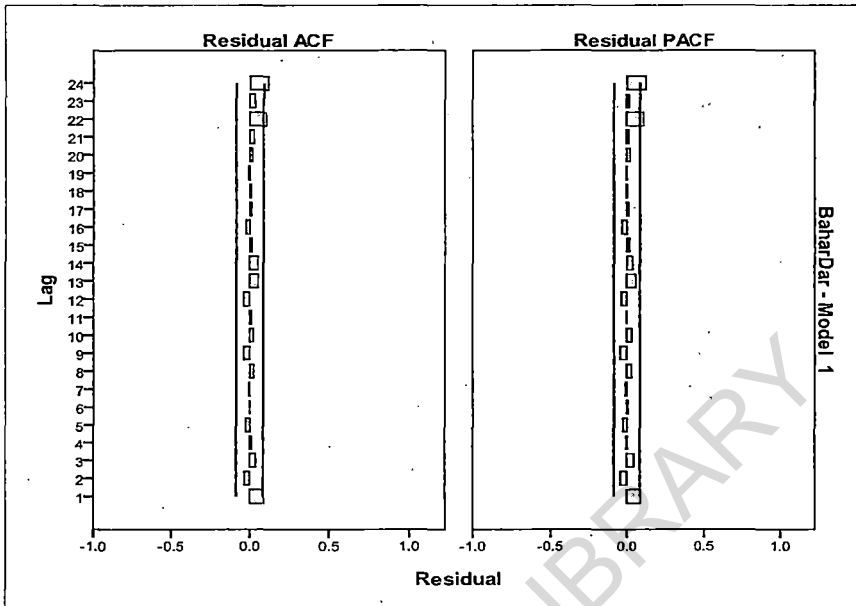


Figure (33): Autocorrelation and partial autocorrelation function of rainfall (mm) for Bahar Dar station.

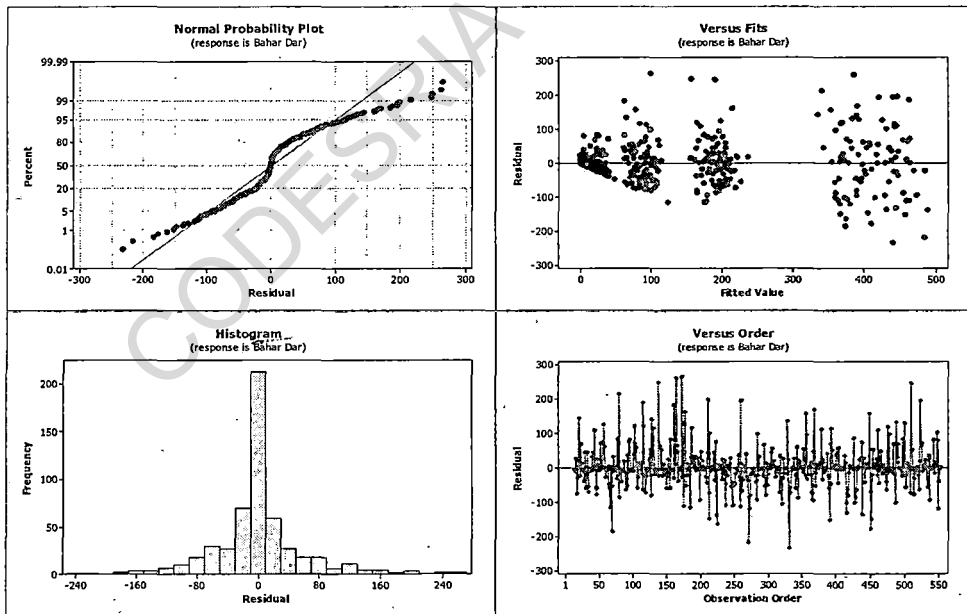


Figure (34): Residual plots of Bahar Dar ARIMA model $(0,0,0)_x(1,1,1)_{12}$.

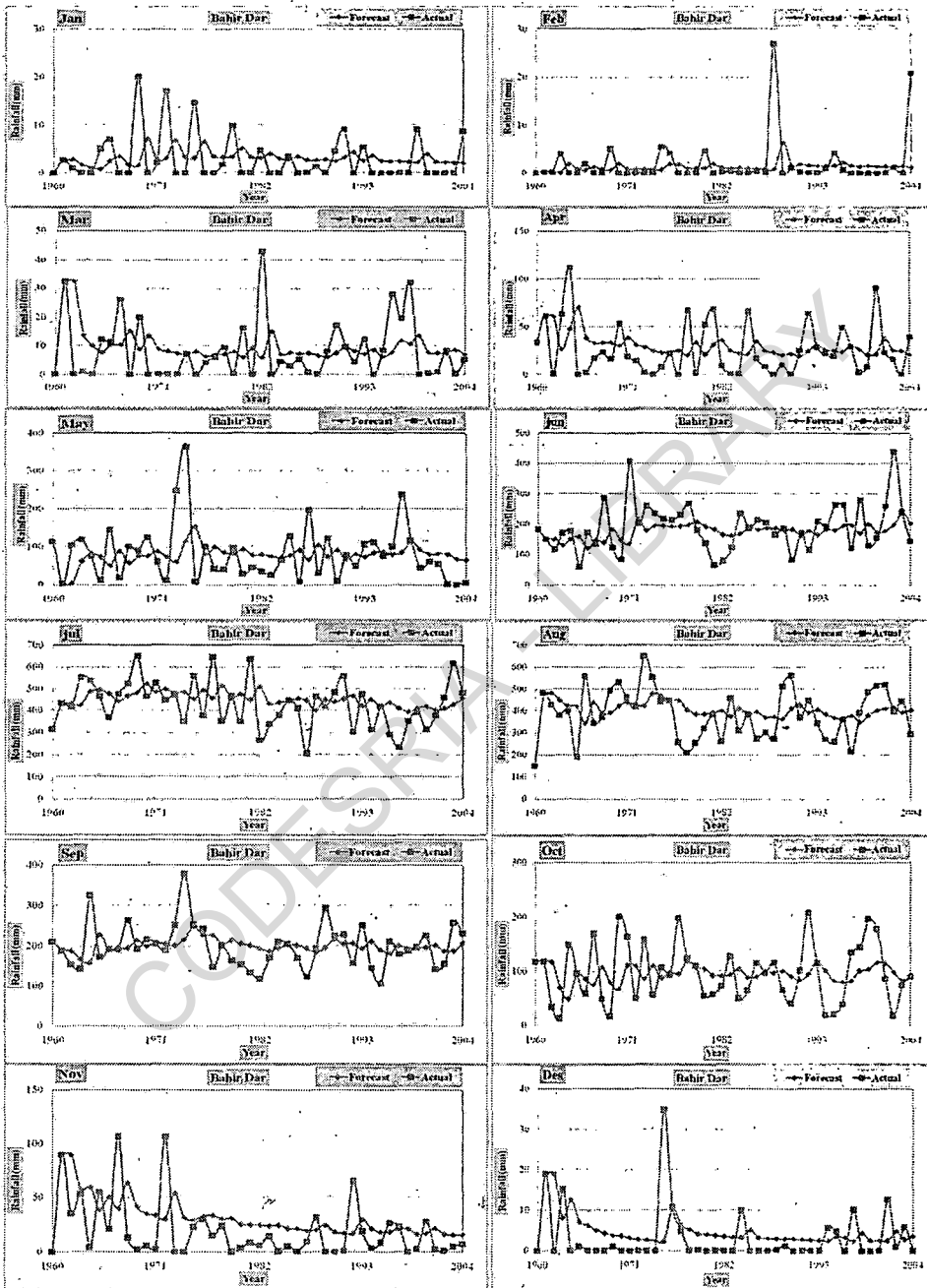


Figure (35): Trend of monthly rainfall for Bahir Dar.

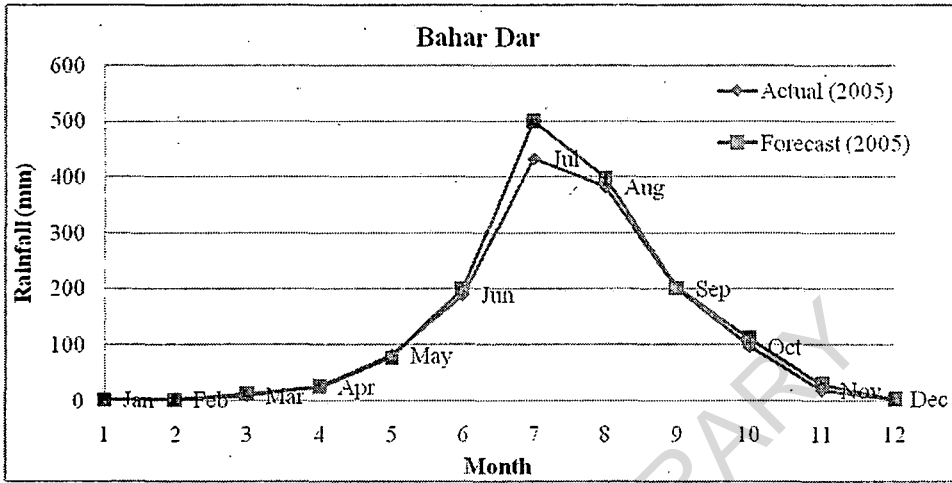


Figure (36): Actual and forecasting Bahar Dar rainfall for the year 2005.

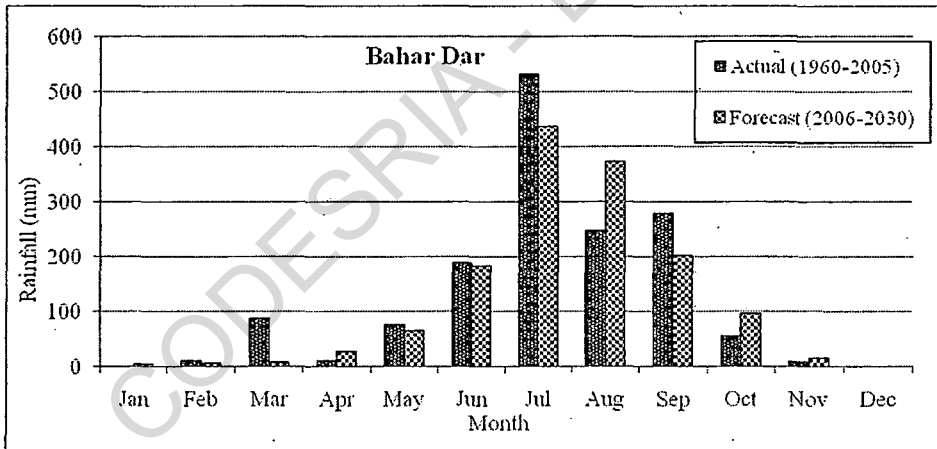


Figure (37): Comparison between actual and forecast period according to mean monthly rainfall (mm) for Bahar Dar station.

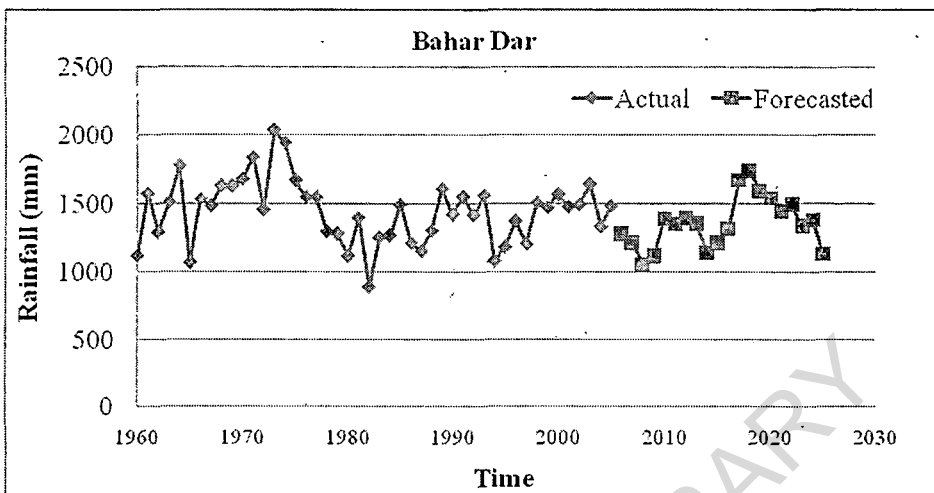


Figure (38): Observed and forecasted Ethiopian rainfall for Bahar Dar station.

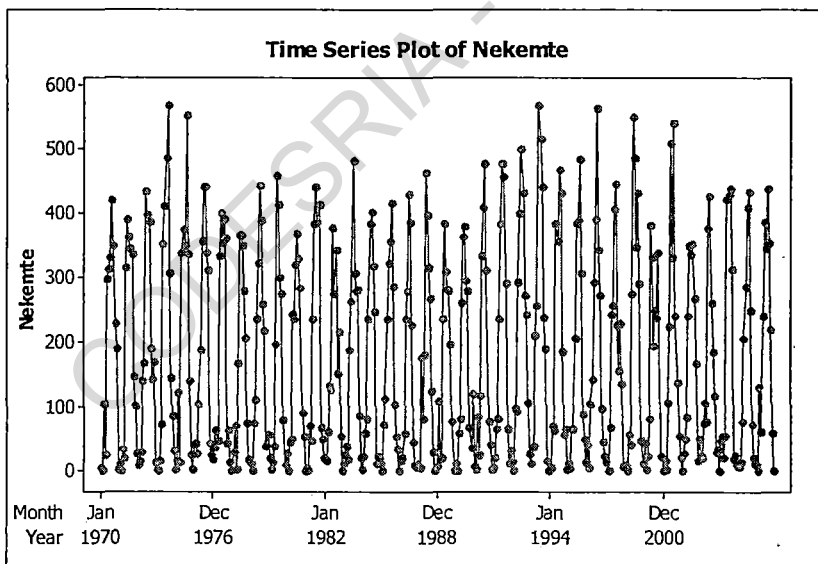


Figure (39): Time series plot of Nekemte station.

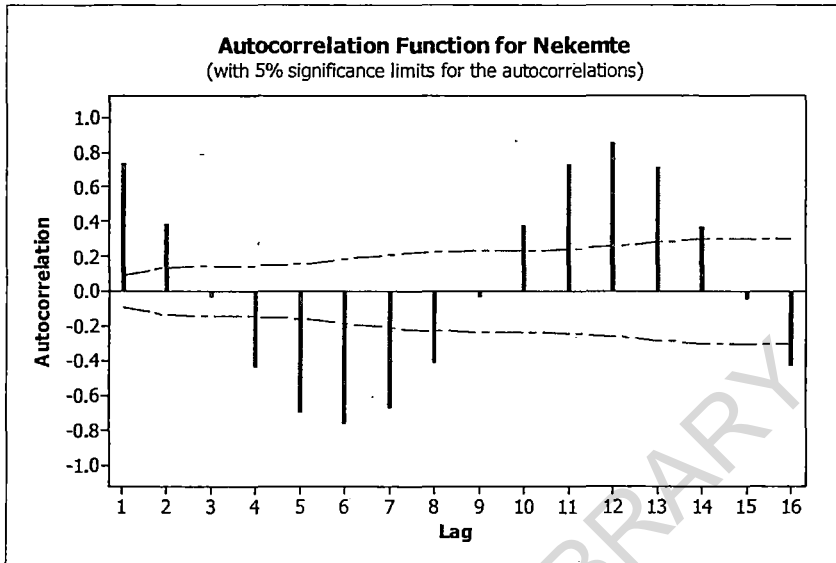


Figure (40): Autocorrelation function of rainfall (mm) for Nekemte station.

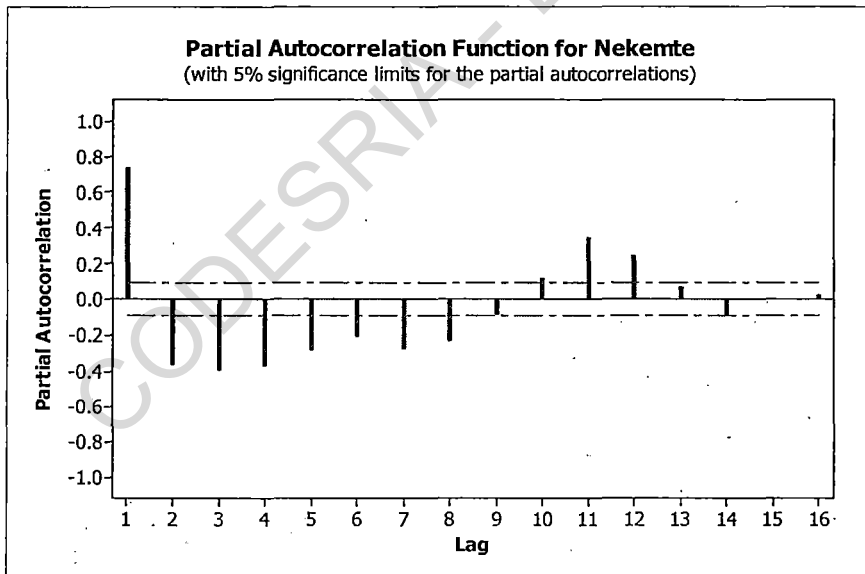


Figure (41): Partial autocorrelation function of rainfall (mm) for Nekemte station.

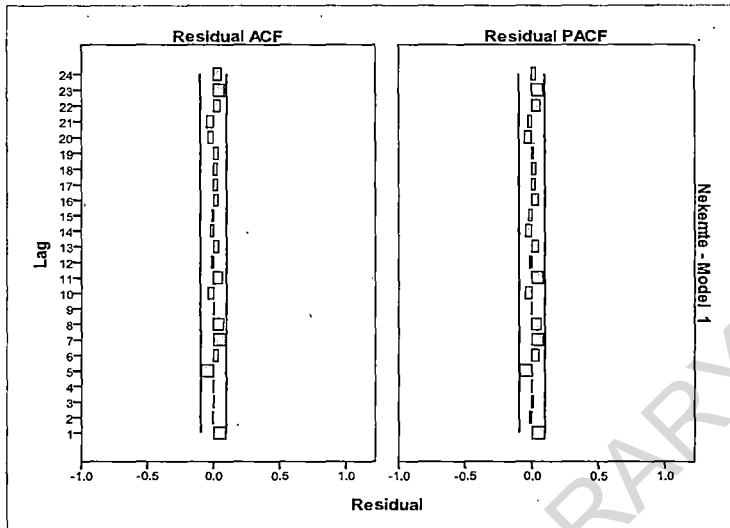


Figure (42): Autocorrelation and partial autocorrelation function of rainfall (mm) for Nekemte station.

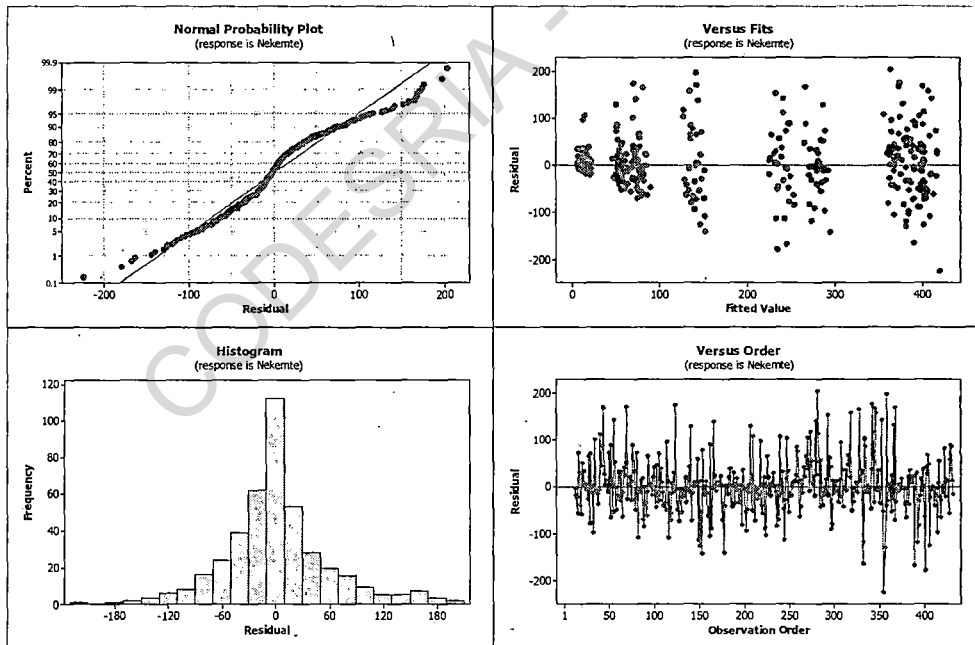


Figure (43): Residual plots of Nekemte ARIMA model $(0,0,0) \times (1,1,1)_{12}$.

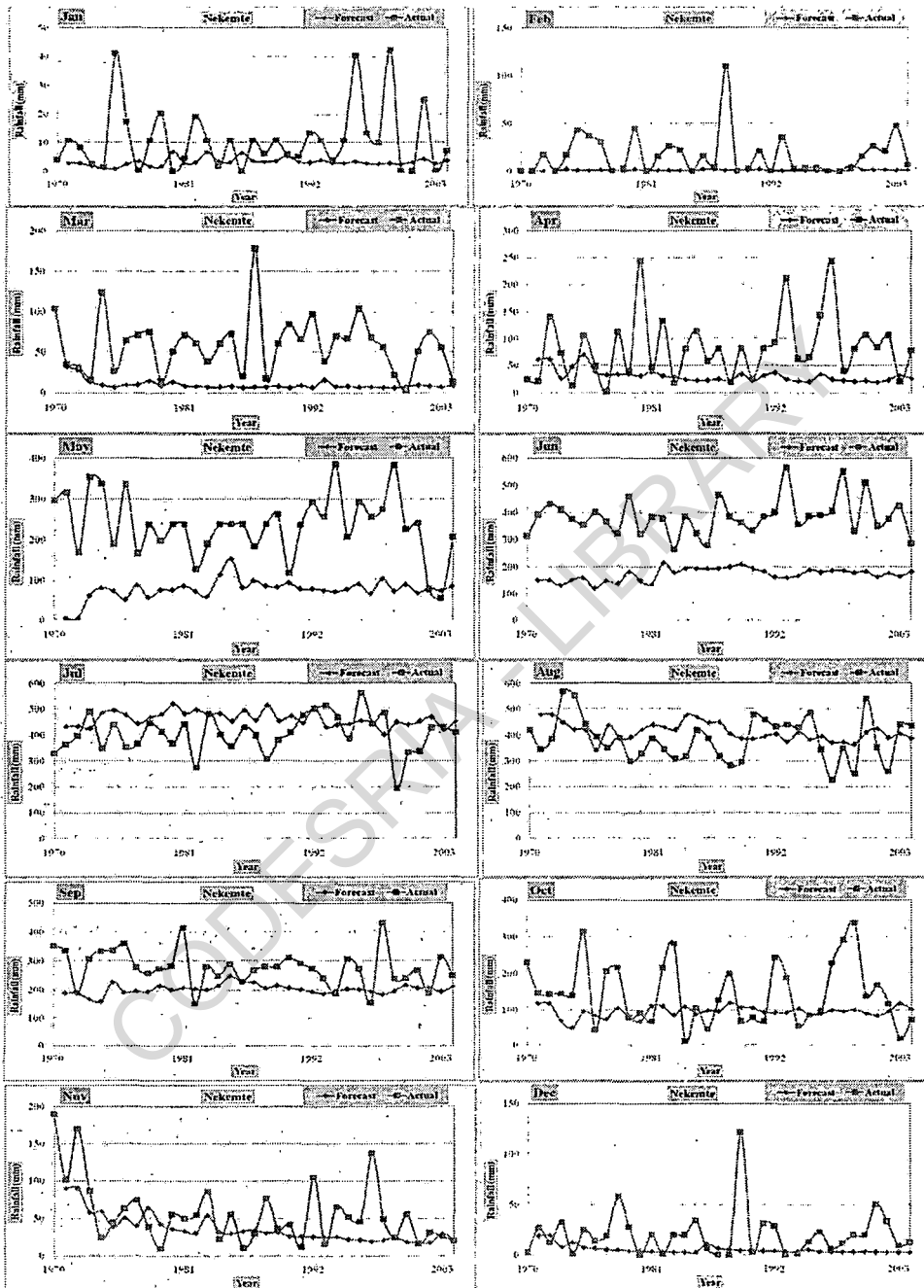


Figure (44): Trend of monthly rainfall for Nekemte station.

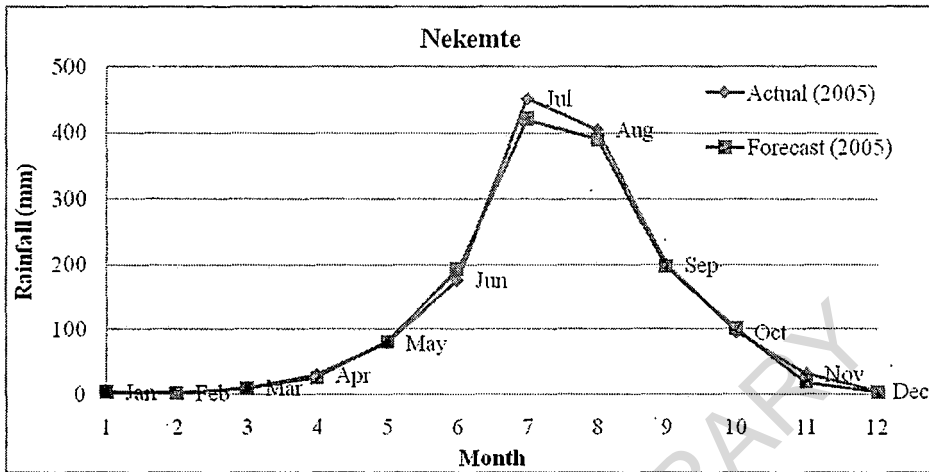


Figure (45): Actual and forecasting Nekemte rainfall for the year 2005.

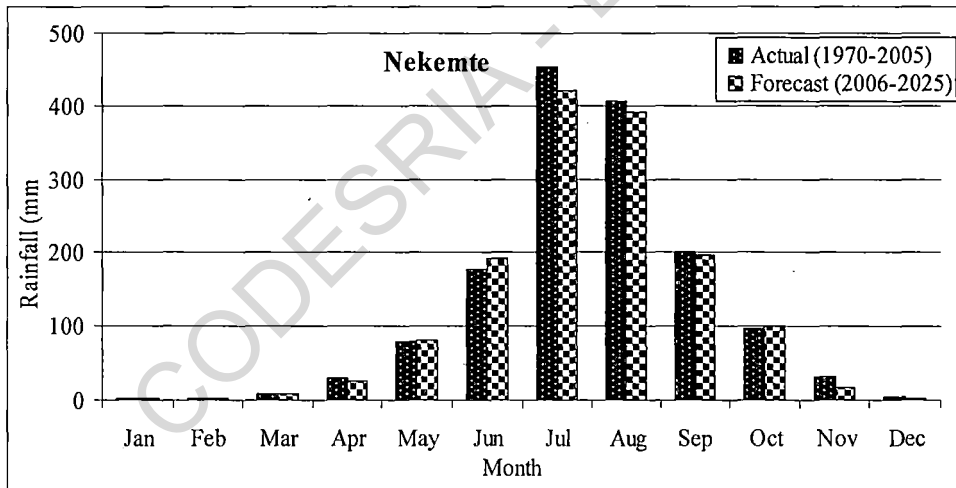


Figure (46): Comparison between actual and forecast period according to mean monthly rainfall (mm) for Nekemte station.

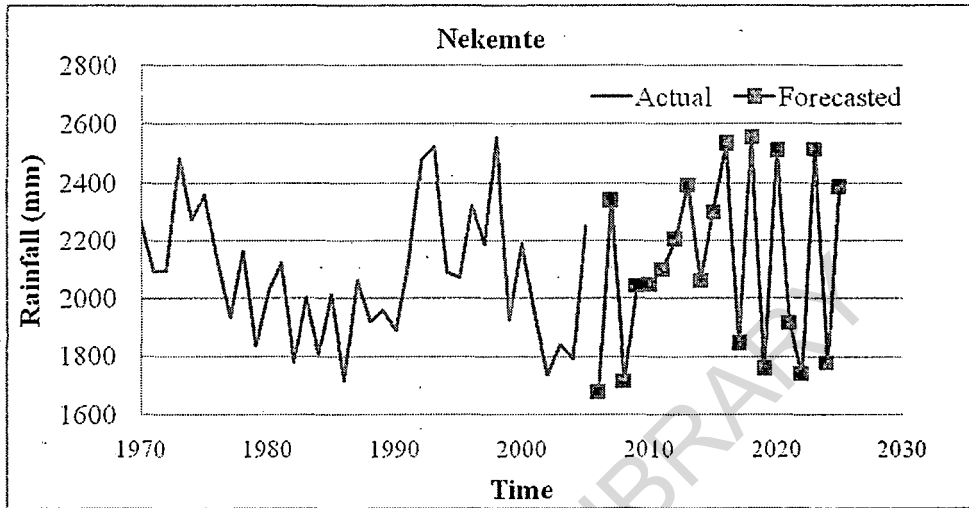


Figure (47): Observed and forecasted Ethiopian rainfall for Nekemte station.

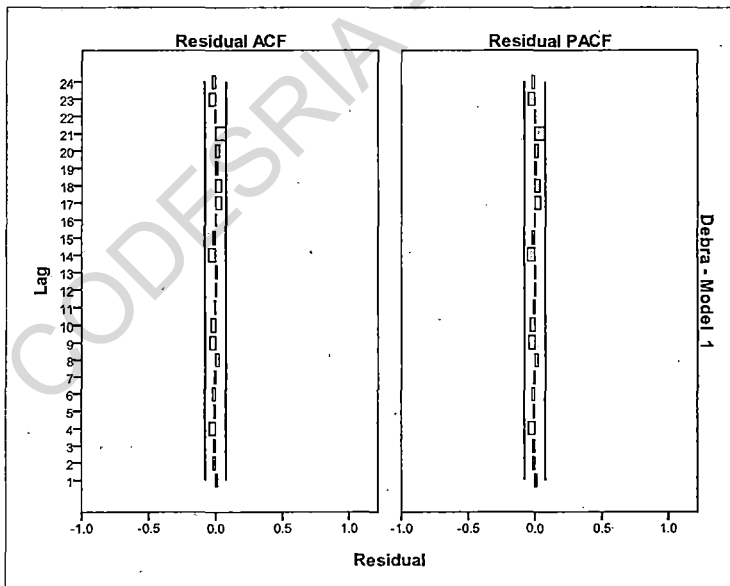


Figure (48): Autocorrelation and partial autocorrelation function of rainfall (mm) for Debra Markos station.

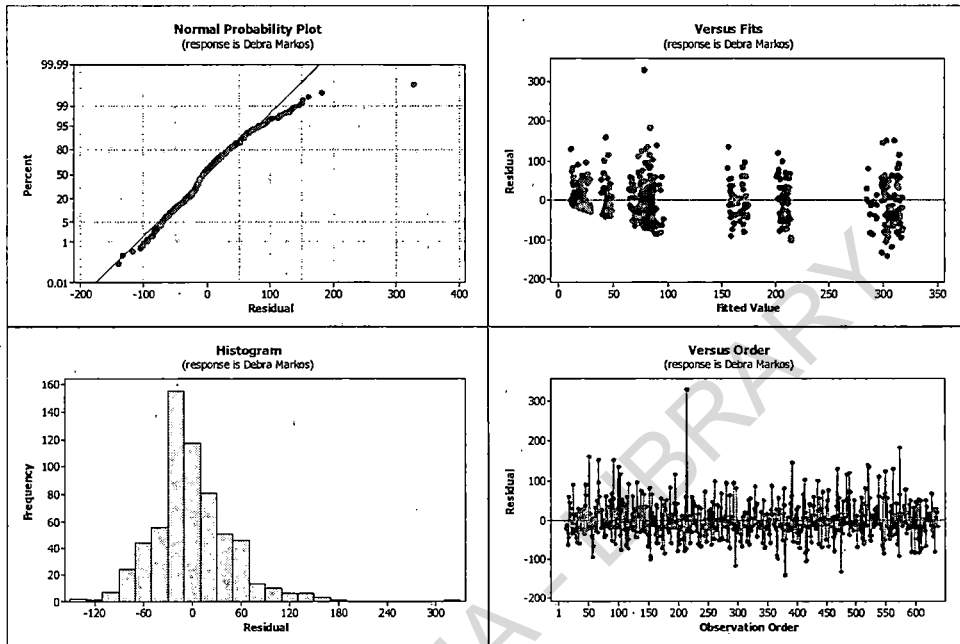


Figure (49): Residual plots of Debra Markos ARIMA model $(0,0,0) \times (0,1,1)_{12}$.

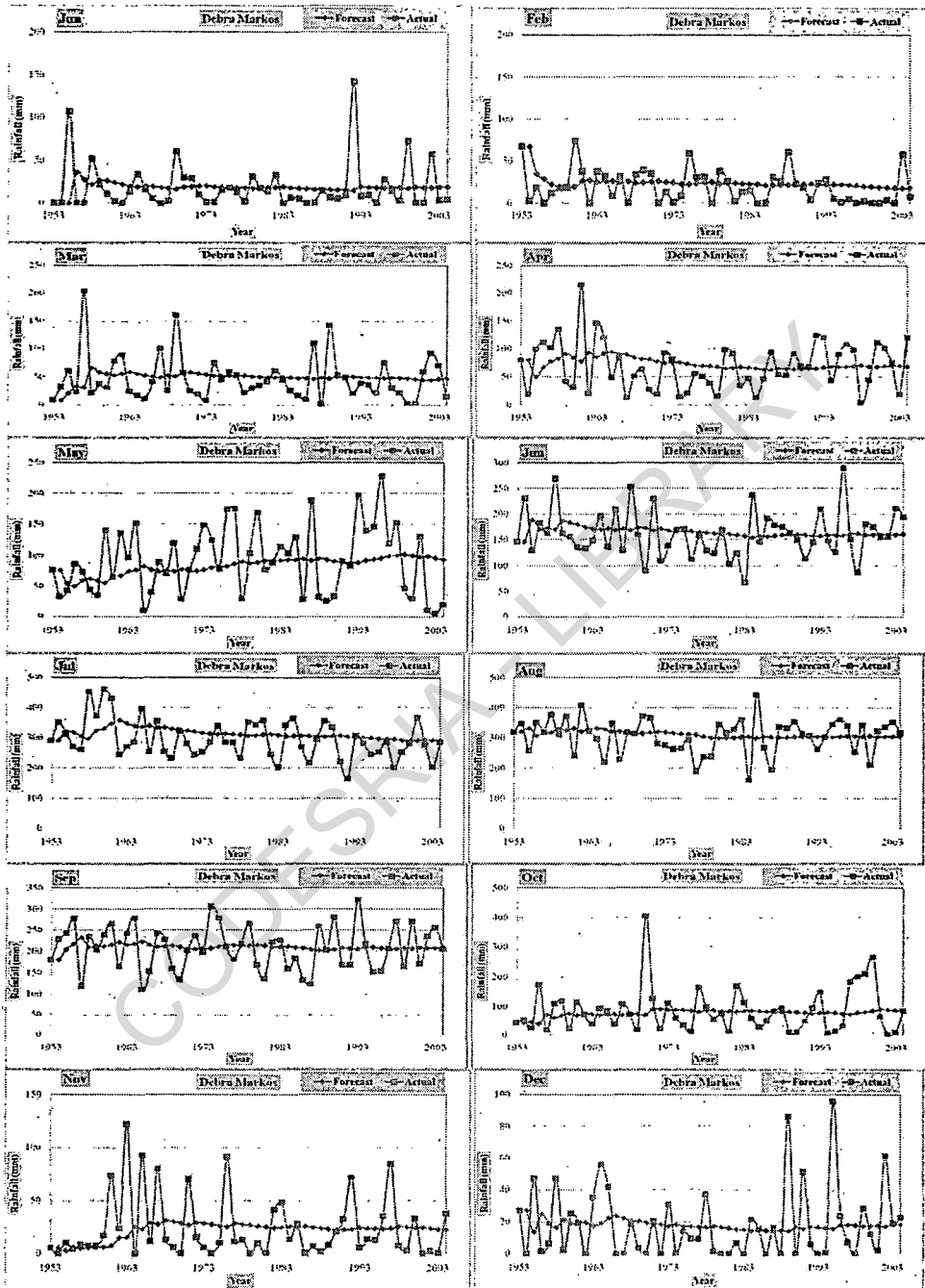


Figure (50): Trend of monthly rainfall for Debra Markos.

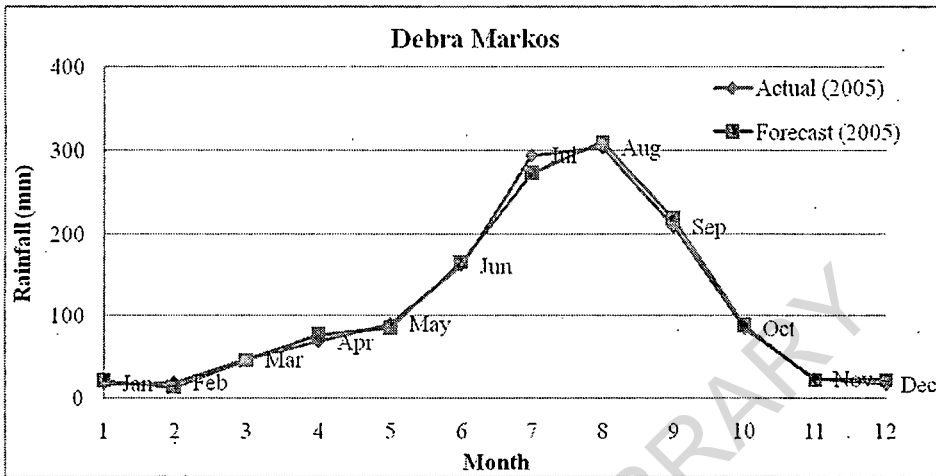


Figure (51): Actual and forecasting Debra Markos rainfall for the year 2005.

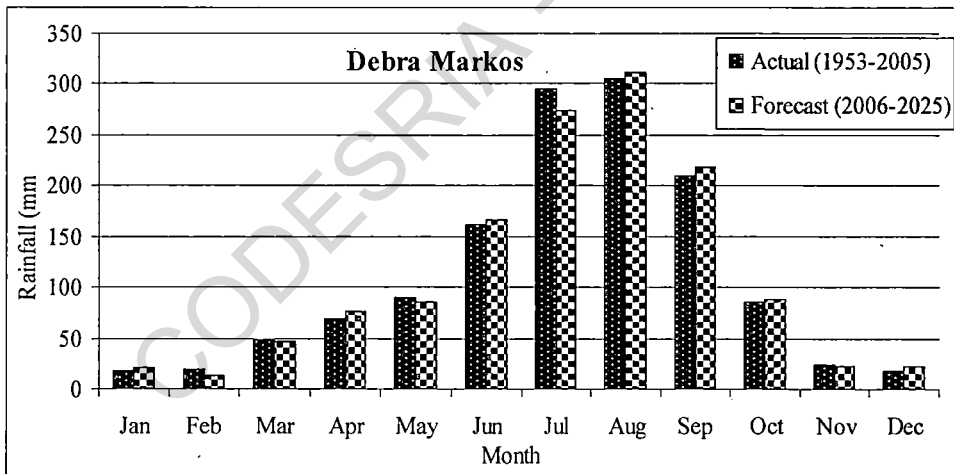


Figure (52): Comparison between actual and forecast period according to mean monthly rainfall (mm) for Debra Markos station.

4.29. Future climate change over Ethiopia

It is found that the best trend equations for mean annual maximum temperature was cubic equation as it had highest value for R^2 then quadratic equation so both equations can represent the mean annual maximum temperature trend during the study period than linear equation although most of researches depend on linear equation only to represent the trend.

After analyses of the trend equations, the data had been obtained which help us to predict the period from (2006-2030) for the selected study stations and this data when represented by a diagram it is noted that data of cubic equation take extreme curve where it was highly positive or negative trend.

From this result it cannot be depend on cubic equation only in the prediction so this difference may be need long period (not less than 100 years) to show the whole frequency period by cubic equation.

After selection of the best trend equation for mean annual maximum and minimum temperature through the study period we depend on this equation to predict the temperature trend for 2006-2030, about 25 year can be forecast, selection of some meteorological stations from different parts of the country to represent most of Ethiopian regions as Addis Ababa (Central part of the country), Arbamich (Southern Ethiopia), Assosa (Western Ethiopia), Gonder (Northern Ethiopia) and Jijiga (Eastern Ethiopia), it is found that all stations will have a small increase in mean annual maximum temperature as regarding quadratic and cubic trend equation but it is found that every station can be represented by either quadratic or cubic trend equation (Figures 53, 54, 55, 56 and 57), but three stations (Assosa, Gonder and Jijiga (Figure 60, 61 and 62)) will have

increase in mean annual minimum temperature as regarding quadratic or cubic trend equation and the other two stations (Addis Ababa and Arbamich (Figures 58 and 59)) will have decrease in mean annual minimum temperature as regarding quadratic or cubic trend equation.

The results of IPCC's mid-range emission scenario show that compared to the 1961-1990 average mean annual temperature across Ethiopia will increase by between 0.9 and 1.1°C by the year 2030 and from 1.7 to 2.1°C by the year 2050. The temperature across the country could rise by between 0.5 and 3.6°C by 2080, whereas precipitation is expected to show some increase (*Tadega, 2007*). Unlike the temperature trends, it is very difficult to detect long-term rainfall trends in Ethiopia, due to the high inter-annual and inter-decadal variability. According to *Feyissa (2010)*, between 1951 and 2006, no statistically significant trend in mean annual rainfall was observed in any season. The results of the IPCC's mid-range emission scenario show that compared to the 1961-1990 annual precipitation show a change of between 0.6 and 4.9% and 1.1 to 18.2% for 2030 and 2050, respectively. The percentage change in seasonal rainfall is expected to be up to about 12% over most parts of the country (*Feyissa, 2010*).

The results of atmospheric general circulation model (MRI-AGCM) shows that mean of annual maximum and minimum temperatures in Ethiopia in the middle of 21st century will increase by 1.17°C and 1.59°C respectively relative to the present end of 20th century. The significant increase of maximum temperature will be in the central highlands and southern parts of Ethiopia (*Fekadu, 2009*).

McSweeney, et al., (2008): Ethiopia – UNDP Climate Change Country Profiles report a 1.3°C increase between 1960 and 2006, an average

rate of 0.28°C per decade. The increase in temperature in Ethiopia has been most rapid in (July, August and September) at a rate of 0.32°C per decade. Other studies show a smaller increase, for example: *Conway, et al., (2011)* report rises of approximately 0.5°C from 1961-2000, Also in the *McSweeney, et al., (2008)*, the National Meteorological Agency reports increases of 0.37°C every 10 years from 1951-2006.

Rainfall patterns in Ethiopia have been reported in some studies. A decline of annual and summer rainfall in eastern, southern, and southwestern Ethiopia was found, but no trend was detected over central, northern, and northwestern Ethiopia (*Shang, et al., 2011*).

The strong inter annual and inter-decadal variability in Ethiopia's rainfall makes it difficult to detect long-term trends. There is not a statistically significant trend in observed mean rainfall in any season in Ethiopia between 1960 and 2006. Decreases in (July, August and September) rainfall observed in the 1980 have shown recovery in the 1990 and 2000 (*McSweeney, et al., 2008*).

Previous time-series studies of rainfall patterns in Ethiopia have been carried out at various spatial (e.g. regional, national) and temporal (e.g. annual, seasonal, monthly) scales. *Cheung, et al., (2008)* determined that summer rainfall (Kiremt) in the central highlands of Ethiopia declined in the second half of the 20th century, while *Seleshi and Zanke, (2004)* failed to find such a trend over central, northern, and northwestern Ethiopia. Instead, they found a decline of annual and Kiremt rainfall in eastern, southern, and southwestern Ethiopia since 1982. *Funk, et al., (2005)* confirmed the *Seleshi and Zanke, (2004)* findings of annual rainfall decline in southwestern and eastern Ethiopia, but argued that while rainfall has been

declining in the Northeast since 1996, Kiremt rain has been consistent (i.e. no trends) for the entire nation since the 1960. In contrast to *Funk, et al., (2005)*, *Conway, (2000)* reported that there are no recent trends in rainfall over the northeastern Ethiopian highlands.

Many of the contradictions in previous findings on rainfall trends and climate extremes in Ethiopia may be explained by the arbitrary division of the study area as well as the quality of the available data (*Cheung, et al., 2008*).

After analyses of rainfall data and its prediction for the period 2006-2030 for four stations (Addis Ababa, Bahir Dar, Debermarkos and Nekemte), it is noted that rainfall oscillation trend and there was minimal increase through this period (Figures 63, 64, 65 and 66).

The trend of annual rainfall computed by the Mann-Kendall test (Figure 67), indicate that there was no significant trend in the forecasted annual rainfall at the mean of the four stations (Addis Ababa, Bahir Dar, Debremarkos and Nekemte), Also it is noted that the period from 2006–2030, the average precipitation is increase slightly and the variability between years is increase.

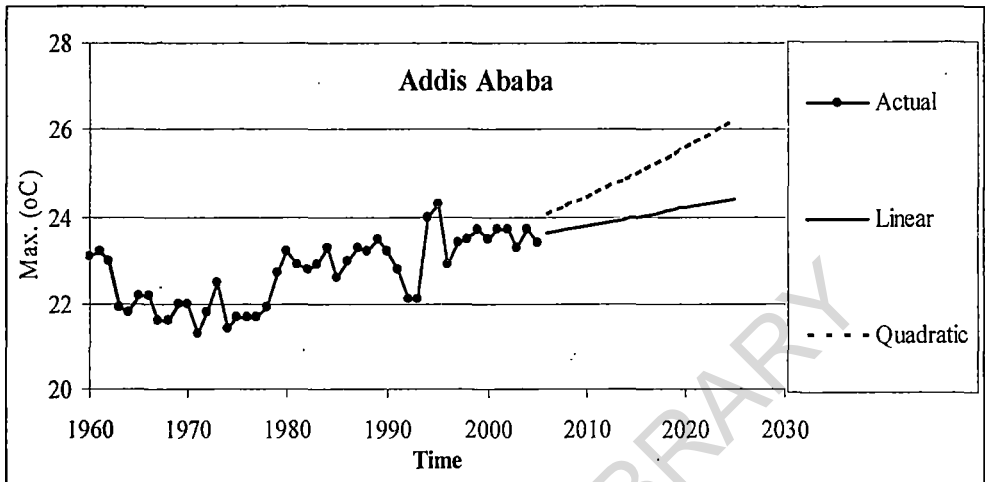


Figure (53): Actual and forecasted mean annual maximum temperature for Addis Ababa.

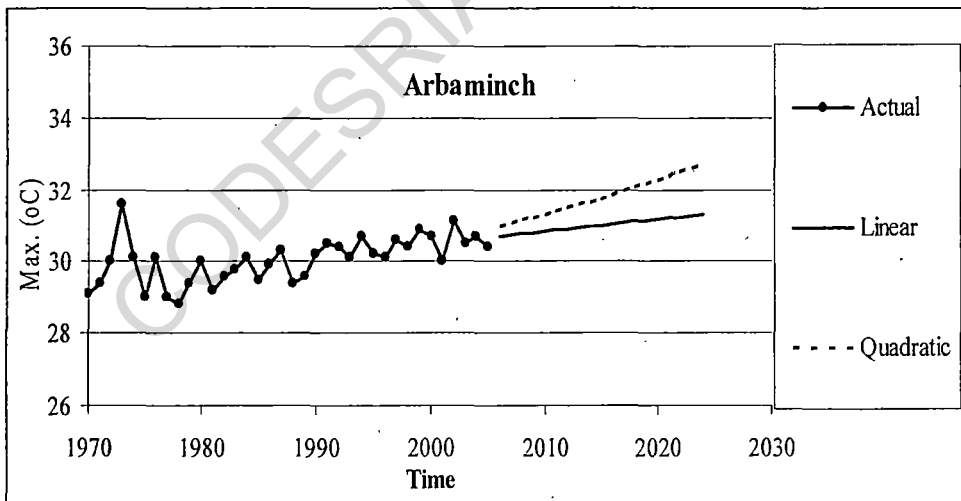


Figure (54): Actual and forecasted mean annual maximum temperature for Arbaminch.

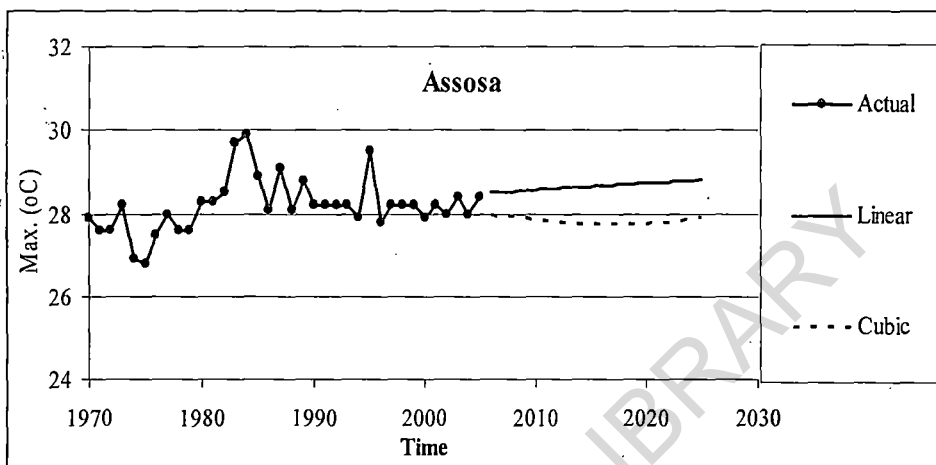


Figure (55): Actual and forecasted mean annual maximum temperature for Assosa.

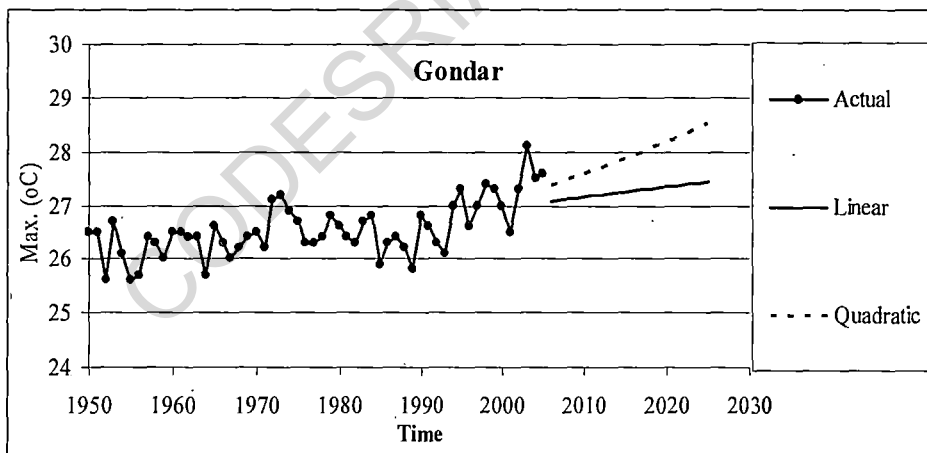


Figure (56): Actual and forecasted mean annual maximum temperature for Gondar.

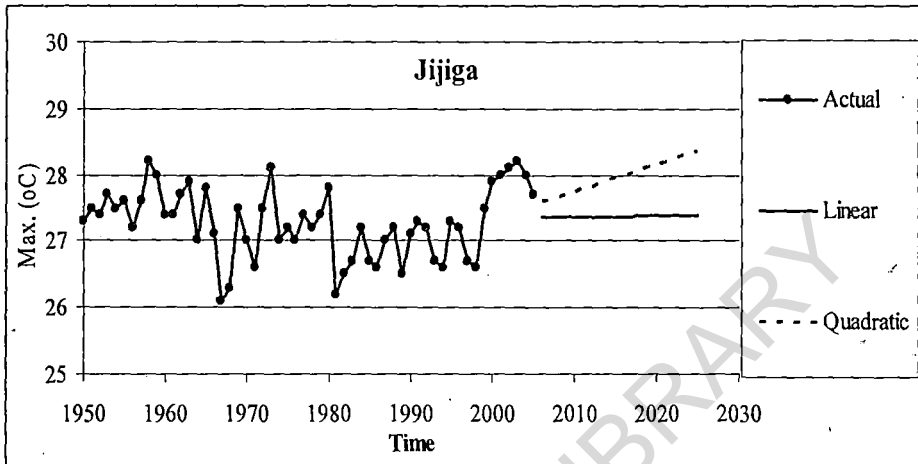


Figure (57): Actual and forecasted mean annual maximum temperature for Jijiga.

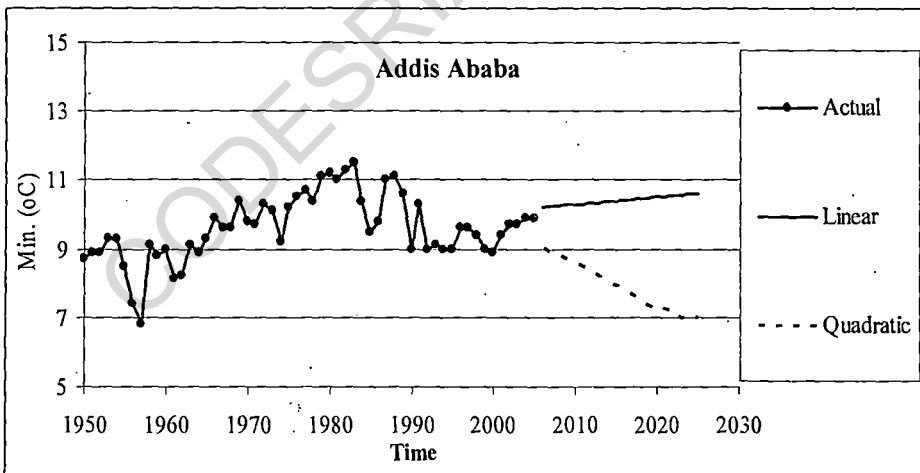


Figure (58): Actual and forecasted mean annual minimum temperature for Addis Ababa.

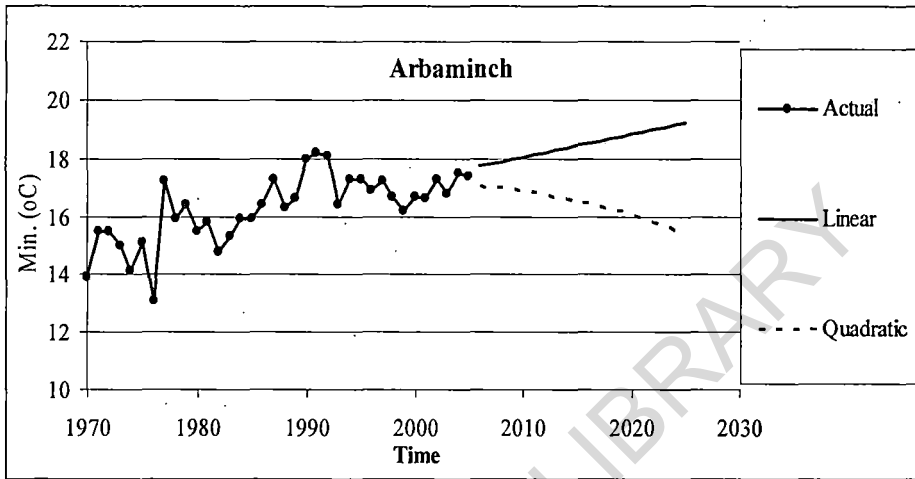


Figure (59): Actual and forecasted mean annual minimum temperature for Arbaminch.

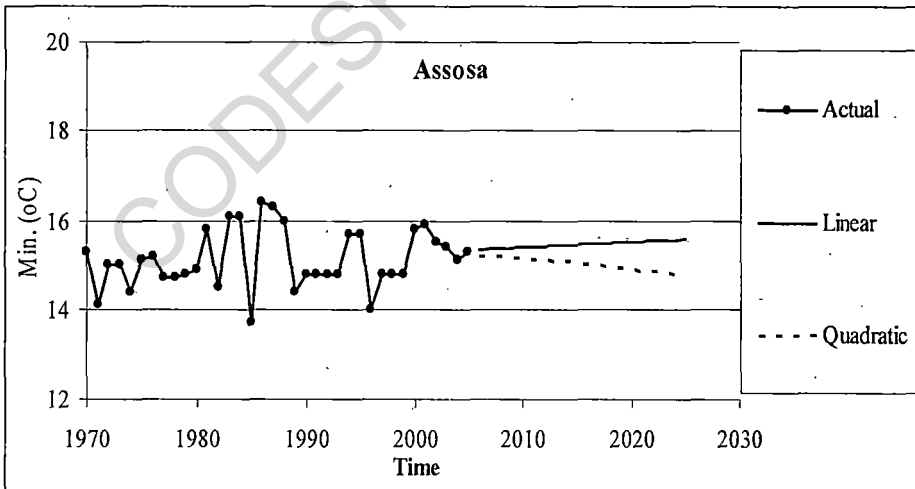


Figure (60): Actual and forecasted mean annual minimum temperature for Assosa.

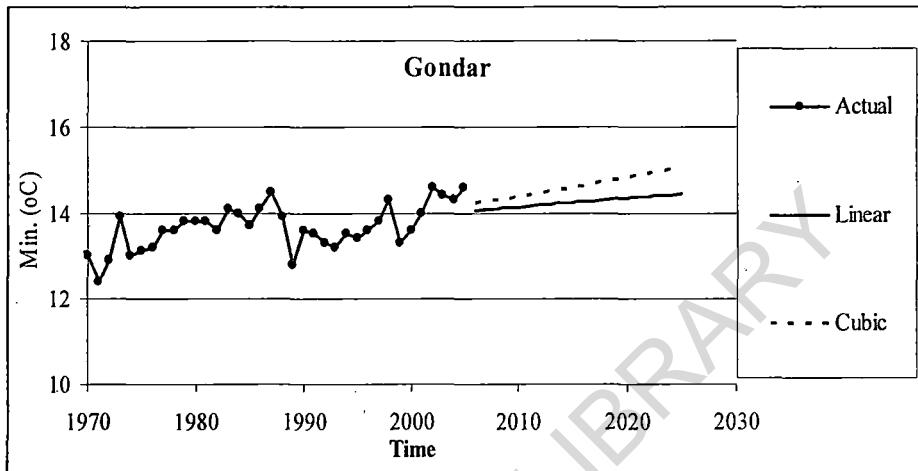


Figure (61): Actual and forecasted mean annual minimum temperature for Gondar.

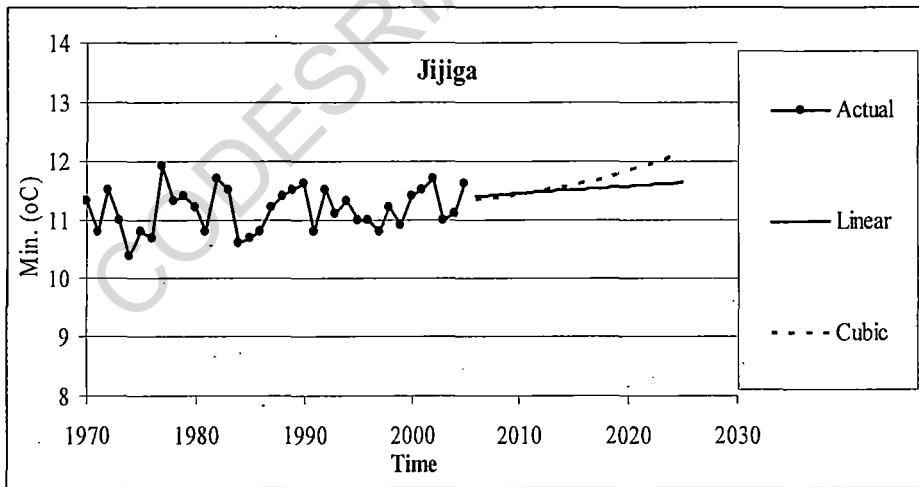


Figure (62): Actual and forecasted mean annual minimum temperature for Jijiga.

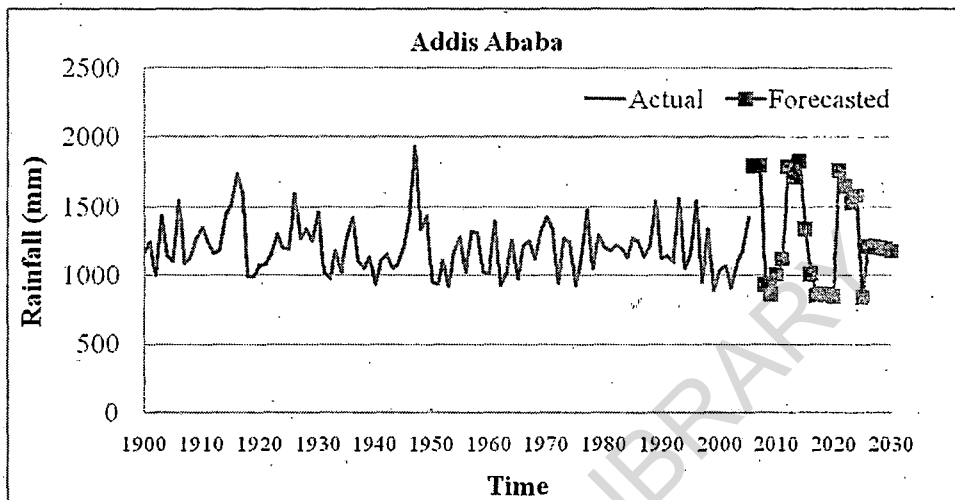


Figure (63): Actual and forecasted annual precipitation for Addis Ababa.

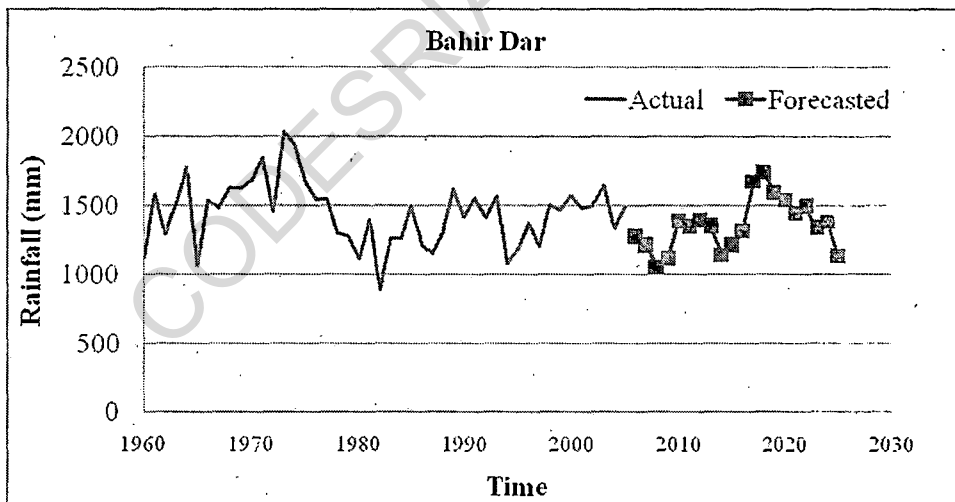


Figure (64): Actual and forecasted annual precipitation for Bahir Dar.

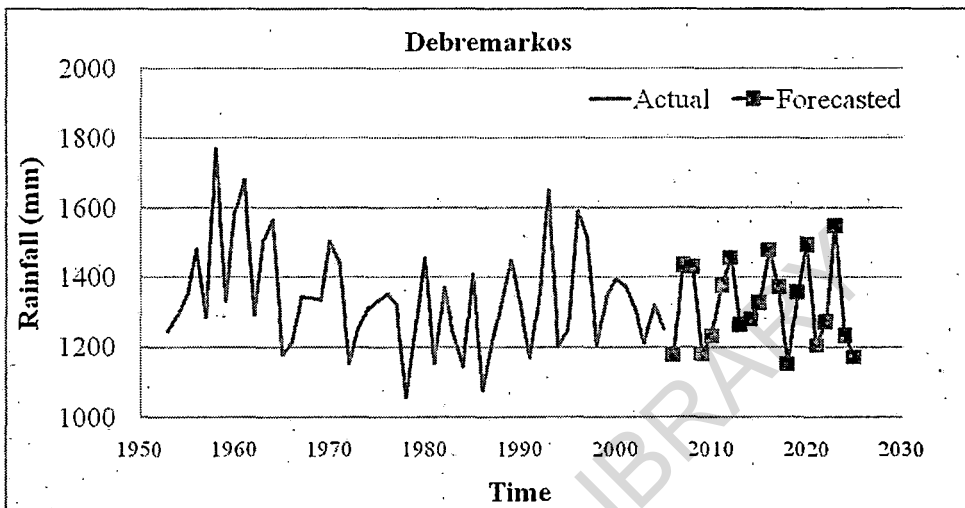


Figure (65): Actual and forecasted annual precipitation for Debremerkos.

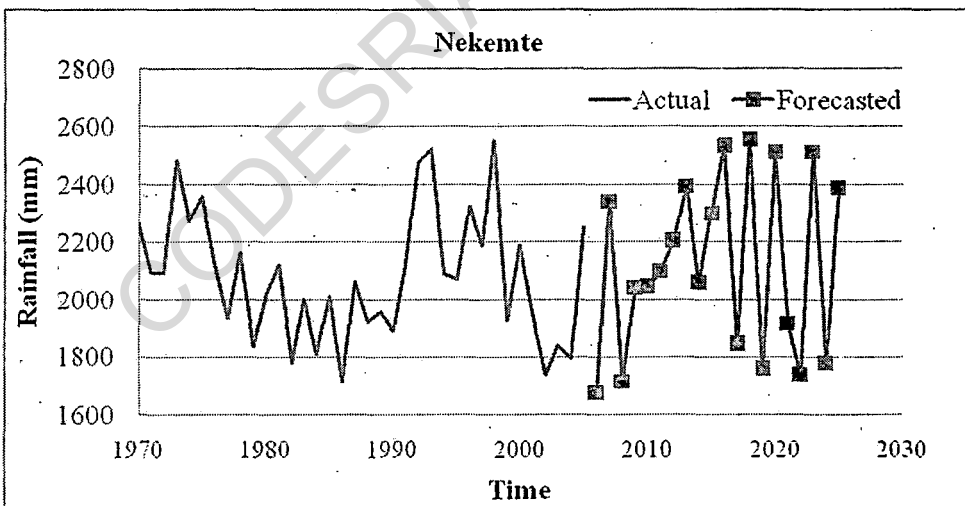


Figure (66): Actual and forecasted annual precipitation for Nekemte.

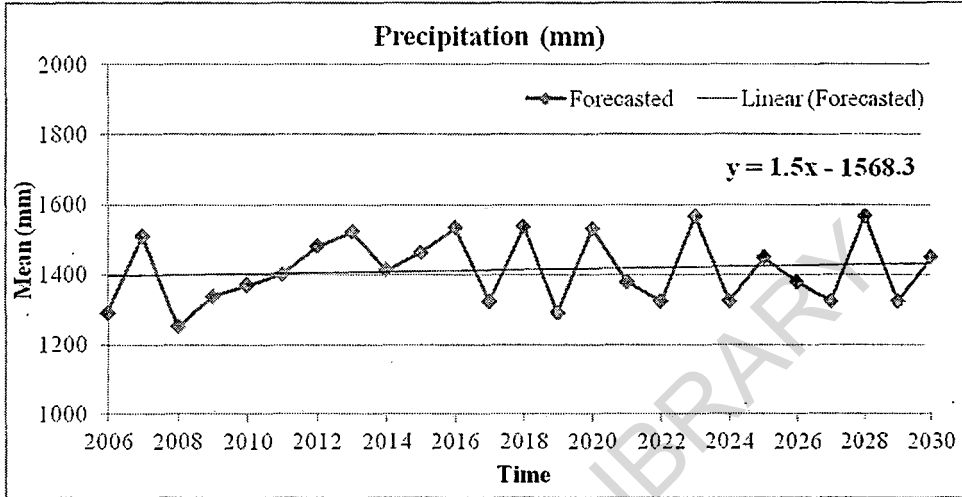


Figure (67): Annual precipitation forecast for four stations (Addis Ababa, Bahir Dar, Debremarkos and Nekemte).

4.30. Trend analysis of the Nile Basin

The trends in stream flow computed by the Mann-Kendall test, the results indicate that there was no significant trend in the observed annual runoff at all stations El Diem, Khartoum, Malakal, Dongola and Aswan ($R^2 = 0.033, 0.00, 0.14, 0.09$ and 0.002 , respectively). It is noted that, trend in the flow TS increased for the Blue Nile at (El Diem and Khartoum station), while the flow TS decreased for White Nile at Malakal station (Figure 68). A comparison of the historical inflow data at Mongalla (33.3 km^3) and outflow data at Malakal (29.7 km^3) shows a negative balance of 3.6 km^3 . Taking into account that the Sobat River contributes an average 13.5 km^3 of water per year to the flow at Malakal one can easily conclude that more than half of the river inflow is lost by evaporation, evapotranspiration and ground water losses (*Sutcliffe and Parks, 1999*).

Some literatures have considered climate change and variability of Nile flow. *Conway and Hulme (1996)* studied the variability in precipitation and streamflow on the whole Nile. They found the main cause for the historical fluctuation in main Nile runoff was the fluctuation in precipitation. In addition they found no correlation in precipitation and runoff between Blue Nile and White Nile and the precipitation and runoff over the upper Blue Nile basin displayed no significant temporal trend.

Sutcliffe and Parks (1999) showed that Blue Nile and Atbara flows are variable and declined in 1970 and 1980, Main Nile stations showed high flow up to 1990 and the variable flows until 1970 and low flow since 1970.

Using Pettitt the possible change points were examined for the mean annual runoff and the possible change-points were indicated as upper values of the probability curve, in this study, the flow TS were checked for the

absence of step trends using annual flows based on hydrological year. The annual flows were computed from the observed monthly flows. Pettitt test was used to identify possible step trends in the flow TS for the Blue Nile, White Nile, and main Nile River. The probability higher than 0.8 is considered statistically significant (Agor, 2003), and the flow TS is checked for the absence of step trends only if the probability is higher than 0.8. Pettitt test suggests that there are possible step trends for flow at El Diem, Khartoum, Malakal, Dongola, and Aswan after the hydrological years 1992, 1987, 1971, 1979, and 1988 respectively. The results of step trend analyses are summarized in (Table 45) and presented in (Figure 70). The trends analyses were carried out at 95% confidence level.

Since 1988 and 1993, the flow of the Blue Nile has increased significantly as observed at Khartoum and El Diem stations (Figure 69). The means of flow before and after 1988 and 1993 are significantly different at 95% confidence level. Difference in means causing instability of the mean, for the TS at Khartoum it was stable in both mean and variance while it was stable in variance and not stable in mean at El Diem. The flow TS of the Blue Nile were found to be stable in the variance at both stations.

The minimum and maximum annual observed flow at El Diem is 29.9 Bm³, and 67.25 Bm³, respectively. The minimum and maximum flows occurred in 1984 and 1988, respectively. Similarly, the minimum and maximum annual observed flow at Khartoum is 16 Bm³, and 70.35 Bm³, respectively, and occurred in 1984 and 1989, respectively. The average annual flow of the Blue Nile observed at El Diem and Khartoum is 46.24 Bm³ and 43.1 Bm³, respectively. It has to mention that in 1988 Sudan had experienced huge and devastating flood (Sutcliffe, et al., 1989).

On the contrary, for the White Nile flow, the analysis showed that there is statistically significant flow reduction after 1972 causing step trend in the TS (Figure 69). The flow TS is stable in the variance but not in the mean. It has to be mentioned that only few data-points are used for the split record test (Pettitt test), and that constrains making solid judgment about the presence of step trend after 1972. However, there is no doubt about the flow decrease of the White Nile. *Ageel, et al., (2010)*, used data from 1965 to 2000, have found an annual flow reduction of about 97.43 Bm^3 .

The mean annual flow of the White Nile observed at Malakal is about 30.7 Bm^3 . The minimum and maximum annual observed flow at Malakal is 25 Bm^3 , and 39.3 Bm^3 , respectively, and occurred in 1984 and 1965, respectively. The maximum flow had occurred when the water level of Victoria Lake is very high, the White Nile flow declines too, this suggests the strong control of Lake Victoria on the White Nile flow.

The minimum and maximum annual observed flow at Aswan is 2901.3 Bm^3 , and 7453.6 Bm^3 , respectively. The minimum and maximum flows occurred in 1985 and 1989, respectively. The average annual flow of the Nile observed at Aswan is 5004.2 Bm^3 . The flow TS of the Nile were found to be stable in the variance and mean at this station.

In this study, the flow TS of the Atbra River is not analyzed, but *Ageel, et al., (2010)* have found that the Atbra River flow is increasing with an annual amount of about 615.65 Bm^3 , using data from 1986 to 2000, and they did not observe step trend in the TS. As the step trends are more likely due to the climatic change effect, and as the climate change effects occur gradually, therefore, the exact location of the step trends could be slightly shifted.

The flow TS of the Nile, as observed at Dongola, showed to be stable in the variance but not in the mean, i.e. there is no step trend in the Nile River flows (figure 70). As the Blue Nile, and Atbra River flows increase, and as the White Nile flow decreases, and as the Nile River flow fairly remains constant, this implies fixed amount of water used within the Sudan, and implies that the decrease of the White Nile flow is counterbalanced by the increase of the Blue Nile and Atbra River flows. The flow reduction of the White Nile could be due to the effect of climate change, as more water evaporated from the East African lakes and the swamps in the southern Sudan. And it seems that the evaporated water from the White Nile basin falls as precipitation over the Blue Nile basin, causing an increase of the Blue Nile flows. However, the total amount of water remains fairly constant, as there is no step trend in the Nile flows.

Our findings are consistent with the Ministry of Irrigation and Water Resources, 2009, findings (figure 69), which shows the control of the Blue Nile and Atbra River on the Nile flow, and the Nile flow is less controlled by the White Nile. The White Nile represents the base flow of the Nile, while the Blue Nile and Atbra River represent the flood flows of the Nile.

Table (45): Step trend analyses.

Station	Year	F-test	t-test
El Diem 45.93 Bm ³ /y	1965 to 1992 1993 to 2005	p-value = 0.503 True, TS is stable in the variance	p-value= 0.023 False, TS is not stable in the mean
Khartoum 42.78 Bm ³ /y	1965 to 1987 1988 to 2005	p-value = 0.199 True, TS is stable in the variance	p-value = 0.094 True, TS is stable in the mean
Malakal 30.9 Bm ³ /y	1965 to 1971 1972 to 2005	p-value = 0.636 True, TS is stable in the variance	p-value = 0.001 False, TS is not stable in the mean
Dongola 71.29 Bm ³ /y	1965 to 1979 1980 to 2005	p-value = 0.883 True, TS is stable in the variance	p-value = 0.004 False, TS is not stable in the mean
Aswan 5004.14 Bm ³ /y	1969 to 1988 1989 to 2005	p-value = 0.437 True, TS is stable in the variance	p-value = 0.105 True, TS is stable in the mean

* For mean flow the whole dataset is used

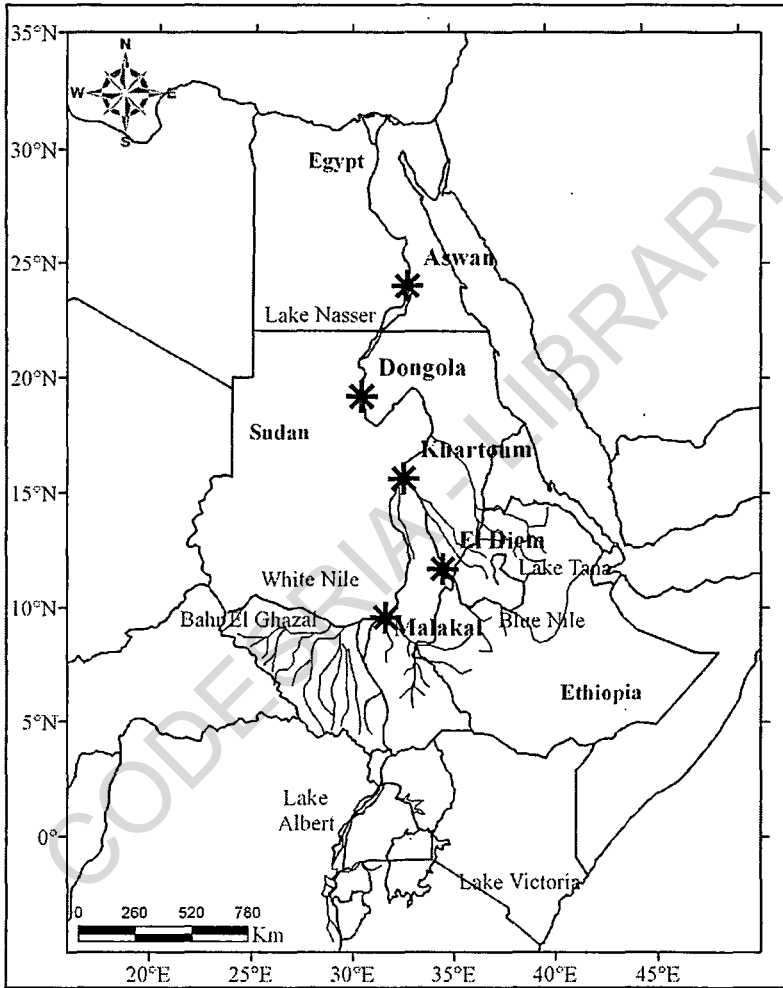


Figure (68): Location of Nile river flow stations.

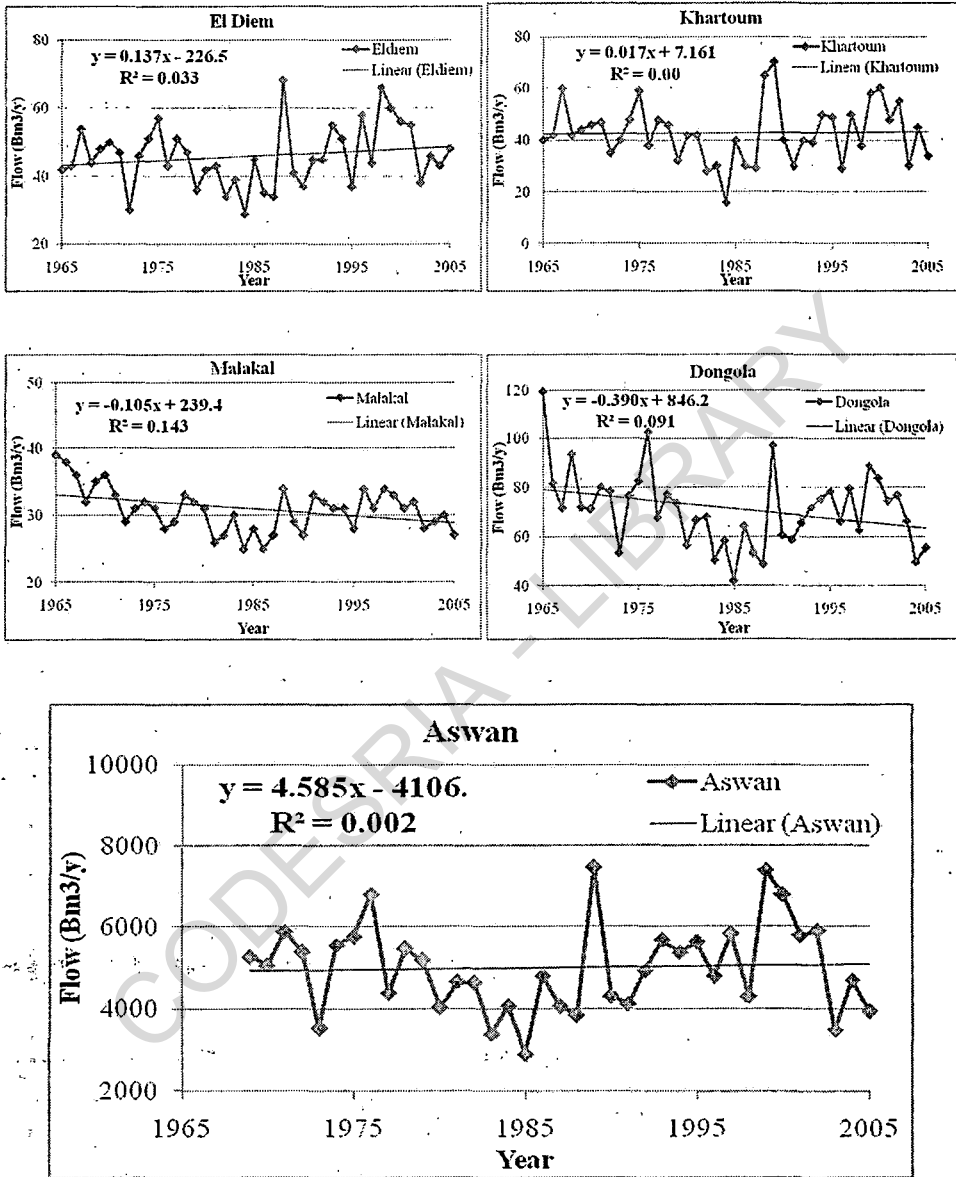


Figure (69): Observed discharge data for El Diem, Khartoum, Malakal, Dongola and Aswan.

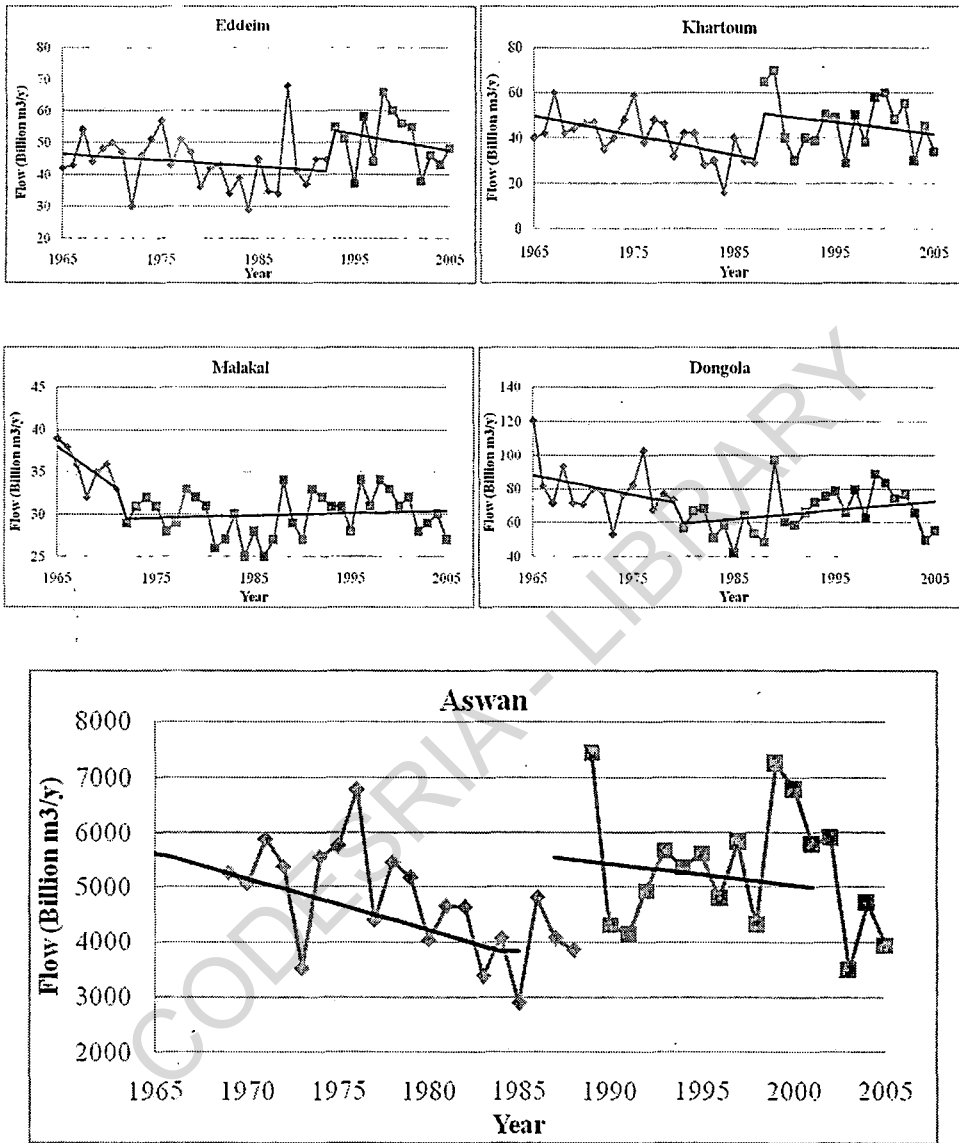


Figure (70): Step trends for: El Diem, Khartoum, Malakal, Dongola and Aswan stations.

Conclusion



COLESON'S LIBRARY

CONCLUSIONS

This study has presented analysis of the spatial and temporal behavior of rainfall, maximum and minimum temperature using data obtained from twenty six meteorological stations of Ethiopia from the year 1950 to 2005. The main findings of the study are summarized below.

1. After analyses of all climatic data for (Annual maximum and minimum temperature) of all stations in Ethiopia, we found that P_{out} value of all data for each station were more than all annual values for this station through the study period, while in the annual rainfall, we found that the total number of corrected values is only twelve stations shown in, total annual rainfall values in these stations were higher than P_{out} value so it were replaced by the corresponding P_{out} value.
2. According to the statistical test for homogeneity, all data series under study were shown as homogeneous data, except rainfall for some stations.
3. Different statistical characteristics like mean and coefficients of variation (CV) of annual maximum temperature over different stations under consideration in Ethiopia are calculated, we found that the study period from (1950-2005) had mean (22.4-34.81), standard deviation (0.4-0.8), variance (0.1-0.7) and coefficients of variation (1.1%-3.48%), while annual minimum temperature, we found that the study period from (1950-2005) had mean (9.4-22.7), standard deviation (0.4-1.4), variance (0.2-2.1) and coefficients of variation (3.2%-12.3%).
4. We found that gradual increase in the mean for maximum temperature from the 1st Quarter (25%) to the last 3rd Quarter (75%) for all stations [1st Quarter (25%) < median < 3rd Quarter (75%)].

5. Trend lines were estimated by linear regression, quadratic and cubic equation, using the least squares method, and the slope of the regression line tested at the 0.05 level of statistical significance.
6. According to the least-square method test for trend, positive trends of the mean annual maximum temperature (Long period) were observed at all study stations. The trends ranged between 0 and 0.06 °C/years at Diredawa station (East Ethiopia).
7. In general the characteristics of minimum and maximum temperatures in Ethiopia reveal significant increasing trends, but the rate was slightly higher for minimum than maximum temperature in almost all study stations during observation period.
8. The findings of the study show positive trends in the annual mean maximum and minimum temperatures with 95% significance levels. The annual maximum temperature increased by 0.027°C, while the minimum temperature experienced an increase of 0.02°C in Ethiopia over the 55-year period.
9. The trend analysis on the significant climate parameters indicated that Rainfall trends of Ethiopia from 1950-2005 has been decreasing in most of station 16 out of 26 stations and this decrease was minimal through the study period, while 8 out of 26 (Arbaminch, Awash, Awassa, Debre Zeit, Dessie, Jima, Harer and Wonji) stations showed increase in rainfall and this increase was minimal and an overall increase in the mean annual minimum and maximum temperatures in the study area.
10. After selecting the most appropriate model, it was found that ARIMA model $(0,0,0) \times (1,1,1)_{12}$, $(0,0,0) \times (1,1,1)_{12}$, $(0,0,0) \times (0,1,1)_{12}$ and $(0,0,1) \times (0,1,1)_{12}$ is among several models that passed all statistic tests

required in the Box-Jenkins methodology for Bahar Dar, Nekemte, Debre Markos and Addis Ababa respectively, of the North, West and middle of Ethiopia.

11. The Blue Nile flow TS were found to be stable in the variance and mean, i.e. there is step trend. Since 1988, the Blue Nile flows have increased significantly, as observed at Khartoum flow measuring stations but decreased in trend of White Nile flow TS at Malakal station.
12. The White Nile flow TS were found to be also stable in the variance but not in the mean, i.e. there is step trend. Since 1972, the White Nile flows have decreased significantly, as observed at Malakal measuring station.
13. The Nile flow TS were found to be stable in variance and not stable in the mean. The Nile flow TS were analyzed for the flow observed at Dongola station.
14. The Nile flow TS were found to be stable in both the variance and the mean, Nile flow TS were found to be increased during the study period at Aswan station.



Recommendations

COLESLAKE LIBRARY

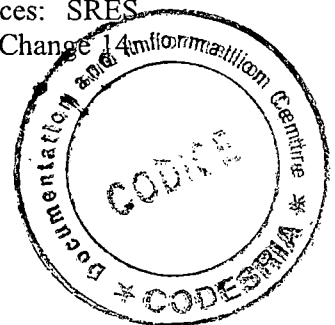
RECOMMENDATIONS

Generally from this specific study the following four main points are strongly recommended:

1. Using prediction model to predict Ethiopian rainfall and fluctuations of the Nile flooding should include historical long periods to obtain good results.
2. To obtain on general feature of rainfall at Nile River water resources, the study should include each region separately because of geographic difference in these regions also difference in local and universal climatic factors.
3. In order to assure the development of water resource and agricultural efficiency of poor countries like Ethiopia as well as the region of Africa, further studies which incorporate the impact of climate change with land use and land cover change, plus sediment inflow to the reservoirs should be undertaken by using more than one and more finer resolution of Global Circulation Models (GCMs). These studies should also investigate the adaptation options for the impact of climate change consequences.
4. Study of more meteorological stations are needed to exactly predict the climate change variations with full confident level since the available climatic stations are widely spaced.

REFERENCES

- Abdullah, M.A., and AlMazroui, M.A., (1998):** Climatological study of the southwestern region of Saudi Arabia, I. Rainfall analysis, *Climate research*, 9: pp 213-223.
- Abebe, D., (2010):** Future climate of Ethiopia from PRECIS Regional Climate Model Experimental Design, http://www.metoffice.gov.uk/media/pdf/o/9/PRECIS_Experimental_Design.
- Ageel, I., Bushara, and Abdelrahim, T., (2010)** Investigation of step trends of the Nile River flow time series, *Nile Basin Water Science & Engineering Journal*, Vol.3, Issue2.
- Agor, M.L., (2003):** Assessment of the long-term rainfall runoff relation of the Geul Catchment, MSc Thesis, UNESCO- IHE, Delft, The Netherlands.
- Aguilar E, Auer I, Brunet M, Thomas C. Peterson and Wieringa J., (2004):** Guidelines on climate metadata and homogenization, WMO/TD No. 1186.
- Akaike, H., (1974):** A New Look at Statistical Model Identification, *IEEE Transactions on Automatic Control*, 19: pp 716-723.
- Al-Ansari, N., and Baban S. M., (2005):** Rainfall Trends in the Badia Region of Jordan, *Surveying and Land Information Science*; Dec; 65, 4, ProQuest Science Journals, 233.
- Al-Ansari, N.A., Shamali, B., and Shatnawi, A., (2006):** Statistical analysis at three major meteorological stations in Jordan, *Al Manara Journal for scientific studies and research* 12, pp 93-120.
- Alexandersson, A., (1995):** Homogeneity testing, multiple breaks and trends, In: *Proceedings of the 6th International Meeting on Statistical Climatology*, Galway, Ireland, pp 439-441.
- Amy, C., (2006):** Assessing the impacts of climate change on river Basin management: a new method with application to the Nile River, PhD Thesis, The Academic Faculty, School of Civil and Environmental Engineering, Georgia Institute of Technology, Georgia.
- Arnell, N. W., (2004):** Climate change and global water resources: SRES emissions and socio-economic scenarios, *Global Environmental Change*, pp 31-52.



- Arsano, Y., (2007):** Ethiopia and the Nile Dilemmas of National and Regional Hydropolitics, PhD Thesis, Department of Political Sciences and International Relations, Addis Ababa University, Ethiopia.
- Bayoumi, B., (2006):** Assessment of vulnerability and adaptation of water resources to climate change in Egypt, water resources management consultant, <http://www.arabwatercouncil.org/administrator/Modules/Events>.
- Bejene, T., Lettenmaier, D., and Kabat, P., (2007):** Hydrologic Impacts of Climate Change on the Nile River Basin: Implications of the 2007 IPCC Climate Scenarios, ALTERRA Green World Research, Wageningen University and Research Centre, P.O. Box 47, 6700 AA Wageningen, the Netherlands.
- Box, G.E., and Jenkins, G.M., (1976):** Time Series Analysis: Forecasting and Control, Revised Edition, Holden-Day, San Francisco.
- Box, G.E., Jenkins, G.M., and Reinsel, G.C., (1994):** Time series analysis: Forecasting and control, Pearson Education, Delhi.
- Buishand, T.A., (1982):** Some methods for testing the homogeneity of rainfall records, *J. Hydrology* 58: pp 11-27.
- Camberlin P., (2009):** Nile Basin Climates. In "The Nile: Origin, Environments, Limnology and Human Use", Dumont, Henri J. (Ed.), *Monographiae Biologicae*, Springer, pp 307-333.
- Camberlin, P., and Philippon, N., (2002):** The East African March-May Rainy Season: Associated Atmospheric Dynamics and Predictability over the 1968-97 period, *Journal of Climate*, 15: pp 1002-1019.
- Chen, S., SHI, Y., GUO, Y., and Zheng Y., (2010)** Temporal and spatial variation of annual mean air temperature in arid and semiarid region in northwest China over a recent 46 year period, *Journal of arid land*, VOL. 2, NO. 2, pp 87-97.
- Cheung, W., Gabriel, B. S., and Singh, A., (2008):** Trends and spatial distribution of annual and seasonal rainfall in Ethiopia, *International journal of climatology*, *Int. J. Climatol.* 28: pp 1723-1734.
- Collier, P., and Dercon, S., (2008):** African agriculture in 50 years: smallholders in a rapidly changing world, FAO Expert Meeting on How to Feed the

World in 2050, Food and Agriculture Organization of the United Nations, Economic and Social Development Department, FAO.

- Conway, D., (2000):**The climate and hydrology of the Upper Blue Nile River, *The Geogr. J.* 166: pp 49–62.
- Conway, D., (2005):**From headwater tributaries to international river: observing and adapting to climate variability and change in the Nile Basin, *Global Environmental Change* 15: pp 99- 114.
- Conway, D., and Hulme M., (1993):**Recent fluctuations in precipitation and runoff over the Nile sub basins and their impact on main Nile discharge, *Climatic Change* 25: pp 127-151.
- Conway, D., Hulme, M., (1996):**The impacts of climate variability and future climate change in the Nile basin on water resources in Egypt, *International Journal of Water Resources Development* 12, 261–280.
- Conway, D., Lisa, E., and Schipper, F., (2011):**Adaptation to climate change in Africa: Challenges and opportunities identified from Ethiopia, *Global Environmental Change* 21, 227–237, <http://dx.doi.org/10.1016/j.gloenvcha.2010.07.013>
- Conway, D., Persechino, A., ArdoinBardin, S., Hamandawana, H., Dieulin, C., and Mahe, G., (2008):**Rainfall and water resources variability in sub-Saharan Africa during the 20th century, *Journal of Hydrometeorology* 10: pp 41-59.
- Dao-yi, G., and Changhoi, H., (2004):** Intra-seasonal variability of wintertime temperature over East Asia, *international journal of climatology*, 24: pp 131–144.
- Degaetano, A.T., Eggleston, K.L., and Knapp, W.W., (1995)**A method to estimate missing maximum and minimum temperature observations, *J. Appl. Meteorol.* 34: pp 371-380.
- Draper, N.R., and Smith, H., (1998):**Applied Regression Analysis, John Wiley and Sons, New York.
- Eischeid, J.K., Baker, C.B., Karl, T.R., and Diaz H.F., (1995):** The quality control of long-term climatological data using objective data analysis, *J. Appl. Meteorol.* 34: pp 2787-2795.

- Elshamy, M.E., Seierstad, I.A., and Sorteberg, A., (2009)** Impacts of climate change on Blue Nile flows using bias-corrected GCM scenarios, *J. of Hydrol., Earth Syst, Sci.*, 13: pp 551–565.
- El-Tantawi, A. M., (2005):** Climate Change in Libya and Desertification of Jifara Plain Using Geographical Information System and Remote Sensing Techniques, Ph.D. thesis, Department of Geography, Mainz University, Germany.
- ENMA (Ethiopia National Meteorological Agency), (2001):** Initial National Communication of Ethiopia to the United Nations Framework Convention on Climate Change (UNFCCC), National Meteorological Services Agency (NMSA), Addis Ababa, Ethiopia.
- ENMA (Ethiopia National Meteorological Agency), (2011):** Annual climate bulletin for the year 2011, National Meteorological Services Agency (NMSA), Addis Ababa, Ethiopia.
- FAO, (2005):** Factors affecting the development and management of water resources for agriculture in the Nile Delta, FAO-AGLW internal notes.
- Fekadu T.B., (2009):** Impact assessment of global climate change on some components of hydrometeorology in Ethiopia: applying atmospheric general circulation model, MSc Thesis, Kochi University of Technology.
- Feyissa G., (2010):** Comparative Analysis of Climate Variability and Impacts in Central Rift Valley and Adjacent Arsi Highlands Using GIS and Remote Sensing, M.Sc, Department of Earth Sciences, Faculty of Science, Addis Ababa University, Addis Ababa.
- Folland, C.K., and Salinger, M.J., (1995):** Surface temperature trends and variations in New Zealand and the surrounding ocean, 1871–1993, *Int. J. Climatol.*, 15, pp 1195–1218.
- Fraedrich, K., and Bantzer, C., (1991):** A note on fluctuations of the Nile River flood levels (715-1470), *Theor. Appl. Climatol.*, 44: pp 167-171.
- Funk, C., Senay, G., Asfaw, A., Verdin, J., Rowland, J., Michaelson, J., Eilerts, G., Korecha, D., and Choularton, R., (2005)** Recent drought tendencies in Ethiopia and equatorial-subtropical eastern Africa, Washington DC, FEWS-NET.

- Gebrehiwot, T., and Anne V.A., (2013):** Assessing the evidence of climate variability in the northern part of Ethiopia, *Journal of Development and Agricultural Economics* Vol. 5(3): pp 104-119.
- Gerretsadikan Aand Sharma, M (2011):** Modeling and forecasting of rainfall data of mekele for Tigray region (Ethiopia), *Statistics and Applications* Volume 9, Nos. 1&2, pp. 31-53.
- Gleick, P.H., (1991):** The vulnerability of runoff in the Nile basin to climatic changes, *The Environmental Professional*, 13, 66–73.
- Haile, T., (1988):** Causes and Characteristics of Drought in Ethiopia, *Ethiopian Journal of Agricultural, Sciences*, 10: pp 85 – 97
- Heino, R., (1994):** Climate in Finland during the Period of Meteorological Observations, *Finnish Meteorological Institute Contributions*, 12: pp 209.
- Hulme, M., (1994):** Global climate change and the Nile basin. In: Howell, P.P., Allan, J.A. (Eds.), *The Nile Sharing a Scarce Resource*, Cambridge University Press, Cambridge, pp. 139–162.
- Hulme, M., Doherty R., Ngara, T., New, M., and Lister, D., (2001):** African climate change: 1900–2100, *Climate Research*, Vol. 17: pp 145–168.
- IBM, (2010):** IBM SPSS Statistics 19 Core System User's Guide, <http://www.spss.com/>
- IPCC, (2001):** Climate change; impacts, adaptation and mitigation, *The Third Assessment Report of the Intergovernmental Panel on Climate Change*, Cambridge University Press, UK, p 650.
- IPCC, (2007):** Climate Change 2007: Impacts, Adaptation and Vulnerability. Contribution of Working Group II to the Fourth Assessment Report of the Intergovernmental Panel on Climate Change (IPCC), Parry, M.L., Canziani, O.F., Palutikof, J.P., vander Linden, P.J., and Hanson, C.E., (Eds) Cambridge University Press, Cambridge, UK, pp 1000.
- IPCC, (2008):** Climate Change and Water, *IPCC Technical Paper VI*, Bryson Bates, Zbigniew W. Kundzewicz and Shaohong Wu, Cambridge University Press, Cambridge, UK, pp 214.
- Kemp, W.P., Burnell, D.G., Everson, D.O., and Thomson, A.J., (1983):** Estimating missing daily maximum and minimum temperatures, *J. Climate Appl. Meteorol.* 22, pp 1587-1593.

- Kim, U., Kaluarachchi, J. J. and Smakhtin, V. U. (2008):** Climate Change Impacts on Hydrology and Water Resources of the Upper Blue Nile River Basin, Ethiopia, Colombo, Sri Lanka: International Water Management Institute (IWMI) Research Report 126, p 27.
- Makridakis, S., and Hison, M., (1995):** ARMA models and the box Jenkins methodology, Printed at INSEAD, 95/45/TM, Fontainebleau, France.
- McSweeney, C., New, M., and Lizcano, G., (2008)** UNDP Country Change Profiles: Ethiopia, Oxford, UK: UNDP, <http://country-profiles.geog.ox.ac.uk>.
- Meigh, J.R., McKenzie, A.A., Austin, B.N., Bradford, R.B., and Reynard, N.S., (1998):** Assessment of Global water Resources – phase II, Estimates of present and future water availability in Eastern and Southern Africa, Center for Ecology and Hydrology, Wallingford.
- Mert O., (2005):** North Sea – Caspian pattern and its influence on the Hydrometeorological parameters over Turkey, M.Sc., Istanbul technical University, Eurasia institute of earth sciences, Turkey.
- Meseret, M. K., (2009):** Climate change and crop agriculture in Nile Basin of Ethiopia: measuring impacts and adaptation options, MSc Thesis, department of economics, school of graduate studies, Addis Ababa University, Ethiopia.
- Mitchell, J.M., Dzerdzevskii, B., Flohn, H., Hofmery, W. L., Lamb, H.H., Rao, K.N., and Wallen, C.C., (1966):** Climatic change, WMO Tech. Note 79, WMO No. 195, TP-100- Geneva.
- Mohamed, M. E., (2006):** Causes and Impact of Desertification in the Butana Area of Sudan, M.Sc, Faculty of Natural and Agricultural Sciences, University of the Free State, Bloemfontein, South Africa.
- Mohamed, Y. A., Van Den Hurk, B. J., Savenije, H. H., and Bastiaanssen, W. G., (2005):** Hydroclimatology of the Nile: results from a regional climate model, Hydrology and Earth System Sciences, 9, pp 263–278.
- Montgomery, D.C., and Johnson, L.A., (1967):** Forecasting and time series analysis, McGraw-Hill Book Company, [http://www.abebooks.com/Forecasting-Time Series-Analysis-Montgomery-Douglas/1323032148/bd](http://www.abebooks.com/Forecasting-Time-Series-Analysis-Montgomery-Douglas/1323032148/bd), McGraw-Hill.

- Moustafa, T., (2007):** The Past and the Future of Flood Management in the Eastern Nile Basin, http://www.inbo-news.org/IMG/pdf/Nile_Flood_Management_abstract.pdf.
- Mulugeta, H., (2009):** Evaluation of Climate Change Impact on Upper Blue Nile Basin Reservoirs (Case Study on Gilgel Abay Reservoir, Ethiopia), M.Sc, Science in Hydraulics and Hydropower Engineering, School of Post Graduate Studies, Arba Minch University, Ethiopia.
- Naill, P.E., and Momani, M., (2009):** Time series analysis model for rainfall data in Jordan: A Case Study for Using Time Series Analysis, American Journal of Environmental, Vol. 5, pp 599-600.
- National climatic data center:** Africa (volume 1-2-3-5), Data for periods 1951-1960, 1961-1970, 1971-1980 and 1981-90, USA.
- Nicholson, S. E., (1996):** A review of climate dynamics and climate variability in Eastern Africa, The Limnology, Climatology and Paleoclimatology of the East African Lakes, T. C. Johnson and E.O. Odada, Eds., Gordon and Breach, pp 25-56.
- Nicholson, S.E., and Kim, J., (1997):** The relationship of the El Niño Southern Oscillation to African rainfall, Int. J. Climatol., 17: pp 117–135.
- Paulhus, J.L., and Kohler, M.A., (1952):** Interpolation of missing precipitation records, Monthly Weather Rev. 80, pp 129-133.
- Rusticucci, M., and Renom, M., (2004):** Homogeneity and quality control of long time series of daily temperature in Uruguay, Universidad de Buenos Aires, Ciudad Universitaria Pab II, 1428 Buenos Aires, Argentina, <http://www.actlife.eu/medias/60-time-series-analysis-and-current-climate-trends-estimatesforavanti.pdf>
- Salas, J.D., and Boes, D.C., (1980):** Shifting Level Modeling of Hydrologic Series: Advances in Water Resources, 3, pp 59-63.
- Salas, J.D., Delleur, J.W., Yevjevich V., and Lane, W.L., (1980):** Applied modeling of hydrologic time series, II Water Resources Publications, Littleton, Colorado.
- Salmi, T., M. Anu, A. Pia, R. Tuija, and A. Toni., (2000):** Detecting trends of annual values of atmospheric pollutants by the Mann-Kendall test and Sen's slope estimates –the Excel template application MAKESENS, Finnish

Meteorological Institute, Library P.O.Box 503, FIN-00101 Helsinki, Finland.

- Seleshi, Y., and Camberlin, P., (2006):**Recent Changes in Dry Spell and Extreme Rainfall Events in Ethiopia, *Theoretical and Applied Climatology*, 83, pp 181–191.
- Seleshi, Y., and Demaree, G.R., (1995):**Rainfall variability in the Ethiopian and Eritrean highlands and its links with the Southern Oscillation index, *J. Biogeography*, 22: pp 945-952.
- Seleshi, Y., and Zanke, U., (2004):**Recent Changes in Rainfall and Rainy Days in Ethiopia, *International Journal of Climatology*, 24: pp 973–983.
- Sene, K.J., (2000):** Theoretical estimates for the influence of Lake Victoria on flows in the Upper White Nile, *Hydrological Sciences Journal* 45, 125–145.
- Sene, K.J., Tate, E.L. and Farquharson, F.A., (2001):**Sensitivity studies of the impacts of climate change on White Nile flows, *Climatic Change* 50:177-208.
- Setegn, S. G., Srinivasan, R., and Dargahi, B., (2008):**Hydrological modelling in the Lake Tana Basin, Ethiopia using SWAT model: *Open Hydrology Journal*, v. 2, p. 49-62.
- Shahin, M., (1985):** Hydrology of the Nile Basin, *Developments in Water Science*, 21, Elsevier, Amsterdam, pp 575.
- Shang, H., Yan, J., Gebremichael, M., and Ayalew, S., (2011)**Trend Analysis of Extreme Precipitation in the Northwestern Highlands of Ethiopia with a Case Study of Debre Markos, Manuscript prepared for *Hydrol. Earth Syst. Sci.* with version 3.2 of the LATEX class copernicus.cls.
- Stepanek, P., and Zahradnicek P., (2009):** Experiences with data quality control and homogenization of daily records of various meteorological elements in the Czech Republic in the period 1961–2010, *Quarterly Journal of the Hungarian Meteorological Service*, Vol. 117, No. 1: pp 123–141.
- Strzepek, K., Yates, D.N., (1996):**Economic and social adaptations to climate change impacts on water resources: a case study of Egypt, *Water Resources Development* 12, 229–244.

- Strzepek, K., Yates, D.N., Yohe, G., Tol, R.J., Mader, N., (2001)** Constructing 'not implausible' climate and economic scenarios for Egypt, Integrated Assessment 2, 139–157.
- Sutcliffe, J. V., and Parks, Y. P., (1999)**: The Hydrology of the Nile, IAHS Special Publication no. 5, IAHS Press, Institute of Hydrology, Wallingford, Oxfordshire OX10 8BB, UK.
- Sutcliffe, J., Dugdale, G., and Milford, J., (1989)**: The Sudan flood of 1988, Hydrological sciences journal, 34 (3), pp 355-364.
- Tadege, A., (2007)**: Climate change national adaptation Programme of action of Ethiopia, ministry of water resources and national meteorological agency, Addis Ababa, Ethiopia.
- Tate, E., Sutcliffe, J., Conway, D., and Farquharson, F., (2004)**: Water balance of Lake Victoria: Update to 2000 and climate change modelling to 2100, Hydrological Sciences Journal, 49(4): pp 563-574.
- Thom, H.C., (1966)**: Some methods of climatological analysis, WMO Tech. Note 81, WMO No.199, TP. 03, Geneva.
- Tronci, N., Molteni, F., and Bozzini, M., (1986)**: A comparison of local approximation methods for the analysis of meteorological data, Arch, Meteorol., Geophys. Bioclimatol., 36, pp 189-211.
- Tsonis, A., Hunt, A. G., and Elsner, J. B., (2003)**: On the relation between ENSO and global climate change, Meteorol. Atmos. Phys., 84: pp 229– 242.
- Wale, A., Rientjes, T., Gieske, A., and Getachew, H., (2009)**: Ungauged catchment contributions to Lake Tana's water balance, Hydrological processes, DOI: 10.1002/hyp.
- Wang, Y., Li, X., and Miao, Q. L.(2004)**: Analyses on variety characteristics of temperature, Arid Land Geography, 27 (1): pp 41–46.
- WMO, (1981a)**: Manual on the Global Observing System, WMO-No, 544, World Meteorological Organization, Geneva.
- WMO, (1981b)**: Guide to Agricultural Meteorological Practices WMO-No, 134, World Meteorological Organization, Geneva.
- WMO, (1989)**: Guide on the global observing system, World Meteorological Organization, WMO (Series); no. 488.

- WMO, (1993):** Guide on the global data-processing system, World Meteorological Organization, WMO (Series); no. 305.
- Xia, Y, Fabian, P., Stohl A, and Winterhalter, M., (1999)** Forest climatology: estimation of missing values for Bavaria, Germany, Agricultural and Forest Meteorology 96, pp 131-144.
- Yates, D., and Strzepek, K., (1998):** Modeling the Nile basin under climatic change, Journal of Hydrologic Engineering, 3: pp 98-108.
- Yue, S., Pilon, P., and Cavadias, G., (2002):** Power of the Mann-Kendall and Spearman's rho tests for detecting monotonic trends in hydrological series, J. Hydrol. 259: pp 254-271.
- Zakaria, S., Nadhir AlAnsari, N., and Knutsson, S., (2013):** Rainwater Harvesting Using Recorded and Hypothetical Rainfall Data Scenarios Journal of Earth Sciences and Geotechnical Engineering, vol. 3, no. 2: pp 21-42.
- Zelalem, K., Yasir, A., and Tammo, S., (2009):** Trends in rainfall and runoff in the Blue Nile Basin: 1964-2003, Hydrological Processes vol. 24 issue 25: pp 3747-3758.
- The Global Historical Climate Network Dataset (GHCN):**
<http://www.ncdc.noaa.gov/pub/data/ghcn/v2>.



Arabic Summary

COLESVILLE LIBRARY

تأثير التغير المناخي على منابع مياه نهر النيل وتقلبات فيضانه في اثيوبيا

رسالة مقدمة من

مصطفى عبد الحميد محمد عطية

بكالوريوس العلوم (قسم الفلك والأرصاد الجوية) - جامعة الأزهر - 2001 - دبلوم الدراسات الإفريقية
(الموارد الطبيعية) - 2005 - ماجستير العلوم في الدراسات الإفريقية (موارد جوية) 2008 - محمد
البحوث والدراسات الإفريقية - جامعة القاهرة

للحصول على درجة دكتوراه العلوم

في الدراسات الإفريقية

(الموارد الطبيعية - موارد جوية)

الإشراف العلمي

الأستاذ الدكتورة/ فوزية إبراهيم مرسى

أستاذ الأرصاد الجوية - محمد البحوث والدراسات الإفريقية

جامعة القاهرة

الدكتور/ عبداللطيف عيسوى عواد

أستاذ مساعد الأرصاد الجوية - هيئة الأرصاد الجوية

المصرية

الدكتور/ عباس محمد شراقي

أستاذ مساعد الجيولوجيا الاقتصادية - محمد

البحوث والدراسات الإفريقية - جامعة القاهرة

المستخلص

تعد التغيرات المناخية من أهم الظواهر التي تسبب تحديات كبيرة على المستوى الكوني فأن التغير في معدلات الأمطار وفي توزيعها المكاني ، يمكن أن يؤدي إلى حدوث تغيرات كبيرة في الدورة الهيدرولوجية مثل زيادة معدلات التبخر لمياه المحيطات وزيادة سرعة تبخر المياه من اليابسة مما يؤدي إلى وصول كمية أقل من مياه الأمطار إلى مصادر الأنهار ومن المتوقع أن تأتي هذه التغيرات مصحوبة بأنماط جديدة لسقوط الأمطار وإحداث مناخ أكثر تطرفاً مثل الأعاصير والفيضانات والجفاف.

1. تهدف الدراسة الى التعرف على أثر التغيرات المناخية على منابع مياه نهر النيل الموسمية وكذلك على تذبذب فيضاناته حيث تتأثر مياه نهر النيل بالتغيرات المناخية.
2. دراسة التغيرات المناخية لعناصر درجتى الحرارة العظمى والصغرى وكذلك كمية الامطار خلال الفترة 1950-2005.
3. التنبؤ بالتغيرات المتوقعة لعناصر درجتى الحرارة العظمى والصغرى وكذلك كمية الامطار خلال الفترة المستقبلية 2006-2030م.
4. تقييم التغيرات في تدفق مياه نهر النيل عند المحطات الواقعة على مجرى النيل الازرق وعطبرة والنيل الرئيس عند دنقلا واسوان.

تعتمد الدراسة على بيانات درجة الحرارة العظمى والصغرى وكمية الامطار الشهرية لمانبع نهر النيل الموسمية (الهضبة الاثيوبية) وكمية الجريان السطحي عند بعض المحطات الموجودة على مجرى النيل الازرق والابيض والنيل الاساسى قبل السد العالى فى السودان وبعد السد عند اسوان تم الحصول على هذه البيانات من هيئة الارصاد الجوية الاثيوبية وبعض المصادر الاخرى لسد الفجوات الموجودة خلال فترة الدراسة ثم تم تقييم هذه البيانات باستخدام طرق مختلفة منها الجودة و التجانس بين البيانات لكل محطة.

من نتائج التحليل وجد ان متوسط درجة الحرارة العظمى والصغرى أخذت الاتجاه الموجب خلال الفترة من (1950-2005) وذلك بالنسبة لكل المحطات ولكن هذه الزيادة فى الاتجاه كانت صغيرة (0.04 لدرجة الحرارة العظمى و0.07 لدرجة الحرارة الصغرى خلال فترة الدراسة) وعلى العكس وجد ان كمية المطر أخذت الاتجاه السالب مع اختلاف القيم السالبة لمعظم المحطات (16 من 26 محطة).

تعد عملية التنبؤ اساساً لكل عمليات التخطيط العلمي ، بأعتبره سمة من سمات العصر الحديث في جميع مجالات الحياة ، اذ انه يساعد المختصين على اتخاذ القرارات اللازمة ووضع الخطط المستقبلية لتقادي المشكلات القائمة ولا سيما تلك التي تمس حياة الإنسان على سطح الأرض. وتعد دراسة كميات الأمطار المتساقطة من المواضيع المهمة في اغلب دول العالم ومنها منطقة الدارسة. يعد أسلوب تحليل السلاسل الزمنية من الأساليب الإحصائية الجديرة بالاهتمام، والتي تطورت كثيراً، وأصبح بالإمكان استخدامها لغرض التوقع للمستقبل. يتكون تحليل السلاسل الزمنية من مراحل متسلسلة تبدأ بمرحلة التشخيص للنموذج والتي تعد المرحلة الأهم، وتليها مرحلة تقدير المعلومات للنموذج، ومن ثم مرحلة فحص مدى الملاءمة للنموذج. وتأتي المرحلة الأخيرة وهي مرحلة التكهّن أو التنبؤ. من التحليل وجد أن سلسلة كمية الامطار الشهرية انها غير مستقرة فى المتوسط وان هناك اتجاه عام واضح فى السلسلة. تم تحقيق استقرارية السلسلة الزمنية بعد اخذ الفرق الاول للبيانات وبعد مطابقة معاملات الارتباط الذاتى والجزئى للسلسلة الزمنية مع السلوك النظرى لدالتى الارتباط الذاتى والجزئى فقد اتضح أن دالة الارتباط الذاتى تتناقص تدريجياً مع فترات الازاحة. تم تحليل السلاسل الزمنية باستخدام طريقة (Box & Jenkins) فى التحليل (التشخيص، التقدير، اختبار ملائمة النموذج، التنبؤ). لايجاد افضل نموذج للتنبؤ بكمية الامطار التي تسقط على دولة اثيوبيا عن بعض محطات الارصاد وذلك بالاعتماد على البيانات الشهرية لهذه المحطات للفترة (1900-2005)، تم الاعتماد على استخدام معايير المفاضلة بين عدة نماذج وهي (أقل قيمة لتباين النموذج-أقل قيمة لمجموع مربعات الخطأ. معيار معلومات آيك) جد أن النماذج الملائمة للبيانات هي نموذج الانحدار الذاتى المتكامل هو $(0,0,0)x(1,1,1)2$ لمحطة Bahar Dar, Nekemte اما النموذج الملائم لمحطة DebreMarkos هو $(0,0,0)x(0,1,1)2$ بينما النموذج $(0,0,1)x(0,1,1)2$ كان هو الملائم عند محطة Addis Ababa. باستخدام هذه النماذج للتنبؤ بكمية الامطار على حوض النيل الازرق للفترة (2006-2030) وجد أن كمية الامطار تزداد خلال هذه الفترة ولكن هذه الزيادة صغيرة. تم استخدام معادلة مان كاندل (Mann-Kendall test) لمعرفة الاتجاه العام للتدفق المائى للنيل الازرق عند محطات الاديم، خرطوم بينما محطة ملكال للنيل الابيض و محطة دنقلا للنيل الاساسى خلال فترة الدراسة. وجد ان معامل التحديد (R^2) صغير عن كل المحطات كذلك وجد ان الاتجاه العام للتدفق النهري للنيل الازرق فى زيادة عند محطة الاديم والخرطوم بينما العكس للنيل الابيض عند محطة ملكال. أظهرت النتائج أيضاً أن التغيرات المتوقعة لتدفقات النيل الرئيسى عند دنقلا تنشأ من الزيادة في معدلات سقوط الأمطار والتدفقات على حوضي النيل الأزرق.

(الكلمات الدالة: حوض نهر النيل- موارد مياه نهر النيل- النيل الازرق-الفيضانات-التغير المناخي- الاتجاه السلاسل الزمنية- نموذج (ARIMA).

الملخص العربي

المقدمة

تعد التغيرات المناخية من أهم الظواهر التي تسبب تحديات كبيرة على المستوى الكوني فإن التغير في معدلات الأمطار وفي توزيعها المكاني ، يمكن أن يؤدي إلى حدوث تغيرات كبيرة في الدورة الهيدرولوجية مثل زيادة معدلات التبخر لمياه المحيطات وزيادة سرعة تبخر المياه من اليابسة مما يؤدي إلى وصول كمية أقل من مياه الأمطار إلى مصادر الأنهار ومن المتوقع أن تأتي هذه التغيرات مصحوبة بأنماط جديدة لسقوط الأمطار وإحداث مناخ أكثر تطرفاً مثل الأعاصير والفيضانات والجفاف. فالتغيرات المناخية ولاسيما الزيادات المسجلة في درجات الحرارة قد أثرت في النظم الفيزيائية والإحيائية في أنحاء عديدة من العالم، وتعد الموارد المائية من أكثر النظم حساسة لتغير المناخ. فالدراسات جميعها حول التغير المناخي للكرة الأرضية، تؤكد تأثير التغير المناخي في كمية الموارد المائية ونوعيتها، وكذلك زيادة الظواهر المناخية المتطرفة مثل الجفاف والفيضانات والانهيارات الثلجية والأعاصير.

ومما لا شك فيه أن مصر باعتبارها جزء لا يتجزأ من دول العالم فإنها وبالتأكيد سوف تتعرض لخطر تلك التغيرات المناخية والتي سوف تؤثر حتماً على مواردها الطبيعية متمثلة في الزراعة والموارد المائية. لقد بات من الواضح أن مصر تتعرض لضغوط متزايدة على استخدامات الموارد المائية المتاحة لها كنتيجة للنمو السكاني واحتياجات التنمية، يضاف إلى ذلك تغير المناخ الذي يضيف المزيد من الضغوط على الوضع الحالي للموارد المائية، ومن هنا فإنه قد أصبح من الضروري بالنسبة لمتخذي القرار الإهتمام برفع مستوى المعرفة بالتأثيرات المحتملة لتغير المناخ وما قد يؤدي إليه من تأثيرات سلبية. تشير التقديرات الدولية الى عدة سيناريوهات بينها ما أشار الى نقص موارد نهر النيل نتيجة لتحرك أحزمة الامطار من فوق الهضبة الأثيوبية والتي تمثل ٨٥ % من موارد مصر من المياه. ومن الجدير بالذكر أن بعض الدراسات الحديثة التي اهتمت بالتنبؤ بالآثار المستقبلية للتغيرات المناخية على مياه نهر النيل قد توصلت إلى حدوث تراجع في معدل تدفق المياه في نهر النيل بنحو ٢٠ % حتى عام 2040 م . بينما يتنبأ سيناريو واحد فقط بحدوث ارتفاع في معدل التدفق لمياه نهر النيل بعد عام ٢٠٤٥م.

تهدف الدراسة الى ما يلى:

- تهدف الدراسة الى التعرف على أثر التغيرات المناخية على منابع مياه نهر النيل الموسمية وكذلك على تذبذب فيضانه, حيث تتأثر مياه نهر النيل بالتغيرات المناخية.
- دراسة التغيرات المناخية لعناصر درجتى الحرارة العظمى والصغرى وكذلك كمية الامطار خلال الفترة 1950-2005.
- التنبؤ بالتغيرات المتوقعة لعناصر درجتى الحرارة العظمى والصغرى وكذلك كمية الامطار خلال الفترة المستقبلية 2006-2030م.
- تقييم التغيرات فى تدفق مياه نهر النيل عند المحطات الواقعة على مجرى النيل الازرق وعطبرة والنيل الرئيس عند دنقلا واسوان.

البيانات المستخدمة:

تعتمد الدراسة على بيانات درجة الحرارة العظمى والصغرى وكمية الامطار الشهرية لمانبع نهر النيل الموسمية (الهضبة الاثيوبية) وكمية الجريان السطحى عند بعض المحطات الموجودة على مجرى النيل الازرق والابيض والنيل الاساسى قبل السد العالى فى السودان وبعد السد عند اسوان تم الحصول على هذه البيانات من هيئة الارصاد الجوية الاثيوبية وبعض المصادر الاخرى لسد الفجوات الموجودة خلال فترة الدراسة ثم تم تقييم هذه البيانات باستخدام طرق مختلفة منها الجودة و التجانس بين البيانات لكل محطة.

حساب الاتجاهات لعناصر المناخ فى اثيوبيا

هذا التحليل يكاد يكون المهيمن على هذه الدراسة فمن هذا التحليل نستطيع ان نتعرف على شكل المنحنى لكل من درجة الحرارة العظمى والصغرى وكمية الامطار خلال فترة الدراسة سواء بالزيادة أو النقص. من المقارنة بين معادلات الاتجاه سواء كانت معادلة من الدرجة الاولى او الثانية او الثالثة اوالمعادلة الاسية وجد ان افضل معادلة لتمثيل الاتجاه هى المعادلة من الدرجة الثانية لمعظم المحطات وهذا ينطبق على البيانات الخطية اما البيانات الغير خطية فتستخدم معادلة مان كاندل (Mann-Kendall test). من نتائج التحليل وجد ان متوسط درجة الحرارة العظمى والصغرى أخذت الاتجاه الموجب خلال الفترة من (1950-2005) وذلك بالنسبة لكل المحطات ولكن هذه

الزيادة فى الاتجاه كانت صغيرة (0.04) لدرجة الحرارة العظمى و0.07 لدرجة الحرارة الصغرى خلال فترة الدراسة) وعلى العكس وجد إن كمية المطر أخذت الاتجاه السالب مع اختلاف القيم السالبة لمعظم المحطات (16 من 26 محطة).

تحليل السلاسل الزمنية للأمطار والجريان السطحي

تعد عملية التنبؤ اساساً لكل عمليات التخطيط العلمي ، بأعتبره سمة من سمات العصر الحديث في جميع مجالات الحياة ، اذ انه يساعد المختصين على اتخاذ القرارات اللازمة ووضع الخطط المستقبلية لتفادي المشكلات القائمة ولا سيما تلك التي تمس حياة الإنسان على سطح الأرض. وتعد دراسة كميات الأمطار المتساقطة من المواضيع المهمة في اغلب دول العالم ومنها منطقة الدراسة. يعد أسلوب تحليل السلاسل الزمنية من الأساليب الإحصائية الجديرة بالاهتمام، والتي تطورت كثيراً، وأصبح بالإمكان استخدامها لغرض التوقع للمستقبل. ويعتمد أسلوب تحليل السلاسل الزمنية على تتبع الظاهرة (أو المتغير) على مدى زمني معين (عدة سنوات مثلاً)، ثم يتوقع للمستقبل بناءً على القيم المختلفة التي ظهرت في السلسلة الزمنية وعلى نمط النمو في القيم. يتكون تحليل السلاسل الزمنية من مراحل متسلسلة تبدأ بمرحلة التشخيص للنموذج والتي تعد المرحلة الأهم. وتليها مرحلة تقدير المعلومات للنموذج، ومن ثم مرحلة فحص مدى الملاءمة للنموذج. وتأتي المرحلة الأخيرة وهي مرحلة التكهّن أو التنبؤ.

من التحليل وجد أن سلسلة كمية الامطار الشهرية انها غير مستقرة فى المتوسط وان هناك اتجاه عام واضح فى السلسلة. تم تحقيق استقرارية السلسلة الزمنية بعد اخذ الفرق الاول للبيانات وبعد مطابقة معاملات الارتباط الذاتى والجزئى للسلسلة الزمنية مع السلوك النظرى لدالتى الارتباط الذاتى والجزئى فقد اتضح أن دالة الارتباط الذاتى تتناقص تدريجياً مع فترات الاراحة. تم تحليل السلاسل الزمنية باستخدام طريقة (Box & Jenkins) فى التحليل (التشخيص، التقدير، اختبار ملائمة النموذج، التنبؤ). لايجاد افضل نموذج للتنبؤ بكمية الامطار التى تسقط على دولة اثيوبيا عن بعض محطات الارصاد وذلك بالاعتماد على البيانات الشهرية لهذه المحطات للفترة (1900-2005)، تم الاعتماد على استخدام معايير المفاضلة بين عدة نماذج وهى (أقل قيمة لتباين النموذج-أقل قيمة لمجموع مربعات الخطأ- معيار معلومات أكايك) جد أن النماذج الملائمة للبيانات هى نموذج الانحدار الذاتى المتكامل هو $(0,0,0) \times (1,1,1)$ لمحطة Bahar Dar, Nekemte اما النموذج الملائم

لمحطة DebreMarkos هو $(0,0,0) \times (0,1,1)$ بينما النموذج $(0,0,1) \times (0,1,1)$ كان هو الملانم عند محطة Addis Ababa. باستخدام هذه النماذج للتنبؤ بكمية الامطار على حوض النيل الازرق للفترة (2006-2030) وجد أن كمية الامطار تزداد خلال هذه الفترة ولكن هذه الزيادة صغيرة.

تم استخدام معادلة مان كاندل (Mann-Kendall test) لمعرفة الاتجاه العام للتدفق المائي للنيل الازرق عند محطات الديم، خرطوم بينما محطة ملكال للنيل الابيض و محطة دنقلة للنيل الاساسى خلال فترة الدراسة. وجد ان معامل التحديد (R^2) صغير عن كل المحطات كذلك وجد ان الاتجاه العام للتدفق النهري للنيل الازرق فى زيادة عند محطة الديم والخرطوم بينما العكس للنيل الابيض عند محطة ملكال. أظهرت النتائج أيضا أن التغيرات المتوقعة لتدفقات النيل الرئيسي عند دنقلا تنشأ من الزيادة في معدلات سقوط الأمطار والتدفقات على حوضي النيل الأزرق.